Renewable additives for poly(vinyl chloride) and poly(lactide) blends

Matthew W. Halloran

Department of Chemical Engineering

McGill University

October 2022

A thesis submitted to McGill University in partial fulfillment of the requirements of the degree
of
Doctor of Philosophy

Abstract

The success and widespread use of commercialized plastics was made possible through the development of suitable chemical additives that are blended with polymers during processing to generate new materials with enhanced mechanical or thermal properties. While they serve as essential components in many applications, most polymer additives are synthesized from fossil-based feedstocks. Accordingly, the investigation of renewably sourced polymer additives is a rapidly growing field of study as the public and industry shift away from their reliance on the petroleum industry.

As one of the most widely produced chemical additives, plasticizers are blended during manufacturing to improve the processability and flexibility of brittle polymers such as poly(vinyl chloride) (PVC) and poly(lactide) (PLA). Depending on the application of the desired material, plasticizer content can reach upwards of 50 weight percent in the resultant blend. However, most plasticizers are not covalently bound to the polymer matrix and are prone to leaching out of the blend over time which results in environmental contamination and eventual mechanical failure of the product. Due to the increased awareness of the negative environmental and health impacts of traditional *ortho*-phthalate plasticizers and their metabolites, significant efforts have been made to develop alternative plasticizers which are both non-toxic and resistant to leaching. Concurrently, the demand for the substitution of fossil-based feedstocks with renewably sourced alternatives has generated interest in the production of effective bio-based plasticizers for both PVC and PLA.

Alternatively, the impact strength of brittle polymers such as PLA can be enhanced through the incorporation of a minority rubbery phase during blending to produce rubber toughened PLA blends. While effective, achieving adequate compatibilization between the two immiscible phases is non-trivial and often requires the use of pre-made or *in situ* formed graft copolymers during blending. Usually, this is achieved using commercially available compatibilization agents or through the addition of external catalysts that are often derived from petroleum-based feedstocks which compromises the sustainable nature of PLA. As such, the development of renewably sourced rubber toughening agents for PLA is of great interest.

The main objective of the work reported in this doctoral thesis was to exploit renewably sourced chemical feedstocks to develop plasticizers and rubber toughening agents for PVC and PLA with similar, or superior properties to existing petroleum-based additives. Initial work was aimed at gaining further insights into the complex relationship between chemical structure and plasticizer leaching, while establishing the use of quantitative proton nuclear magnetic resonance (^{1}H NMR) as a reliable tool to monitor plasticizer leaching over time. To this end, a series of bio-based branched heptyl-succinate compounds was developed and studied as plasticizers for PVC. It was found that a higher degree of branching led to a significant decrease (two to ten-fold) in plasticizer leaching relative to commercial di(2-ethylhexyl) phthalate (DEHP). However, compounds functionalized with three or more heptyl-succinate branches performed poorly as plasticizers and produced blends with inferior elongation at break (EL%<45%) and glass transition temperatures (T_gs>9 °C) to DEHP (EL% = 96%, T_g = -7 °C). This work highlighted the inherent challenges associated with developing both effective and leaching resistant plasticizers.

Building from this initial work, a family of glycerol-succinate based compounds was developed and studied as plasticizers to produce flexible PLA and PVC materials with potential applications as food packaging. PLA blends containing 20 weight% plasticizer produced films with improved elongation at break values (up to 435%) relative to neat PLA (6% EL%), while the T_g of the blends was reduced by up to 45 °C from that of neat PLA (T_g ~ 60 °C). The glycerol compounds were also shown to function as effective PVC plasticizers as elongations at break of up to 97% were achieved in conjunction with a reduction in T_g of up to 86 °C. Furthermore, a cell-viability assay confirmed little to no toxicity of the newly developed compounds over a seven-day time period.

Finally, the terpene monomer farnesene was used as a building block for the design of bio-based elastomeric rubber toughening agents for PLA. A novel catalyst free-method was exploited to achieve reactive compatibilization to create toughened PLA blends exhibiting a 16- and 10-fold increase in impact strength and elongation at break, respectively, over neat PLA.

Taken together, the work reported in this doctoral thesis illustrates the potential of renewably sourced building blocks for the development of chemical additives that can modulate the material properties of PVC and PLA.

Résumé

Le succès et l'utilisation généralisée des plastiques commercialisés ont été rendus possibles grâce au développement d'additifs chimiques appropriés qui sont mélangés avec des polymères pendant le traitement, ce qui donne de nouveaux matériaux aux propriétés mécaniques ou thermiques améliorées. Bien qu'ils servent de composants essentiels dans de nombreuses applications, la plupart des additifs polymères sont synthétisés à partir de matières premières d'origine fossile. En conséquence, l'étude des additifs polymères d'origine renouvelable est un domaine d'étude en croissance rapide alors que la communauté scientifique s'éloigne de sa dépendance à l'égard de l'industrie pétrolière.

En tant que l'un des additifs chimiques les plus largement produits, les plastifiants sont mélangés pendant la fabrication pour améliorer l'aptitude au traitement et la flexibilité des polymères fragiles tels que le poly(chlorure de vinyle) (PVC) et le poly(lactide) (PLA). En fonction de l'application du matériau souhaité, la teneur en plastifiant peut atteindre plus de 50 % en poids dans le mélange résultant. Cependant, la plupart des plastifiants ne sont pas liés de manière covalente à la matrice polymère et sont susceptibles de s'échapper du mélange au fil du temps, ce qui entraîne une contamination de l'environnement et une éventuelle défaillance mécanique du produit. En raison de la prise de conscience accrue des impacts négatifs sur l'environnement et la santé des plastifiants ortho−phtalates traditionnels et de leurs métabolites, des efforts importants ont été déployés pour développer des plastifiants alternatifs à la fois non toxiques et résistants à la lixiviation. Parallèlement, la demande de remplacement des matières premières d'origine fossile par des alternatives d'origine renouvelable a suscité un intérêt pour la production de plastifiants biosourcés efficaces pour le PVC et le PLA.

Alternativement, la résistance aux chocs des polymères fragiles tels que le PLA peut être améliorée par l'incorporation d'une phase caoutchouteuse minoritaire pendant le mélange pour produire des mélanges de PLA durcis au caoutchouc. Bien qu'efficace, l'obtention d'une compatibilité adéquate entre les deux phases non miscibles n'est pas triviale et nécessite souvent l'utilisation de copolymères greffés préfabriqués ou formés in situ pendant le mélange. Habituellement, ceci est réalisé en utilisant des agents de compatibilisation disponibles dans le commerce ou par l'ajout d'un catalyseur externe qui sont souvent dérivés de matières premières à base de pétrole, ce qui compromet la nature durable du PLA. En tant que tel, le développement d'agents de durcissement de caoutchouc d'origine renouvelable pour le PLA est d'un grand intérêt.

L'objectif principal des travaux rapportés dans cette thèse de doctorat était d'exploiter des matières premières chimiques d'origine renouvelable pour développer des plastifiants et des agents de durcissement du caoutchouc pour le PVC et le PLA avec des propriétés similaires ou supérieures aux additifs à base de pétrole existants. Les travaux initiaux visaient à mieux comprendre la relation complexe entre la structure chimique et la lixiviation des plastifiants, tout en établissant l'utilisation de la résonance magnétique nucléaire quantitative du proton (RMN 1H) comme outil fiable pour surveiller la lixiviation des plastifiants au fil du temps. À cette fin, une série de composés biosourcés d'heptyl-succinate ramifié a été développée et étudiée comme plastifiants pour le PVC. Il a été constaté qu'un degré plus élevé de ramification entraînait une diminution significative (de deux à dix fois) de la lixiviation du plastifiant par rapport au phtalate de di (2-éthylhexyle) (DEHP) commercial. Cependant, les composés fonctionnalisés avec trois branches heptyl-succinate ou plus se sont mal comportés en tant que plastifiants et ont produit des mélanges avec un allongement à la rupture inférieur (EL% <45%) et des températures de transition vitreuse (Tgs>9 °C) au DEHP (EL% = 96% , Tg = -7 °C). Ce travail a mis en évidence les défis inhérents au développement de plastifiants efficaces et résistants à la lixiviation.

À partir de ces travaux initiaux, une famille de composés à base de succinate de glycérol a été développée et étudiée en tant que plastifiants pour produire des matériaux flexibles en PLA et en PVC avec des applications potentielles comme emballage alimentaire. Les mélanges de PLA contenant 20 % en poids de plastifiant ont produit des films avec des valeurs d'allongement à la rupture améliorées (jusqu'à 435 %) par rapport au PLA pur (6 % EL %), tandis que les Tg ont été réduites jusqu'à 45 °C par rapport à celles du PLA pur (Tg ~ 60 °C). Il a également été démontré que les composés de glycérol fonctionnent comme des plastifiants efficaces du PVC, car des allongements à la rupture allant jusqu'à 97 % ont été obtenus en conjonction avec une réduction de la Tg allant jusqu'à 86 °C. De plus, un test de viabilité cellulaire a confirmé peu ou pas de toxicité des composés nouvellement développés sur une période de sept jours.

Enfin, le farnesene monomère terpénique a été utilisé comme élément de base pour la conception d'agents de renforcement de caoutchouc élastomère biosourcé pour le PLA. Une nouvelle méthode sans catalyseur a été exploitée pour obtenir une compatibilisation réactive afin de créer des mélanges de PLA durcis présentant une augmentation de 16 et 10 fois de la résistance aux chocs et de l'allongement à la rupture, respectivement, par rapport au PLA pur.

Acknowledgements

First and foremost, I would like to express my deep gratitude to my three supervisors Prof. Milan Marić, Prof. Richard Leask, and Prof. Jim Nicell, for all the support, guidance, and freedom to pursue any direction with my research during the course of my degree. Moreover, I would like to thank them for providing me with this opportunity and taking a chance by hiring me despite my lack of background knowledge in the field.

I am forever grateful to the many colleagues, past and present, who supported me throughout my PhD and made the experience both a memorable, and bearable one. I would like to especially mention and thank Dr. Roya Jamarani who helped to train and guide me throughout the early parts of my degree. I will always remember the many laughs we shared as well as our road trips to Cambridge. I also express special appreciation to Mr. Frank Caporuscio and Mr. Gerald Lepkyj for their constant help with broken down lab equipment, Mr. Ranjan Roy and Mr. Andrew Golsztajn for their help with analytical equipment, and Ms. Lisa Danielczak for her help with the cytotoxicity assay.

To all the great lab-mates in the Marić and Leask lab who I had the opportunity to learn from and work alongside over the years: Adrien, Georges, Sharmaine, Farhad, Mohammad, Masa, Gabrielle, Kevin, Lauren, Alex, Marc, and Neil. To all my friends in the department, I feel honoured to have worked among such amazing people- thank you for all the great memories.

I would also like to extend my deepest gratitude to Taylor Gretzinger for her constant support and encouragement. Thank you for believing in me, listening to me complain, and celebrating the small victories with me along the way.

Finally, I would like to thank to my parents and family for their constant words of encouragement, unwavering support, and belief in me during my degree. This meant more to me than I think you realize, and this PhD would not have been possible without you.

Table Of Contents

List of Figures

List of Tables

List of Schemes

Contribution of Authors

This thesis is manuscript-based and contains four original research articles which have been published in peer-reviewed journals. The author contributions for each manuscript are outlined below.

Article 1 (Chapter 3)

Halloran, M.W.; Nicell, J. A.; Leask, R. L.; Marić, M. Small molecule plasticizers for improved migration resistance: Investigation of branching and leaching behaviour in PVC blends. *Mater. Today Commun.* **2021,** *29*, 102874.

Matthew Halloran developed, planned, and executed all experiments in this article as well as prepared the manuscript for publication and response to reviewers. Richard Leask, Jim Nicell, and Milan Marić funded the work, guided the direction of the study, aided in the design of experiments, guided the interpretation of data, and contributed to the editing of the manuscript before submission.

Article 2 (Chapter 4)

Halloran, M.W.; Danielczak, L; Nicell, J. A.; Leask, R. L.; Marić, M. Highly Flexible Polylactide Food Packaging Plasticized with Nontoxic, Biosourced Glycerol Plasticizers. *ACS Appl. Polym. Mater.* **2022**, *4* (5), 3608-3617.

Matthew Halloran planned and executed experiments in this article as well as prepared the manuscript for publication and response to reviewers. Lisa Danielczak helped with the design and execution of the cytotoxicity assay, while Matthew Halloran analyzed and interpreted the results. Richard Leask, Jim Nicell, and Milan Marić funded the work, contributed to the design of experiments, and aided in the editing of the manuscript before submission.

Article 3 (Chapter 5)

Halloran, M.W.; Nicell, J. A.; Leask, R. L.; Marić, M. Bio-based glycerol plasticizers for flexible poly(vinyl chloride) blends. *J. Appl. Poly. Sci.* **2022**, *139* (32), e52778.

Matthew Halloran planned and executed all experiments in this article in addition to preparing the manuscript for publication and response to reviewers. Richard Leask, Jim Nicell, and Milan Marić provided funding for the research, contributed to the design of experiments, and aided in the editing of the manuscript before the initial and final submission.

Article 4 (Chapter 6)

Halloran, M.W.; Nicell, J. A.; Leask, R. L.; Marić, M. Toughening poly(lactide) with bio-based poly(farnesene) elastomers. *ACS Appl. Polym. Mater.* **2022**, *Just Accepted,* DOI: 10.1021/acsapm.2c01183.

Matthew Halloran planned and executed all experiments in this publication in addition to preparing the manuscript for publication and crafting the response to reviewers. Richard Leask, Jim Nicell, and Milan Marić provided funding for the research, contributed to the design of experiments, guided the interpretation of the data, and aided in the editing of the manuscript before the initial and final submission.

1 Introduction

Growing concerns associated with the depletion of fossil fuel reserves in conjunction with improvements in the extraction of valuable feedstock chemicals from biomass resources has stimulated significant interest not only in the development of renewably sourced polymers but also additives that are necessary for producing functional plastics.[1] Most commercial plastics contain chemical additives such as plasticizers, lubricants, stabilizers, and impact modifiers which are added during the manufacturing process to enhance the properties of the base resin.[2] These additives serve as vital components in the production of commodity plastics providing a wide range of physical and mechanical properties, which have significantly influenced our way of life.[1] While effective, many of these chemical additives are derived from petroleum precursors.[3] Thus, the development of renewably sourced polymer additives which can replace conventional non-renewable products is an active area of research and serves as the overarching goal of this doctoral thesis.

Poly(vinyl chloride) (PVC) is one of the most commonly used synthetic thermoplastics in the world, with approximately 50 million tons produced per year,[4] and is used in a variety of commodity items such as packaging, car interiors, pool liners, and medical tubing.[5] Since PVC is a brittle material with poor processing properties, numerous additives are used during manufacturing to provide thermal stability and improve its mechanical properties.[6] Plasticizers are arguably the most significant of these additives, owing to their remarkable ability to lower the glass transition temperature (T_g) and impart flexibility into an otherwise brittle polymer matrix.[7] Although effective and widely used, plasticizers are prone to leaching over time as they are not covalently bound to the PVC backbone which results in widespread environmental contamination and a significant reduction in mechanical properties of the material.[8] Therefore, the development of leaching-resistant PVC plasticizers is an active area of research which has resulted in a number of notable advancements over the years.[9] However, most of these reports have taken a narrow approach to this problem that neglects a comprehensive view that takes into account both functionality and sustainability of the plasticizer.

In a much broader sense, a truly sustainable solution to move away from plastics derived from fossil fuels would be to implement the use of renewably sourced polymers. As one of the most widely studied renewably sourced and compostable polymers, poly(lactide) (PLA), has found suitable applications in the packaging industry and biomedical field owing to its biocompatability.[10, 11] Similar to PVC, PLA is a brittle polymer with poor thermal stability that often relies on the use of additives, such as plasticizers or impact modifiers, during manufacturing to help to impart flexibility and toughness into the blend.[12] While effective, many of the reported examples rely on the use of petroleum-derived feedstocks when designing functional additives for PLA[13] which compromises its renewable nature.

In recognition of this, the motivation for the work in this thesis was driven by the need to identify and exploit renewably sourced feedstocks to develop polymer additives for PVC and PLA with real-world applications.

1.1 Objectives

The overarching goal of this thesis research was to develop renewably sourced chemical additives for PVC and PLA which can serve as viable replacements for current petroleum-derived compounds. To accomplish this goal, multiple parameters were taken into consideration including use of renewable chemical feedstocks, benign and scalable syntheses, permanence of the additives in the blends, toxicity of the additives, effectiveness of additives relative to existing commercial compounds, theoretical and experimental evolution of compatibility, and designing additives for environmental biodegradation (Figure 1.1).

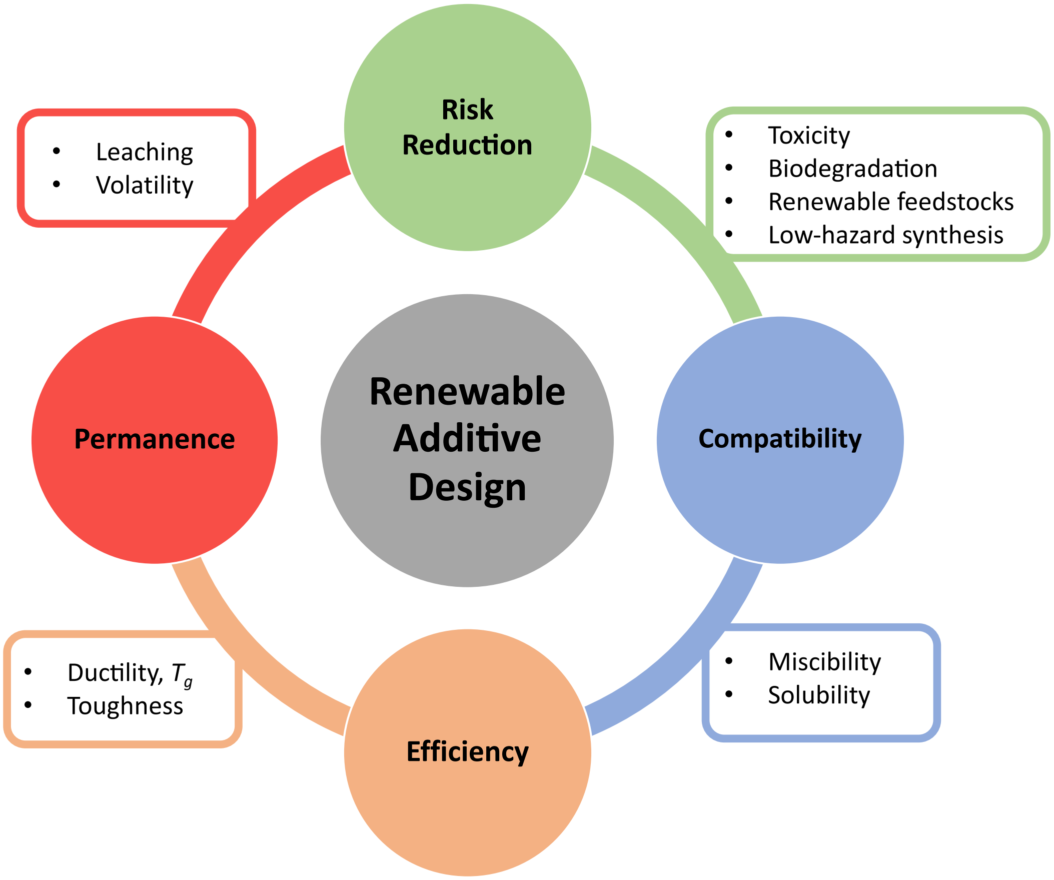

Figure 1.1. Parameters taken into consideration during the design of renewable additives for PVC and PLA.

In line with this, studies were conducted to understand the relationship between permanence and chemical structure of small molecule plasticizers in blends with PVC and PLA while evaluating their efficiency to improve the mechanical properties of the resulting blends. Finally, as an alternative approach to plasticization, bio-based elastomeric additives were studied as impact modifiers for PLA. As such, the following specific objectives were pursued:

1. To (a) evaluate the relationship between branching and permanence of small molecule plasticizers in PVC blends to allow for further development of low leaching plasticizers with the hypothesis that higher degrees of branching results in lower leaching; and (b) demonstrate the use of quantitative ^{1}H NMR as a reliable analytical tool to measure plasticizer leaching.
2. To (a) synthesize and evaluate the potential of renewably sourced glycerol-succinate derivatives to function as plasticizers for PLA in comparison to commercial standards, (b)

identify optimal alkyl chain length for plasticization performance and permanence, and (c) establish the need for a wide scope of testing requirements for alternative plasticizers.

3. To (a) demonstrate the dual functionality of the glycerol compounds to function as plasticizers for PLA and PVC and (b) establish structural similarities between what constitutes an effective plasticizer for these two distinct polymer matrices.
4. To evaluate the potential of the terpene monomer, farnesene, as a building block for the design of rubber toughening agents to improve the impact strength of PLA.

1.2 Thesis Organization

This manuscript-based thesis consists of eight chapters, four of which have been published as peer-reviewed journal articles. In Chapter 2, a background of polymer additives is provided in which the development and use of renewably sourced PVC plasticizers, PLA plasticizers, and PLA rubber toughening agents is presented. This literature review forms the foundation upon which the work reported in Chapters 3 through 6 is built, each of which present details of the investigations conducted as outlined below.

- In Chapter 3, a series of compounds with varying degrees of branching were synthesized to investigate the relationship between branching and permanence in small molecule plasticizers. Additionally, the use of quantitative ^{1}H NMR was evaluated as an analytical tool to measure plasticizer leaching.
- Chapter 4 details efforts directed towards developing glycerol-based plasticizers for PLA with potential applications as flexible food packaging materials. This included the evaluation of two different blend preparation techniques (solvent-casting of films versus melt-mixing) to obtain a comprehensive set of data. Additionally, the toxicity of the plasticizers was evaluated using a mammalian cell cytotoxicity assay.
- As a follow up to this work, Chapter 5 describes the investigation of the glycerol compounds as effective PVC plasticizers, while comparing their thermal, mechanical, morphological, and migration behavior alongside the commercial *ortho*-phthalate alternative plasticizer, DOTP.

- The final manuscript presented in Chapter 6 discusses the development of farnesene-based rubber toughening agents for PLA.

The manuscripts presented in Chapters 3 to 6 are followed by Chapters 7 and 8 which include a brief discussion that supplements what is already presented in the individual chapters, concluding remarks in relation to the objectives, an outline of the original contributions made to the field arising from this work, and recommendations for future work.

2 Background

To pursue the objectives of this thesis, this work builds upon key findings reported in the literature related to the development of renewably sourced additives for PVC and PLA. A background discussion on PVC and plasticizers is provided in conjunction with an overview describing the mechanism of action of plasticizers. This is followed by a summary of several relevant examples of succinate-based plasticizers which have been developed for use in PVC blends. Thereafter, PLA-based blends are discussed in the context of renewably sourced plasticizer development and rubber toughening agents. The examples discussed in this section highlight notable advancements in the field and help to provide appropriate background material, while also drawing attention to areas which require further investigation.

2.1 Poly(vinyl chloride) Blends

Poly(vinyl chloride) (PVC) is the third most widely produced thermoplastic in the world, with production levels nearing 50 million tons in 2019.[4] The presence of chlorine atoms on alternating bonds throughout the backbone imparts a polar nature to the polymer and generates weak dipole-dipole interactions. (Figure 2.1).[6] These weak interactions hinder the mobility of the polymer chains and render the material rigid and brittle below its glass transition temperature (T_g) of 80 °C, i.e., the temperature at which a polymer transitions from a hard, glassy state, into a soft or rubbery state.[14]

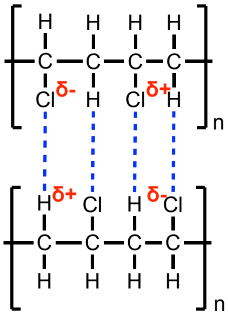

Figure 2.1. Chemical structure of PVC indicating dipole-dipole interactions.

In spite of this, rigid PVC (rPVC), which is also known as unplasticized PVC, finds numerous applications in the construction sector where it is used in window frames, piping, flooring, and rigid films.[15] To broaden the scope of application, plasticizers are blended with PVC which help to reduce the T_g and introduce significant flexibility into the resultant blend.[16] Nearly 90% of all plasticizers which are produced globally are used in blends with PVC owing to its unique ability to accept high loadings of plasticizer into the polymer matrix.[16] It is hypothesized that the presence of the polar chlorine atoms in the polymer backbone improve compatibilization with plasticizers, while the microcrystalline regions of PVC that are dispersed within a predominantly amorphous polymer matrix permit the polymer to retain its mechanical strength when blended with high loadings of plasticizer.[6]

2.1.1 Plasticizers

Plasticizers are typically small, organic, ester-based molecules which are blended with PVC during the manufacturing process.[7] Their main function is to impart flexibility into an otherwise brittle polymer matrix; however, their incorporation into a polymer blend also leads to a reduction in the T_g, a modification of melt rheology, and an improvement in melt processability by lowering the fusion temperatures of the blend.[17] Plasticizers can be classified as either internal or external, with the latter being the most common. Internal plasticizers are chemically introduced into the polymer backbone through grafting or copolymerization methods, whereas their external counterparts are blended with the polymer at elevated temperatures and are not covalently bound to the backbone.[18] Given that external plasticizers are added post-polymerization during blending, the final polymeric properties of the material can be specifically tailored in a much simpler and cost-effective manner relative to internal plasticization.

Despite their cost effectiveness and widespread use, external plasticizers are not covalently bound to PVC which permits their diffusion in and out of the blend over time. As such, and after migrating to the surface of the blend, the plasticizer can leach out into its surroundings, resulting in human exposure and environmental contamination.[19, 20] The most commonly used commercial plasticizer, di(2-ethylhexyl) phthalate (DEHP) (Figure 2.2), has garnered negative attention due to the detection of its presence in a variety of environmental samples as well the detrimental health effects of its metabolites.[21] In particular, the primary metabolite mono(2-ethylhexyl) phthalate (MEHP) is a known human endocrine disruptor and displays anti-androgenic effects.[22, 23] Due to these negative health implications, the use of DEHP and structurally similar phthalates has been regulated in consumer items in many developed nations including the United States, the European Union, and Canada.[21] However, the widespread use and low-cost production of phthalate-based plasticizers have hindered the development and adoption of safer, non-toxic replacements in industrial processes. Nevertheless, owing to the adverse health effects of phthalates and increased regulatory pressure that restrict their use, there is a growing incentive to develop alternative plasticizers which can replace the existing problematic ones on the market.

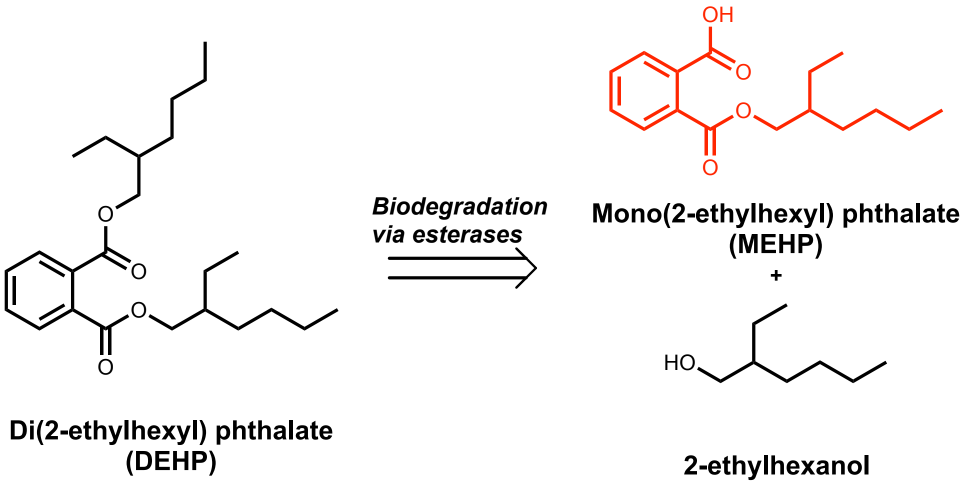

Figure 2.2. DEHP and its primary metabolites MEHP, and 2-ethylhexanol.

2.1.2 Plasticizer Mechanism of Action

Despite the widespread commercial use of plasticizers for nearly a century, their precise mechanisms of action are not fully understood, which has, to a certain extent, hampered the development of efficient phthalate alternatives. Several theories of plasticization exist, with each theory partially building upon its predecessor.[24] The first of these theories, known as the lubricity theory, was developed by Kirkpatrick in 1940.[25] It states that a plasticizer in PVC acts as a molecular lubricant which enables the polymer chains to flow freely over one another by reducing intermolecular friction when a force is applied. In this conceptual model, a specific functional group on the plasticizer is strongly attracted to the PVC polymer and acts as a solvent, whereas other functional groups act as lubricants. Shortly after this development, Aiken and coworkers proposed the gel theory of plasticization which states that plasticizers are free to move throughout the three-dimensional polymer network, disrupting PVC chain-chain interactions thereby imparting flexibility to the material.[26] It is hypothesized that external plasticizers moved freely within the gel structure to solvate and de-solvate different sites in a dynamic fashion depending on the types of forces present. This theory helped to explain why externally plasticized PVC softens more upon exposure to heat than its internally plasticized counterpart.

In the 1950s and 1960s, the free volume theory of plasticization was put forth in an effort to explain the reduced T_g that was observed upon the addition of plasticizers in PVC blends.[27] It was observed that the specific volume of a polymer decreased in a linear fashion as temperature decreased, until the T_g was reached. It was postulated that the increased specific volume above the T_g was attributable to the free volume that existed between the molecules. In general, free volume can be defined as the difference between the specific volume at a specified temperature of interest, and a reference temperature. By increasing the free volume of the polymer, a plasticization effect is observed. This increase in free volume can be attained by increasing the overall molecular mobility of the polymer chains through a variety of methods:

1. Increasing the number of end groups present in the polymer backbone
2. Increasing the amount of side chains attached to the backbone (internal plasticization)
3. Adding external plasticizers
4. Increasing backbone mobility and creation of empty space through molecular geometry

Since external plasticizers are commonly small organic molecules in relation to the polymer they are blended with, they contain a higher end-group concentration which leads to an overall increase in the free volume. Additionally, this theory allowed for a rational prediction of T_g for plasticizer-polymer blends. However, although useful, it does not consider the compatibility nor the permanence of the plasticizer in the blend, therefore, limiting its applications. Taken together, these theories, despite their limitations, are useful in informing the structural design and development of alternative plasticizers.

2.1.3 Renewably Sourced PVC Plasticizers

The restrictions placed on the commercial use of *ortho*-phthalates coupled with the desire to transition away from the use of petroleum feedstocks has resulted in increasing interest in the exploitation of renewably sourced building blocks for the design of alternative plasticizers. In this context, this area of research has grown considerably over the last two decades and has produced a number of notable examples reported in the literature.[4] This has led to the development of several structural classes of alternative plasticizers including maleates, vegetable oil derivatives, citrates, succinates, and malic acids, just to name a few.[4] However, for the sake of brevity, only the most relevant examples directly pertaining to the work in this thesis will be discussed here.

2.1.3.1 Succinate-Ester Plasticizers

Described as one of the top 12 building block chemicals by the US Department of Energy,[28] succinic acid (1,2-diethane dicarboxylic acid) has emerged as a promising platform chemical for the design of numerous consumer items in the food, agricultural, and pharmaceutical industries.[29] Moreover, recent advancements in the area of biotechnology and biomass extraction have demonstrated the efficiency of producing succinic acid through fermentation processes which are both high yielding and cost competitive with existing petrochemical methods.[29] As a result of this, succinic acid has been extensively investigated as a renewable building block for the design of alternative plasticizers.

To this end, a number of succinate diester compounds were synthesized and evaluated as potential phthalate replacement plasticizers (Figure 2.3a).[30, 31] As a point of reference, the plasticization performance of the diester compounds in PVC blends was benchmarked against DEHP and Hexamoll® DINCH (diisononyl cyclohexane 1,2 dicarboxylate - another commonly used commercially available diester plasticizer) (Figure 2.3b). Specifically, the T_g of the blends, mechanical properties (e.g., tensile strength, surface hardness), rheological properties, biodegradation, and leaching behavior were investigated. Amongst the compounds tested, it was found that succinate esters functionalized with linear alkyl chain lengths between six- and eight carbons in length provided the highest plasticization efficiency (i.e., improvement in mechanical properties) in PVC blends (comparable or superior to DINCH and DEHP), and were shown to biodegrade into innocuous metabolites in under three weeks.[32]

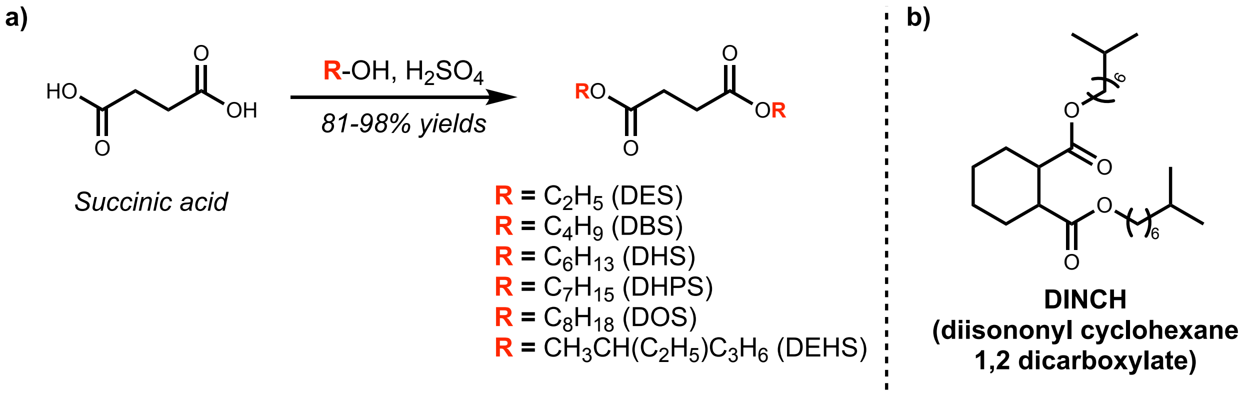

Figure 2.3. a) Synthesis and chemical structures of various succinate diester plasticizers; b) Chemical structure of DINCH.

Moreover, by using the renewably sourced 1-heptanol as the alcohol coupling reagent, Elsiwi *et al.* developed a fully renewably sourced plasticizer, diheptyl succinate (DHPS) (Scheme 2.3a).[30] Relative to DEHP, DHPS produced PVC blends with comparable tensile and thermal properties, and was shown to readily biodegrade in only two weeks. While promising, DHPS was subsequently shown to have comparably high rates of leaching in comparison to traditional *ortho*-phthalate plasticizers.[33]

Due to the important environmental and health concerns linked to plasticizer leaching, significant efforts have been made to develop alternative plasticizers with reduced rates of leaching.[9] Previous work has shown that poly(ε-caprolactone)-based (PCL) polymeric and oligomeric plasticizers demonstrate superior migration resistance than lower molecular weight diester plasticizers.[34, 35] This body of work led to the development of a family of PCL triol and diol succinates (Figure 2.4), which were investigated as low-migratory plasticizers alongside commercially available diisononyl phthalate (DINP).[33] In general, it was found that the PCL plasticizers produced blends with comparable mechanical, thermal, and rheological properties to both DINP and DHPS blends. However, they demonstrated superior resistance to leaching than DINP and DHPS (two- to ten-fold less leaching), with the butyl (C4) functionalized PCL-triol-succinate displaying the lowest leaching over time followed by the heptyl (C7), and decyl (C10) analogues. It was also shown that the linear, PCL-diol-succinate plasticizer displayed comparable leaching behavior to the branched PCL-triol-succinate compounds. From this, it was concluded that there was no observable relationship between the branching in the chemical structure of the plasticizer and its leaching behavior within the family of oligomeric compounds studied.[33]

In contrast, the relationship between branching and leaching within small molecule plasticizers has not been previously explored in the literature, which makes the design of effective phthalate alternative plasticizers challenging. Therefore, a fundamental understanding of this relationship within small molecule plasticizers is essential to develop viable replacements.

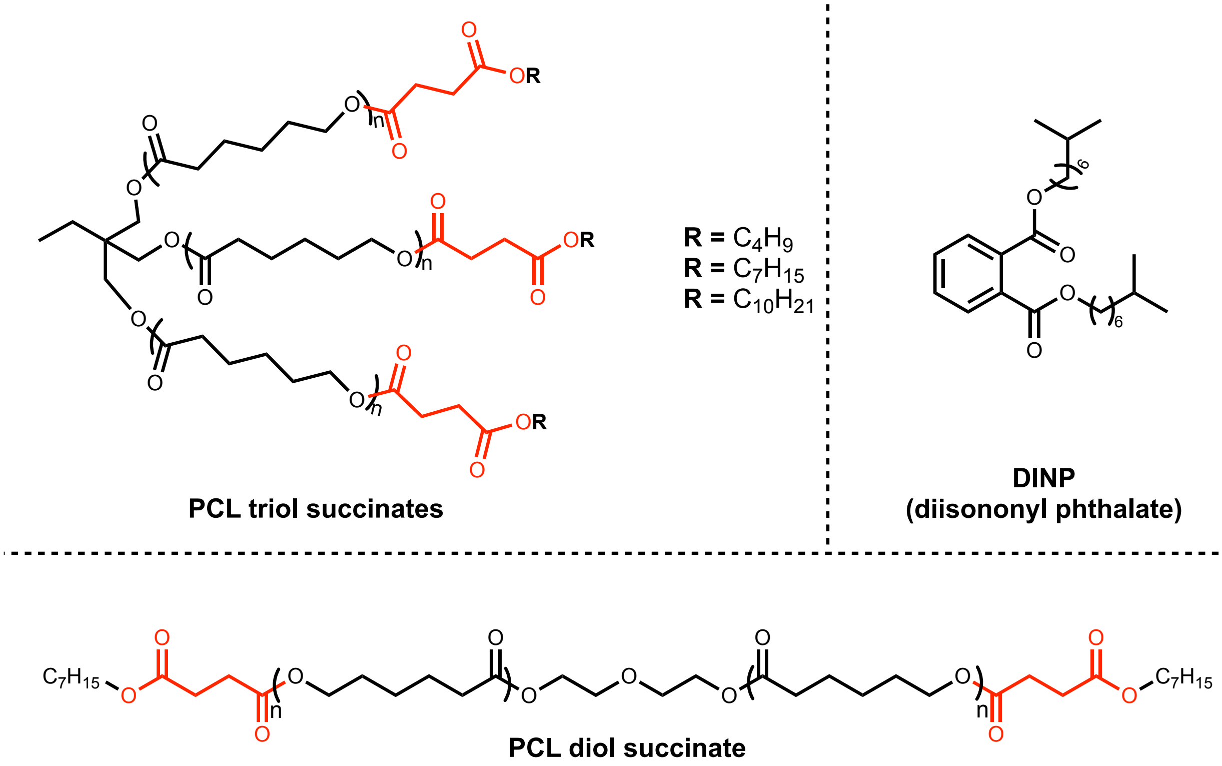

Figure 2.4. Chemical structures of PCL triol and diol succinates and DINP investigated as low-migratory plasticizers for PVC.

2.2 Poly(lactide) Blends

As an alternative to traditional petroleum-derived polymers such as PVC, poly(styrene) (PS), or poly(ethylene terephthalate) (PET), poly(lactide) (PLA) has received considerable attention owing to its renewable nature and compostability.[36, 37] Industrially, PLA is commonly synthesized through a two-step sequence which involves the dehydration of the bio-sourced lactic acid monomer to provide the cyclic di-ester (lactide), which then undergoes ring opening polymerization (ROP) in the presence of a metal catalyst to generate a high molecular weight PLA polymer species (Scheme 2.1). Owing to its high tensile strength and modulus, PLA has found applications in certain packaging applications, and in the medical field as sutures or implants due to its biocompatibility.[12] In addition, its ability to be processed using conventional polymer processing equipment and techniques such as extrusion and film blowing have established PLA as a promising replacement for PET or PS.[38] However, significant limitations of PLA include its inherent brittleness and poor thermal stability, which has restricted its widespread use to certain applications.[39]

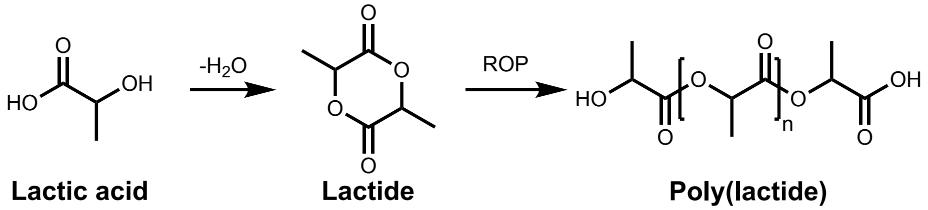

Scheme 2.1. Industrial synthesis of high molecular weight poly(lactide).

Two commonly used approaches to enhance the material properties of PLA are through the addition of plasticizers (usually small molecule ester-based), or through the incorporation of polymeric rubber toughening agents (Table 2.1).[12] A summary of each strategy is provided in Table 2.1, which highlights the advantages and disadvantages associated with each. In general, plasticizers are used to produce flexible PLA films, whereas rubber toughening agents are used to produce impact modified bulk specimens. Similar to PVC plasticizers, PLA plasticizers can be problematic as they are prone to leaching over time which has, to a certain extent, limited its use in certain applications.[11] Regardless of the application or strategy taken, there is a strong incentive to implement the use of renewably sourced building blocks when designing chemical additives for PLA.

Table 2.1. Commonly employed strategies to improve the mechanical properties of PLA.[12]

Strategy	Description	Example	Pros	Cons
Plasticization	Blending small molecules (usually ester-based)	Citrate esters (Acetyl tributyl citrate (ATBC), poly(ethylene glycol) (PEG))	High flexibility, tensile toughness, low cost, can be renewably sourced	Leaching (environmental, health, and mechanical issues)
Rubber Toughening	Blending functionalized immiscible rubbery component, sometimes via reactive blending	Poly(ethylene) (PE) with glycidyl methacrylate functionalized Pes	Increase impact resistance, tensile toughness	Need to use/synthesize functionalized rubbery phase, can be challenging to compatibilize

2.2.1 Renewably Sourced PLA Plasticizers

In contrast to what is seen in the PVC plasticizer literature, there are considerably fewer reports of renewably sourced PLA plasticizers being developed, with most examples having been reported in the last 15 years. This is mainly due to the fact that PLA is more challenging to manipulate in the melt owing to its susceptibility to undergo hydrolytic degradation at elevated temperatures during processing,[40] its historically expensive cost of production,[41] as well as its significantly lower market share value in relation to petroleum derived polymers such as PVC.[42] Thus, for many years, PLA was used exclusively in selected biomedical applications. However, advancements were made to its manufacturing process in the early 2000s[41] which improved yields and decreased the cost of PLA production. As a result of this, the scope of application of PLA-based materials has increased dramatically in recent years, with significant attention being given to the development of chemical additives which can be blended with PLA to enhance its material properties.

In a similar context to additive design for PVC, increasing focus has been placed on exploiting renewably sourced building blocks when designing chemical additives for PLA. This has led to the development of several structural classes of ester-based PLA plasticizers including functionalized glycerols,[43] citrate esters,[44] levulinic acids,[45] tartaric acids,[46] malic acids,[47] and soybean oils.[48]

2.2.1.1 Functionalized Glycerol Plasticizers

The renewable nature of glycerol and the relative ease in which its three hydroxyl groups can be manipulated for further synthetic transformations have established glycerol as a high-value building block for the design of consumer items.[49] While glycerol itself has shown promise as a plasticizer for the production of biodegradable starch films,[50] attempts at applying it as a plasticizer for PLA have been unsuccessful as it produces brittle blends which were observed to phase separate.[51] This is likely do its highly polar nature arising from the three hydroxyl groups, which make it incompatible with PLA and prevent it from effectively plasticizing the matrix.[52] Therefore, to increase compatibility, there have been a handful of studies which were aimed at investigating the potential of functionalized glycerol derivatives to serve as plasticizers for PLA.

In line with this, Wan *et al.* investigated the use of glycerol tribenzoate (GTB) and glycerol triacetate (GTA) as potential plasticizers for PLA (Figure 2.5).[43] In general, it was shown that GTA functioned more effectively to plasticize PLA, as it produced blends with lower T_g values, higher flexibility, and greater stability over time (assessed via extended aging tests), than GTB. Although no microscopy was conducted on the blends to assess compatibility, it was hypothesized that the small acetate groups on GTA were more effective at penetrating the PLA matrix than the rigid and bulky benzoate groups; thereby generating a larger increase in free volume. Overall, this work demonstrated the potential of functionalized glycerol derivatives to serve as plasticizers for PLA and provided a basis for future work in the area.

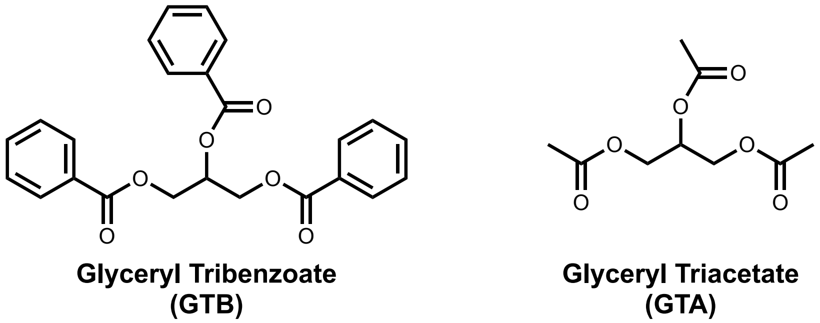

Figure 2.5. Chemical structures of benzoate and acetate functionalized glycerol plasticizers by Wan *et al* (redrawn).[43]

Building upon this work, Pettchwattana *et al.* evaluated the effect of carbon chain length on plasticization efficiency of functionalized glycerols using tributyrin, trilaurin, and tristearin in blends with PLA (Figure 2.6).[51] Scanning electron microscopy (SEM) analysis of the blends indicated phase separation for the blends plasticized with trilaurin and tristearin, while the shorter chain tributyrin produced homogenous blends with PLA. It was also shown that blends plasticized with tributyrin produced the highest improvement in elongation at break, Izod impact strength, and depression of T_g, whereas negligible improvements were seen using the longer carbon chain derivatives. Coupled with the work from Wan and coworkers, this work demonstrated that glycerols functionalized with shorter alkyl chains function more effectively to plasticize PLA than bulky aromatic groups or long carbon chains. Given that their scope of investigated compounds was limited and included a broad range of alkyl chain lengths, a more in-depth study focused on the effect of alkyl chain length of functionalized glycerol plasticizers, which also includes an analysis of their leaching behaviour, is needed.

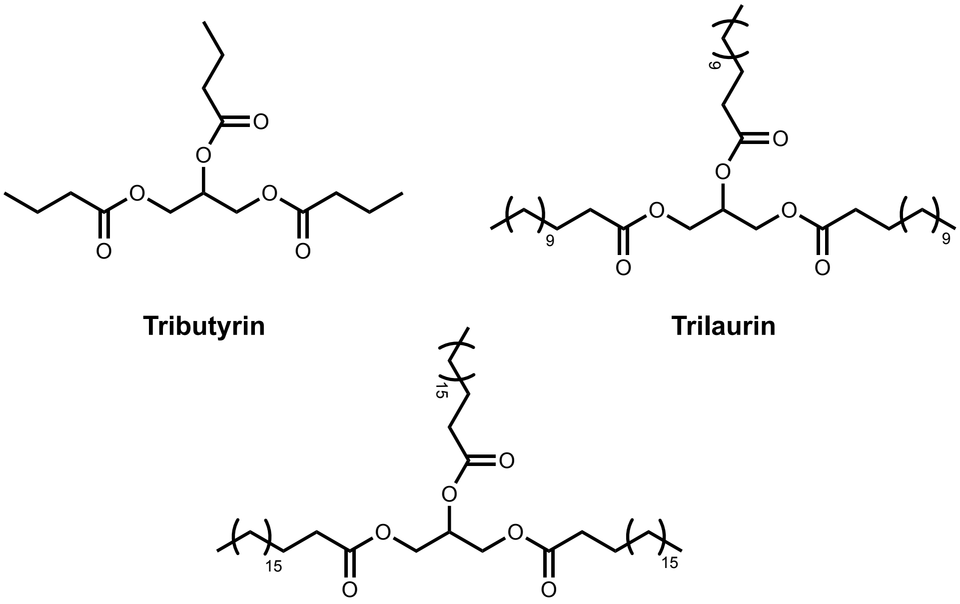

Tributyrin

Trilaurin

Tristearin

Figure 2.6. Chemical structures of glycerol plasticizers evaluated by Pettchwattana *et al* (redrawn).[51]

2.2.2 Rubber Toughening PLA

Aside from the addition of plasticizers, the mechanical properties of PLA can be enhanced through the incorporation of a minority rubbery polymer during blending; a technique known as rubber toughening.[53] Whereas plasticizers are commonly used to reduce the T_g of the blend and impart flexibility, the addition of rubbery polymers primarily leads to an increase in the impact strength of the resultant blend. The impact strength of a material can be defined as the energy that it can absorb before fracturing,[54] and is commonly described as "material toughness" in the polymer blend literature.[53] The impact strength of a polymer is dependent on both intrinsic (i.e., molecular weight distribution, morphology, crystallinity) and extrinsic (i.e., temperature, test speed, specimen thickness) factors.[54] Therefore, by incorporating a rubbery component into a polymer matrix, such as PLA, the intrinsic factors of the resultant blend will have significant influence on the toughness of the final material.

As a homopolymer, PLA has a low impact strength of ~26 J/m which has inhibited its use in many commodity items which require high material toughness such as certain food packaging, construction materials, and automotive parts.[12] As such, significant efforts have been made over the last several decades to improve the impact strength of PLA via rubber toughening,[13] which has resulted in "super-toughened" PLA blends with impact strengths of up to 800 J/m in some cases.[13] One of the most common and economically viable approaches to rubber toughen PLA is through polymer blending in which one (or more) rubbery components are blended with PLA during processing.[13] This approach is advantageous as it allows the operator to easily manipulate the final properties of the material by modifying the components and their loadings in the blend, and is analogous to modifying the plasticizer loadings in a blend to obtain different material properties.

While polymer blending has proven effective at producing impact-modified PLA, achieving compatibilization between PLA and an immiscible rubbery phase has proven challenging, which usually results in phase separation upon blending due to unfavorable chemical interactions between the polymer constituents (i.e., repulsive forces).[55] To alleviate the unfavorable interactions and increase compatibility between the phases, suitable graft copolymers can be synthesized prior to blending (often lactide groups grafted onto a compatibilizer), or graft copolymers can be formed *in situ* during blending (known as reactive compatibilization).[13]

An example of the former is provided in Scheme 2.2, wherein Mauck *et al.* grafted lactide units onto an acrylated epoxidized soybean oil (AESO) derivative before blending with PLA.[56] The AESO's dual functionality serves two separate purposes. The lactide functionalized AESO contained hydroxyl groups which could aid in compatibilization with PLA while the highly reactive acrylate groups could react at elevated temperatures to generate a cross-linked polymer network. The resulting PLA-ASEO blends demonstrated increased elongation at break values (roughly 10-fold) over neat PLA, while SEM images indicated relatively fine blend morphology (droplet sizes ~1.5 μm). The authors concluded that the enhanced material properties were a result of transesterification reactions which occurred between AESO and PLA, as well as cross-linking occurring between AESO molecules.

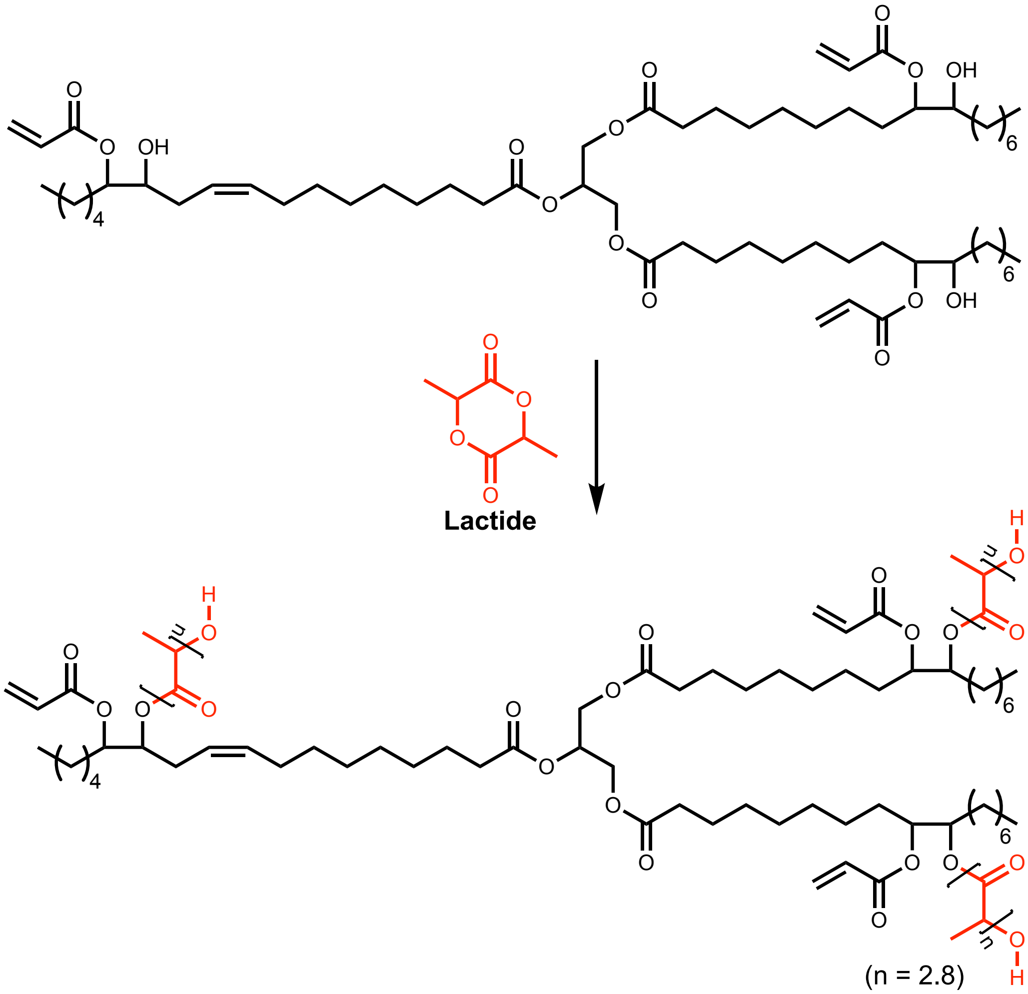

Scheme 2.2. Lactide grafted (average of 2.8 lactide units per arm) acrylated epoxidized soybean oil by Mauck *et al.* (redrawn).[56]

Alternatively, reactive compatibilization can be leveraged to form graft copolymers *in situ* during the blending process. One limitation of this approach is the need to first pre-functionalize the rubber toughening agent with reactive groups such as epoxides, anhydrides, or acids,[57] which can react with the acid and/or hydroxyl end-groups on PLA. Secondly, achieving adequate reactivity between the functional groups in the short period of time (usually <10 mins) during blending often requires the use of an external metal-based catalyst, or by raising the blending temperature to above 220 °C which degrades the PLA.[13] Despite these limitations, reactive compatibilization remains the most widely used strategy to produce impact modified PLA owing to its scalability, low cost, and overall rubustness.[13, 53, 58]

An example of this is shown in Scheme 2.3, wherein Thurber *et al.* blended the commercially available epoxy-functionalized poly(ethylene) with PLA in the presence of a cobalt octoate ($Co(Oct)_2$) catalyst to promote graft copolymer formation *in situ*.[59] In relation to the non-catalyzed blends, the blends produced with $CoOct_2$ showed a 2-fold increase in elongation at break and tensile toughness (taken as the area under the stress-strain curve), coupled with a much finer phase morphology. Moreover, by monitoring the reaction process through torque measurements in the mixer, a rapid increase in torque was observed upon the addition of the cobalt catalyst, whereas no increase was observed in the non-catalyzed blends. In general, an increase in torque during mixing is indicative of a chemical reaction occurring (either cross-linking or graft copolymer formation) as the newly formed species will have a higher viscosity.[59] Overall, this work demonstrated the efficiency of cobalt-mediated catalysis to promote reactive compatibilization between two immiscible phases. While effective, one shortcoming of this example (as well as many others in the literature)[13] is its reliance on the petroleum-derived poly(ethylene) as a compatibilization agent. Additionally, the use of the cobalt catalyst which remains a part of the final blend is problematic as $Co(Oct)_2$ has been shown to be extremely toxic to aquatic life, and can cause fertility issues in humans.[60] Therefore, a rubber toughening strategy which relies on the use of renewably-sourced building blocks to achieve reactive compatibilization in the absence of toxic external catalysts would be of great interest.

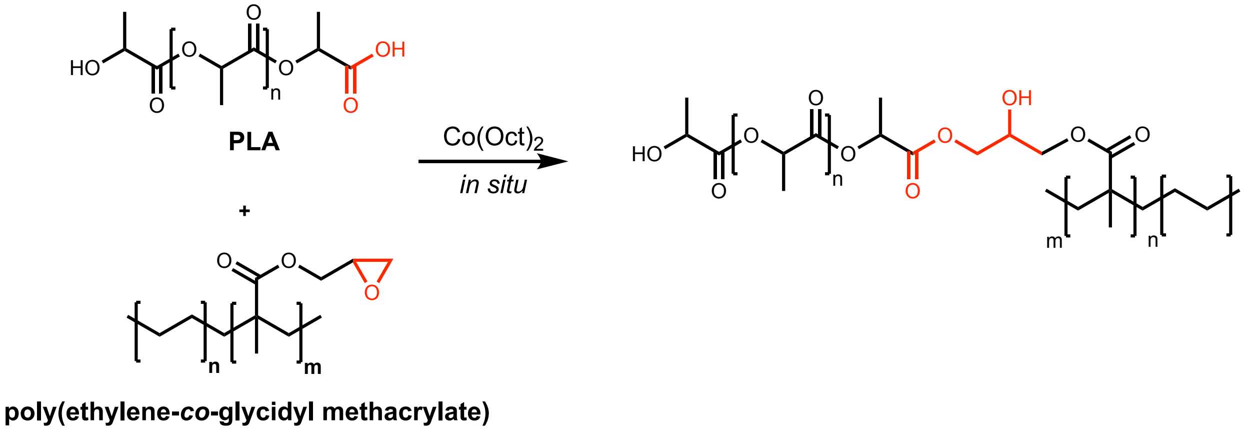

Scheme 2.3. Cobalt-mediated epoxide ring opening leading to graft copolymer formation by Thurber *et al.* (redrawn)[59]

2.2.2.1 Renewably Sourced Rubber Toughening Agents

To preserve the sustainable nature of PLA, many research groups have turned their focus towards the development of renewable rubber toughening agents for PLA. Several different renewable resources have been exploited including biomass derived polyesters, natural rubbers, bio-elastomers, functionalized plant oils, and microbially produced polyesters.[61] Given the diverse scope of chemical structures which have been explored as renewable toughening agents for PLA, multiple techniques have been employed to achieve compatibilization, with some being more successful than others.[61]

As a naturally occurring extract obtained from a variety of plant sources, natural rubber (cis-1,4-poly(isoprene)) has been used in a number of applications throughout history owing to its abundance, high stretch ratio, and elastomeric properties.[62] Additionally, the alkene group on the polymer backbone serves as a potential site for further functionalization. Owing to these favorable properties, it has been explored as a potential rubber toughening agent for PLA. For example, Chen *et al.* investigated the use of natural rubber (NR) in conjunction with its epoxidized derivative (ENR) in blends with PLA (Figure 2.7).[63, 64] As expected, blends produced with NR demonstrated phase separation and no improvement in impact strength in relation to neat PLA.[63] However, upon the addition of the radical initiator dicumyl peroxide (DCP), cross-linking reactions occurred in the melt to aid in compatibilization. This resulted in a highly cross-linked blend with an impressive 21-fold increase in impact strength over neat PLA.

Natural rubber (NR)
(cis-1,4-poly(isoprene))

Epoxidized natural
rubber (ENR)

Figure 2.7. Chemical structures of natural rubber and epoxidized natural rubber used as toughening agents for PLA.

As a follow-up to this work, Chen *et al.* went on to evaluate ENR as a toughening agent in blends with PLA.[64] The epoxy groups were predicted to aid in compatibilization between the rubber phase and PLA, while also providing a site for potential reactivity with the acid/hydroxyl end-groups on PLA. In the presence of DCP, the ENR/PLA blends underwent both cross-linking and transesterification reactions to produce toughened blends which exhibited a 15-fold increase in impact strength over neat PLA.

Taken together, these collective examples reported by Chen demonstrate the potential of unsaturated rubbery elastomers to function as rubber toughening agents for PLA while also demonstrating an alternative reactive compatibilization strategy which relies on the use of a radical initiator. Nonetheless, the requirement for an external catalyst (albeit in low quantities) to obtain reactivity is not ideal and leaves room for further improvement in this area.

In summary, the examples discussed above highlight recent advancements in the development of renewably sourced additives for PVC and PLA blends while also drawing attention to existing deficiencies and limitations in this area. In this context, the work reported in this thesis aims to target these deficiencies while illustrating the potential of renewably sourced building blocks in the design of chemical additives for PVC and PLA.

3 Small molecule plasticizers for improved migration resistance: Investigation of branching and leaching behaviour in PVC blends

Matthew W. Halloran,[1] Jim A. Nicell,[2] Richard L. Leask,[1] Milan Marić*[1]

[1]Department of Chemical Engineering, McGill University, 3610 University Street, Montréal, QC, Canada, H3A 0C5
[2]Department of Civil Engineering, McGill University, 817 Sherbrooke Street West, Montreal, Quebec, Canada, H3A 0C3

*corresponding author:

3.1 Preface

The following manuscript was published in 2021 in the journal *Materials Today Communications*. As discussed in Chapter 2, plasticizer leaching poses significant environmental and health concerns which has resulted in the prohibition of the use of several phthalate ester plasticizers in commercial products. To address the important issue of leaching and to mitigate such concerns, a fundamental understanding of the relationship between plasticizer molecular structure and its permanence in PVC blends is needed.

In this work, a family of plasticizers was synthesized, and each were evaluated for their plasticization efficiency as well as permanence in blends with PVC. The main objective of this work was to study the relationship between branching in small molecule plasticizers and their degree of migration into hexanes and vegetable oil to mimic the grease-prone environments in which plasticized PVC encounters, such as human skin or food items. While previous studies have investigated this relationship using polymeric plasticizers, sufficient data for small molecule plasticizers was lacking. Furthermore, in order to evaluate leaching, a method based on ^{1}H NMR spectroscopy was developed and tested for its ability to accurately monitor and quantify plasticizer leaching. Overall, the goal was to establish a relationship between the number of branches present in the molecule and its permanence in the blend.

3.2 Abstract

The influence of branching on plasticizer effectiveness and migration behavior of heptyl-succinate plasticizers blended with poly(vinyl chloride) (PVC) was evaluated. An increase of branching led to a decrease in migration of the plasticizers into both hexanes and vegetable oil medias. Additionally, a quantitative ^{1}H-NMR method was used to identify plasticizer concentration in the leachates and compared to a gravimetric standard test method. Overall, the quantitative ^{1}H-NMR method proved to be a more direct method to assess leaching. In comparison to commercial plasticizer di(2-ethylhexyl) phthalate (DEHP) and alternative plasticizer diheptyl succinate (DHPS), all of the branched species displayed superior migration resistance into hexanes (two to ten-fold). The glass transition temperatures and stress at break data indicated that the plasticizers comprised of up to three branches functioned as well as, or better than DEHP and DHPS. However, there was a decrease in plasticizer efficiency with compounds comprised of four or more branches.

3.3 Introduction

External plasticizers are chemical additives that are blended with polymers to decrease their glass transition temperature (T_g) as well as improve flexibility, ductility and processing characteristics.[1-3] Approximately 90% of all plasticizers produced are used in blends with poly(vinyl chloride) (PVC) [4] to generate a wide range of commercial products including medical tubing, construction, packaging materials, and films.[5] They constitute a class of non-volatile organic molecules comprised of a broad range of molecular weights which are added in concentrations of up to 40% by weight to PVC.[6] In 2018 alone, nearly 7.7 million metric tonnes of plasticizer were produced industrially to plasticize PVC, with phthalate diesters accounting for approximately two-thirds of this production.[4] Within this family of phthalates, 3.24 million metric tonnes of di(2-ethylhexyl) phthalate (DEHP) were produced for use in blends with PVC, making DEHP the most widely produced industrial plasticizer.[4]

Given that external plasticizers are not covalently bound to the PVC backbone, their migration and leaching out of the blend is unavoidable over time, resulting in widespread contamination and accumulation in the environment.[7-10] In particular, DEHP and its metabolites have been detected in a variety of samples including landfill runoff,[11] food products,[12] bottled water,[13] marine life, [14] and human blood samples.[15, 16] In addition to the ubiquitous presence of DEHP in the environment which is problematic in itself, the initial microbial hydrolysis of this plasticizer yields two stable metabolites, mono(2-ethylhexyl) phthalate (MEHP) and 2-ethylhexanoic acid,[17] which have been shown to be toxic.[9, 18-24] These findings have resulted in the regulation of DEHP and structurally similar phthalates in a variety of consumer items in many developed nations including the United States, the European Union, and Canada.[25-27] Ultimately, the growing implementation of such regulations that are designed to protect human and ecosystem health have created an urgent need for the development and production of alternative, safer, non-toxic plasticizers with permanence in the polymer blend.

While leaching poses significant environmental concerns, the diffusion and loss of plasticizer also leads to a degradation of the mechanical properties of PVC products, resulting in a stiffer and more brittle polymer.[28] In line with this, significant efforts have been made to address the issue of plasticizer leaching which has ultimately led to the development of a number of proposed alternative strategies including internal plasticization (i.e., forming a covalent bond between plasticizer and PVC),[29] the use of polymeric or oligomeric plasticizers,[30] plasma surface coating of plasticized PVC, [31] and incorporation of ionic liquids and nanoparticles.[32] While many of these strategies have been proven to prevent or diminish the rate of plasticizer leaching, the widespread utilization and industrial implementation of these methods is plagued by their complexity and high cost of production.[33] Additionally, having the ability to blend native PVC with external plasticizers at varying concentrations tailored for specific uses renders this approach the most economically and industrially feasible.

The design of branched and hyper-branched plasticizers for reduced leaching rates has previously been investigated by several groups;[34-36] however, these reports were centered upon high molecular weight oligomeric and polymeric plasticizers. While these studies are significant to the field, there is a lack of information regarding the relationship of branching and leaching within small molecule plasticizers. In response to this, in this work, we developed a novel series of small molecule heptyl-succinate branched compounds (see Figure 3.1a) and evaluated their plasticization efficiency in conjunction with their leaching behaviour. Plasticization efficiency of each candidate was assessed using tensile testing, surface hardness measurements, differential scanning calorimetry (DSC), and thermal gravimetric analysis (TGA) to characterize mechanical and thermal properties, while leaching tests were conducted in hexanes and vegetable oil media and then analyzed using a quantitative ^{1}H NMR technique.[37] As a direct comparison of performance, each analysis was conducted in parallel with the commercial plasticizer, DEHP, and a promising replacement plasticizer, diheptyl succinate (DHPS) (see Figure 3.1b).[38] In conjunction with exploring the structural relationship between branching and leaching within small molecule plasticizers, a further aim of this work was to establish the use of quantitative ^{1}H NMR as a reliable tool to assess plasticizer leaching.

(a) Novel analogs investigated in this study

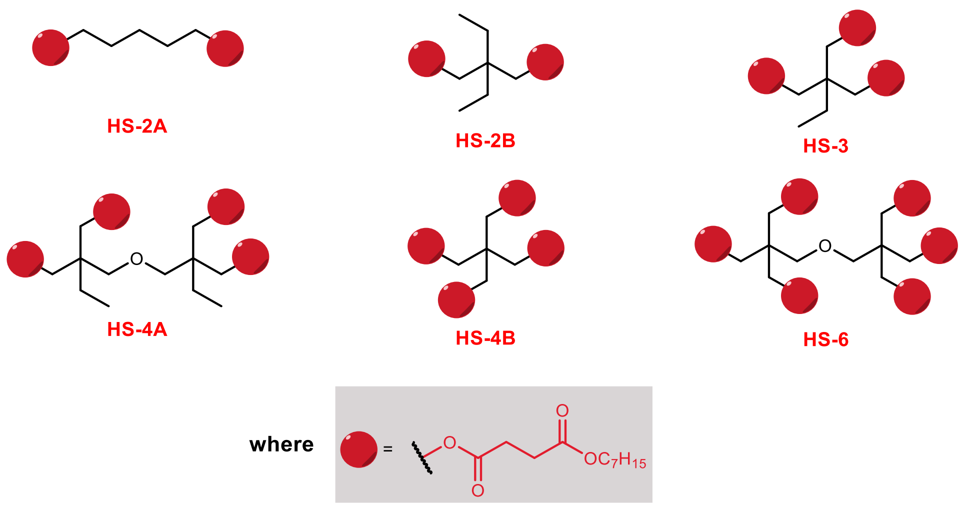

(b) Control Compounds

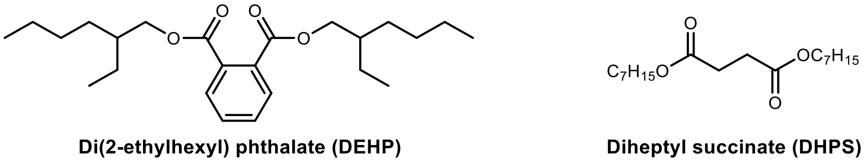

Figure 3.1. Compounds investigated in this study: (a) Novel heptyl-succinate branched analogs investigated in the study (Red ball represents a heptyl succinate arm); (b) Current industrial standard DEHP and alternative plasticizer DHPS (diheptyl succinate).

3.4 Methods and Materials

3.4.1 Materials and Reagents

Unplasticized PVC (UPVC; K50) was supplied by Solvay Benvic (Chevigny, France). n-heptanol (99.9%) that was made from renewable feedstocks was purchased from Arkema (King of Prussia, PA). Sulfuric acid (98%), stearic acid (97%), hexanes, toluene, and benzene were purchased from Fisher Scientific (Montreal, QC) and epoxidized soybean oil from Galata Chemicals (Southbury, CT). 1,3,5-trimethoxylbenzene (99%), DEHP (99%), 1,5-pentanediol (97%), trimethylolpropane (97%), pentaerythritol (98%), succinic anhydride (99%) dipentaerythritol (technical grade), and 2,2-diethyl-1,3-propanediol (99%) were purchased from Millipore Sigma (Oakville, ON). No name® 100% pure vegetable oil was purchased from a local grocery store (Montreal, QC).

3.4.2 Synthesis of Plasticizers

DHPS was synthesized according to the procedure previously reported.[38] Each of the six branched structures were synthesized according to the two-step sequences described below. The ^{1}H NMR spectra and characterization data are provided in Appendix A.

3.4.2.1 Synthesis of monoheptyl succinate

In a 1 L round bottomed flask, succinic anhydride (100.0 g, 0.99 mol, 1 equiv.) and *n*-heptanol (141.3 mL, 0.99 mol, 1 equiv.) were dissolved in toluene (300 mL) and refluxed for 6 hours. The reaction mixture was then cooled to room temperature, and the toluene was removed under reduced pressure to afford monoheptyl succinate (210.5g, 0.97 mol) as a pale-yellow oil in a 98% yield which was used without further purification.

3.4.2.2 Conditions I: Synthesis of HS-2A, HS-2B, HS-3, HS-4A

Monoheptyl succinate (1.05 equiv. for each hydroxyl group w.r.t polyol) was mixed with the appropriate polyol (1 equiv.) in the presence of sulfuric acid (0.15 equiv.) in a 500 mL round bottomed flask and refluxed in benzene using a Dean-Stark apparatus for 4 hours. The reaction mixture was cooled to room temperature and benzene was removed under reduced pressure to afford the compounds as oils which were used without further purification. Each compound was named according to the number of heptyl succinate arms it contained, where HS represents heptyl succinate, and the number corresponds to the number of branches.

3.4.2.3 Conditions II: Synthesis of HS-4B, HS-6

Monoheptyl succinate (1.05 equiv. for each hydroxyl group w.r.t polyol) was mixed with the appropriate polyol (1 equiv.) in the presence of sulfuric acid (0.15 equiv.) in a three-necked 500 mL round bottomed flask under a stream of N_2 gas for 3 hours at 125 °C. The reaction mixture was then cooled to room temperature, dissolved in dichloromethane (50 mL), filtered, and then concentrated under reduced pressure to afford the desired compounds as light-yellow oils which were used without further purification.

3.4.3 Extrusion of PVC/plasticizer blends

In accordance with methods previously described,[39] blends at plasticizer concentrations of 28.6 wt% (40 parts per hundred rubber, phr) were prepared through a two-step extrusion process using a Haake Minilab conical intermeshing twin-screw extruder (Thermo Electron Corporation, Beverly, MA). In the first step, blends containing 20 phr of plasticizers were prepared in 3 g batches containing 20 phr plasticizer, 4 phr epoxidized soybean oil (heat stabilizer), and 5 phr stearic acid (lubricant). The batches were fed into the extruder and the extrudate was manually cut into small pieces. Each extruded batch was subsequently recycled through the extruder a second time to facilitate adequate mixing. In the second step, an additional 20 phr of the plasticizer was added and the material was passed through the extruder twice. The extruder was operated at 130 °C with a screw speed of 30 rpm throughout.

3.4.4 Production of tensile bars and leaching disks

In accordance with methods previously described [39], tensile test bars and circular disks for leaching tests were produced using a heated manual hydraulic press (press: Carver, Wabash, IN; temperature controllers: Watlow, St. Louis, MO) and steel molds. The 40 phr blends were placed into the molds and pressed at 165 °C in the following manner: 5 minutes at 5 metric tonnes, 10 minutes at 10 metric tonnes, 30 minutes at 15 metric tonnes. Tensile test bar dimensions adhered to the standardized testing protocol ASTM-D638 for tensile properties: thickness (T_0), 1.4 mm;

width of narrow section (W_0), 3.3 mm; length of narrow section, 17.8 mm; overall length 64 mm; overall width, 10 mm. Leaching disk dimensions: radius 12.5 mm; thickness, 1 mm.

3.4.5 Thermal Gravimetric Analysis (TGA)

The thermal stability of the plasticized PVC blends was evaluated using a TA Instruments Q500 (New Castle, DE) under nitrogen flow of 90 mL/min from 25 to 600 °C at a heating rate of 10 °C/min. The onset temperature at weight loss with 5% is reported in Appendix A (Table A1) for comparison purposes.

3.4.6 Differential Scanning Calorimetry (DSC)

The glass transition temperature, T_g, of each blend at 40 phr was measured by temperature-modulated differential scanning calorimetry (mDSC) using a TA Instruments Q2000 (New Castle, DE). Two heating cycles from -90 to 100 °C superimposed by a sinusoidal modulation of 1.27 °C with a period of 60 s were carried out. The T_g was then determined from the reversible heat flow of the second heating cycle using the automated glass/step transition tool in the TA Instruments Universal Analysis 2000 software.

3.4.7 Hardness Testing

The surface hardness of the 40 phr plasticized PVC blends was evaluated using a micro-indenter (Nanovea PB1000 with Nano module, stainless steel ball tip of 1 mm diameter) in accordance with a previously described method [39]. The measurements were collected at room temperature and repeated three times on each test disk at three different locations on the disk. After the indenter had reached its zero point, it built up a contact load of 0.3 mN and then the tip was forced into the sample at a rate of 30 mN/min until a load of 20 mN was reached. The tip was then removed at the rate of 30 mN/min. Indentation depth was recorded automatically with the software (Nanovea Nano Hardness Tester). A Matlab® program was then used to calculate the surface hardness. Briefly, a stiffness term was derived from the slope of the first third of the unloading curve, in addition to the estimated contact area and indentation depth. The result is then expressed in units of MPa.

3.4.8 Tensile Testing

Testing was performed using a Shimadzu Easy Test instrument (Kyoto, Japan) equipped with a 500 N load cell in accordance with a previously developed protocol.[38] Each specimen was desiccated for at least 48 hours at room temperature prior to analysis. The dimensions of each test specimen were recorded using a digital micrometer. Test bars were clamped and subjected to a strain rate of 5 mm/min. The stress-strain curves were used to obtain values for strain (% elongation) and stress at break.

3.4.9 Leaching

The American Society for Testing and Materials (ASTM) Method D1239-14, "Resistance of Plastic Films to Extraction by Chemicals" was used as a template. As was previously reported,[40] the weight loss method for quantification, which is an indirect measure of leaching, can be problematic as PVC blends can suffer from swelling when exposed to certain media. Therefore, we avoided this issue entirely by directly measuring leaching by performing a quantitative analysis of the leachates using ^{1}H-NMR [37]. All test specimens were desiccated at room temperature for at least 48 hours and weights were measured prior to leaching tests. Leaching into hexanes was performed at 50 °C for 4 hours. Leaching into vegetable oil was performed at 40 °C for durations of two and four weeks. These durations and temperatures were selected to allow for adequate amounts of plasticizer to be detected using ^{1}H-NMR as well as compare their relative percentage of leaching over time.

For each sample, two PVC disks of known weight containing 40 phr plasticizer were suspended in a 250-mL wide-mouth Erlenmeyer flask using an aluminum wire containing 200 mL of media. The flask was plugged with a rubber stopper, wrapped in Parafilm® and placed in a shaker at 100 RPM for the time periods and temperatures mentioned above. Each experiment was run in triplicate. At the end of the time periods, the disks were removed from the flasks, rinsed with 70% ethanol, dried with a Kim Wipe towel and weighed. Leachates were retained for further analysis.

3.4.10 ^{1}H NMR analysis of leachates

Treatment of leachates varied between media types. For hexanes, the leachate was transferred into a 500-mL round-bottom flask and concentrated under reduced pressure. The concentrated leachate was then dissolved by the addition of 2 mL of an internal standard solution of 1,3,5-trimethoxylbenzene (10 mg/mL) in deuterated chloroform ($CDCl_3$) which was subsequently analyzed using ^{1}H-NMR. For vegetable oil, the leachate was transferred to a separatory funnel and extracted with methanol (50 mL × 3). The methanol extracts were combined in a 250-mL round-bottom flask and concentrated under reduced pressure. The leachate was then dissolved by the addition of 3 mL of an internal standard solution of 1,3,5-trimethoxylbenzene (5 mg/mL) and analyzed in the same manner as described above.

The plasticizer concentration in the leachates was calculated by comparing the integral values of the internal standard (1,3,5-trimethoxybenzene), with that of each plasticizer using Equation (i):

$$C_x = \frac{I_x}{I_{cal}} \cdot \frac{N_{cal}}{N_x} \cdot C_{cal} \qquad \text{(i)}$$

where C_x is the concentration of the plasticizer in the leachate; I_x is the integral value of the plasticizer peak; I_{cal} is the integral value of the internal standard peak; N_{cal} is the number of protons represented by internal standard peak; N_x is the number of protons represented by the plasticizer peak; and C_{cal} is the concentration of the internal standard.

3.4.11 ^{1}H NMR Spectroscopy

^{1}H-NMR spectra were collected using a Bruker AVIIIHD 500 MHz spectrometer (MA, USA) with an average of 16 scans using deuterated chloroform ($CDCl_3$) as the solvent. Multiplicities are reported using the following abbreviations: s = singlet; d = doublet; t = triplet; q = quartet; m = multiplet (range of multiplet is given).

3.4.12 Statistics

Statistical analysis was performed with GraphPad Prism 5 software. Difference between the mean values of the plasticizer types were analyzed by one-way-ANOVA test with a Bonferroni post-test to evaluate differences between each type. A p value less than 0.05 was interpreted as significant.

3.5 Results

3.5.1 Synthesis of Plasticizers

This study explored the effect of molecular weight and branching on permanence of a series of succinate plasticizers in PVC blends. As we have previously investigated the efficacy of a linear diheptyl succinate (DHPS) as a bio-sourced renewable alternative to conventional petroleum-derived plasticizers,[38] we aimed to expand upon this by using DHPS as a platform molecule during the design of our branched analogs. In line with this, a series of analogs with 2 to 6 heptyl succinate arms were synthesized using commercially available polyols, and monoheptyl succinate (Scheme 3.1). Briefly, succinic anhydride and *n*-heptanol were reacted at elevated temperatures in toluene to afford monoheptyl succinate (MHPS). MHPS was then reacted with a variety of polyols in the presence of catalytic amounts of sulfuric acid in benzene to provide the desired branched analogs (Scheme 3.1, Conditions I). To overcome the poor solubility of pentaerythritol and dipentaerythritol in organic solvents, modified conditions from Elsiwi *et al.*[38] were used which employed the use of a solvent-free esterification at elevated temperatures (Scheme 3.1, Conditions II). Each analog was then characterized with ^{1}H NMR.

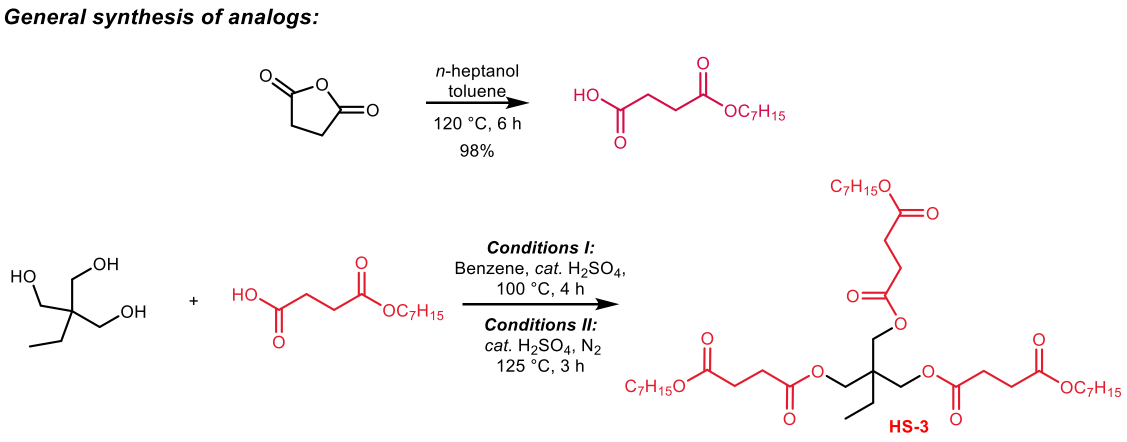

Scheme 3.1. General sequence for the synthesis of heptyl-succinate branched analogs. Conditions I were used to synthesize **HS-2A**, **HS-2B**, **HS-3**, and **HS-4A**, while Conditions II were adapted for the synthesis of **HS-4B** and **HS-6**. Each compound was named according to the number of heptyl succinate arms it contained, where HS represents heptyl succinate, and the number corresponds to the number of branches.

3.6 Plasticizer Efficiency

3.6.1 Glass Transition Temperature

To evaluate the series of branched compounds for their ability to function as plasticizers, they were extruded at a concentration of 40 phr to produce blends which were subjected to thermal and mechanical testing. As can be seen in Table 3.1, each of the compounds showed a significant reduction in T_g relative to neat PVC (~ 80 °C),[3] which indicated their ability to function as plasticizers. It was found that the linear two-armed **HS-2A** produced the largest decrease in T_g, while the branched **HS-2B** and **HS-3** had a T_g comparable to that of DEHP. In general, as the molecular weight and number of succinate-arms increased, the reduction in T_g was less pronounced, indicating decreased plasticization efficiency.

Table 3.1. Mechanical and thermal properties of PVC/plasticizer blends at 40 phr. Averages and standard deviations are reported for $n = 3$ specimens. Refer to Figure 1 for plasticizer structures.

Plasticizer	**# Arms**	**Strain at break (%EL)[a]**	**Stress at break (MPa)[a]**	**T_g (°C)**	**Surface hardness (MPa)**
[b]DEHP	0	96 ± 4	11.8 ± 0.1	-7.3	0.83 ± 0.05
[c]DHPS	0	93 ± 7	5.5 ± 0.4	-23.2	0.63 ± 0.03
HS-2A	2	145 ± 2	16.5 ± 0.1	-24.2	0.68 ± 0.06
HS-2B	2	88 ± 7	7.0 ± 0.9	-7.6	0.89 ± 0.13
HS-3	3	100 ± 7	9.7 ± 1.5	-6.5	0.98 ± 0.11
HS-4A	4	93 ± 15	11.3 ± 1.0	8.9	1.00 ± 0.09
HS-4B	4	40 ± 13	7.9 ± 0.8	12.1	1.08 ± 0.20
HS-6	6	5 ± 0.1	12.0 ± 0.5	13.1	1.23 ± 0.06

[a] $n = 3$, [b] data taken from [39], [c] data taken from [38]

3.6.2 Tensile Strength

The tensile data, including strain at break and stress at break, is presented in Table 3.1 and Figures 3.2a and 3.2b, respectively. A significant difference was observed in the strain at break amongst the compounds tested ($p < 0.001$, one-way ANOVA). The tensile testing results indicated that **HS-2B**, **HS-3**, and **HS-4A** showed statistically equivalent strain at break values to both DEHP and DHPS ($p > 0.05$, Bonferroni post-test), while compounds **HS-4B** and **HS-6** displayed significantly lower values ($p < 0.001$, Bonferroni post-test). Interestingly, despite the structural similarities amongst **HS-2A** and **HS-2B**, **HS-2A** exhibited a significantly higher strain at break value of 145 ± 2 compared to 88 ± 2 for **HS-2B** ($p < 0.001$, Bonferroni post-test). These results suggest that within this subset of compounds, as the number of arms increases above four, a sharp decline in elongation is observed.

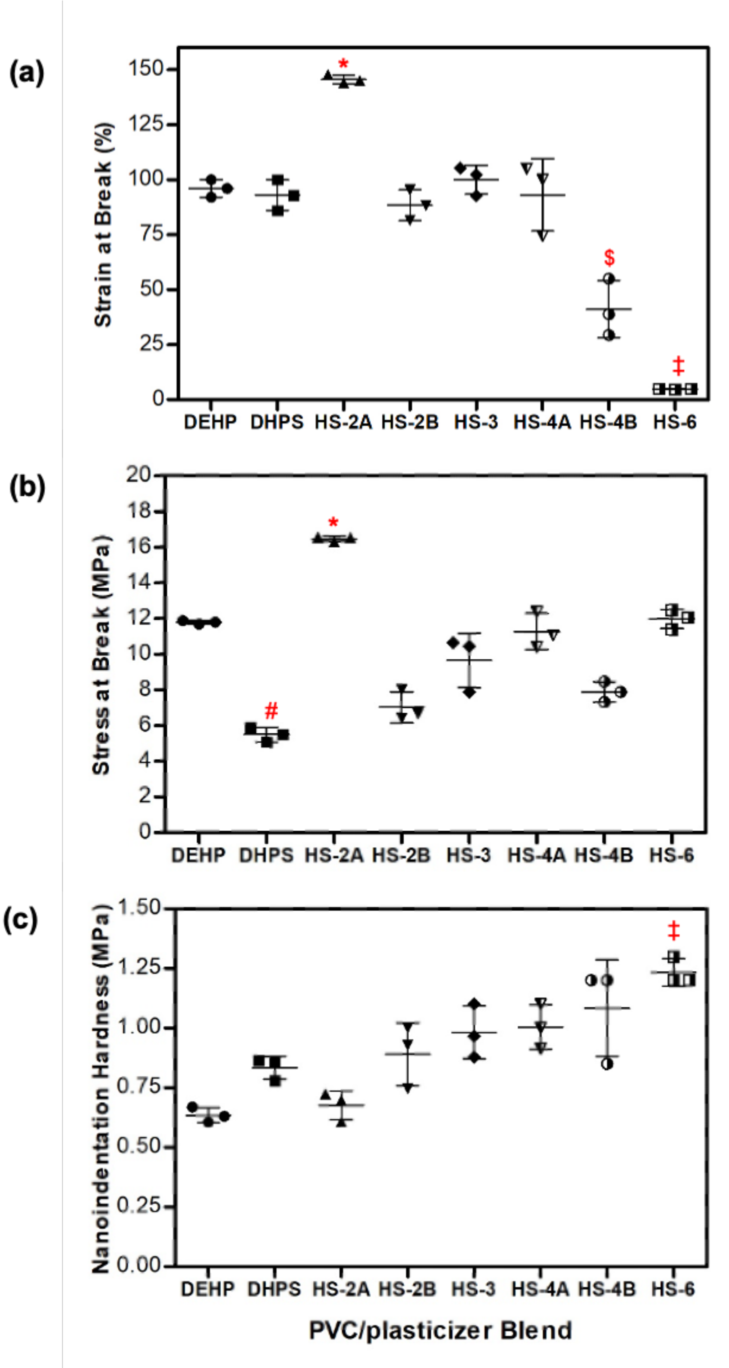

Figure 3.2. (a) Strain at break and stress at break (b) for PVC/plasticizer blends at 40 phr. (c) Surface hardness (in MPa) for PVC/plasticizer blends at 40 phr. Error bars represent one standard deviation with mean shown ($n = 3$ replicates). Refer to Figure 1 for plasticizer structures. Symbols above error bars indicate statistically significant differences ($p < 0.001$, Bonferroni post-test). (a) **HS-2A** (*), **HS-4B** ($), **HS-6** (‡) statistically significantly different than all other plasticizers; (b) DHPS (#) statistically significantly different than all except **HS-2B** and **HS-4B**; (c) **HS-6** (‡) statistically significantly different than DEHP and **HS-2A.**

A significant difference was observed in the stress at break amongst all of the compounds tested ($p < 0.001$, one-way ANOVA); however, there was no observable trend relating to their molecular structures. There was no significant difference between compounds **HS-3**, **HS-4A**, **HS-6** with respect to DEHP ($p > 0.05$, Bonferroni post-test), whereas **HS-2A** displayed a significantly higher stress at break of 16.5 ± 0.1 ($p < 0.001$, Bonferroni post-test).

3.6.3 Surface hardness by Nano-indentation

The results obtained for the surface hardness measurements of the plasticized blends are presented in Figure 3.2c and Table 3.1. There was a significant difference in the surface hardness amongst the blends measured ($p < 0.001$, one-way ANOVA). A significant difference between DEHP and the higher branched species **HS-3**, **HS-4A**, **HS-4B**, and **HS-6** was observed ($p < 0.05$, Bonferroni post-test). This difference was also observed between the linear **HS-2A** and the branched **HS-3**, **HS-4A, HS-4B**, and **HS-6** ($p < 0.05$, Bonferroni post-test). However, no significant differences in the surface hardness were observed between the plasticizers containing three or more branches ($p > 0.05$, Bonferroni post-test).

3.7 Plasticizer Leaching

Initial leaching tests were conducted under accelerated conditions in hexanes at 50 °C for 4 hours in accordance with a modified version of the ASTM standard. Initial masses taken of the PVC/plasticizer disks following the leaching experiments showed weight gains in all of the disks, except for DHPS (Table A2, Appendix A). This weight gain was not unexpected and was attributed to absorption of the hexanes into the PVC matrix leading to swelling. Therefore, each concentrated leachate sample was spiked with an internal standard of known concentration which was then used to directly quantify plasticizer concentration with ^{1}H NMR. The results for the series of compounds, DHPS, and DEHP are shown in Figure 3.3a and summarized in Table 3.2. The percent plasticizer leached out of the disks was then calculated based on the mass of plasticizer present in the 40 phr disks. The accuracy of this quantitative approach is demonstrated as the results were reproducible with small calculated standard deviations amongst the triplicate experiments. There was a significant difference in the net leaching amongst the blends measured ($p < 0.001$, one-way ANOVA). Additionally, a significant difference between both DEHP and DHPS and all of the branched heptyl-succinate species was observed ($p < 0.001$, Bonferroni post-test). Within the series of candidate plasticizers, a difference between the linear **HS-2A** and the other branched compounds was also observed ($p < 0.001$, Bonferroni post-test). The relationship between molecular weight and percent of plasticizer leaching into hexanes is shown in Figure 3.3b. A clear trend was observed in which the higher molecular weight plasticizers exhibited the lowest net leaching overall.

Table 3.2. ^{1}H NMR analysis data for leaching into hexanes.

Plasticizer	MW (g/mol)	# Arms	% Plasticizer Leached[a]
DEHP	390.56	-	9.3 ± 0.60
DHPS	314.47	-	20.8 ± 0.80
HS-2A	500.67	2	5.9 ± 0.20
HS-2B	528.73	2	3.9 ± 0.30
HS-3	728.96	3	3.1 ± 0.10
HS-4A	1043.38	4	2.4 ± 0.10
HS-4B	929.20	4	2.7 ± 0.40
HS-6	1443.85	6	2.1 ± 0.30

[a] Errors represent one standard deviation (n = 3 repeats were performed in each case).

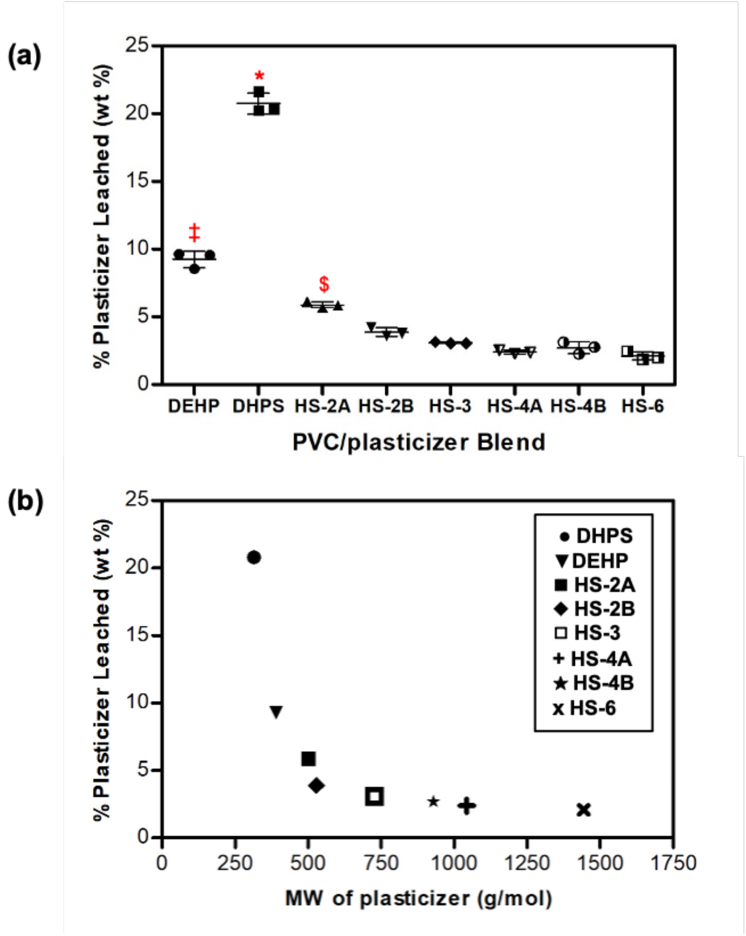

Figure 3.3. (a) Percent of plasticizer leaching into hexanes for four hours at 50 °C detected using quantitative ^{1}H-NMR. Error bars represent one standard deviation with mean shown (n = 3 replicates). Refer to Figure 1 for plasticizer structures. Symbols above error bars indicate statistically significant differences. DEHP (‡), DHPS (*), and **HS-2A** ($) statistically significantly different ($p < 0.001$, Bonferroni post-test) than all other plasticizers. (b) Percent of plasticizer leaching into hexanes versus molecular weight (MW) of the plasticizer.

To further explore the migration behaviour of this family of compounds, additional leaching tests were conducted in vegetable oil at durations of two- and four-weeks at 40 °C. Vegetable oil was selected to mimic the grease-prone environmental conditions in which plasticized PVC is exposed to when it comes into contact with both food products and human skin. Two time points were chosen in order to study the evolution of leaching over time, while 40 °C was selected to ensure ample quantities of plasticizer were present in the leachate for an accurate analysis. The leaching results for the two- and four-week time points are presented in Figures 3.4a and 3.4b, respectively and summarized in Table 3.3. Over both timepoints, there was a significant difference in the net leaching amongst the blends measured ($p < 0.001$, one-way ANOVA) as well as a similar trend of increased branching and decreased net leaching was observed. A significant difference between DHPS and all of the branched species was observed ($p < 0.001$, Bonferroni post-test), as well as between the linear **HS-2A** and the higher branched compounds ($p < 0.001$, Bonferroni post-test) over both durations. While the overall percentage of plasticizer leached was lower into vegetable oil than into hexanes, an analogous trend was seen, with DHPS displaying the highest percentage over both measurement periods.

Table 3.3. ^{1}H NMR analysis data for leaching into vegetable oil.

Plasticizer	**MW (g/mol)**	**# Arms**	**% Plasticizer leached after**[a]	
			2 weeks	**4 weeks**
DEHP	390.6	-	2.1 ± 0.20	3.0 ± 0.30
DHPS	314.5	-	7.5 ± 0.50	8.3 ± 0.90
HS-2A	500.6	2	2.9 ± 0.20	4.1 ± 0.20
HS-2B	528.7	2	1.5 ± 0.20	1.9 ± 0.40
HS-3	728.9	3	0.80 ± 0.10	1.30 ± 0.03
HS-4A	1043.4	4	0.50 ± 0.01	0.70 ± 0.03
HS-4B	929.2	4	0.60 ± 0.10	0.80 ± 0.03
HS-6	1443.9	6	0.40 ± 0.03	0.50 ± 0.01

[a] Errors represent one standard deviation (n = 3 repeats were performed in each case).

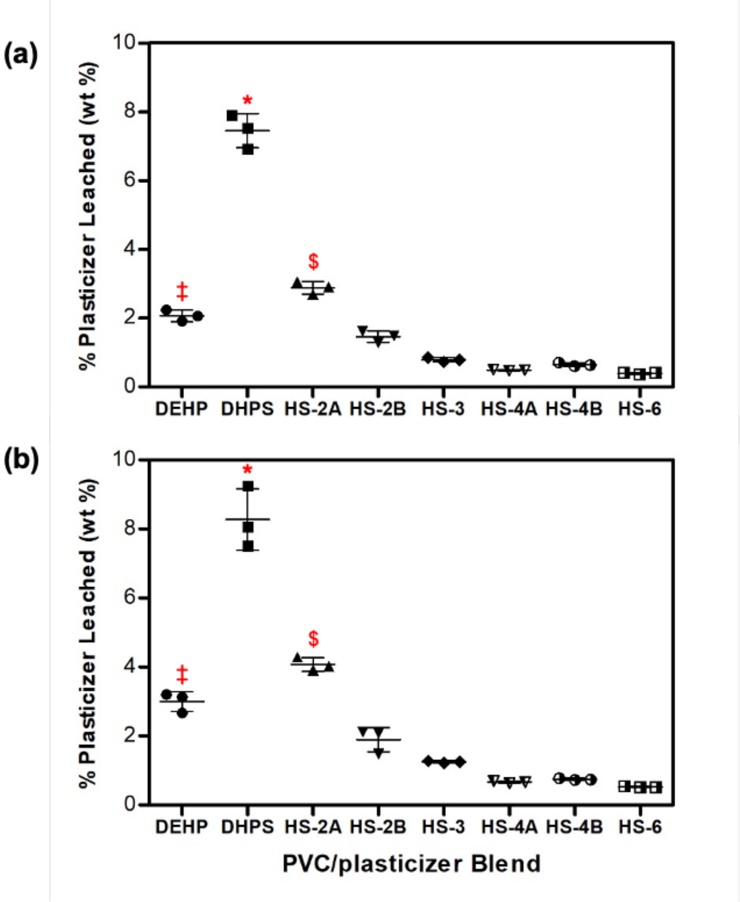

Figure 3.4. Percentage of plasticizer leached into vegetable oil for two weeks (a) and four weeks (b) at 40 °C and detected using quantitative ^{1}H NMR. Error bars represent one standard deviation (n = 3 replicates). Refer to Figure 1 for plasticizer structures. Symbols above error bars indicate statistically significant differences. DHPS (*) statistically significantly different ($p < 0.001$, Bonferroni post-test) than all other plasticizers. DEHP (‡) and **HS-2A** ($) statistically significantly different ($p < 0.001$, Bonferroni post-test) than all other plasticizers (except for **HS-2A** versus DEHP over four weeks).

3.8 Discussion

Despite the societal pressures applied to industry and consumers to transition away from petroleum-derived products and move towards renewably sourced alternatives, the global demand for PVC plasticizers continues to increase. Therefore, until this transition can be fully realized, there remains a need for the development of non-toxic replacement plasticizers for PVC. However, for a newly developed alternative to be deemed a viable replacement for phthalates, it must function as effectively, or more effectively to plasticize PVC. In addition, leaching behaviour and biodegradability should be taken into consideration. As a result of this, the search for a viable replacement is one that is currently ongoing.

In the present study, a class of heptyl-succinate plasticizers was developed and tested using a series of commercially available polyols to investigate the overall effect of branching on plasticization efficiency and permanence in the blend. Each compound was extruded with PVC at 40 phr alongside DEHP and DHPS for comparison purposes and subjected to a series of mechanical and thermal tests to evaluate their effectiveness as plasticizers. It was found that as the number of heptyl-succinate arms increased above four, the stiffness of the blends increased, while the plasticization performance decreased. However, the higher branched plasticizers displayed superior migration resistance to both DEHP and DHPS into hexanes and vegetable oil medias.

3.9 Structural Considerations for Plasticization

From a structural standpoint, there are several key features which govern the effectiveness of a plasticizer. For a plasticizer to be compatible with PVC as well as impart flexibility into the blend, it must consist of both polar, and non-polar moieties.[41] The polar components are necessary to serve as compatibilizers between the plasticizer and the polar PVC chains, while the non-polar components serve to disrupt the PVC chain-chain interactions and increase the free volume of the polymer, thereby imparting flexibility.[41] Typically, the polar moieties consist of ester groups while the non-polar moieties consist of aromatic groups or alkyl chains.[42] However, the development of plasticizers that are compatible with PVC, that can efficiently function to impart flexibility, and that display low levels of leaching out of the blend remains challenging.

Previously, it has been shown that succinate diesters with varying alkyl chain lengths can function effectively as plasticizers, readily biodegrade into innocuous metabolites, and display comparable rates of leaching to DEHP in aqueous media.[38-40, 43] Here, this family of compounds was broadened further through the synthesis of branched heptyl-succinate plasticizers. Within this series of compounds, the plasticization efficiency decreased with increased branching and molecular weight. In particular, compounds **HS-4B** and **HS-6**, which are comprised of four and six heptyl-succinate arms respectively, performed poorly as plasticizers. This was evinced by their low strain at break values, high surface hardness values, and relatively high T_g values when compared to the control compounds (see Table 3.1). This finding proved interesting as it was expected that increasing the number of heptyl-succinate arms would increase the number of chain ends and thereby increase the free volume of the polymer matrix to decrease the T_g of the blend. However, this proved not to be the case within this family of compounds as a deleterious effect was observed when the number of branches/end groups was increased. Whether this loss in efficacy is the result of incompatibility between the higher molecular weight compounds and PVC remains unclear at this time and is a subject that is worthy of future investigation.

3.10 Structural Considerations for Leaching

Despite the fact that the ASTM gravimetric analysis is routinely used as the nearly universal standard to quantify plasticizer leaching, this method can suffer from significant limitations. Foremost, PVC blends are prone to swelling and absorption when exposed to certain types of media, making the subsequent weight-loss quantification challenging.[40] Additionally, the blends are often comprised of multiple additives and stabilizers which are also assumed to participate in leaching but are often left unaccounted for during analysis. Therefore, to bypass these potential constraints, ^{1}H NMR was used to quantify plasticizer concentration in the leachates. While ^{1}H NMR analysis has previously been used to quantify plasticizer concentration in a variety of commercial PVC samples,[44, 45] this report demonstrates its applicability as an analytical screening tool for plasticizer leaching.

Initial leaching experiments were conducted under accelerated conditions in hexanes at 50 °C for a period of four hours, which provided a primary rapid test of our plasticizer candidates and validated our quantitative analysis method. It was found that as the number of heptyl-succinate arms increased from two to six, there was an observable decrease in the leaching percentage from 5.9% to 2.1%, with all analogs displaying lower values than DEHP (9.3%) and DHPS (20.8%). As can be seen in Figure 3.3, DHPS displayed the highest percentage of leaching, two-fold more than DEHP, and between four and tenfold higher than the branched analogs. This result can be rationalized as DHPS is a non-polar, hydrophobic compound with high solubility in hexanes and therefore its tendency to migrate out of the blend and into this media is not unexpected. Additionally, as it is a low molecular weight, non-branched plasticizer, its ability to embed itself into the PVC matrix is lower than its branched counterparts, permitting a faster rate of diffusion out of the blend.

To simulate a more realistic leaching environment for plasticized PVC samples, additional experiments were conducted into vegetable oil media at durations of two and four weeks. Over both durations, an analogous trend was observed in which the analogs displayed lower net leaching as the number of branches increased. Similarly, DHPS displayed the lowest resistance to migration into vegetable oil over both time points. Interestingly, there was a relatively small increase in leaching observed amongst all plasticizers between two and four weeks, suggesting a non-linear relationship between leaching and time within the investigated timeframe.

In addition to the effect of branching, previous studies have reported a strong correlation between increased molecular weight with lower rates of leaching with a series of oligomeric plasticizers.[34, 46] This relationship was further demonstrated in this work as the highest molecular weight species (**HS-4A**, **HS-4B**, **HS-6**) displayed the lowest percentage of leaching in both media types. By increasing the molecular weight as well as the number of branches, the diffusion of the plasticizer out of the blend will occur at a much slower rate as it becomes more entangled within the PVC matrix.

Despite the higher branched analogs **HS-4B** and **HS-6** displaying a higher resistance to leaching in both media types, they did not function effectively as plasticizers as their blends with PVC displayed poor mechanical and thermal properties. It was hypothesized that the decrease in plasticization ability was due to the imbalance between polar and non-polar moieties present in the higher branched species. In general, they contained a higher number of polar ester functional groups than non-polar alkyl chains; rendering them compatible with the polar PVC backbone and resistant to migration but hindering their ability to disrupt the PVC chain-chain interactions and impart flexibility. This highlights the challenge associated with developing replacement plasticizers which are not only compatible with PVC and display a high resistance to leaching but can also impart flexibility to the blend.

3.11 Conclusion

In this work, the relationship between branching and plasticizer effectiveness as well as permanence in the blend within a family of small molecule heptyl-succinate compounds was investigated. Overall, it was found that a higher degree of branching and a higher molecular weight led to a decreased rate of leaching into both hexanes and vegetable oil medias when compared to

DEHP and DHPS. Despite displaying a higher permanence in the blend, the higher branched analogs **HS-4B** and **HS-6** did not perform adequately as plasticizers, as they produced stiffer blends with poor tensile properties and higher T_gs compared to the controls as well as the other branched species. However, the lower branched species proved effective as plasticizers as they produced blends with equal or superior elongation at break and T_g values to DEHP and DHPS and displayed a higher resistance to leaching. This work validates that an increase of branching and molecular weight leads to a decrease in overall migration within small molecule plasticizers as well as establishes the use of ^{1}H NMR spectroscopy to accurately quantify plasticizer concentration in leachates.

3.12 Acknowledgments

This research was funded using grants from the Natural Sciences and Engineering Research Council of Canada (NSERC; Collaborative Research and Development Grants, CRDPJ 543853-2019 and Discovery Grants Program, RGPIN 05948-2019, RGPIN 06161-2018, 2016-03792) and the James McGill Chair program of McGill University. Student support was provided through McGill Engineering Doctoral Awards program of the Faculty of Engineering of McGill University.

3.13 References

1. Bocqué, M.; Voirin, C.; Lapinte, V.; Caillol, S.; Robin, J.-J., Petro-based and bio-based plasticizers: Chemical structures to plasticizing properties. *J. Polym. Sci., Part A-1: Polym. Chem.* **2016,** *54* (1), 11-33.

2. Fischer, I.; Schmitt, W. F.; Porth, H. C.; Allsopp, M. W.; Vianello, G., Poly(vinyl chloride). In *Ullmann's Encyclopedia of Industrial Chemistry*, Wiley-VCH: Weinheim, Germany, 2014

3. Sears, J. K.; Darby, J. R., *The Technology of Plasticizers*. John Wiley New York, NY, USA, 1982.

4. Ceresana, Ceresana's latest report details growth and change for global plasticizers market. *Additives for Polymers* **2019,** (6), 11.

5. Kumar, S., Recent Developments of Biobased Plasticizers and Their Effect on Mechanical and Thermal Properties of Poly(vinyl chloride): A Review. *Ind. Eng. Chem. Res.* **2019,** *58* (27), 11659-11672.

6. Vieira, M. G. A.; da Silva, M. A.; dos Santos, L. O.; Beppu, M. M., Natural-based plasticizers and biopolymer films: A review. *Eur. Polym. J.* **2011,** *47* (3), 254-263.

7. Erythropel, H. C.; Maric, M.; Nicell, J. A.; Leask, R. L.; Yargeau, V., Leaching of the plasticizer di(2-ethylhexyl)phthalate (DEHP) from plastic containers and the question of human exposure. *Appl. Microbiol. Biotechnol.* **2014,** *98* (24), 9967-9981.

8. Staples, C. A.; Peterson, D. R.; Parkerton, T. F.; Adams, W. J., The environmental fate of phthalate esters: A literature review. *Chemosphere* **1997,** *35* (4), 667-749.

9. Surhio, M. A.; Talpur, F. N.; Nizamani, S. M.; Talpur, M. K.; Afridi, H. I.; Khaskheli, A. A.; Bhurgri, S.; Surhio, J. A., Leaching of phthalate esters from different drinking stuffs and their subsequent biodegradation. *Environ. Sci. Pollut. Res.* **2017,** *24* (22), 18663-18671.

10. Velazquez, S.; Bi, C. Y.; Kline, J.; Nunez, S.; Corsi, R.; Xu, Y.; Ishaq, S. L., Accumulation of di-2-ethylhexyl phthalate from polyvinyl chloride flooring into settled house dust and the effect on the bacterial community. *PeerJ* **2019,** *7*.

11. Wowkonowicz, P.; Kijenska, M., Phthalate release in leachate from municipal landfills of central Poland. *PLoS One* **2017,** *12* (3).

12. Heinemeyer, G.; Sommerfeld, C.; Springer, A.; Heiland, A.; Lindtner, O.; Greiner, M.; Heuer, T.; Krems, C.; Conrad, A., Estimation of dietary intake of bis(2-ethylhexyl)phthalate (DEHP) by consumption of food in the German population. *Int. J. Hyg. Environ. Health* **2013,** *216* (4), 472-480.

13. Al-Saleh, I.; Shinwari, N.; Alsabbaheen, A., Phthalates residues in plastic bottled waters. *J. Toxicol.* **2011,** *36* (4), 469-478.

14. Gunaalan, K.; Fabbri, E.; Capolupo, M., The hidden threat of plastic leachates: A critical review on their impacts on aquatic organisms. *Water Res.* **2020,** *184*, 116170.

15. Eckert, E.; Muller, J.; Hollerer, C.; Purbojo, A.; Cesnjevar, R.; Goen, T.; Munch, F., Plasticizer exposure of infants during cardiac surgery. *Toxicol Lett* **2020,** *330*, 7-13.

16. Koch, H. M.; Preuss, R.; Angerer, J., Di(2-ethylhexyl)phthalate (DEHP): human metabolism and internal exposure-- an update and latest results. *Int J Androl* **2006,** *29* (1), 155-65; discussion 181-5.

17. Nalli, S.; Cooper, D. G.; Nicell, J. A., Metabolites from the biodegradation of di-ester plasticizers by Rhodococcus rhodochrous. *Sci. Total Environ.* **2006,** *366* (1), 286-294.

18. Camacho, L.; Latendresse, J. R.; Muskhelishvili, L.; Law, C. D.; Delclos, K. B., Effects of intravenous and oral di (2-ethylhexyl) phthalate (DEHP) and 20% Intralipid vehicle on neonatal rat testis, lung, liver, and kidney. *Food Chem. Toxicol.* **2020**, 111497.

19. Cuenca, L.; Shin, N.; Lascarez-Lagunas, L. I.; Martinez-Garcia, M.; Nadarajan, S.; Karthikraj, R.; Kannan, K.; Colaiácovo, M. P., Environmentally-relevant exposure to diethylhexyl phthalate (DEHP) alters regulation of double-strand break formation and crossover designation leading to germline dysfunction in Caenorhabditis elegans. *PLoS Genet.* **2020,** *16* (1), e1008529.

20. Fan, J.; Traore, K.; Li, W.; Amri, H.; Huang, H.; Wu, C.; Chen, H.; Zirkin, B.; Papadopoulos, V., Molecular Mechanisms Mediating the Effect of Mono-(2-Ethylhexyl) Phthalate on Hormone-Stimulated Steroidogenesis in MA-10 Mouse Tumor Leydig Cells. *Endocrinology* **2010,** *151* (7), 3348-3362.

21. Horn, O.; Nalli, S.; Cooper, D.; Nicell, J., Plasticizer metabolites in the environment. *Water Res.* **2004,** *38* (17), 3693-3698.

22. Ingram, N.; Dishinger, C.; Wood, J.; Hutzler, J. M.; Smith, S.; Huskin, M., Effect of the Plasticizer DEHP in Blood Collection Bags on Human Plasma Fraction Unbound Determination for Alpha-1-Acid Glycoprotein (AAG) Binding Drugs. *AAPS J.* **2019,** *21* (1).

23. Martinez-Arguelles, D. B.; Guichard, T.; Culty, M.; Zirkin, B. R.; Papadopoulos, V., In Utero Exposure to the Antiandrogen Di-(2-Ethylhexyl) Phthalate Decreases Adrenal Aldosterone Production in the Adult Rat1. *Biol. Reprod.* **2011,** *85* (1), 51-61.

24. Piché, C. D.; Sauvageau, D.; Vanlian, M.; Erythropel, H. C.; Robaire, B.; Leask, R. L., Effects of di-(2-ethylhexyl) phthalate and four of its metabolites on steroidogenesis in MA-10 cells. *Ecotox. Environ. Safe.* **2012,** *79*, 108-115.

25. EU. 1999/0238(Cod): Child Health Protection: Phthalates, Dangerous Substances, Safety of Toys. https://oeil.secure.europarl.europa.eu/oeil/popups/ficheprocedure.do?lang=en&reference=1999/0238 (accessed March 2022).

26. Prohibition of Children's Toys and Child Care Articles Containing Specified Phthalates. https://www.federalregister.gov/documents/2017/10/27/2017-23267/prohibition-of-childrens-toys-and-child-care-articles-containing-specified-phthalates (accessed March 2022).

27. Phthalates Regulations. https://laws-lois.justice.gc.ca/eng/regulations/SOR-2016-188/page-1.html (accessed March 2022).

28. Wei, X.-F.; Linde, E.; Hedenqvist, M. S., Plasticiser loss from plastic or rubber products through diffusion and evaporation. *NPJ Mater. Degrad.* **2019,** *3* (1), 18.

29. Najafi, V.; Abdollahi, H., Internally Plasticized PVC by Four Different Green Plasticizer Compounds. *Eur. Polym. J.* **2020**, 109620.

30. Lee, K. W.; Chung, J. W.; Kwak, S. Y., Highly Branched Polycaprolactone/Glycidol Copolymeric Green Plasticizer by One-Pot Solvent-Free Polymerization. *ACS Sustain. Chem. Eng.* **2018,** *6* (7), 9006-9017.

31. Zhang, X. X.; Zhang, C.; Hankett, J. M.; Chen, Z., Molecular Surface Structural Changes of Plasticized PVC Materials after Plasma Treatment. *Langmuir* **2013,** *29* (12), 4008-4018.

32. Dias, A. M. A.; Marceneiro, S.; Braga, M. E. M.; Coelho, J. F. J.; Ferreira, A. G. M.; Simoes, P. N.; Veiga, H. I. M.; Tome, L. C.; Marrucho, I. M.; Esperanca, J.; Matias, A. A.;

Duarte, C. M. M.; Rebelo, L. P. N.; de Sousa, H. C., Phosphonium-based ionic liquids as modifiers for biomedical grade poly(vinyl chloride). *Acta Biomater.* **2012,** *8* (3), 1366-1379.

33. Czogała, J.; Pankalla, E.; Turczyn, R., Recent Attempts in the Design of Efficient PVC Plasticizers with Reduced Migration. *Materials* **2021,** *14* (4), 844.

34. Choi, W.; Chung, J. W.; Kwak, S. Y., Unentangled Star-Shape Poly(epsilon-caprolactone)s as Phthalate-Free PVC Plasticizers Designed for Non-Toxicity and Improved Migration Resistance. *ACS Appl. Mater. Inter.* **2014,** *6* (14), 11118-11128.

35. Feng, Y. C.; Chu, Z. Z.; Man, L. M.; Hu, Y.; Zhang, C. Q.; Yuan, T.; Yang, Z. H., Fishbone-Like Polymer from Green Cationic Polymerization of Methyl Eleostearate as Biobased Nontoxic PVC Plasticizer. *ACS Sustain. Chem. Eng.* **2019,** *7* (23), 18976-18984.

36. Lee, K. W.; Chung, J. W.; Kwak, S. Y., Synthesis and characterization of bio-based alkyl terminal hyperbranched polyglycerols: a detailed study of their plasticization effect and migration resistance. *Green Chem.* **2016,** *18* (4), 999-1009.

37. Singh, S.; Roy, R., The application of absolute quantitative 1H NMR spectroscopy in drug discovery and development. *Expert Opin. Drug Discov.* **2016,** *11* (7), 695-706.

38. Elsiwi, B. M.; Garcia-Valdez, O.; Erythropel, H. C.; Leask, R. L.; Nicell, J. A.; Maric, M., Fully Renewable, Effective, and Highly Biodegradable Plasticizer: Di-n-heptyl Succinate. *ACS Sustain. Chem. Eng.* **2020,** *8* (33), 12409-12418.

39. Erythropel, H. C.; Shipley, S.; Bormann, A.; Nicell, J. A.; Maric, M.; Leask, R. L., Designing green plasticizers: Influence of molecule geometry and alkyl chain length on the plasticizing effectiveness of diester plasticizers in PVC blends. *Polymer* **2016,** *89*, 18-27.

40. Kastner, J.; Cooper, D. G.; Maric, M.; Dodd, P.; Yargeau, V., Aqueous leaching of di-2-ethylhexyl phthalate and "green" plasticizers from poly(vinyl chloride). *Sci. Total Environ.* **2012,** *432*, 357-364.

41. *Handbook of Plasticizers, 3rd Edition*. 2017; p 1-858.

42. Jamarani, R.; Erythropel, H. C.; Nicell, J. A.; Leask, R. L.; Maric, M., How Green is Your Plasticizer? *Polymers* **2018,** *10* (8).

43. Erythropel, H. C.; Dodd, P.; Leask, R. L.; Maric, M.; Cooper, D. G., Designing green plasticizers: Influence of alkyl chain length on biodegradation and plasticization properties of succinate based plasticizers. *Chemosphere* **2013,** *91* (3), 358-365.

44. Duchowny, A.; Adams, A., Compact NMR Spectroscopy for Low-Cost Identification and Quantification of PVC Plasticizers. *Molecules* **2021,** *26* (5).

45. Genay, S.; Feutry, F.; Masse, M.; Barthélémy, C.; Sautou, V.; Odou, P.; Décaudin, B.; Azaroual, N., Identification and quantification by (1)H nuclear magnetic resonance spectroscopy of seven plasticizers in PVC medical devices. *Anal Bioanal Chem* **2017,** *409* (5), 1271-1280.

46. Shi, G. X.; Cooper, D. G.; Maric, M., Poly(epsilon-caprolactone)-based 'green' plasticizers for poly(vinyl choride). *Polym. Degrad. Stab.* **2011,** *96* (9), 1639-1647.

4 Highly flexible polylactide food packaging plasticized with non-toxic, bio-sourced glycerol plasticizers

Matthew W. Halloran,[1] Lisa Danielczak,[1] Jim A. Nicell,[2] Richard L. Leask,[1] Milan Marić*[1]

[1]Department of Chemical Engineering, McGill University, 3610 University Street, Montréal, QC, Canada, H3A 0C5

[2]Department of Civil Engineering, McGill University, 817 Sherbrooke Street West, Montreal, Quebec, Canada, H3A 0C3

*corresponding author

4.1 Preface

The following manuscript was published in 2022 in the journal *ACS Applied Polymer Materials* and served as our first reported successful attempt at developing plasticizers for PLA. This work stems from the desire to shift the focus of the research from the field of PVC plasticizers into the area of renewably sourced and biodegradable polymers, which would represent an additional important step toward the development of green alternatives to plastics. Although commercial plasticizers for PLA already exist, many have petroleum derived origins which take away from the sustainable nature of PLA. Thus, the focus of this work was to develop renewably sourced plasticizers for PLA using a straightforward, and benign synthesis route.

Building on the results presented in the first manuscript, a series of glycerol-succinate plasticizers were developed that had been functionalized with a range of alkyl chain lengths. These were then evaluated as plasticizers for PLA in solvent-cast film and melt-mixed samples, which have important potential applications as food packaging materials. In addition to evaluating mechanical, thermal, and morphological properties of the blends, extensive migration studies were performed using different food simulant environments. Finally, a cytotoxicity assay was used to evaluate acute toxicity of the plasticizers over a seven-day period. Ultimately, the main objectives of this work were to develop alternative, renewably sourced plasticizers for PLA, to show that they can be used to produce flexible films and bulk specimens, and finally to demonstrate and establish the value of toxicity testing when developing new plasticizers.

4.2 Abstract

Polylactide (PLA) is a promising bio-sourced and biodegradable polymer substitute for traditional petroleum-based products. Despite its recognized potential, its widespread adoption is restricted by its brittleness and low ductility and, thus, to enhance its material properties, plasticizers must be blended with PLA to lower the glass transition temperature (T_g) and impart flexibility into the blend. As such, this work focused on the synthesis of a family of bio-sourced plasticizers for applications in flexible food packaging using glycerol, succinic anhydride, and alcohols of varying chain lengths. The effect of chemical structure on plasticization performance, migration, blend morphology, and toxicity were evaluated and compared to the commercial plasticizer acetyl tributyl citrate (ATBC). Plasticizer/PLA blends were prepared using solvent-casting as well as melt-mixing to produce thin films and bulk specimens. At loadings of 20 wt%, improved flexibility (up to 435% elongation) was observed in films with the glycerol plasticizers relative to neat PLA (6% elongation), while T_g's were reduced by up to 45 °C from that of neat PLA ($T_g \sim 60$ °C). Phase morphologies evaluated with SEM showed good incorporation of the plasticizers into the PLA matrix. Leaching behaviour of the plasticized blends were evaluated in different food simulants and showed that plasticizers comprised of branched, or longer alkyl chains produced 2- to 6-fold lower migration rates compared to those with short alkyl chains. Finally, plasticizer candidates were shown to be non-toxic and did impact HepG2 cell viability over a period of 7 days in an *in vitro* mammalian cell assay.

4.3 Introduction

A growing global awareness of the ramifications brought on by the manufacture, use, and accumulation of petroleum-derived plastics in the environment has resulted in significant interest in the development of sustainably sourced polymeric materials.[1] This has resulted in the development of a number of promising alternative bio-based polymers which have been shown to be both biodegradable and biocompatible.[2, 3] Although bio-based polymers currently account for only about one percent of the estimated 368 million tonnes of plastics produced annually, their market is projected to expand as the global production capacities are poised to increase from 2.11 million tonnes in 2020 to 2.87 million tonnes by 2025.[4] Within this group of alternatives, polylactide (PLA) has emerged as one of the leading replacements for conventional petroleum-derived polyethylene terephthalate (PET) and polystyrene (PS).[5] As a bio-sourced synthetic polymer, PLA is derived from animal and plant sources,[6] and has shown to be biodegradable under industrial composting conditions.[7] Having similar mechanical properties to both PET and PS,[8, 9] PLA has high tensile strength and modulus which make it suitable for certain packaging applications, 3D printing, and in the medical field for sutures and drug delivery owing to its biocompatability.[10-12]

Despite its wide scope of application, PLA suffers from several drawbacks including its brittleness, low ductility, and poor tensile properties.[13] These important drawbacks have limited its use in certain applications such as food packaging, for which high flexibility, elongation and toughness are essential.[12] One of the commonly used approaches to modify the impact toughness and ductility of PLA is through reactive blending between PLA and an immiscible rubbery polymer, such as polyethylene,[14] poly(1,4-*cis*-isoprene),[15] or epoxy-based styrenes.[16] While this approach has considerable promise, it often requires the use of complicated synthetic procedures to selectively install reactive functional groups on the rubbery phase, which has, to some extent, limited its widespread use.[17] Alternatively, the use of external plasticizers (herein simply referred to as plasticizers) which are blended with PLA to help lower the glass transition temperature (T_g) of the polymer, impart flexibility, and improve processing characteristics is an industrially adopted practice.[18, 19]

Although the addition of plasticizers to PLA is an accepted method to improve its mechanical properties, plasticizers are prone to migration and leaching out of the blend as they are not covalently bound to the polymer backbone.[19] This compromises the integrity of the product[20] and can lead to widespread environmental contamination and potential human exposure.[21, 22] Consequently, the investigation of plasticizer accumulation in the environment[23] as well as the health effects of plasticizer exposure on both humans[24, 25] and animals[26] remains an area of active research. To date, there have been numerous plasticizers developed for the production of flexible PLA including but not limited to citrate esters,[27] polyethylene glycol analogs,[28] levulinic acids,[29] tartaric acids,[30] malic acids,[31] and functionalized epoxidized soybean oils.[32] While many of these have demonstrated promise, the global push towards sustainable commodity plastics has resulted in the demand for alternative plasticizers synthesized from simple, renewably sourced feedstock chemicals.[33] Additionally, to mitigate risk while avoiding the regrettable substitution of one problematic plasticizer with another,[34] the toxicology of these alternative plasticizers must be taken into consideration.

In line with this, the goal of this work was to design a family of non-toxic bio-based plasticizers for flexible food packaging materials, while evaluating the effect of chemical structure on plasticization performance, surface morphology, and migration behaviour in blends with PLA. The green platform chemical, glycerol, was exploited as a building block to synthesize a series of glycerol-succinate bio-plasticizers functionalized with different alcoholic substituents which were then compared with the commercial standard plasticizer acetyl tributyl citrate (ATBC). In addition, we aimed to compare the thermal stabilities and surface morphologies of blends prepared using two different types of commonly employed preparation techniques (solvent casting of films vs. melt-mixing) to evaluate our family of plasticizers under both laboratory and industrial relevant conditions. Finally, the cytotoxicity of the plasticizers was investigated through an *in vitro* mammalian cell assay using Human Hepatocellular Carcinoma (HepG2) cells.

4.4 Experimental Methods

4.4.1 Materials and Reagents

Polylactic acid (Ingeo Bioworks 2003D, MFI = 6 g/10min (210 °C/2.16 kg) and density = 1.24 g/cm^3) was purchased from Nature-Works LLC (Minnetonka, MN). Succinic anhydride (99%), glycerol (99%), 2-ethylhexanol (99.6%), 1-butanol (99.8%), *n*-hexanol (99%), magnesium sulfate (99.5%), sodium bicarbonate (ACS reagent), and *p*-toluene sulfonic acid monohydrate (98.5%) were purchased from Sigma Aldrich (Oakville, ON). *n*-heptanol (99.9%) was purchased from Arkema (King of Prussia, PA). Ethyl acetate (ACS grade), *iso*-propanol (ACS grade), toluene (ACS grade), dichloromethane (ACS grade), acetic acid (99.5%), ethanol (ACS grade), water (LCMS grade), dimethyl sulfoxide (99%), Dulbecco's Modified Eagle Medium (DMEM), Penicillin Streptomycin solution, and Fetal Bovine Serum (FBS) were purchased from Fisher Scientific (Montreal, QC). Tributyl 2-acetylcitrate (ATBC) (98%) was used as a reference plasticizer and was purchased from Sigma-Aldrich (Oakville, ON). Cell-Counting Kit-8 (CCK-8) was purchased from Cedarlane Laboratories Ltd (Burlington, ON).

4.4.2 Synthesis of Plasticizers

See Appendix B for full experimental and characterization information regarding the synthesis of the plasticizers. Briefly, the appropriate mono-succinate (3.8 eq.) was reacted with glycerol (1 eq.) and *p*-toluene sulfonic acid monohydrate (0.03 eq.) under bubbling N_2 at 110 °C for 18 hours to afford the crude glycerol analogs as oils. Crude reaction mixtures were dissolved in ethyl acetate (50 mL), washed with saturated sodium bicarbonate (25 mL), dried over magnesium sulfate, filtered, and concentrated under reduced pressure to afford the glycerol-succinate (GS) analogs as clear to yellow oils in yields ranging from 82-95%. Each compound was named according to the alcohol substituent on the GS core.

4.4.3 Solvent-Casting of Films

Neat PLA (nPLA) and plasticized films were prepared using solvent-casting. PLA films were produced using 10 and 20 weight percent (wt%) of plasticizer using blends of 2.5 g total weight. Each blend was produced by combining the appropriate weights of PLA and plasticizer into a 50-mL round-bottomed flask and stirring at room temperature for 1 hour in 25 mL of dichloromethane. The films were then cast into a circular glass dish (diameter = 120 mm), covered with aluminum foil, and left in a fumehood to dry for 48 hours. The films were then peeled from the dish and dried in a vacuum oven at 40 °C for 48 hours to remove residual solvent. The thickness of the obtained films was 0.14 ± 0.02 mm. Each blend was named according to the plasticizer weight percentage it is comprised of (i.e., a 20 wt% blend of ATBC is denoted as ATBC-20).

4.4.4 Melt Mixing of PLA/plasticizer blends

Melt-mixed blends at plasticizer concentrations of 10 and 20 wt% were prepared using a Rheocord System 40 double arm internal batch mixer (Haake Buchler). The PLA pellets were dried under vacuum for 24 hours at 40 °C to remove residual moisture before use. 50 g batches of each blend were pre-weighed and stirred by hand briefly before being added to the batch mixer and mixed for 10 minutes at 170 °C with a rotation rate of 50 rpm. The batches were then quenched into a liquid nitrogen bath to freeze the morphology and stored for further analysis. nPLA was processed under the same conditions for comparison purposes. Blends were named in the same manner as described above.

4.4.5 Scanning Electron Microscopy (SEM)

The morphology of the samples was investigated with scanning electron microscopy (SEM), using a FEI Quanta 450 Environmental Scanning Electron Microscope (FE-ESM) operating under high vacuum and acceleration voltage of 5.0 kV. The specimens were freeze-fractured with liquid nitrogen and mounted on aluminum stubs with carbon tape and glue. All samples were sputter-coated with 4 nm of platinum prior to analysis using a Leica Microsystems EM ACE600 High Resolution Sputter Coater.

4.4.6 Production of Tensile Bars

Tensile test bars of melt-mixed blends were produced using compression molding with a heated manual hydraulic press (Carver Manual Hydraulic Press with Watlow temperature controllers, St. Louis, MO) and steel molds. The blends were manually cut into small fragments and dried in a vacuum oven at 40 °C for 24 hours before being placed into the molds and pressed at 170 °C in the following manner: 5 minutes at 5 metric tonnes followed by 5 minutes at 10 metric tonnes. Tensile test bar dimensions adhered to the standardized testing protocol ASTM-D638 for tensile properties: i.e., a thickness (T_0) of 1.4 mm; a width of narrow section (W_0) of 3.3 mm; a length of narrow section of 17.8 mm; an overall length of 64 mm; and an overall width of 10 mm. The exact dimensions (thickness/width) of each specimen were recorded using an electronic caliper prior to testing.

4.4.7 Thermal Gravimetric Analysis (TGA)

The thermal stability of the PLA blends was evaluated using a TA Instruments Discovery 5500 (New Castle, DE) instrument under nitrogen flow of 25 mL/min from 25 to 500 °C at a heating rate of 10 °C/min. The onset temperature at weight loss with 5% (T_5) is reported (see Appendix B, Table B1 and B2) for comparison purposes.

4.4.8 Differential Scanning Calorimetry (DSC)

The glass transition temperature (T_g) of each blend was measured by differential scanning calorimetry (DSC) using a TA Instruments Q2000 (New Castle, DE) under a nitrogen atmosphere using the following heat/cool/heat cycle. The samples were heated from 25-200 °C at a rate of 20

°C per minute, held constant at 200 °C for two minutes, then cooled to -30 °C at a rate of 10 °C per minute and held constant for two minutes at -30 °C. The samples were then heated to 200 °C at a rate of 20 °C per minute. The T_g was then determined from the reversible heat flow of the second heating cycle using the automated glass/step transition tool in the TA Instruments Universal Analysis 2000 software which finds the inflection point in the thermogram. The melting (T_m) and cold crystallization (T_{cc}) temperatures were taken from the second heating scan. The crystallinity (X_c) was calculated using equation (1) with the melt and crystallization enthalpies where ΔH_m, ΔH_{cc}, ΔH_m^0, and w_{PLA} represent the enthalpy of melting, the enthalpy of cold crystallization, the enthalpy of melting for 100% crystalline PLA, and the weight percent of PLA in the blend, respectively. A value of 93.15 J/g was taken as the melting enthalpy for 100% crystalline PLA (see Appendix B, tables B5 and B8 for calculated values).[35]

$$X_c = \frac{\Delta H_m - \Delta H_{cc}}{\Delta H_m^0 \times w_{PLA}} \times 100\% \qquad (1)$$

4.4.9 Tensile Testing

Testing was performed using a Shimadzu (Kyoto, Japan) Easy Test instrument equipped with a 500 N load cell in accordance with a previously developed protocol.[22] For the film specimens, samples were cut into rectangular strips with dimensions of 5 mm width x 60 mm length x 0.14 ± 0.02 mm thickness and stored in a desiccator until the testing was performed. Test strips were clamped and subjected to a strain rate of 20 mm/min with a constant gauge length of 30 mm. At least five specimens were tested for each sample. *For the blended/compression molded samples,* test bars were clamped and subjected to a strain rate of 5 mm/min with a constant gauge length of 36 mm. The stress-strain curves were used to obtain values for strain (% elongation), stress at break, and the early extensional modulus (0-5% strain).

4.4.10 Plasticizer Leaching

The American Society for Testing and Materials (ASTM) Method D1239-14, “Resistance of Plastic Films to Extraction by Chemicals” was used as a template. Films blended with 20 wt% of plasticizer were used. Specimens were cut into square fragments measuring 2 cm x 2 cm and dried in a vacuum oven for 24 hours at 40 °C. Three food simulants were selected for leaching analysis: water, 10% v/v ethanol in water, and 3% v/v acetic acid in water over time points of one, five, and ten days at a temperature of 60 °C. Each specimen was pre-weighed, placed into a 24-mL glass vial containing 20 mL of each simulant and then placed into an incubator shaker set at 60 rpm for the specified time frame. Each experiment was run in triplicate. At the end of the time periods, the film specimens were removed from the vials, wiped with tissue paper, and dried in a vacuum oven at room temperature for 7 days. The film specimens were then re-weighed, and the percent mass loss was calculated using equation (2), as follows:

$$Mass\ Loss\ (\%) = \frac{W_i - W_f}{W_i} \times 100\% \tag{2}$$

where W_i is the initial mass of the specimen and W_f is the final mass

4.4.11 Cell Viability Assay

The human hepatocellular carcinoma (HepG2) cell line was used in this assay. Cells were thawed from stock and cultured using an established protocol.[36] After culture, the cell count was obtained with a Bio-Rad TC20 cell counter. Stock solutions were then prepared at different concentrations for the standard curve and test wells. The cell-counting kit (CCK-8), which uses a [2-(2-methoxy-4-nitrophenyl)-3-(4-nitrophenyl)-5-(2,4-disulfophenyl)-2H-tetrazolium] salt (WST-8), was purchased and used according to the manufacturer's instructions. In brief, the WST-8 reagent produces a formazan dye upon reduction by a metabolically active cell to allow for a direct quantification of viable cells and evaluate cytotoxicity. HepG2 cells were collected and counted using a Bio-Rad TC20 cell counter. Cells were then plated in 96-well plates at a concentration of 5000 cells/well and incubated for 24 hours to allow for cell adhesion. The media was removed and 150 µL of sterilized solutions comprised of cell media and 500 µM of each plasticizer in 0.5% v/v DMSO (to improve solubility) were added to the appropriate wells and the plates returned to the incubator. A negative control of 0.5% v/v DMSO was added to the cells in the absence of plasticizer to account for toxicity of the solvent, while a positive control of 10% v/v DMSO was employed. Each solution was run in triplicate on the same plate. At time points of one and seven days, the media was removed, and 100 µL of media containing 10% v/v WST-8 reagent was added to each well and the plates returned to the incubator for two hours. After two hours, absorbance values at 450 nm were read using a Bio-Rad Benchmark Plus plate reader (CA, USA). Each absorbance value was normalized with respect to values obtained from wells containing cells seeded at 5000 cells/well. Each plate was analyzed in triplicate.

4.4.12 ^{1}H NMR Spectroscopy

^{1}H NMR spectra were collected using a Bruker AVIIIHD 500 MHz spectrometer (MA, USA) with an average of 16 scans using deuterated chloroform ($CDCl_3$) as the solvent.

4.4.13 Statistics

Statistical analysis was done using GraphPad Prism 5 software. Difference between the mean values of the plasticizer types were analyzed by a one-way-ANOVA test with a Bonferroni post-test to evaluate differences between each type. A *p* value less than 0.05 was interpreted as significant.

4.5 Results and Discussion

4.5.1 Synthesis of Plasticizers

A family of six glycerol-succinate analogs with different alcohol chain lengths were synthesized and evaluated as plasticizers for flexible PLA-based food packaging applications. Glycerol is an ideal building block for the design of green plasticizers as it is a non-toxic, renewably sourced chemical containing three alcohol functional groups for further synthetic manipulation. Here, glycerol was used as a platform molecule to design a series of succinate derivatives bearing different alcohol substituents to investigate the effect of alcohol chain length and substitution pattern on plasticization efficiency, surface morphology, migration behaviour, and toxicity in blends with PLA.

Each analog was synthesized following the same two-step sequence (Figure 4.1). The appropriate mono-substituted acid was reacted with glycerol in the presence of catalytic amounts of *para*-toluene sulfonic acid (*p*TsOH•H_2O) under solvent-free conditions to afford the desired analogs as light yellow or clear oils. Initial attempts to esterify the secondary alcohol of glycerol were unsuccessful at reaction times of 4 hours. However, increasing the reaction time to 18 hours led to complete conversion and provided the fully esterified products, which was confirmed with ^{1}H NMR (see Appendix B for spectra). This approach avoids the use of organic solvent during the reaction, reaches high yields and conversions with very low catalyst loadings, and generates only water as a by-product during the esterification.

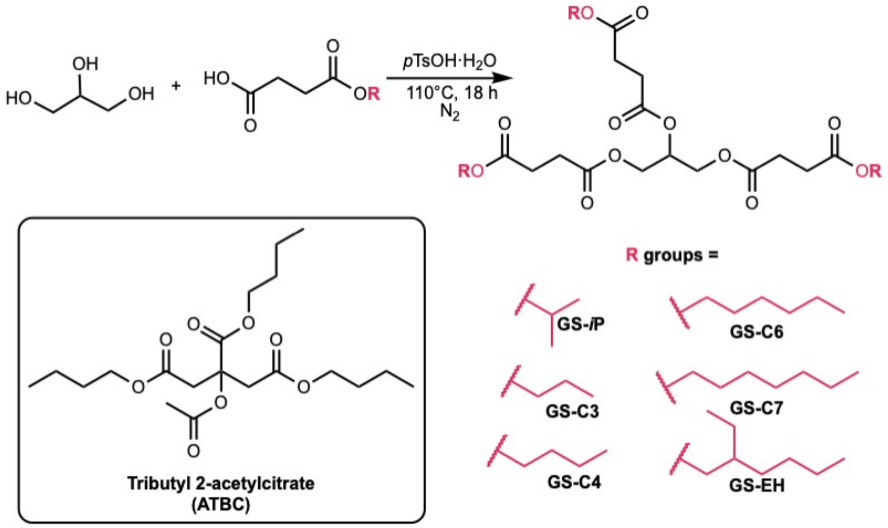

Figure 4.1. Synthesis and structures of glycerol-based plasticizers and commercially available ATBC used for comparison purposes in this study.

4.5.2 Theoretical Prediction of Compatibility of Glycerol Analogs with PLA

For a molecule to function effectively as a plasticizer, it must be both miscible and compatible with the host polymer system it is blended with.[37] In the case of a plasticizer-polymer system, this type of relationship can be evaluated with Hansen Solubility Parameters (HSP) in which theoretical predictions are made based on the chemical structure and molecular weight of the plasticizer in relation to the host polymer.[38] For a plasticizer to be deemed compatible, it must have similar solubility parameters to its host polymer as well as have a relative energy difference (RED) value of less than 1.[39] Here, the HSP values of each plasticizer candidate were calculated using the Hoftyzer-Van Krevelen method[40] and compared to both PLA as well as ATBC (Appendix B, Table B9). Our calculated value of the solubility parameter for PLA of 20.6 (MJ/m^3)$^{1/2}$ was consistent with reported literature values which range from 20.1-21.9 (MJ/m^3)$^{1/2}$.[29, 41] The calculated RED values of ATBC and our plasticizer candidates ranged from 0.6-0.7, indicating that they were theoretically miscible with PLA.

4.5.3 Investigation as Plasticizers

In addition to investigating the plasticization efficiency of this class of bio-based plasticizers for PLA, we also evaluated two different types of commonly employed blend preparation techniques used in the literature (i.e., solvent casting of films versus melt-mixing). While solvent-casting is a generally accepted method of sample preparation for small-scale screening of new plasticizers, this processing technique is not one which is used industrially.[42, 43] Therefore, we wanted to establish the efficiency of this class of plasticizers under both laboratory and industrially relevant testing conditions while also comparing the thermal properties and surface morphologies of the blends arising from the two preparation techniques.

4.5.3.1 Thermal Properties of the Blends

To evaluate the plasticization efficiency of the compounds, films containing 10 and 20 wt% of each candidate plasticizer were prepared through solvent casting. In each case, flexible and transparent films were obtained after evaporation of the solvent. The thermal stabilities of the film blends were then evaluated with thermal gravimetric analysis (TGA) to evaluate the effect of alkyl chain length and branching on blend stability with the onset temperature at weight loss with 5% (T_5) reported for comparison (see Appendix B, Table B1). The film blends produced with the glycerol analogs displayed higher T_5 values at both 10 and 20 wt% (ranged between 244 to 293 for 10wt% and 195 to 271 °C for 20wt%) loadings (except for GS-C4-20) than blends produced with ATBC (T_5 of 222 and 207 °C for 10 and 20wt%, respectively). In comparison, the thermal stabilities of the melt-mixed blends prepared with the glycerol analogs also displayed higher thermal stabilities than blends produced with ATBC (see Appendix B, Table B2). In general, the thermal stability was higher for the analogs comprised of longer alkyl chains.

Each blend was then evaluated using DSC to obtain the glass transition (T_g), melting (T_m), cold crystallization (T_{cc}) temperatures, and crystallinity (X_c) of the blends. The obtained DSC thermograms for films blends are presented in Figure 4.2. When compared to nPLA with a T_g of 59 °C, the glycerol analogs reduced the T_g between 22-26 °C at loadings of 10 wt%. A more pronounced decrease in T_g was found at 20 wt% plasticizer loadings where values as low as 15 °C were obtained for blends produced with the glycerol analogs. Between these, it was found that analogs comprised of longer, linear alkyl chains produced blends with the lowest T_g value observed at 20 wt% loadings, whereas the branched GS-EH did not produce the same desirable effect. As expected, the addition of the glycerol analogs slightly depressed the melting temperatures of the blends (Table B3) relative to nPLA, while the increase in plasticizer loading from 10 to 20 wt% did not have a significant effect as comparable T_m values were obtained at both loadings. Cold crystallization was present in all the film blends, except for nPLA, ATBC-20 and GS-EH-10 and GS-EH-20 (see Table B4, for values), with the largest exotherms observed for the blends produced with the glycerol analogs comprised of C6 and C7 alkyl chains.

In contrast, the DSC thermograms of the melt-mixed blends display slightly different thermal transition temperatures than those observed for the solvent-cast films (Figure B1); however, each glycerol analog effectively reduced the T_g of nPLA to between 25-36 °C, with GS-C4-20 displaying the lowest T_g of 24 °C.

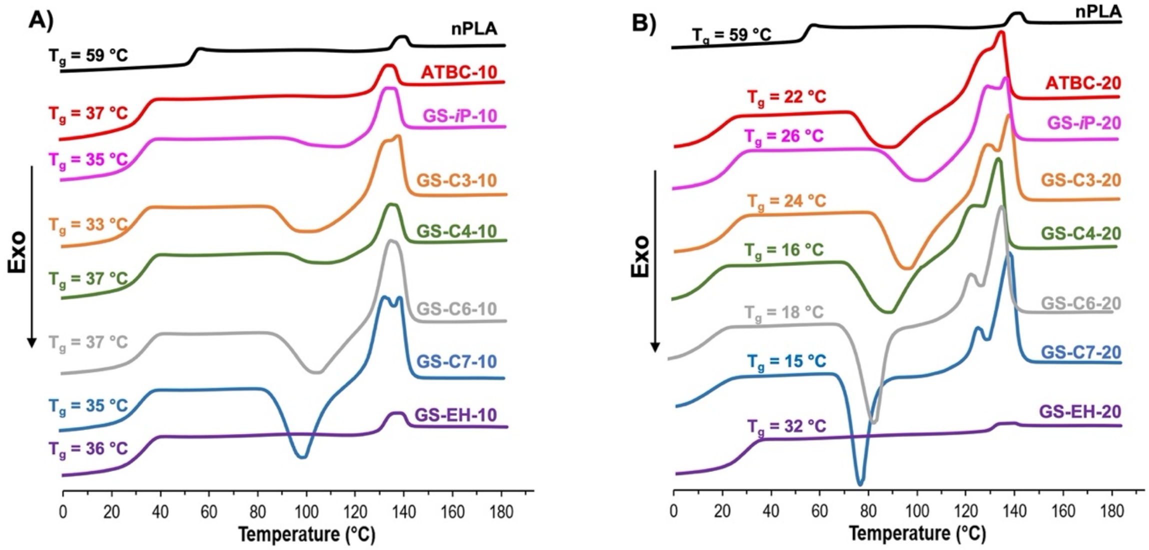

Figure 4.2. DSC thermograms of PLA film blends obtained from the second heating cycle with (A) 10 wt% and (B) 20 wt% glycerol plasticizers.

4.5.3.2 Mechanical Properties

Since PLA is known for its brittleness, low ductility, and poor tensile properties,[44] the addition of an effective plasticizer should enhance flexibility while increasing the elongation at break.[19] Tensile testing data of the solvent-cast film blends is summarized in Figure 4.3, with all plasticized blends showing an increase in elongation, and a decrease of modulus and stress at break compared to nPLA. Significant differences were observed in the modulus, stress at break, and elongation at break amongst the compounds tested at both 10 and 20 wt% plasticizer loading ($p < 0.001$). A representative stress versus strain in % elongation curve for 20 wt% plasticized films shows typical plasticizing behaviour for all blends, with the highest elongation of 435% obtained for GS-*i*P-20 (Figure 3A). An increase of plasticizer loading from 10 to 20 wt% did not have a significant effect on the elongation or stress at break for analogs comprised of alkyl chains greater than three carbons in length ($p > 0.05$). The early extensional modulus (0-5% strain) ranged from 71 MPa to 659 MPa for the 20 wt% blends, and from 221 MPa to 725 MPa for the 10 wt% blends. It has previously been shown that an elongation at break of 522% and a stress at break of 21 MPa were obtained with PLA films plasticized with 20 wt% epoxidized soybean oil methyl ester,[32] while an elongation at break of around 460% and a stress at break of 40 MPa were obtained using 20 wt% of a glycerol-based levulinic acid derivative.[29] Therefore, the obtained results for our glycerol-based succinates are comparable to previous literature reports as well as the commercial standard ATBC.

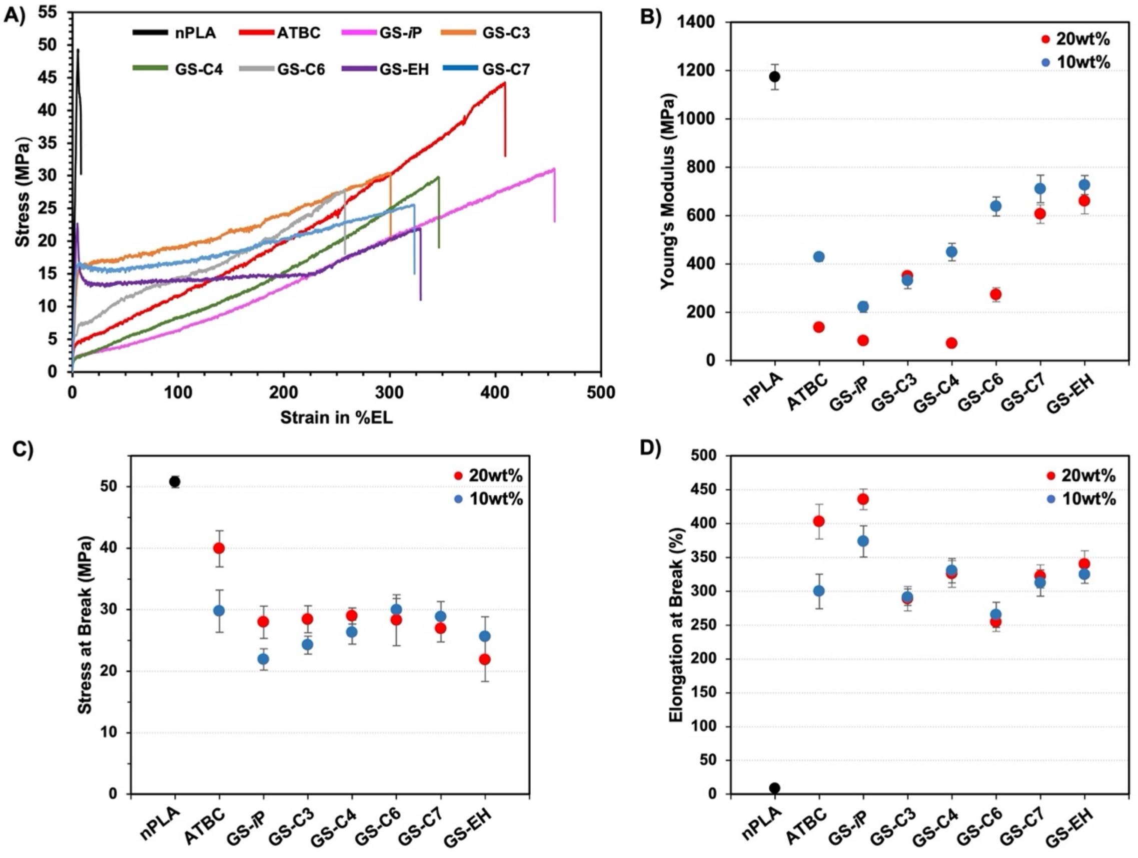

Figure 4.3. Mechanical properties of PLA film blends at 10 and 20 wt% plasticizer loadings: (A) Representative stress vs. strain in % elongation curves; (B) Young's modulus; (C) Stress at break; (D) Elongation at break (*n*=5, error bars represent standard deviation, means are shown).

The tensile testing data for the 10 and 20 wt% melt-mixed blends is summarized in Figure 4.4. Significant differences were observed in the modulus, stress at break, and elongation at break amongst the compounds tested at 20 wt% plasticizer loading ($p < 0.001$). In contrast to the solvent-cast films, the melt-mixed blends containing 10 wt% plasticizer displayed very poor tensile properties, with no significant differences observed in the modulus and elongation at break between any of the 10 wt% blends and nPLA ($p > 0.05$). Although the plasticizers and PLA form miscible blends at 10% loading, no improvement in mechanical properties was observed. This finding agrees with a previous report by Jeong and coworkers wherein the inability of their plasticizers to improve the tensile properties of PLA in bulk specimens at 10 wt% plasticizer loadings was also observed.[45] This is believed to be a direct result of antiplasticization,[37] in which low loadings of plasticizers produce blends with increased tensile strength, but decreased elongation. At low loadings, the majority of the plasticizer molecules can be hydrogen-bonded to the PLA backbone and restrict their ability to move freely within the polymer matrix and plasticize the blend. Conversely, blends prepared with 20 wt% plasticizer loadings displayed remarkable tensile properties. An increase in elongation of up to 257% for GS-C6 was obtained, while significant reduction in the modulus were observed for all 20 wt% blends (except for GS-EH). A representative stress versus strain in % elongation curve is presented in Figure 4A which shows standard plasticizing behaviour as the test bars displayed typical necking before fracture (see Figure S5). Interestingly, GS-EH was unable to improve the tensile properties of PLA at 20 wt% loading, as no significant difference was found between their elongation at break or modulus when compared to nPLA ($p > 0.05$). Although structurally similar to ATBC, the branched glycerol analogs contain two additional ester groups and overall longer carbon chains to allow them to be both miscible with the polar PLA backbone, but also increase the free volume of the polymer matrix to effectively plasticize the blend.[19]

Overall, the glycerol analogs functioned to effectively plasticize PLA at both 10 and 20 wt% loadings and produce highly flexible and ductile solvent-cast films reaching elongations of up to 435%. In comparison, the melt-mixed blends plasticized with 10 wt% of the glycerol compounds showed negligible improvements in tensile properties relative to nPLA, while at 20 wt% loadings the plasticized blends showed significant improvement in ductility/flexibility with elongations up to 257% reached. The stark difference observed in the tensile properties at 10 wt% plasticizer loadings between the solvent-cast films and the melt-mixed blends is attributed to the size effect,[46, 47] in which thinner specimens demonstrate higher elongation than their thicker counterparts comprised of the same microstructure. This demonstrates the ability of these compounds to produce both highly flexible PLA films as well as bulk specimens while establishing their potential applicability for a variety of PLA-based food packaging materials.

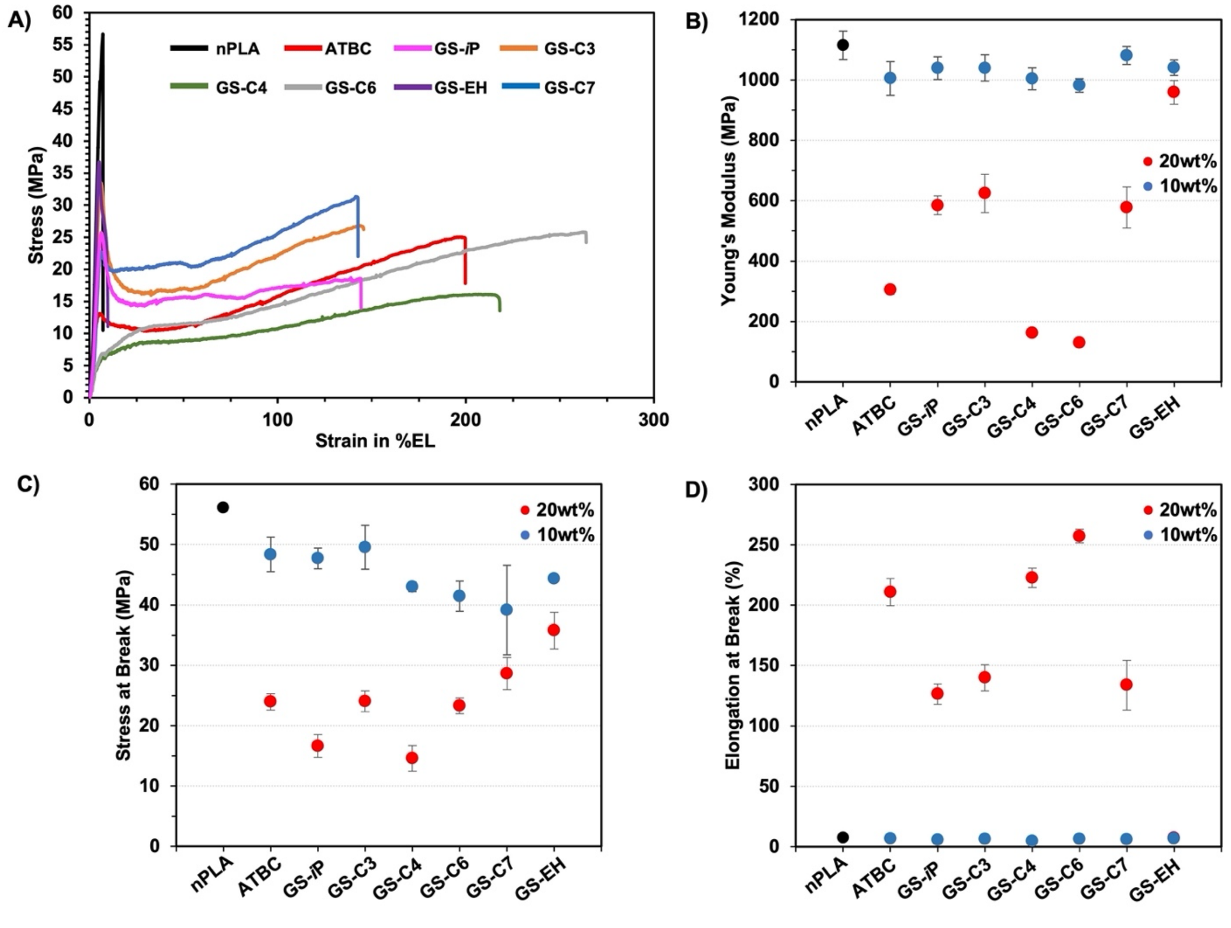

Figure 4.4. Mechanical properties of PLA melt-mixed blends at 20wt% plasticizer loadings: (A) Representative stress vs. strain in % elongation curves; (B) Young's modulus; (C) Stress at break; (D) Elongation at break (*n*=5, error bars represent standard deviation, means are shown).

4.5.3.3 Morphology of Blends

SEM of the freeze-fractured surfaces was used to characterize the morphology of both the solvent casted film blends (Figure 4.5) and the melt-mixed blends (Figure 4.6) at 20 wt% loadings of the plasticizers (see Figures B3 and B4 for additional SEM images). The fractured surfaces of the films produced with ATBC, GS-C3, GS-*i*P, and GS-C4 all show relatively uniform incorporation of the plasticizer within the PLA matrix, which is demonstrated by a homogenous surface absent of any droplet formation or apparent phase separation. However, when observing blends produced with GS-C6, GS-EH, and GS-C7, an apparent phase separation occurs, which is evident by the formation of droplets and/or pores within the PLA matrix. Despite the presence of droplets and/or pores within the matrix, these three blends still showed significant improvements in tensile and thermal properties relative to nPLA.

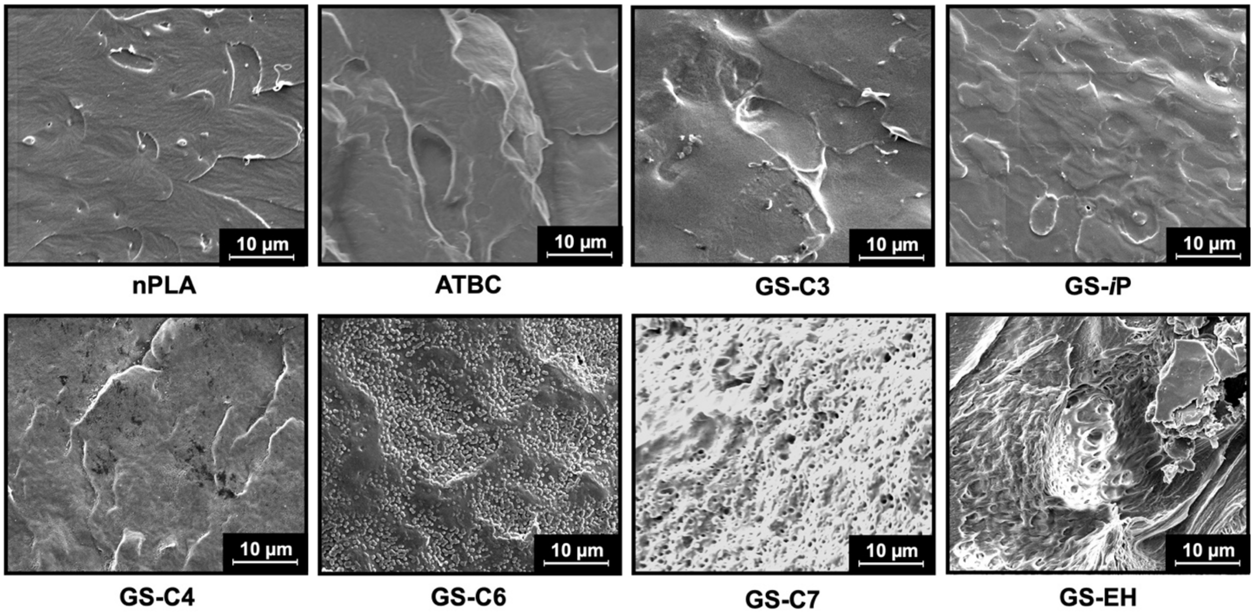

Figure 4.5. Freeze fractured surface SEM images of nPLA and 20 wt% solvent-cast film blends (2500× magnification).

In contrast, SEM images taken of the melt-mixed samples revealed different surface morphologies for several of the blends. While smooth, homogenous surfaces were observed in films produced with GS-*i*P and GS-C4, the melt-mixed blends show signs of droplet formation and potential phase separation. In the case of GS-C6, there was no sign of droplet formation in the melt-mixed blend and instead, a homogenous surface was observed. This observation of a well-compatibilized blend agrees with the remarkable tensile results obtained for GS-C6-20. Both preparation techniques yielded homogeneous morphologies with ATBC and GS-*i*P. The highly porous surface morphology obtained with GS-EH-20 is interesting as this unique architecture could be exploited for applications which require porous PLA materials, such as bone scaffolds.[48]

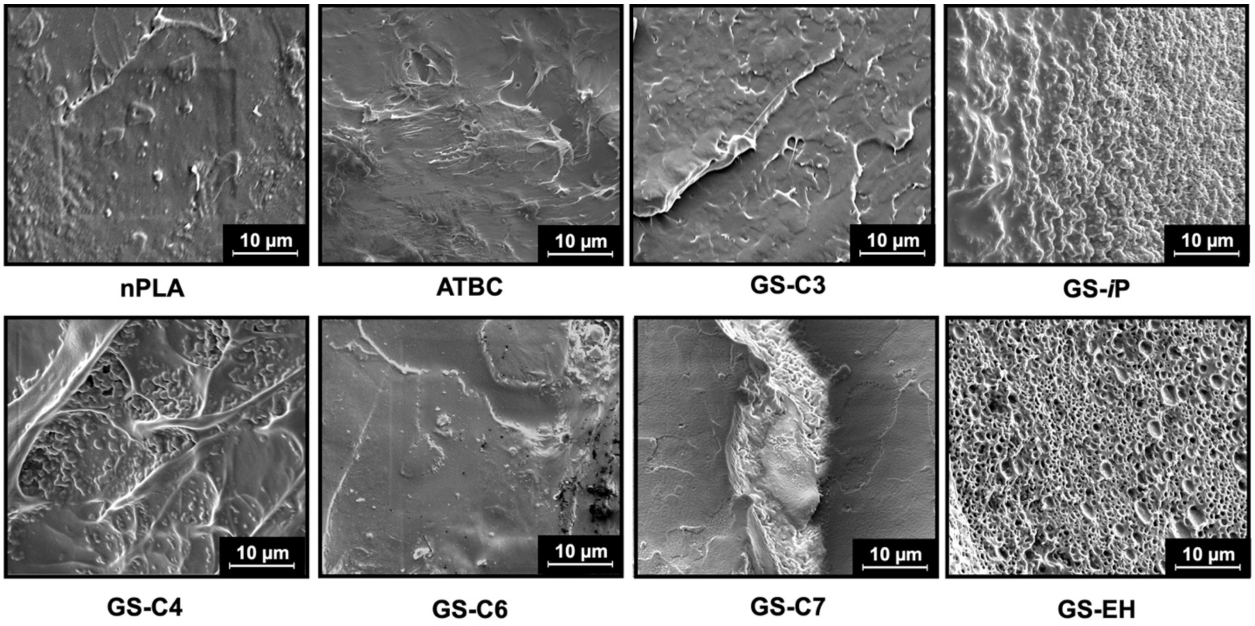

nPLA ATBC GS-C3 GS-*i*P

GS-C4 GS-C6 GS-C7 GS-EH

Figure 4.6. Freeze fractured surface SEM images of nPLA and 20 wt% melt-mixed blends (2500× magnification).

4.5.4 Plasticizer Leaching

The migration levels of each blend at 20 wt% were evaluated into three different food simulants to evaluate the applicability of each compound as potential plasticizers in food packaging material. Films were exposed to water, 3% v/v acetic acid, and 10% v/v ethanol for durations of one, five, and ten days at a temperature of 60 °C to monitor the evolution of migration over time (Figure 4.7). Significant differences amongst the blends were observed across all three simulants tested ($p < 0.001$). Previous studies have shown that lower molecular weight, more hydrophilic plasticizers generate higher degrees of migration out of PLA blends over time.[29, 49] A similar relationship was observed in our case as the blends produced with plasticizers comprised of longer alkyl chains exhibited the lowest percentage of mass loss over time. This effect of alkyl chain length was apparent amongst the plasticizers examined as GS-*i*P, functionalized with an *iso*-propyl chain, consistently displayed a higher mass loss after ten days than all other analogs tested ($p < 0.05$). In contrast, the blends produced with plasticizers functionalized with longer hexyl (GS-C6) and heptyl (GS-C7) alkyl chains displayed the lowest mass losses into all three simulants amongst the glycerol analogs, while ATBC exhibited the lowest mass loss overall.

Mass loss of the nPLA films remained relatively constant between 5-8% over time into all three simulants tested. This is attributed to the hydrolytic cleavage degradation of the ester bonds of the polymer into smaller oligomeric fragments.[50] Interestingly, blends produced with ATBC and GS-C6 exhibited a lower mass loss than nPLA into all three simulants examined ($p < 0.05$), suggesting that these plasticizers provide an added stability to the PLA matrix when exposed to aqueous solutions.

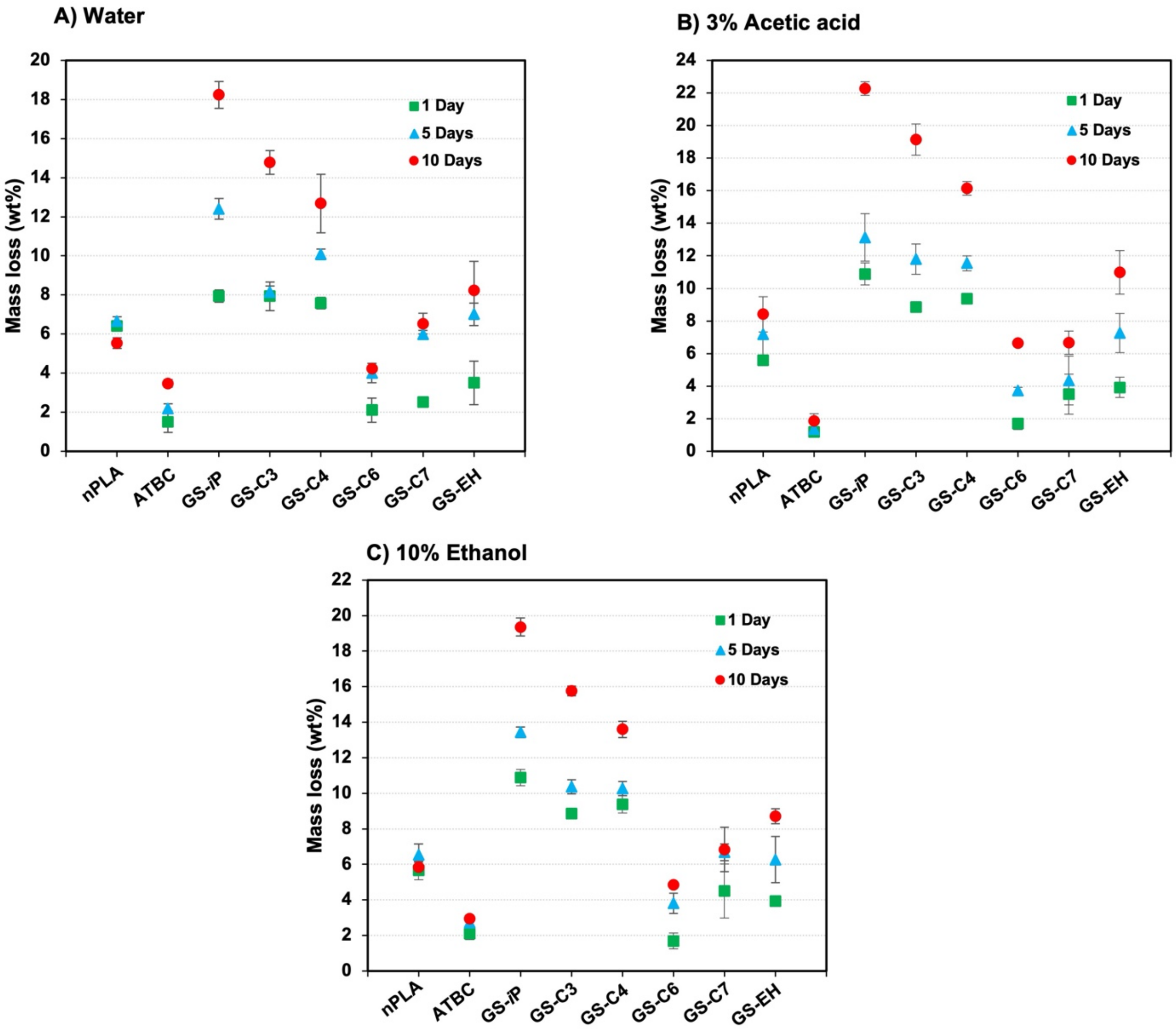

Figure 4.7. Mass loss due to leaching of nPLA and 20 wt% plasticized PLA film blends for durations of 1, 5, and 10 days in (A) water, (B) 3% v/v aqueous acetic acid, and (C) 10% v/v aqueous ethanol. (n=3, error bars represent standard deviation, means are shown).

4.5.5 Cell Viability Assay

While there are a number of promising alternative plasticizers for PLA being developed and reported in the literature,[51] the majority of these reports focus solely on the mechanical, thermal, and migration behaviour of the blends being produced and often overlook the evaluation of toxicity. The few examples which do include this type of analysis are essential in our progress towards developing all-encompassing green and sustainable plasticizers while avoiding regrettable substitution.[34] In line with this, we screened our new family of glycerol plasticizers for their cytotoxicity using an *in vitro* WST-8 cell viability assay[52] with HepG2 cells. The WST-8 reagent produces a formazan dye upon reduction by a metabolically active cell to allow for a direct quantification of viable cells and analysis of cytotoxicity. Plasticizers were administered to HepG2 cells at a concentration of 500 μM in 0.5% v/v DMSO (i.e., to enhance solubility in cell media) and absorbance readings were taken at time points of one and seven days. Despite the slight decrease in absorbance values after one day exposure to the plasticizers (Figure 4.8), there was no significant difference found between any of the plasticizers and the 0.5% v/v DMSO control ($p > 0.05$). However, after seven days exposure time, there was a significant difference found amongst the plasticizers tested ($p < 0.001$). Specifically, the absorbance values at day seven for GS-C7 and GS-EH were found to be significantly different than all the other plasticizers tested ($p < 0.05$), indicating a higher toxicity of these two longer chained or branched analogs. In contrast, there was no significant difference found between the shorter chain analogs (C6 or less) or ATBC with the 0.5% v/v DMSO control after seven days of exposure ($p > 0.05$). With GS-*i*P, GS-C3, GS-C4, and ATBC, the absorbance values increased between one and seven days which indicates that the cells were able to continue to proliferate in the presence of these compounds. Taken together, the results from this assay establish that the glycerol analogs comprised of alkyl chains equal to or shorter than C6 did not affect cell viability, whereas the longer chain or branched compounds demonstrated low to moderate levels of cytotoxicity and cell death. Follow-up work to investigate the biodegradation of the parent compounds, the identification of metabolites, and evaluation of their toxicity is proposed for future study.

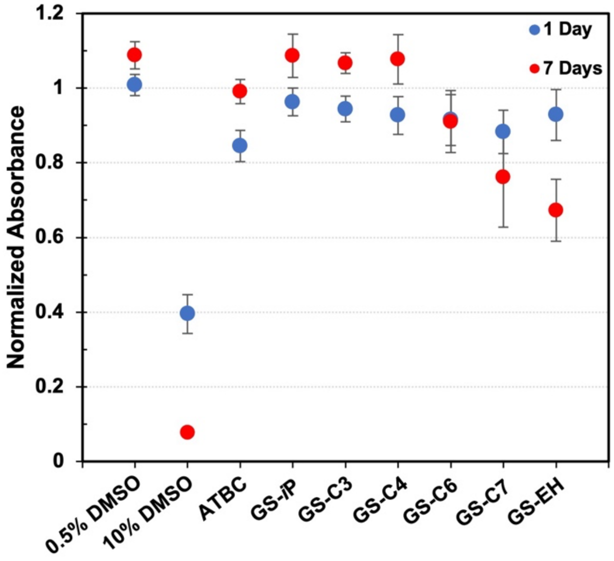

Figure 4.8. Normalized absorbance of HepG2 cells with and without the addition of plasticizers at 500 µM. 0.5% v/v DMSO was used as negative control while 10% v/v DMSO was used a positive control (*n*=3, error bars represent standard deviation, means are shown).

4.6 Conclusions

A family of bio-based plasticizers were designed and synthesized using solvent-free reaction conditions to produce flexible PLA which has potential applications as food packaging materials. Blends at 10 and 20 wt% plasticizer loadings were prepared using both solvent-casting and melt-mixing and analyzed to evaluate the effect of alkyl capper chain length and branching on plasticization efficiency and compared to blends produced using ATBC. In general, both the film and melt-mixed blends displayed higher thermal stability than blends prepared with ATBC. All glycerol analogs significantly reduced the T_g of nPLA, with the longer, linear substituted analogs providing the highest decrease in T_g of 44 °C relative to nPLA. The blends had excellent thermal stabilities with no significant decomposition observed below 208 °C at 20 wt% plasticizer loadings. Elongation at break values of up to 435% at 20 wt% plasticizer loadings were obtained in solvent-cast films, while the melt-mixed bulk samples reached elongation at break values up to 257%. The surface morphologies of the solvent-cast films and melt-mixed samples showed relatively smooth, homogenous mixtures for blends produced with plasticizers comprised of linear alkyl chains six carbons or smaller, whereas highly porous morphologies were obtained with branched or longer carbon chains. When exposed to different aqueous food simulants, film blends plasticized with shorter alkyl chain groups showed the highest degree of migration over time with up to 22% mass loss observed after ten days, while GS-C6 blends displayed excellent migration resistance (<7% mass loss). Finally, the glycerol plasticizers comprised of alkyl chains six carbons or less were shown to be non-toxic through an *in vitro* mammalian cell toxicity assay. Taken together, this work demonstrates the applicability of this family of bio-plasticizers to produce highly flexible, low leaching, and non-toxic PLA blends which have the potential to be used to manufacture PLA-based food packaging materials.

4.7 Funding

This research was funded using grants from the Natural Sciences and Engineering Research Council of Canada (Collaborative Research and Development Grants, CRDPJ 543853-2019 and Discovery Grants Program, RGPIN 05948-2019, RGPIN 06161-2018, 2016-03792) and the James McGill Chair program of McGill University. Student funding was provided by the Fonds de Recherche du Québec - Nature et Technologie (FRQNT), which granted Matthew W. Halloran a Doctoral Scholarship administered under the B2X program.

4.8 Acknowledgements

The authors would like to thank the McGill Chemistry Material Characterization facility for use of their facility. The operation of MC2 and their staff are supported by the Quebec Center for Advanced Materials (QCAM). They would also like to acknowledge and thank Dr. Robin Stein for running the ^{1}H NMR samples, and Mr. Gerald Lepkyj for his help with the Haake batch mixer.

4.9 References

1. Geyer, R.; Jambeck, J. R.; Law, K. L., Production, use, and fate of all plastics ever made. *Sci. Adv.* **2017,** *3* (7), e1700782.

2. Babu, R. P.; O'Connor, K.; Seeram, R., Current progress on bio-based polymers and their future trends. *Prog. Biomater.* **2013,** *2* (1), 8.

3. Vieira, M. G. A.; da Silva, M. A.; dos Santos, L. O.; Beppu, M. M., Natural-based plasticizers and biopolymer films: A review. *Eur. Polym. J.* **2011,** *47* (3), 254-263.

4. Bioplastics market data. https://www.european-bioplastics.org/market/ (accessed July 15th, 2022).

5. Sangeetha, V. H.; Deka, H.; Varghese, T. O.; Nayak, S. K., State of the art and future prospectives of poly(lactic acid) based blends and composites. *Polym. Compos.* **2018,** *39* (1), 81-101.

6. Zaaba, N. F.; Jaafar, M., A review on degradation mechanisms of polylactic acid: Hydrolytic, photodegradative, microbial, and enzymatic degradation. *Polym. Eng. Sci.* **2020,** *60* (9), 2061-2075.

7. Karamanlioglu, M.; Preziosi, R.; Robson, G. D., Abiotic and biotic environmental degradation of the bioplastic polymer poly(lactic acid): A review. *Polym. Degrad. Stab.* **2017,** *137*, 122-130.

8. Girija, B. G.; Sailaja, R. R. N.; Madras, G., Thermal degradation and mechanical properties of PET blends. *Polym. Degrad. Stab.* **2005,** *90* (1), 147-153.

9. Rouabah, F.; Dadache, D.; Haddaoui, N., Thermophysical and Mechanical Properties of Polystyrene: Influence of Free Quenching. *ISRN Polymer Sci.* **2012,** *2012*, 161364.

10. Balla, E.; Daniilidis, V.; Karlioti, G.; Kalamas, T.; Stefanidou, M.; Bikiaris, N. D.; Vlachopoulos, A.; Koumentakou, I.; Bikiaris, D. N., Poly(lactic Acid): A Versatile Biobased Polymer for the Future with Multifunctional Properties—From Monomer Synthesis, Polymerization Techniques and Molecular Weight Increase to PLA Applications. *Polymers* **2021,** *13* (11), 1822.

11. Jamshidian, M.; Tehrany, E. A.; Imran, M.; Jacquot, M.; Desobry, S., Poly-Lactic Acid: Production, Applications, Nanocomposites, and Release Studies. *Compr. Rev. Food Sci. Food Saf.* **2010,** *9* (5), 552-571.

12. Reichert, C. L.; Bugnicourt, E.; Coltelli, M. B.; Cinelli, P.; Lazzeri, A.; Canesi, I.; Braca, F.; Martinez, B. M.; Alonso, R.; Agostinis, L.; Verstichel, S.; Six, L.; De Mets, S.; Gomez, E. C.; Issbrucker, C.; Geerinck, R.; Nettleton, D. F.; Campos, I.; Sauter, E.; Pieczyk, P.; Schmid, M., Bio-Based Packaging: Materials, Modifications, Industrial Applications and Sustainability. *Polymers* **2020,** *12* (7).

13. Farah, S.; Anderson, D. G.; Langer, R., Physical and mechanical properties of PLA, and their functions in widespread applications — A comprehensive review. *Adv. Drug Deliv. Rev.* **2016,** *107*, 367-392.

14. Thurber, C.; Gu, L.; Myers, J. C.; Lodge, T. P.; Macosko, C. W., Toughening polylactide with a catalyzed epoxy-acid interfacial reaction. *Polym. Eng. Sci.* **2018,** *58* (1), 28-36.

15. Kowalczyk, M.; Piorkowska, E., Mechanisms of plastic deformation in biodegradable polylactide/poly(1,4-cis-isoprene) blends. *J. Appl. Polym. Sci.* **2012,** *124* (6), 4579-4589.

16. Quiles-Carrillo, L.; Montanes, N.; Lagaron, J. M.; Balart, R.; Torres-Giner, S., In Situ Compatibilization of Biopolymer Ternary Blends by Reactive Extrusion with Low-Functionality Epoxy-Based Styrene–Acrylic Oligomer. *J. Polym. Environ.* **2019,** *27* (1), 84-96.

17. Nagarajan, V.; Mohanty, A. K.; Misra, M., Perspective on Polylactic Acid (PLA) based Sustainable Materials for Durable Applications: Focus on Toughness and Heat Resistance. *ACS Sustain. Chem. Eng.* **2016,** *4* (6), 2899-2916.

18. Bocqué, M.; Voirin, C.; Lapinte, V.; Caillol, S.; Robin, J.-J., Petro-based and bio-based plasticizers: Chemical structures to plasticizing properties. *J. Polym. Sci., Part A-1: Polym. Chem.* **2016,** *54* (1), 11-33.

19. Godwin, A. D., 28 - Plasticizers. In *Applied Plastics Engineering Handbook*, Kutz, M., Ed. William Andrew Publishing: Oxford, 2011; pp 487-501.

20. Wei, X.-F.; Linde, E.; Hedenqvist, M. S., Plasticiser loss from plastic or rubber products through diffusion and evaporation. *NPJ Mater. Degrad.* **2019,** *3* (1), 18.

21. Billings, A.; Jones, K. C.; Pereira, M. G.; Spurgeon, D. J., Plasticisers in the terrestrial environment: sources, occurrence and fate. *Environ. Chem.* **2021,** *18* (3), 111-130.

22. Halloran, M. W.; Nicell, J. A.; Leask, R. L.; Marić, M., Small molecule plasticizers for improved migration resistance: Investigation of branching and leaching behaviour in PVC blends. *Mater. Today Commun.* **2021,** *29*, 102874.

23. Wright, R. J.; Bosch, R.; Gibson, M. I.; Christie-Oleza, J. A., Plasticizer Degradation by Marine Bacterial Isolates: A Proteogenomic and Metabolomic Characterization. *Environ. Sci. Technol.* **2020,** *54* (4), 2244-2256.

24. Chen, Y. H.; Wu, Y. J.; Chen, W. C.; Lee, T. S.; Tsou, T. C.; Chang, H. C.; Lo, S. W.; Chen, S. L., MEHP interferes with mitochondrial functions and homeostasis in skeletal muscle cells. *Biosci Rep* **2020,** *40* (4).

25. Vasconcelos, A. L.; Silva, M. J.; Louro, H., In vitro exposure to the next-generation plasticizer diisononyl cyclohexane-1,2-dicarboxylate (DINCH): cytotoxicity and genotoxicity assessment in human cells. *J. Toxicol. Environ. Health - A: Curr. Issues* **2019,** *82* (9), 526-536.

26. Gunaalan, K.; Fabbri, E.; Capolupo, M., The hidden threat of plastic leachates: A critical review on their impacts on aquatic organisms. *Water Res.* **2020,** *184*, 116170.

27. Chaos, A.; Sangroniz, A.; Gonzalez, A.; Iriarte, M.; Sarasua, J. R.; del Rio, J.; Etxeberria, A., Tributyl citrate as an effective plasticizer for biodegradable polymers: effect of plasticizer on free volume and transport and mechanical properties. *Polym. Int.* **2019,** *68* (1), 125-133.

28. Chaos, A.; Sangroniz, A.; Fernandez, J.; del Rio, J.; Iriarte, M.; Sarasua, J. R.; Etxeberria, A., Plasticization of poly(lactide) with poly(ethylene glycol): Low weight plasticizer vs triblock copolymers. Effect on free volume and barrier properties. *J. Appl. Polym. Sci.* **2019,** *137* (28).

29. Xuan, W. X.; Hakkarainen, M.; Odelius, K., Levulinic Acid as a Versatile Building Block for Plasticizer Design. *ACS Sustain. Chem. Eng.* **2019,** *7* (14), 12552-12562.

30. Zawada, K.; Plichta, A.; Jańczewski, D.; Hajmowicz, H.; Florjańczyk, Z.; Stępień, M.; Sobiecka, A.; Synoradzki, L., Esters of Tartaric Acid, A New Class of Potential "Double Green" Plasticizers. *ACS Sustain. Chem. Eng.* **2017,** *5* (7), 5999-6007.

31. Park, M.; Choi, I.; Lee, S.; Hong, S. J.; Kim, A.; Shin, J.; Kang, H. C.; Kim, Y. W., Renewable malic acid-based plasticizers for both PVC and PLA polymers. *J. Ind. Eng. Chem.* **2020,** *88*, 148-158.

32. Zych, A.; Perotto, G.; Trojanowska, D.; Tedeschi, G.; Bertolacci, L.; Francini, N.; Athanassiou, A., Super Tough Polylactic Acid Plasticized with Epoxidized Soybean Oil Methyl Ester for Flexible Food Packaging. *ACS Appl. Polym. Mater.* **2021,** *3* (10), 5087-5095.

33. Robert, T.; Friebel, S., Itaconic acid – a versatile building block for renewable polyesters with enhanced functionality. *Green Chem.* **2016,** *18* (10), 2922-2934.

34. Maertens, A.; Golden, E.; Hartung, T., Avoiding Regrettable Substitutions: Green Toxicology for Sustainable Chemistry. *ACS Sustain. Chem. Eng.* **2021,** *9* (23), 7749-7758.

35. Nerkar, M.; Ramsay, J. A.; Ramsay, B. A.; Kontopoulou, M., Dramatic Improvements in Strain Hardening and Crystallization Kinetics of PLA by Simple Reactive Modification in the Melt State. *Macromol. Mater. Eng.* **2014,** *299* (12), 1419-1424.

36. Donato, M. T.; Tolosa, L.; Gómez-Lechón, M. J., Culture and Functional Characterization of Human Hepatoma HepG2 Cells. *Methods. Mol. Biol.* **2015,** *1250*, 77-93.

37. Mascia, L.; Kouparitsas, Y.; Nocita, D.; Bao, X., Antiplasticization of Polymer Materials: Structural Aspects and Effects on Mechanical and Diffusion-Controlled Properties. *Polymers* **2020,** *12* (4), 769.

38. Hansen, C. M., Polymer additives and solubility parameters. *Prog. Org. Coat.* **2004,** *51* (2), 109-112.

39. Hansen, C. M., *Hansen solubility parameters: a user's handbook*. CRC press: 2007.

40. Van Krevelen, D. W.; Te Nijenhuis, K., *Properties of polymers: their correlation with chemical structure; their numerical estimation and prediction from additive group contributions*. Elsevier: 2009.

41. Murariu, M.; Da Silva Ferreira, A.; Alexandre, M.; Dubois, P., Polylactide (PLA) designed with desired end-use properties: 1. PLA compositions with low molecular weight ester-like plasticizers and related performances. *Polym. Adv. Technol.* **2008,** *19* (6), 636-646.

42. Bao, R.-Y.; Yang, W.; Wei, X.-F.; Xie, B.-H.; Yang, M.-B., Enhanced Formation of Stereocomplex Crystallites of High Molecular Weight Poly(l-lactide)/Poly(d-lactide) Blends from Melt by Using Poly(ethylene glycol). *ACS Sustain. Chem. Eng.* **2014,** *2* (10), 2301-2309.

43. Castro-Aguirre, E.; Iñiguez-Franco, F.; Samsudin, H.; Fang, X.; Auras, R., Poly(lactic acid)—Mass production, processing, industrial applications, and end of life. *Adv. Drug Deliv. Rev.* **2016,** *107*, 333-366.

44. Jem, K. J.; Tan, B., The development and challenges of poly (lactic acid) and poly (glycolic acid). *Adv. Ind. Eng. Polym. Res.* **2020,** *3* (2), 60-70.

45. Jeong, H.; Yuk, J. S.; Lee, H.; Kang, S.; Park, H.; Park, S. H.; Shin, J., Lactide-derived ester oligomers for highly compatible poly(lactide) plasticizer produced through an eco-friendly process: renewable resources, biodegradation, enhanced flexibility, and elastomeric performance. *Green Chem.* **2021,** *23* (19), 7549-7565.

46. Armstrong, R. W., Size effects on material yield strength/deformation/fracturing properties. *J. Mater. Res.* **2019,** *34* (13), 2161-2176.

47. Zhu, T. T.; Bushby, A. J.; Dunstan, D. J., Materials mechanical size effects: a review. *Mater. Technol.* **2008,** *23* (4), 193-209.

48. Rodrigues, N.; Benning, M.; Ferreira, A. M.; Dixon, L.; Dalgarno, K., Manufacture and Characterisation of Porous PLA Scaffolds. *Procedia CIRP* **2016,** *49*, 33-38.

49. Andersson, S. R.; Hakkarainen, M.; Albertsson, A.-C., Tuning the Polylactide Hydrolysis Rate by Plasticizer Architecture and Hydrophilicity without Introducing New Migrants. *Biomacromolecules* **2010,** *11* (12), 3617-3623.

50. Elsawy, M. A.; Kim, K.-H.; Park, J.-W.; Deep, A., Hydrolytic degradation of polylactic acid (PLA) and its composites. *Renewable Sustainable Energy Rev.* **2017,** *79*, 1346-1352.

51. Alhanish, A.; Abu Ghalia, M., Developments of biobased plasticizers for compostable polymers in the green packaging applications: A review. *Biotechnol. Prog.* **2021,** *37* (6), e3210.

52. Chamchoy, K.; Pakotiprapha, D.; Pumirat, P.; Leartsakulpanich, U.; Boonyuen, U., Application of WST-8 based colorimetric NAD(P)H detection for quantitative dehydrogenase assays. *BMC Biochem.* **2019,** *20* (1), 4.

5 Bio-based glycerol plasticizers for flexible Poly(vinyl chloride) blends

Matthew W. Halloran,[1] Jim A. Nicell,[2] Richard L. Leask,[1] Milan Marić*[1]

[1]Department of Chemical Engineering, McGill University, 3610 University Street, Montréal, QC, Canada, H3A 0C5

[2]Department of Civil Engineering, McGill University, 817 Sherbrooke Street West, Montreal, Quebec, Canada, H3A 0C3

*corresponding author

5.1 Preface

The following manuscript was published in 2022 in the *Journal of Applied Polymer Science* and served as a follow-up study to the manuscript presented in Chapter 4. As discussed in Chapter 2, both PLA and PVC have the unique ability to accept plasticizers into their polymer matrices to significantly improve their material properties. Despite their many inherent differences, effective plasticizers for PLA and PVC are usually ester-based compounds comprised of polar and non-polar groups which help to interact with the polar backbone of the polymer, while also increasing the free volume of the matrix. Therefore, to further broaden the scope of application of the proven non-toxic, bio-derived glycerol compounds, they were subsequently evaluated as PVC plasticizers. The main objective of this work was to evaluate these compounds as dual-purpose plasticizers for two distinct polymer matrices to demonstrate a wider scope of application. To the best of our knowledge, there are very few existing studies which evaluate plasticizer efficiency with different host polymers.

5.2 Abstract

A series of glycerol-based compounds were investigated for their application as plasticizers for flexible poly(vinyl chloride) (PVC) blends. The effect of plasticizer chemical structure on the performance, migration behaviour, and blend morphology were evaluated and compared to blends produced using the commercial plasticizer dioctyl terephthalate (DOTP). Blends containing 40 phr

(parts per hundred rubber) of glycerol-based plasticizer showed a considerable reduction (between 54 to 86 °C) in glass transition temperature (T_g) relative to neat PVC ($T_g \sim 80$ °C). Tensile testing of samples prepared with the glycerol analogs demonstrated higher ductility (elongation at break values of up to 97%) than DOTP (elongation at break value of 75%) at identical plasticizer loadings. The surface morphologies showed excellent incorporation of the glycerol plasticizers functionalized with alkyl chains longer than four carbons in length into the PVC matrix, whereas droplet formation was observed in blends with shorter chain glycerol derivatives. Leaching behaviour of the plasticized samples were evaluated into different media and showed that plasticizers comprised of branched, or longer alkyl chains produced 2- to 4-fold lower migration rates compared to those with shorter alkyl chains into polar solutions.

5.3 Introduction

Despite ongoing efforts to move towards sustainably sourced alternative plastics,[1] the demand for petroleum derived materials such as poly(vinyl chloride) (PVC) has continued to increase, with global production values exceeding 49 million tons in 2019.[2] As one of the most commonly used thermoplastics, PVC finds applications in numerous consumer items such as construction materials, medical tubing, films, and packaging materials.[2-5] While rigid, unplasticized PVC (UPVC) is advantageous in select industries, its brittleness and poor tensile properties limit its use in applications that require high flexibility and toughness.[6, 7] To improve the processing characteristics and fine tune the mechanical properties of the final products, external plasticizers (herein referred to as plasticizers) are blended with PVC during the manufacturing process.[7] In particular, plasticizers reduce the glass transition temperature (T_g) of PVC, while significantly improving flexibility and ductility of the final product.[7]

Historically, the global plasticizer market has been dominated by *ortho*-phthalates due to their low-cost of synthesis and excellent compatibility with PVC.[8] However, a growing awareness of their negative health effects on humans and animals[9-13] in conjunction with their pervasive nature in the environment,[14-18] have resulted in widespread restrictions on their production and use in consumer items in many of the developed nations around the world.[19-21] In spite of these well-established health and environmental concerns, the manufacture of *ortho*-phthalates accounted for nearly two-thirds of the 8 million tons of plasticizer produced in 2018.[22] Nevertheless, the rapidly growing phthalate-free plasticizer market is gaining traction and is projected to account for about one-fifth of the global market share by 2026.[22] In line with this, significant efforts have been made to design alternative plasticizers which can function as effectively, or superiorly to, existing *ortho*-phthalates.[23, 24] Concurrently, the motivation to substitute petroleum-based chemicals with renewably-sourced feedstocks has spurred the development of a number of promising bio-based plasticizers for PVC,[5] such as vanillic acid derivatives,[25] waste oil fatty-acids,[26] ricinoleic acid analogs,[27] malic acids,[28] and succinate esters,[29] to name a few.

As one of the major by-products generated during the production of biodiesel, glycerol has emerged as a high-value renewable building block that is commonly used in the synthesis of a variety of downstream products.[30] Glycerol is an ideal starting material for the design of consumer items, such as plasticizers, as it is both non-toxic and contains three hydroxyl groups which can be exploited for further synthetic transformations.[31] As such, a series of bio-based glycerol compounds were recently developed and shown to be effective plasticizers to produce highly flexible polylactide (PLA) materials with improved mechanical toughness.[32] In addition to improving the mechanical properties of PLA, a facile two-step synthetic route was developed to prepare the plasticizers thereby limiting the use of organic solvent while only generating water as a by-product. Furthermore, the compounds were shown to be non-toxic through an *in vitro* cytotoxicity assay. In this work, we aimed to expand the scope of application of these compounds by evaluating their potential as plasticizers for PVC while comparing their thermal and mechanical properties to blends produced using the commercial *ortho*-phthalate alternative plasticizer dioctyl terephthalate (DOTP, also sold under the tradename of Eastman 168) (Figure 5.1). Blends with the glycerol plasticizers at 40 phr (parts per hundred rubber, ~28.6 wt%) loadings were prepared and the effect of chemical structure on plasticization performance, surface morphology, and leaching behaviour were studied to investigate their capacity to function as multi-resin plasticizers for both PLA and PVC.

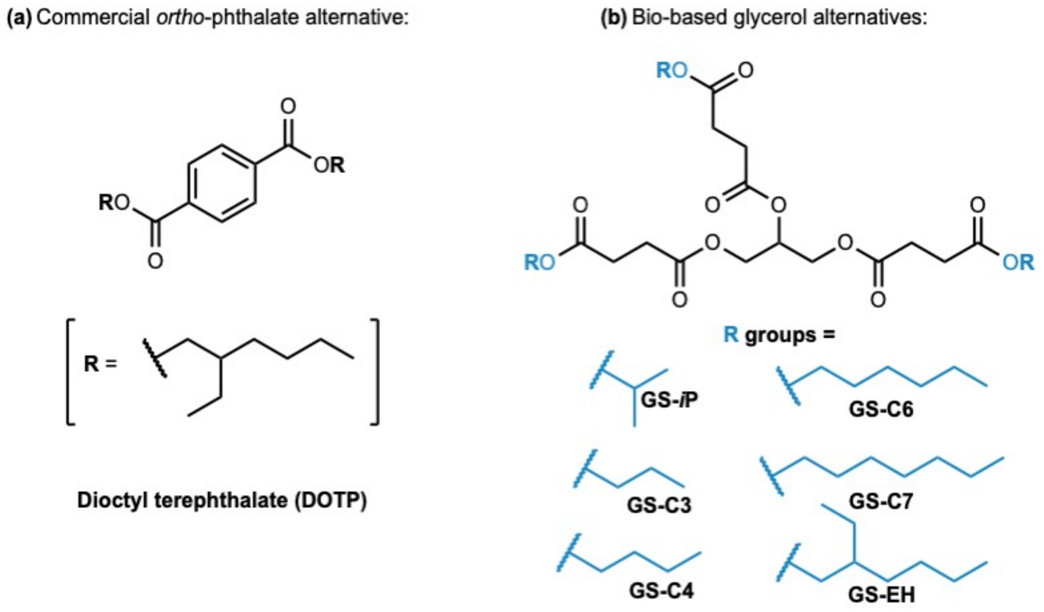

Figure 5.1. Chemical structure of plasticizers investigated in this study: (a) Commercially available dioctyl terephthalate (DOTP); and (b) Bio-based glycerol alternatives.

5.4 Experimental Methods

5.4.1 Materials and Reagents

Unplasticized PVC (UPVC; K50) was supplied by Solvay Benvic (Chevigny, France). *n*-heptanol (99.9%) was purchased from Arkema (King of Prussia, PA). Ethyl acetate (ACS grade), *iso*-propanol (ACS grade), toluene (ACS grade), *n*-hexanes (ACS grade), dichloromethane (ACS grade), ethanol (ACS grade), water (LCMS grade), stearic acid (97%), Sparkleen™ 1 detergent, and hexanes (ACS grade) were purchased from Fisher Scientific (Montreal, QC). Epoxidized soybean oil was purchased from Galata Chemicals (Southbury, CT). Dioctyl terephthalate (96%), succinic anhydride (99%), glycerol (99%), 2-ethylhexanol (99.6%), 1-butanol (99.8%), *n*-hexanol (99%), magnesium sulfate (99.5%), sodium bicarbonate (ACS reagent), and *p*-toluene sulfonic acid monohydrate (98.5%) were purchased from Sigma Aldrich (Oakville, ON). The cell-counting kit-8 (CCK-8) was purchased from Cedarlane Laboratories Ltd (Burlington, ON). The glycerol plasticizers used in this study were synthesized in accordance with a previously reported procedure.[32]

5.4.2 Extrusion of PVC/plasticizer blends

Blends at a plasticizer concentration of 28.6 weight percent (wt%), or 40 parts per hundred rubber (phr), were prepared through a two-step extrusion process with a Haake Minilab conical intermeshing twin-screw extruder (Thermo Electron Corporation, Beverly, MA). Initially, blends containing 20 phr of plasticizers were prepared in 3 g batches containing 20 phr plasticizer, 4 phr epoxidized soybean oil (heat stabilizer), and 5 phr stearic acid (lubricant). The batches were fed into the extruder and the extrudate was manually cut into small pieces. Each extruded batch was subsequently recycled through the extruder a second time to facilitate adequate mixing. In the second step, an additional 20 phr of the plasticizer was added and the material was passed through the extruder twice. The extruder was operated at 140 °C with a constant screw speed of 30 rpm throughout.

5.4.3 Compression Molding

Tensile testing bars were produced with a heated manual hydraulic press (Carver, Wabash, IN) outfitted with a temperature controller (Watlow, St. Louis, MO) using a steel mold. The 40 phr blends were placed into the molds and pressed at 165 °C in the following manner: 5 minutes at 5 metric tonnes, 10 minutes at 10 metric tonnes, and 10 minutes at 15 metric tonnes. Tensile test bar dimensions adhered to the standardized testing protocol ASTM-D638-03 for tensile properties: i.e., a thickness (T_0) of 1.4 mm; the width of narrow section (W_0) of 3.3 mm; a length of the narrow section of 17.8 mm; an overall length of 64 mm; and an overall width of 10 mm. Film specimens with a constant thickness of 0.25 mm were produced for leaching analysis using the same conditions described above using a 100 mm by 100 mm mold.

5.4.4 Thermal Gravimetric Analysis (TGA)

The thermal stability of the plasticized PVC blends was evaluated using a TA Instruments Q500 (New Castle, DE) under nitrogen flow of 90 mL/min from 25 to 600 °C at a heating rate of 10 °C/min.

5.4.5 Differential Scanning Calorimetry (DSC)

The glass transition temperature (T_g) of each blend at 40 phr was measured by temperature-modulated differential scanning calorimetry (mDSC) using a TA Instruments Q2000 (New Castle, DE). Two heating cycles from -90 to 100 °C superimposed by a sinusoidal modulation of 1.27 °C with a period of 60 s were carried out. The T_g was then determined from the reversible heat flow of the second heating cycle using the automated glass/step transition tool in the TA Instruments Universal Analysis 2000 software. See Supporting Information for DSC curves.

5.4.6 Scanning Electron Microscopy (SEM)

The morphology of the samples was investigated using scanning electron microscopy (SEM), using a FEI Quanta 450 Environmental Scanning Electron Microscope (FE-ESM) operating under high vacuum and acceleration voltage of 10.0 kV. The extruded specimens were freeze-fractured with liquid nitrogen and mounted on aluminum stubs with carbon tape. All samples were first etched with *n*-hexanes to selectively remove the plasticizers, and then sputter-coated with 4 nm of platinum prior to analysis using a Leica Microsystems EM ACE600 High Resolution Sputter Coater.

5.4.7 Tensile Testing

Tensile testing was performed with a Shimadzu Easy Test instrument (Kyoto, Japan) equipped with a 500 N load cell in accordance with a previously used protocol.[33] Each specimen was desiccated for at least 48 hours prior to analysis. The exact dimensions of each dumbbell-shaped test specimen were recorded using a digital micrometer and adhered to the dimensions described in ASTM D638-03: thickness (*T*) of 1.4 mm; a width of narrow section (*W*) of 3.3 mm; a length of narrow section (*L*) of 17.8 mm; an overall length of 64 mm; and an overall width of 10 mm. Test bars were clamped and subjected to a strain rate of 5 mm/min. The stress-strain curves were used to obtain values for strain (percent elongation) and stress at break. Five specimens were tested for each blend.

5.4.8 Plasticizer Leaching

The ASTM method D1239-14, “Resistance of Plastic Films to Extraction by Chemicals” was used as a template for leaching tests. Compression molded films blended with 40 phr of plasticizer were used. Film specimens were cut into square fragments measuring 20 mm by 20 mm by 0.25 mm. Four simulants were selected for leaching analysis – water, 50% v/v ethanol in water, hexanes, and 1 wt% Sparkleen™ detergent in water for four hours at 50 °C. Each specimen was pre-weighed, placed into a 24-mL glass vial containing 20 mL of each simulant, capped, and then placed into an incubator shaker set at 60 rpm. Each experiment was run in triplicate. After four hours, the film specimens were removed from the vials, wiped with tissue paper, and dried in a vacuum oven at room temperature for 7 days until a constant weight was reached. The film specimens were then re-weighed, and the percent weight loss of the plasticizer was calculated using Equation (1) where W_i is the initial mass of the specimen, W_f is the final mass of the specimen, and 0.286 represents the weight percentage of plasticizer in the 40 phr blends used:

$$Plasticizer\ Loss\ (\%) = \frac{W_i - W_f}{W_i \times 0.286} \times 100\% \qquad (1)$$

5.4.9 Cell Viability Assay

Testing was conducted according to a previously reported procedure using the human hepatocellular carcinoma (HepG2) cell line and a cell-counting kit (CCK-8).[32] The CCK-8 uses a tetrazolium salt (WST-8) reagent which produces a formazan dye upon reduction by a metabolically active cell to allow for a direct quantification of viable cells left in the culture. Briefly, cells were plated in 96-well plates at a concentration of 5000 cells/well and incubated for 24 hours to allow for cell adhesion. Media was removed and 150 μL of sterilized solutions comprised of cell media and 500 μM of each plasticizer in 0.5% v/v DMSO were added to the appropriate wells and the plates were returned to the incubator. A negative control of 0.5% v/v DMSO was used and a positive control of 10% v/v DMSO was used. Each solution was run in triplicate on the same plate. After one and seven days, samples of the media were removed, and 100 μL of media containing 10% v/v WST-8 reagent was added to each well and the plates were then returned to the incubator for two hours. After two hours, absorbance values at 450 nm were read using a Bio-Rad Benchmark Plus plate reader (CA, USA). Each absorbance value was then normalized with respect to values obtained from wells containing cells seeded at 5000 cells/well. Each plate was analyzed in triplicate and the average absorbance values are reported.

5.4.10 ^{1}H NMR Spectroscopy

^{1}H NMR spectra were obtained using a Bruker AVIIIHD 500 MHz spectrometer (MA, USA) with an average of 16 scans using deuterated chloroform ($CDCl_3$) as the solvent.

5.4.11 Statistical Analysis

Statistical analysis was performed using GraphPad Prism 5 software. Difference between the mean values of the plasticizers were analyzed using a one-way-ANOVA test with a Bonferroni post-test to evaluate differences between each type. A p value less than 0.05 was interpreted as significant.

5.5 Results and Discussion

5.5.1 Theoretical Prediction of Plasticizer Compatibility with PVC

A defining characteristic of an effective plasticizer is its compatibility with the host polymer it is blended with.[34] This complex relationship can be evaluated theoretically using the Hansen Solubility Parameters (HSP) and the interaction radius (IR) in which predictions are made based on the molecular weight and chemical structure of the plasticizer relative to the host polymer.[35] In general, a plasticizer is considered to be compatible with the host polymer if it has similar HSP values and a low interaction radius, which is usually < 8 $J^{1/2}/cm^{3/2}$.[36] Here, the HSP and IR values for PVC, DOTP, and the six glycerol analogs were calculated according to the group contribution methods of Hoftzyer and Van-Krevelen (Table 5.1).[37] Based on these calculations, the glycerol plasticizers substituted with the shorter *iso*-propyl and propyl alkyl chains (GS-*i*P and GS-C3) have the largest IR values of 8.2 and 8.1, respectively, deeming them theoretically less compatible than DOTP and their longer chained counterparts which have IR values ranging from 7.7 to 6.7. While the calculated HSP and IR values help to provide some insight into compatibility between the host polymer and plasticizer molecule, these serve mainly as theoretical predictors that must be verified experimentally.

Table 5.1. Calculated Hansen solubility parameter terms and interaction radii for PVC and plasticizers. See Supporting Information for calculations and formulas used.

	δ ($J^{1/2}/cm^{3/2}$)[a]	**δ_v ($J^{1/2}/cm^{3/2}$)[b]**	**δ_h ($J^{1/2}/cm^{3/2}$)[c]**	**IR ($J^{1/2}/cm^{3/2}$)[d]**
PVC	22.0	21.8	3.0	-
DOTP	18.6	17.6	6.1	6.7
GS-*i*P	19.8	17.4	9.8	8.2
GS-C3	20.0	17.4	9.8	8.1
GS-C4	19.7	17.4	9.3	7.7
GS-C6	19.3	17.4	8.6	7.1
GS-C7	19.2	17.3	8.2	6.8
GS-EH	18.9	17.1	7.9	6.8

[a] Overall Hansen Solubility Parameter. [b] Combination of dispersion (δ_d) and polar forces (δ_p). [c] Hydrogen bonding parameter. [d] Interaction radius

5.5.2 Thermal Stability of Blends

The thermal stabilities of each blend at 40 phr plasticizer loading were evaluated using thermal gravimetric analysis (TGA), with the onset temperature at weight loss with 10% (T_{10}) taken for comparison. The TGA traces of each blend are shown in Figure 5.2 along with the T_{10} values. Amongst the glycerol analogs, the compounds functionalized with longer alkyl or branched chains displayed higher T_{10} values, with the GS-EH blend displaying the highest value of 240 °C. In comparison to the blend prepared with commercial plasticizer DOTP (T_{10} of 238 °C), the glycerol analogs displayed relatively similar T_{10} values; demonstrating that they are also capable of being processed under analogous conditions without any significant decomposition occurring.

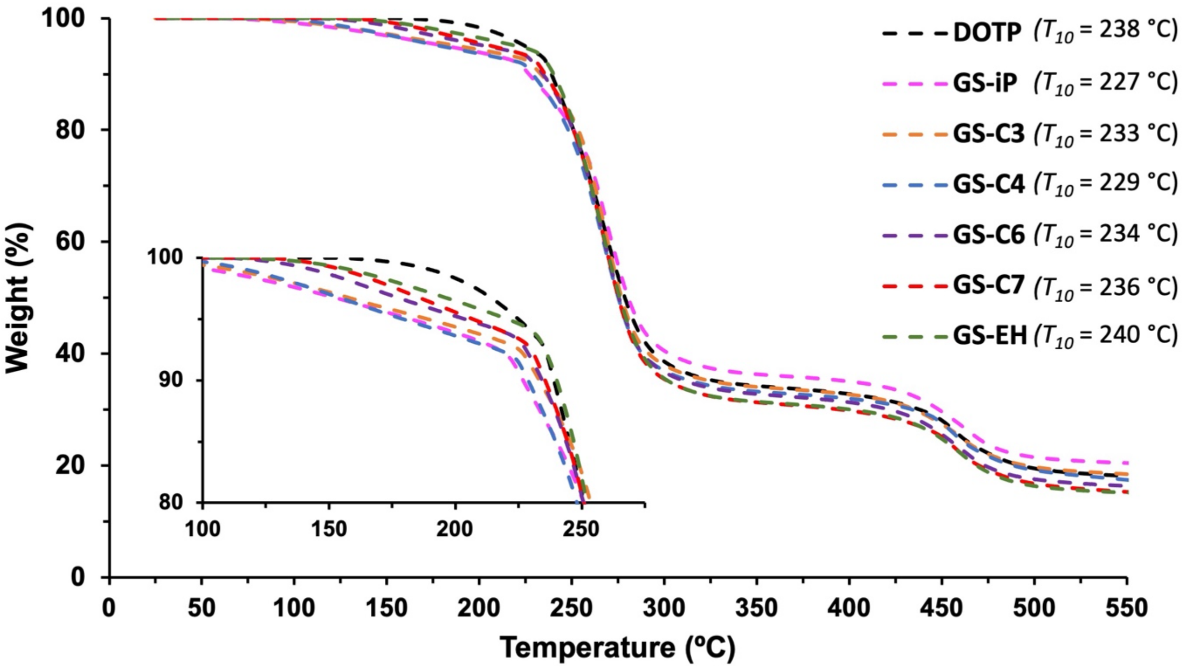

Figure 5.2. TGA traces of PVC/plasticizer blends at 40 phr (i.e., 28.6 wt% plasticizer).

5.5.3 Glass Transition Temperature

In addition to improving the mechanical and processing properties of PVC, an effective plasticizer should reduce the glass transition temperature (T_g) of the blend.[7] Relative to unplasticized PVC (UPVC) with a $T_g \sim 80$ °C,[6] each of the compounds showed a significant reduction in the T_g at both 20 and 40 phr plasticizer loadings (Table 5.2). At 20 phr, the T_g values ranged from 27 °C obtained with GS-C3 to 14 °C obtained with GS-C6, which were comparable to that of DOTP at the same loading (T_g of 16 °C). In contrast, at 40 phr, the T_g values ranged from 10 °C obtained with GS-C3 and GS-*i*P to -8 °C obtained with GS-C7. Apart from the GS-EH 40 phr blend, a noticeable trend amongst the glycerol analogs was observed in that the compounds substituted with the longer alkyl chains displayed the largest reduction in T_g. This is consistent with a previous report in which a greater reduction in T_g was also observed for diester succinate plasticizers functionalized with longer alkyl chains.[38]

Table 5.2. Thermal and mechanical properties of plasticized PVC blends at 20 and 40 phr (i.e., 15.5 and 28.6 wt% plasticizer, respectively).

Plasticizer	T_g – 20 phr blend (°C)	T_g – 40 phr blend (°C)	Strain at break (%EL)[a]	Stress at break (MPa)[a]
DOTP	16	-6	73 ± 6	7.6 ± 0.8
GS-*i*P	23	9	39 ± 1	9.3 ± 0.3
GS-C3	27	10	23 ± 5	4.9 ± 1.4
GS-C4	21	-2	97 ± 9	7.9 ± 0.6
GS-C6	14	-2	80 ± 9	6.9 ± 1.0
GS-C7	16	-8	76 ± 3	7.8 ± 0.6
GS-EH	23	6	76 ± 4	7.9 ± 1.4

[a] 40 phr blend, $n = 5$

5.5.4 Mechanical Properties

The tensile testing results for the PVC blends at 40 phr plasticizer loading are summarized in Figure 5.3, including representative stress versus strain in percent (%) elongation curves, elongation at break data, and stress at break values (values presented in Table 5.2). Significant differences were observed in both the stress at break and elongation at break between the compounds tested at 40 phr plasticizer loading ($p < 0.001$). In comparison with UPVC which is known for its brittleness and poor tensile properties at room temperature,[6] all of the plasticized blends showed significant improvements in elongation at break with average values ranging from 23% for GS-C3, to 97% for GS-C4 (Figure 5.3B). Amongst the glycerol analogs, there was a noticeable effect of the alkyl chain length on elongation at break (GS-*i*P and GS-C3 significantly different than GS-C4, GS-C6, GS-C7, and GS-EH, $p < 0.001$). It has previously been shown that poly(ε-caprolactone) (PCL) star shaped and linear dibenzoate alternative plasticizers demonstrated elongation at break values between 85 and 115% at 40 phr plasticizer loadings,[39, 40] while linear succinate and fumarate based plasticizers obtained elongation at break values of up to 90% at 40 phr loadings.[41] Therefore, the obtained results for the glycerol-succinate plasticizers are comparable to previous reports of alternative plasticizers.

Plasticizers functionalized with alkyl chains containing four or more carbon atoms showed significant improvement in elongation at break relative to UPVC, whereas the shorter chain analogs produced stiffer, less ductile blends. A similar relationship was observed with linear succinate diester plasticizers as the largest improvement in tensile properties was observed for plasticizers functionalized with alkyl chain lengths between four and seven carbons.[38] The complex relationship between chemical structure and plasticizer efficiency is one which has been studied both practically and computationally by many academic groups,[23, 42, 43] and highlights the challenge of striking a fine balance between polar and non-polar functional groups on the plasticizer molecule. The polar functional groups are essential to compatibilize the plasticizer with the polar PVC backbone and serve as hydrogen-bond acceptors, while the non-polar groups disrupt the PVC chain-chain interactions and increase the free volume of polymer matrix[44] (for a more in-depth discussion on this topic as well as additional theories of plasticization, we direct the readers to the works of Daniels and Mascia).[34, 45] In the case of GS-*i*P and GS-C3, they are functionalized with relatively short alkyl chains, which may hinder their ability to effectively permeate the PVC matrix and plasticize the blend; explaining the inferior mechanical and thermal properties of these blends. Conversely, there was no relationship between molecular structure and performance when considering the stress at break values, with only GS-C3 producing significantly different values than the other blends ($p < 0.05$).

Taken together, the tensile results demonstrate that this series of glycerol compounds can effectively plasticize PVC, with the analogs comprised of alkyl chains ranging in length from four to six showing the highest improvements in elongation at break. As these compounds have previously been shown to plasticize PLA, this work demonstrates their added potential as highly effective alternative plasticizers for PVC.

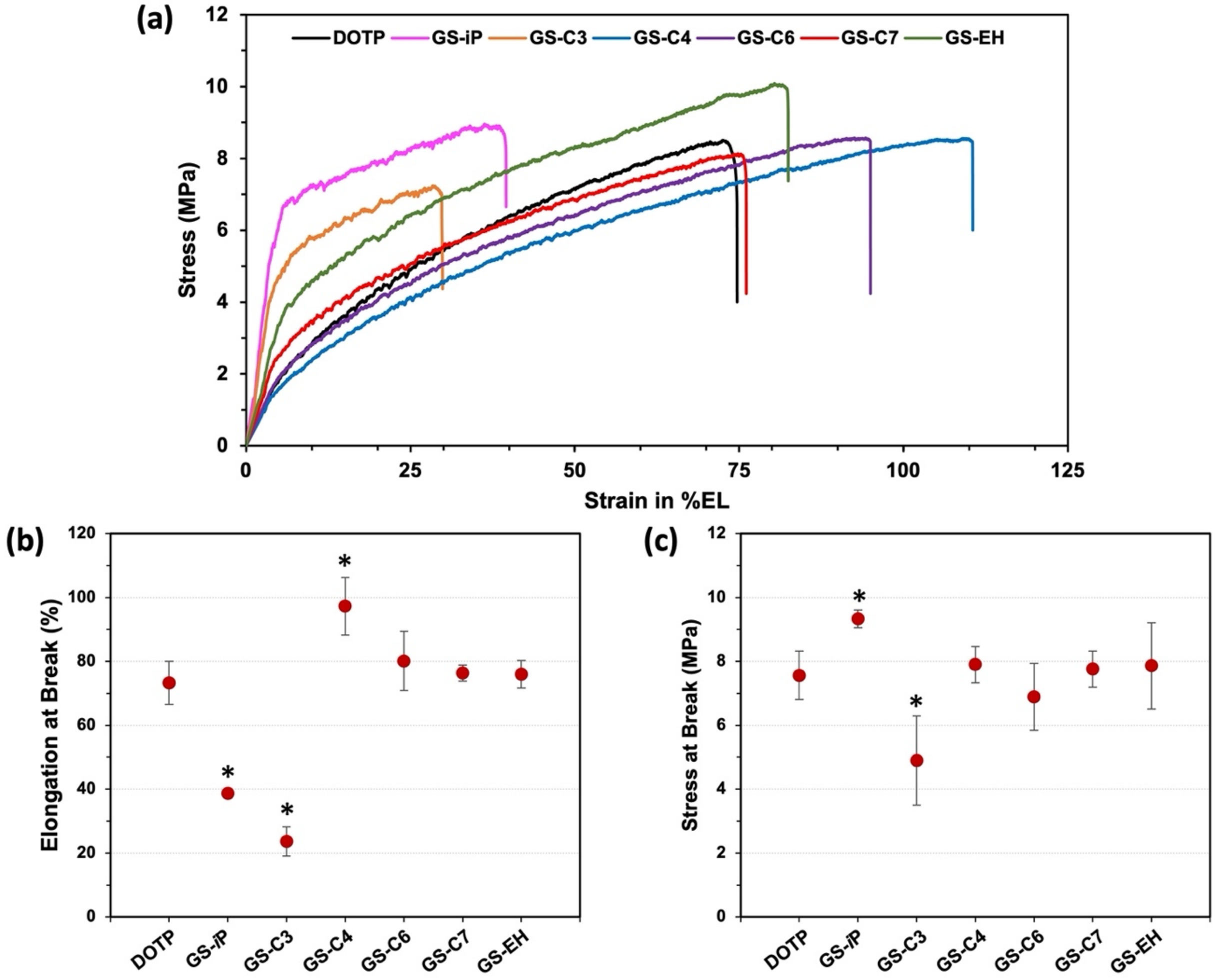

Figure 5.3. Tensile testing results of PVC/plasticizer blends at 40 phr. (a) Representative stress vs. strain curves in % elongation. (b) Elongation at break. (c) Stress at break. ($n = 5$; error bars represent standard deviation; means are shown). Symbols (*) above error bars indicate statistically significant differences ($p < 0.001$, Bonferroni post-test). (b) GS-*i*P, GS-C3, GS-C4 statistically significantly different than DOTP; (c) GS-*i*P, GS-C3 statistically significantly different than DOTP.

5.5.5 Blend Morphology

The morphology of the PVC/plasticizer blends at 40 phr loadings was characterized with SEM (Figure 5.4). Extruded samples were freeze-fractured and etched with *n*-hexanes to selectively remove the plasticizers from the blend and enhance the contrast between phases. The obtained surface morphologies for DOTP, GS-C4, GS-C6, GS-E7, and GS-EH reveal relatively homogenous blends, with very little presence of droplet formation or porosity. In contrast, blends produced with GS-*i*P and GS-C3 reveal highly porous morphologies, suggesting poor miscibility of these compounds in the PVC matrix leading to their coalescence into droplets.[46] These findings further corroborate the notion that the alkyl chain length plays a significant role in the miscibility (and ultimately the effectiveness) of ester-based plasticizers in PVC blends.[41, 47] Additionally, this apparent incompatibility between GS-*i*P and GS-C3 with PVC agrees with our theoretical HSP and IR calculations presented in Table 1.

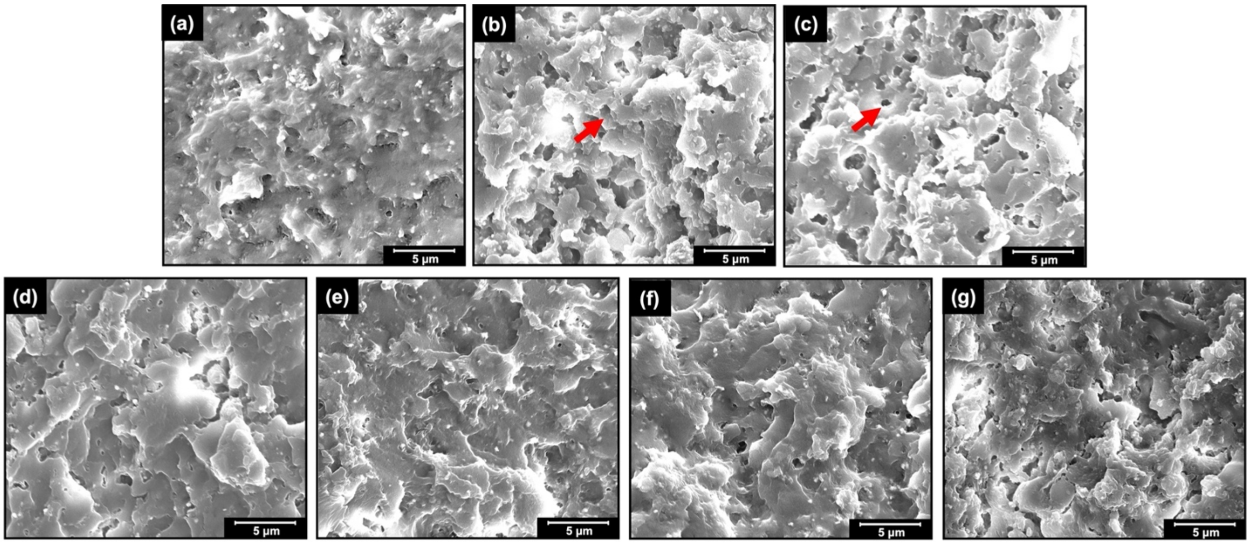

Figure 5.4. Representative SEM images of freeze fractured surface of PVC/plasticizer blends at 40 phr. (a) DOTP, (b) GS-*i*P, (c) GS-C3, (d) GS-C4, (e) GS-C6, (f) GS-C7, (g) GS-EH. (5000× magnification)

5.5.6 Plasticizer Leaching

The leaching behaviour of each blend at 40 phr was evaluated in several different types of solutions under accelerated conditions. Plasticized film samples were exposed to a 1% w/v detergent solution, water, 50% v/v ethanol, and hexanes for a duration of four hours at 50 °C (Figure 5.5). These four simulants were selected to evaluate plasticizer leaching under both polar and non-polar conditions, while studying the relationship between alkyl chain length on migration behaviour. Significant differences amongst the blends were observed across all four of the simulants tested ($p < 0.001$). Overall, moderate to low levels of plasticizer loss (between 4 and 23%) were observed for migration tests into water and the detergent solutions, with statistically equivalent values being obtained between both simulants for each plasticizer ($p > 0.05$). The highest values of plasticizer loss were observed for GS-*i*P and GS-C3 (23% and 22%, respectively), while less than 10% loss was observed with DOTP and GS-EH. Both GS-*i*P and GS-C3 are functionalized with short linear or branched alkyl chains, rendering them more polar, and therefore more soluble into water and the detergent solution. Conversely, the relatively long and branched 2-ethylhexyl chain substituents on DOTP and GS-EH make these compounds more greasy and non-polar, and less likely to migrate out of the PVC matrix into the polar simulants. This structural relationship has been observed previously, wherein longer chain succinates, fumarates, and maleates resulted in lower levels of migration into water.[48] Similarly, studies of plasticizer loss into a 50% ethanolic solution revealed a comparable relationship in that the longer chain species DOTP, GS-C7, and GS-EH exhibited lower levels of migration.

The opposite relationship was observed using hexanes, as the longer chained compounds showed the highest percentage of plasticizer loss; i.e., DOTP, GS-C6, GS-C7, and GS-EH at 55%, 40%, 42%, and 38% loss, respectively. A similar relationship was observed in a series of alkyl-capped PCL star-shaped plasticizers in which the compounds functionalized with longer aliphatic chains displayed higher levels of migration into hexanes.[40] Despite the fact that DOTP and GS-EH are functionalized with the same 2-ethylhexyl chain, the branched structure of GS-EH (which emanates from the glycerol core) allows it to remain further embedded in the PVC matrix and resist migration from the blend when exposed to non-polar media.[33]

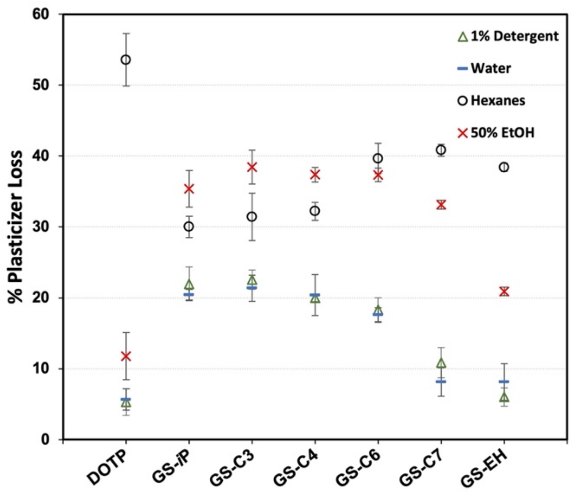

Figure 5.5. Plasticizer loss due to leaching of 40 phr plasticized PVC film blends at 50 °C in 1% w/v detergent solution, water, 50% v/v aqueous ethanol, and hexanes. (n=3; means are shown, with error bars representing standard deviation).

5.5.7 Cytotoxicity

In addition to evaluating the thermal and mechanical properties of the plasticizers in PVC blends, we aimed to investigate their toxicity through an *in vitro* mammalian cell assay. It was previously shown via an *in vitro* cytotoxicity assay that the glycerol compounds functionalized with linear chains of six carbons or less are non-toxic, whereas the longer chain or branched analogs showed mild levels of toxicity over a seven-day period.[32] Here, we also evaluated two widely used phthalate-based plasticizers for their cytotoxicity – di(2-ethylhexyl) phthalate (DEHP), and DOTP. Briefly, each compound was administered to HepG2 cells at a concentration of 500 μM in 0.5% v/v DMSO and absorbance readings were taken at time points of one and seven days to quantify viable cell population. Neither DEHP nor DOTP absorbances were found to be significantly different than the 0.5% v/v DMSO control ($p > 0.05$) after seven-day exposure, suggesting no cytotoxicity of these compounds in our assay (Figure 5.6), and supporting previous reports classifying these compounds as low hazard.[49] When compared to the glycerol compounds after seven-day exposure, the absorbance values of DEHP and DOTP were found to be significantly different than GS-C7 and GS-EH ($p < 0.01$), whereas no difference was found between DEHP/DOTP and the shorter alkyl chain derivatives ($p > 0.05$). Interestingly, although DEHP, DOTP, and GS-EH are functionalized with the same 2-ethylhexyl chain, different levels of cytotoxicity were observed between GS-EH and the phthalates after seven days. This difference in toxicity could be due to different levels of solubility, or to a partial hydrolytic biodegradation occurring over time with GS-EH in which one of the 2-ethylhexyl chains is cleaved and subsequently oxidized to form small quantities of 2-ethylhexanal which has been shown to be toxic.[50] However, over a relatively short incubation time of seven days this would not occur with the phthalate diesters as they have been shown to have higher stability and are more resistant to hydrolysis.[51]

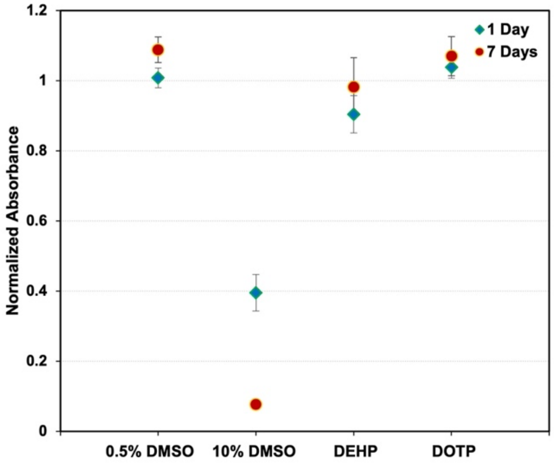

Figure 5.6. Normalized absorbance of HepG2 cells with and without the addition of plasticizers at 500 μM. 0.5% v/v DMSO was used as negative control while 10% v/v DMSO was used a positive control (n = 3; means are shown, with error bars representing standard deviation).

5.6 Conclusions

In this work, a series of glycerol-based compounds were investigated as plasticizers in blends with PVC. At 40 phr plasticizer loadings, all the glycerol plasticizers showed significant reductions in T_g's (ranging from 8 °C to -8 °C) and elongations of up to 97% were achieved with GS-C4. A noticeable effect of structure on plasticization efficiency was observed as the analogs functionalized with alkyl chains shorter than four carbons in length (GS-*i*P and GS-C3) demonstrated inferior thermal and mechanical properties than their longer chain counterparts. The surface morphologies revealed similar structural relationship differences as larger droplet formation was evident in blends plasticized with GS-*i*P and GS-C3, whereas the longer chained analogs formed more homogenous blends. Leaching tests were conducted into several different types of media and demonstrated that the longer chain glycerol analogs, GS-C7 and GS-EH, showed comparable migration behaviour to DOTP when exposed to polar environments. Finally, an *in vitro* cytotoxicity assay revealed no detectable levels of toxicity for either DOTP or DEHP, corroborating previous claims. In summary, this work illustrates an additional application for this family of glycerol compounds that were previously used to plasticize PLA by showing their ability to generate highly flexible PVC materials.

5.7 Funding

This research was supported by the Natural Sciences and Engineering Research Council of Canada (Collaborative Research and Development Grants, CRDPJ 543853-2019 and Discovery Grants Program, RGPIN 05948-2019, RGPIN 06161-2018, 2016-03792) and the James McGill Chair program of McGill University. Student funding was provided by the Fonds de Recherche du Québec - Nature et Technologie (FRQNT), which granted Matthew W. Halloran a Doctoral Scholarship administered under the B2X program.

5.8 Acknowledgements

The authors thank the McGill Chemistry Characterization facility for use of their facility, whose operations are supported by the Quebec Center for Advanced Materials (QCAM). They also acknowledge and thank Lisa Danielczak for her help with the toxicological assay.

5.9 References

1. Rosenboom, J.-G.; Langer, R.; Traverso, G., Bioplastics for a circular economy. *Nat. Rev. Mater.* **2022,** *7* (2), 117-137.

2. Zhang, Z. M.; Jiang, P. P.; Liu, D. K.; Feng, S.; Zhang, P. B.; Wang, Y. T.; Fu, J. H.; Agus, H., Research progress of novel bio-based plasticizers and their applications in poly(vinyl chloride). *J. Mater. Sci.* **2021,** *56* (17), 10155-10182.

3. Groh, K. J.; Backhaus, T.; Carney-Almroth, B.; Geueke, B.; Inostroza, P. A.; Lennquist, A.; Leslie, H. A.; Maffini, M.; Slunge, D.; Trasande, L.; Warhurst, A. M.; Muncke, J., Overview of known plastic packaging-associated chemicals and their hazards. *Sci. Total Environ.* **2019,** *651*, 3253-3268.

4. Jamarani, R.; Halloran, M. W.; Panchal, K.; Garcia-Valdez, O.; Mafi, R.; Nicell, J. A.; Leask, R. L.; Maric, M., Additives to prevent the formation of surface defects during poly(vinyl chloride) calendering. *Polym. Eng. Sci.* **2021,** *61* (4), 1209-1219.

5. Kumar, S., Recent Developments of Biobased Plasticizers and Their Effect on Mechanical and Thermal Properties of Poly(vinyl chloride): A Review. *Ind. Eng. Chem. Res.* **2019,** *58* (27), 11659-11672.

6. Fischer, I.; Schmitt, W. F.; Porth, H. C.; Allsopp, M. W.; Vianello, G., Poly(vinyl chloride). In *Ullmann's Encyclopedia of Industrial Chemistry*, Wiley-VCH: Weinheim, Germany, 2014

7. Godwin, A. D., 28 - Plasticizers. In *Applied Plastics Engineering Handbook*, Kutz, M., Ed. William Andrew Publishing: Oxford, 2011; pp 487-501.

8. Lorz, P. M.; Towae, F. K.; Enke, W.; Jäckh, R.; Bhargava, N.; Hillesheim, W., Phthalic Acid and Derivatives. In *Ullmann's Encyclopedia of Industrial Chemistry*, 2007.

9. Camacho, L.; Latendresse, J. R.; Muskhelishvili, L.; Law, C. D.; Delclos, K. B., Effects of intravenous and oral di (2-ethylhexyl) phthalate (DEHP) and 20% Intralipid vehicle on neonatal rat testis, lung, liver, and kidney. *Food Chem. Toxicol.* **2020**, 111497.

10. Chang, C.-H.; Chen, C.-F.; Tsai, Y.-A.; Wang, S.-L.; Huang, P.-C.; Chen, B.-H.; Wu, M.-T.; Chen, C.-C.; Hsiung, C. A.; Chen, M.-L., The sex-specific association of phthalate exposure with DNA methylation and characteristics of body fat in children. *Sci. Total Environ.* **2020**, 139833.

11. Nadeem, A.; Ahmad, S. F.; Al-Harbi, N. O.; Al-Ayadhi, L. Y.; Attia, S. M.; Alasmari, A. F.; Sobeai, H. M. A.; Bakheet, S. A., Ubiquitous plasticizer, Di-(2-ethylhexyl) phthalate enhances existing inflammatory profile in monocytes of children with autism. *Toxicology* **2020**, 152597.

12. Wang, Y.; Zhu, H.; Kannan, K., A Review of Biomonitoring of Phthalate Exposures. *Toxics* **2019,** *7* (2), 21.

13. Zhang, J.; Powell, C. A.; Kay, M. K.; Park, M. H.; Meruvu, S.; Sonkar, R.; Choudhury, M., A moderate physiological dose of benzyl butyl phthalate exacerbates the high fat diet-induced diabesity in male mice. *Toxicol Res (Camb)* **2020,** *9* (4), 353-370.

14. Baloyi, N. D.; Tekere, M.; Maphangwa, K. W.; Masindi, V., Insights Into the Prevalence and Impacts of Phthalate Esters in Aquatic Ecosystems. *Front. Environ. Sci.* **2021,** *9*.

15. Gunaalan, K.; Fabbri, E.; Capolupo, M., The hidden threat of plastic leachates: A critical review on their impacts on aquatic organisms. *Water Res.* **2020,** *184*, 116170.

16. Henkel, C.; Huffer, T.; Hofmann, T., The leaching of phthalates from PVC can be determined with an infinite sink approach. *Methodsx* **2019,** *6*, 2729-2734.

17. Velazquez, S.; Bi, C. Y.; Kline, J.; Nunez, S.; Corsi, R.; Xu, Y.; Ishaq, S. L., Accumulation of di-2-ethylhexyl phthalate from polyvinyl chloride flooring into settled house dust and the effect on the bacterial community. *PeerJ* **2019,** *7*.

18. Wowkonowicz, P.; Kijenska, M., Phthalate release in leachate from municipal landfills of central Poland. *PLoS One* **2017,** *12* (3).

19. EU. 1999/0238(Cod): Child Health Protection: Phthalates, Dangerous Substances, Safety of Toys. https://oeil.secure.europarl.europa.eu/oeil/popups/ficheprocedure.do?lang=en&reference=1999/0238 (accessed March 2022).

20. Prohibition of Children's Toys and Child Care Articles Containing Specified Phthalates. https://www.federalregister.gov/documents/2017/10/27/2017-23267/prohibition-of-childrens-toys-and-child-care-articles-containing-specified-phthalates (accessed March 2022).

21. Phthalates Regulations. https://laws-lois.justice.gc.ca/eng/regulations/SOR-2016-188/page-1.html (accessed March 2022).

22. Ceresana, Ceresana's latest report details growth and change for global plasticizers market. *Additives for Polymers* **2019,** (6), 11.

23. Bocque, M.; Voirin, C.; Lapinte, V.; Caillol, S.; Robin, J. J., Petro-Based and Bio-Based Plasticizers: Chemical Structures to Plasticizing Properties. *J. Polym. Sci. A* **2016,** *54* (1), 11-33.

24. Chiellini, F.; Ferri, M.; Morelli, A.; Dipaola, L.; Latini, G., Perspectives on alternatives to phthalate plasticized poly(vinyl chloride) in medical devices applications. *Prog. Polym. Sci.* **2013,** *38* (7), 1067-1088.

25. Zhu, H. C.; Yang, J. J.; Wu, M. Y.; Wu, Q. Y.; Liu, J. Y.; Zhang, J. A., Vanillic Acid as a New Skeleton for Formulating a Biobased Plasticizer. *ACS Sustain. Chem. Eng.* **2021,** *9* (45), 15322-15330.

26. Tan, J.; Wang, F.; Wang, W.; Wang, Q.; Wang, X.; Wang, F.; Zhang, M.; Zhu, X., Waste Fatty Acid-Based Methyl Tetraglycol Ester Derived from Dimer Acid Manufacturing as an Efficient and Biodegradable Plasticizer for Poly (vinyl chloride). *ACS Sustain. Chem. Eng.* **2021**.

27. Feng, S.; Zhang, P.; Jiang, P.; Zhang, Z.; Deng, J.; Cao, Z., Synthesis and application of high-stability bio-based plasticizer derived from ricinoleic acid. *Eur. Polym. J.* **2022**, 111125.

28. Park, M.; Choi, I.; Lee, S.; Hong, S. J.; Kim, A.; Shin, J.; Kang, H. C.; Kim, Y. W., Renewable malic acid-based plasticizers for both PVC and PLA polymers. *J. Ind. Eng. Chem.* **2020,** *88*, 148-158.

29. Elsiwi, B. M.; Garcia-Valdez, O.; Erythropel, H. C.; Leask, R. L.; Nicell, J. A.; Maric, M., Fully Renewable, Effective, and Highly Biodegradable Plasticizer: Di-n-heptyl Succinate. *ACS Sustain. Chem. Eng.* **2020,** *8* (33), 12409-12418.

30. Bagnato, G.; Iulianelli, A.; Sanna, A.; Basile, A., Glycerol Production and Transformation: A Critical Review with Particular Emphasis on Glycerol Reforming Reaction for Producing Hydrogen in Conventional and Membrane Reactors. *Membranes (Basel)* **2017,** *7* (2), 17.

31. Ciriminna, R.; Pina, C. D.; Rossi, M.; Pagliaro, M., Understanding the glycerol market. *Eur. J. Lipid Sci. Technol.* **2014,** *116* (10), 1432-1439.

32. Halloran, M. W.; Danielczak, L.; Nicell, J. A.; Leask, R. L.; Marić, M., Highly Flexible Polylactide Food Packaging Plasticized with Nontoxic, Biosourced Glycerol Plasticizers. *ACS Appl. Polym. Mater.* **2022,** *4* (5), 3608-3617.

33. Halloran, M. W.; Nicell, J. A.; Leask, R. L.; Marić, M., Small molecule plasticizers for improved migration resistance: Investigation of branching and leaching behaviour in PVC blends. *Mater. Today Commun.* **2021,** *29*, 102874.

34. Mascia, L.; Kouparitsas, Y.; Nocita, D.; Bao, X., Antiplasticization of Polymer Materials: Structural Aspects and Effects on Mechanical and Diffusion-Controlled Properties. *Polymers* **2020,** *12* (4), 769.

35. Hansen, C. M., Aspects of solubility, surfaces and diffusion in polymers. *Prog. Org. Coat.* **2004,** *51* (1), 55-66.

36. Greco, A.; Brunetti, D.; Renna, G.; Mele, G.; Maffezzoli, A., Plasticizer for poly(vinyl chloride) from cardanol as a renewable resource material. *Polym. Degrad. Stab.* **2010,** *95* (11), 2169-2174.

37. Van Krevelen, D. W.; Te Nijenhuis, K., Chapter 7 - Cohesive Properties and Solubility. In *Properties of Polymers (Fourth Edition)*, Van Krevelen, D. W.; Te Nijenhuis, K., Eds. Elsevier: Amsterdam, 2009; pp 189-227.

38. Erythropel, H. C.; Dodd, P.; Leask, R. L.; Maric, M.; Cooper, D. G., Designing green plasticizers: Influence of alkyl chain length on biodegradation and plasticization properties of succinate based plasticizers. *Chemosphere* **2013,** *91* (3), 358-365.

39. Erythropel, H. C.; Bormann, A.; Nicell, J. A.; Leask, R. L.; Maric, M., Designing Green Plasticizers: Linear Alkyl Diol Dibenzoate Plasticizers and a Thermally Reversible Plasticizer. *Polymers* **2018,** *10* (6).

40. Jamarani, R.; Halloran, M. W.; Panchal, K.; Nicell, J. A.; Leask, R. L.; Marić, M., Poly(ε-caprolactone)-based additives: Plasticization efficacy and migration resistance. *J. Vinyl Addit. Technol.* **2021,** *27* (4), 821-832.

41. Erythropel, H. C.; Maric, M.; Cooper, D. G., Designing green plasticizers: Influence of molecular geometry on biodegradation and plasticization properties. *Chemosphere* **2012,** *86* (8), 759-766.

42. Li, D.; Panchal, K.; Mafi, R.; Xi, L., An Atomistic Evaluation of the Compatibility and Plasticization Efficacy of Phthalates in Poly(vinyl chloride). *Macromolecules* **2018,** *51* (18), 6997-7012.

43. Li, D.; Panchal, K.; Vasudevan, N. K.; Mafi, R.; Xi, L., Effects of molecular design parameters on plasticizer performance in poly(vinyl chloride): A comprehensive molecular simulation study. *Chem. Eng. Sci.* **2022,** *249*, 117334.

44. Marcilla, A.; Beltran, M., 5 - Mechanisms of plasticizers action. In *Handbook of Plasticizers (Third Edition)*, Wypych, G., Ed. ChemTec Publishing: 2017; pp 119-134.

45. Daniels, P. H., A Brief Overview of Theories of PVC Plasticization and Methods Used to Evaluate PVC-Plasticizer Interaction. *J. Vinyl Addit. Technol.* **2009,** *15* (4), 219-223.

46. Sundararaj, U.; Macosko, C. W., Drop Breakup and Coalescence in Polymer Blends: The Effects of Concentration and Compatibilization. *Macromolecules* **1995,** *28* (8), 2647-2657.

47. Erythropel, H. C.; Shipley, S.; Bormann, A.; Nicell, J. A.; Maric, M.; Leask, R. L., Designing green plasticizers: Influence of molecule geometry and alkyl chain length on the plasticizing effectiveness of diester plasticizers in PVC blends. *Polymer* **2016,** *89*, 18-27.

48. Kastner, J.; Cooper, D. G.; Maric, M.; Dodd, P.; Yargeau, V., Aqueous leaching of di-2-ethylhexyl phthalate and "green" plasticizers from poly(vinyl chloride). *Sci. Total Environ.* **2012,** *432*, 357-364.

49. Harmon, J. P.; Otter, R., Green Chemistry and the Search for New Plasticizers. *ACS Sustain. Chem. Eng.* **2018,** *6* (2), 2078-2085.

50. Piche, C. D.; Sauvageau, D.; Vanlian, M.; Erythropel, H. C.; Robaire, B.; Leask, R. L., Effects of di-(2-ethylhexyl) phthalate and four of its metabolites on steroidogenesis in MA-10 cells. *Ecotox. Environ. Safe.* **2012,** *79*, 108-115.

51. Nalli, S.; Cooper, D. G.; Nicell, J. A., Biodegradation of plasticizers by Rhodococcus rhodochrous. *Biodegradation* **2002,** *13* (5), 343-352.

6 Toughening poly(lactide) with bio-based poly(farnesene) elastomers

Matthew W. Halloran,[1] Jim A. Nicell,[2] Richard L. Leask,[1] Milan Marić*[1]

[1]Department of Chemical Engineering, McGill University, 3610 University Street, Montréal, QC, Canada, H3A 0C5

[2]Department of Civil Engineering, McGill University, 817 Sherbrooke Street West, Montreal, Quebec, Canada, H3A 0C3

*corresponding author

6.1 Preface

The following manuscript was published in 2022 in the journal *ACS Applied Polymer Materials.* While promising results were obtained from the work with PLA plasticizers presented in Chapter 4, the underlying concern of plasticizer leaching remained an issue. This naturally suggested that it would be prudent and useful to investigate alternative strategies to modulate the mechanical properties of PLA. In this context, the work presented in this chapter describes efforts directed towards the development of renewably sourced rubber toughening agents which could enhance the impact strength and tensile properties of PLA.

To accomplish this, the terpene monomer, farnesene, was used as a building block for the design of functionalized copolymers which could react with PLA during the blending process to achieve reactive compatibilization between the immiscible phases. The blends were evaluated using a series of techniques including rheology, dynamic mechanical thermal analysis (DMTA), Izod impact testing, tensile testing, and scanning electron microscopy (SEM) to study the effects of chemical composition on the mechanical and thermal properties of the blends. The main objective of this work was to demonstrate the potential of farnesene as a building block for the design of renewably sourced rubber toughening agents for PLA.

6.2 Abstract

The development and application of bio-sourced elastomers which can be blended with poly(lactide) (PLA) to enhance its poor material properties are of great interest as we move towards replacing petroleum-derived plastics with viable alternatives. As such, this work focused on the valorization of the terpene-based monomer, trans-β-farnesene (farnesene), as a building block to design rubber toughening agents to improve the impact strength of PLA blends. Ternary blends consisting of copolymers of farnesene-glycidyl methacrylate (PFGMA), farnesene-methacrylic acid (PFMAA) (20-30 wt% farnesene-copolymers), and PLA exhibited significant improvements in impact strength and elongation at break (i.e., approximately 16-fold and 10-fold, respectively) over neat PLA. Torque mixer measurements and FTIR spectroscopy confirmed the occurrence of epoxy-acid/epoxy-hydroxyl interfacial compatibilization reactions catalyzed through hydrogen bonding interactions. Phase morphologies of the ternary blends were evaluated with scanning electron microscopy (SEM) and showed an approximate 4-fold reduction in particle diameter relative to the binary systems (i.e., from 4.3 to 1.1 μm) with the compatibilized blend morphology deemed stable upon annealing. The toughening mechanism responsible for the improved mechanical properties observed with the ternary blends was also investigated by examining the impact fractured surface morphologies with SEM. A combination of enhanced interfacial adhesion coupled with shear yielding of the matrix was proposed as the main contributing factor to the improvement in mechanical properties observed in the ternary blends.

6.3 Introduction

As a renewably sourced and biodegradable polymer, poly(lactide) (PLA) has been shown to be a promising alternative to petroleum-derived poly(styrene) (PS) and poly(ethylene terephthalate) (PET).[1] Owing to its high tensile strength and modulus, PLA has been found suitable for applications in the packaging industry[2] and the biomedical field where it is used to manufacture implantable medical devices and degradable sutures.[3, 4] Nevertheless, PLA suffers from several shortcomings such as its inherent brittleness and poor tensile properties which have restricted its widespread use as a viable replacement for PET or PS.[5] To address these shortcomings, the most commonly adopted methods to improve the mechanical properties of PLA are through the incorporation of plasticizers which help to lower the glass transition temperature (T_g) of the blend while imparting flexibility,[6] and through blending with an immiscible rubbery polymer to enhance impact toughness.[7]

The latter approach has received considerable attention over the last two decades due to its low cost, efficiency, and ability to fine-tune the mechanical properties by altering the components and composition of the blend.[8, 9] However, achieving adequate compatibilization between PLA and the rubbery phase is not straightforward,[10] and often requires the use of suitable graft or copolymers which can be pre-made or formed *in situ* through reactive compatibilization.[11] In this context, many reports have demonstrated significant improvements in the impact strength and tensile properties of PLA by incorporating poly(ethylene) (PE),[12] acrylonitrile-butadiene-styrene copolymer,[13] poly(ε-caprolactone),[14] poly(butylene succinate),[15] poly(carbonate),[16] and ethylene-glycidyl-methacrylate (EGMA),[17] just to name a few. Despite the excellent mechanical properties obtained with these systems, the use of these additives compromises the sustainable nature of PLA due to their petroleum-derived origins. Consequently, focus has shifted towards toughening PLA with renewably sourced polymers[18] such as natural rubbers,[19, 20] polyhydroxybutyrates,[21] epoxidized corn[22] or soybean oils,[23] and lignocellulosic biomass.[24-26]

Alternatively, terpene-based monomers such as β-myrcene and trans-β-farnesene have emerged as promising building blocks for the development of renewably sourced rubbery materials[27] which exhibit similar properties to poly(isoprene) and poly(butadiene).[28, 29] Both poly(myrcene) and poly(farnesene) (PF) display similarly low T_gs (i.e., ~ -70 °C) in comparison to poly(butadiene) (i.e., with a T_g of -100 °C), while their bottlebrush-like structure with densely-packed, long side chains establishes them as excellent candidates as bio-based elastomeric materials.[30-33] As a naturally-occurring compound found in many essential oils, farnesene can also be produced on large scale from sugar cane fermentation.[34]

Although previous work has demonstrated the effectiveness of myrcene graft copolymers to improve the mechanical properties of both poly(urethane)[35] and PLA,[36] to the best of our knowledge the use of PF as an additive in such applications has not been previously explored. Therefore, this work describes the synthesis and evaluation of functionalized PF derivatives as renewably sourced elastomeric rubber toughening agents in blends with PLA. The rheological, morphological, thermal, and mechanical properties of the blends was investigated as both binary and ternary mixtures with the overarching goal of achieving compatibilization in conjunction with targeting an increase in impact strength. Farnesene copolymers containing modest amounts (10 mol%) of glycidyl methacrylate (GMA) and methacrylic acid (MAA) functionalities were also evaluated as potential reactive compatibilizers for PF/PLA blends which could undergo cross-linking reactions through an acid-epoxy, or transesterification reaction. It was subsequently demonstrated through torque mixer measurements and FTIR spectroscopy that epoxy-acid/epoxy-hydroxyl cross-linking reactions catalyzed through intermolecular hydrogen-bonding interactions occurred in the ternary blends during melt-mixing. In contrast to existing reports which rely on the use of external metal catalysis[37] or high blending temperatures[38] to achieve reactive compatibilization, this approach differs in that it illustrates the efficiency of intermolecular hydrogen-bonding catalysis to obtain rubber toughened PLA blends which we believe could be useful for broader applications in the field of polymer blending.

6.4 Materials and Methods

6.4.1 Materials and Reagents

Poly(lactide) (Ingeo Bioworks 2003D, MFI = 6 g/10min (210 °C/2.16 kg), density = 1.24 g/cm^3, M_n = 43 kg/mol, $Đ$ = 3.0) was purchased from Nature-Works LLC (Minnetonka, MN). Trans-β-farnesene, or Biofene (≥95%), was generously donated by Amyris with thanks to Derek McPhee (Emeryville, CA). Glycidyl methacrylate (GMA, 97%), methacrylic acid (MAA, 99%), deuterated chloroform ($CDCl_3$), and dicumyl peroxide (DCP, 98%) were purchased from Sigma Aldrich (Oakville, ON). The monomers were purified using 1.0 g of aluminum oxide (basic Al_2O_3, activated, Brockmann I) and 0.05 g calcium hydride (≥90%) per 50 mL of monomer. Xylenes (ACS grade), chloroform (ACS grade), and tetrahydrofuran (HPLC grade) were purchased from Fisher Scientific (Montreal, QC).

6.4.2 Experimental Methods

6.4.2.1 Synthesis of PF additives

Poly(farnesene) (PF) was synthesized via conventional free radical polymerization in accordance with a slightly modified version of a previously reported procedure,[39] wherein the reaction was conducted in 50 weight% xylenes (w.r.t. farnesene monomer) instead of in bulk, and the reaction time was increased to 12 hours. Poly(farnesene-co-glycidyl methacrylate) (PFGMA) and poly(farnesene-co-methacrylic acid) (PFMAA) were synthesized under analogous conditions using 10 mol% of glycidyl methacrylate and methacrylic acid, respectively. Hydrogenated PF (HPF) was synthesized according to a previously reported procedure.[39] Monomer conversions were calculated using ^{1}H NMR as previously described.[39] The copolymer composition was equal to the initial monomer composition in the reaction.

6.4.2.2 Melt Mixing of blends

Melt-mixed blends were prepared using a Rheocord System 40 double arm internal batch mixer (Haake Buchler). The PLA pellets and farnesene polymers were dried under vacuum for 24 hours at 50 °C to remove residual moisture before use. Batches of 50 g each blend were pre-weighed and were briefly stirred manually with a spatula before being added to the batch mixer and mixed for 6 minutes at 175 °C with a rotation rate of 100 rpm. The batches were then quenched into a liquid nitrogen bath to freeze the morphology and stored for further analysis. Neat PLA was processed under the same conditions for comparison purposes.

6.4.2.3 Compression Molding of Mechanical Test Bars

Test bars of blends were produced with compression molding using a heated manual hydraulic press (Carver Manual Hydraulic Press with Watlow temperature controllers, St. Louis, MO) and steel molds. Blends were cut into small fragments and dried in a vacuum oven at 50 °C for 24 hours before being placed into the molds and pressed at 175 °C for 5 minutes at 10 metric tonnes. Tensile test bar dimensions were as follows: a thickness (T) of 1.4 mm; a width of narrow section (W) of 3.3 mm; a length of narrow section (L) of 17.8 mm; an overall length of 64 mm; and an overall width of 10 mm. Bars for impact testing with the dimensions of T= 3.0 mm, W= 12.7 mm, and L= 63.5 mm were prepared in the same manner described above. Dynamic thermal mechanical analysis (DMTA) bars were prepared in the same manner with the following dimensions: T= 1.45 mm, L= 45 mm, and W= 10 mm. The exact dimensions (thickness/width) of each specimen were recorded using an electronic caliper prior to testing.

6.4.3 Characterization Methods

6.4.3.1 Mechanical Testing

Tensile testing was performed using a Shimadzu (Kyoto, Japan) Easy Test instrument equipped with a 500 N load cell in accordance with ASTM standard D638-14. Test bars were aged for 48 hours before being clamped and subjected to a strain rate of 5 mm/min. The stress−strain curves were used to obtain values for strain (% elongation), stress at break, and modulus.

Notched Izod impact strength was measured in accordance with ASTM standard D256 using a CEAST Universal Pendulum Impact tester. A minimum of 5 specimens were tested per blend for both tensile and Izod testing.

6.4.3.2 Scanning Electron Microscopy (SEM)

The morphology of the samples was investigated with scanning electron microscopy (SEM), using a FEI Quanta 450 Environmental Scanning Electron Microscope (FE-ESM) operating under high vacuum and acceleration voltage of 10.0 kV. Binary blends were freeze-fractured with liquid nitrogen, while ternary blends were cryo-microtomed using Leica Microsystems EM UC7/FC7 cryo-ultramicrotome (Leica Microsystems, Wetzlar, Germany) with a Diatome diamond knife (Diatome, Nidau, Switzerland) at -120 °C. Cryo-microtomy was used to prepare samples of the ternary blends to obtain higher quality images for particle analysis as images of the freeze-fractured surfaces did not provide enough contrast between phases. All samples were mounted on aluminum stubs with carbon tape and then sputter-coated with 4 nm of platinum prior to analysis using a Leica Microsystems EM ACE600 High Resolution Sputter Coater. Particle analysis was performed using Fiji-ImageJ software to obtain cross-sectional particle areas that were converted to an equivalent sphere diameter. At least 300 particles from four independent SEM images were measured for each blend to ensure reliable statistics. Weight-average particle diameter (d_w) was calculated according to equation (1):

$$d_w = \frac{\sum n_i d_i^2}{\sum n_i d_i} \qquad (1)$$

where n_i is the number of particles with diameter d_i. The particle size polydispersity was calculated as the ratio of weight-average particle diameter to number average particle diameter (d_n), i.e., d_w/d_n.

Selected impact-fractured specimens were also evaluated with SEM to investigate the toughening mechanism by imaging sections adjacent to the notch. Selected samples were thermally annealed above the T_g of PLA at 100 °C in a vacuum oven for 8 hours and imaged to evaluate blend stability. The blends were deemed stable if the dispersed phase particle size did not increase by more than 20% after thermal annealing.[40]

6.4.3.3 Thermal Gravimetric Analysis (TGA)

The thermal stability of the homopolymers and blends was evaluated using a TA Instruments Discovery 5500 (New Castle, DE) instrument under nitrogen flow of 25 mL/min from 25 to 500 °C at a heating rate of 10 °C/min. The onset temperature at weight loss with 10% (T_{10}) is reported for comparison purposes.

6.4.3.4 Differential Scanning Calorimetry (DSC)

The glass transition temperature (T_g) of homopolymers and blends were measured by differential scanning calorimetry (DSC) using a TA Instruments Q2000 (New Castle, DE) under a nitrogen atmosphere using a heat/cool/heat cycle. The samples were heated from 25-170 °C at a rate of 20 °C per minute, held constant at 170 °C for two minutes, then cooled to -90 °C at a rate of 10 °C per minute and held constant for two minutes at -90 °C. The samples were then heated to 170 °C at a rate of 20 °C per minute. The T_g was then determined from the reversible heat flow of the second heating cycle using the automated glass/step transition tool in the TA Instruments Universal Analysis 2000 software. Melting (T_m) and cold crystallization (T_{cc}) temperatures were taken from the second heating scan. Crystallinity (X_c) was calculated using equation (2) below with the melt and crystallization enthalpies where ΔH_m, ΔH_{cc}, ΔH_m^0, and w_{PLA} represent the enthalpy of melting, the enthalpy of cold crystallization, the enthalpy of melting for 100% crystalline PLA, and the weight percent of PLA in the blend, respectively.

$$X_c = \frac{\Delta H_m - \Delta H_{cc}}{\Delta H_m^0 \times w_{PLA}} \times 100\% \tag{2}$$

A value of 93.15 J/g was taken as the melting enthalpy for 100% crystalline PLA.[41]

6.4.3.5 Rheology

Rheological characterization was conducted using an Anton Paar MCR 302 instrument equipped with a CTD 450 convection oven operated under an N_2 atmosphere. Frequency sweep measurements of the homopolymers were conducted using a parallel plate (PP 25, diameter of 25 mm) configuration (1 mm gap) at a temperature of 175 °C to replicate blending conditions. Neat PLA pellets were compression molded into disks of 25 mm diameter and 1 mm thickness, while the poly(*Far*) derivatives were directly loaded onto the plate with a spatula. All samples were stabilized for 10 minutes at 175 °C before beginning the test. The homopolymer samples were measured using a shear strain of 1.0% (within the linear viscoelastic range) and frequency range of 0.1 to 100 rad/s to obtain the storage modulus (G') and complex viscosity (η^*).

6.4.3.6 Dynamic Thermal Mechanical Analysis (DMTA)

Dynamic thermal mechanical analysis (DMTA) was conducted on the blends to evaluate miscibility using the SRF 12 configuration on the MCR 302 instrument with a CTD 450 convection oven operated under an N_2 atmosphere. Compression-molded test bars were loaded in tension, and a temperature ramp was performed from 25 to 150 °C at a rate of 5 °C/min, with an oscillation strain of 0.1% and a frequency of 1 Hz to obtain the storage modulus (G') and tanδ curves.

6.4.3.7 Gel Permeation Chromatography (GPC)

The PF homopolymers' molecular weight distributions were analyzed using GPC. The number average molecular weight (M_n) and dispersity ($Đ = M_w/M_n$) were measured using a Waters Breeze instrument and HPLC-grade THF as an eluent at a flow rate of 0.3 mL/min. The GPC has three Waters Styragel HR columns (HR1 which has a molecular weight measurement range of 10^2 to 5×10^3 g/mol, HR2 with a molecular weight measurement range of 5×10^2 to 2×10^4 g/ mol, and HR4 with a molecular weight measurement range of 5×10^3 to 6×10^5 g/mol), a guard column, as well as a refractive index (RI 2414) detector. The columns were heated to 40 °C throughout analysis. The molecular weights were determined relative to poly-(methyl methacrylate) (PMMA) calibration standards from Varian Inc. (ranging from 875 to 1,677,000 g/mol). The reported molecular weights were all relative to the PMMA standards and not adjusted with Mark−Houwink parameters for universal calibration.

6.4.3.8 Proton Nuclear Magnetic Resonance (^{1}H NMR) Spectroscopy

^{1}H NMR spectra were collected using a Bruker AVIIIHD 500 MHz spectrometer (MA, USA) with an average of 16 scans using deuterated chloroform ($CDCl_3$) as the solvent.

6.4.3.9 Fourier Transform Infrared (FTIR) Spectroscopy

FTIR measurements were conducted using a Perkin Elmer instrument (Spectrum II series) which is equipped with a single bounce diamond attenuated transmission reflectance (ATR) for solids. 32 scans were recorded for each sample over the range 4000−500 cm^{-1} with a normal resolution of 4 cm^{-1}. The farnesene homopolymers were measured as is, whereas neat PLA was solvent cast from chloroform ($CHCl_3$) to produce a thin film for analysis. Ternary blends were stirred in $CHCl_3$ for 48 hours at room temperature to dissolve PLA, PFMAA, and PFGMA, while the cross-linked portions remained insoluble and were collected via syringe and dried. This process was repeated three times to ensure only the cross-linked portions remained before analysis with FTIR. See Appendix D, Figure D6, for a picture of the isolated insoluble fractions.

6.5 Results and Discussion

6.5.1 Synthesis and Characterization of Farnesene Polymers

In contrast to poly(isoprene) and poly(butadiene) which have entanglement molecular weights (M_e) of 3000-5000 g/mol and 1500-1900 g/mol,[42] respectively, PF has a much higher M_e of 50,000 g/mol due to its repeating unit having a higher degree of unsaturation (i.e. 3 vs. 1).[43] Therefore, in order to obtain PF samples with similar viscoelastic properties as poly(isoprene) and poly(butadiene) which could be used to rubber toughen PLA, a molecular weight of 50,000 g/mol or higher is required. Conditions for the synthesis of PF have previously been developed using several different approaches including anionic polymerization,[29] redox free-radical polymerization in emulsion,[44] nitroxide-mediated polymerization in miniemulsions[45] and bulk,[46] and free-radical polymerization (FRP).[39] However, only the FRP conditions are generally amenable to synthesize species with molecular weights greater than 50,000 g/mol.

Here, slightly modified FRP conditions from Luk *et al.*[39] were employed to synthesize a suite of high molecular weight (M_n's of 58-63 kg/mol) farnesene-based polymers (Figure 6.1). The hydrogenated derivative (HPF) has previously been shown to have higher thermal stability, a lower M_e, and higher viscosity relative to its unsaturated counterpart (PF),[39, 42] which are all more favorable characteristics of an elastomeric toughening agent for PLA and was therefore of interest here. With the goal of promoting an interfacial compatibilization reaction to achieve enhanced material properties, epoxy (PFGMA) and carboxylic acid (PFMAA) functionalized derivatives were also synthesized under the same conditions containing only modest amounts of compatibilizer (10 mol%). Both epoxy and carboxylic acid groups have been used previously as successful compatibilization agents between immiscible rubbery polymers and PLA to generate toughened blends.[16, 37, 38, 47-49] Glass transition temperatures (T_g) of the homopolymers ranged between -58.5 to -71.8 °C, while they all exhibited excellent thermal stabilities as the onset temperatures of 10% mass loss ($T_{d,10\%}$) were all well above 300 °C (Table 6.1) (See Appendix D, Figures D1 and D2 for DSC and TGA curves).

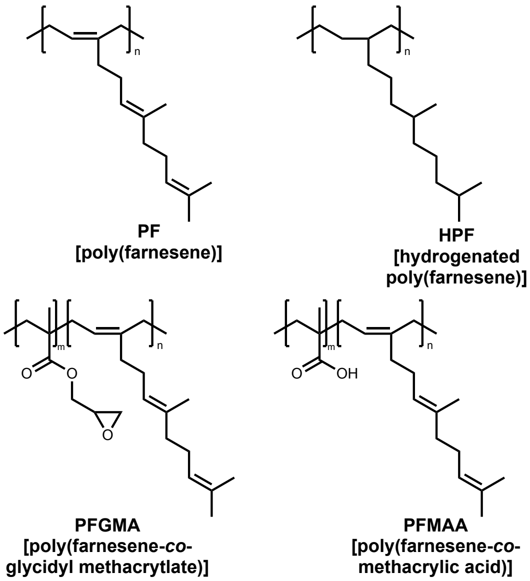

Figure 6.1. Chemical structures of farnesene-based polymers synthesized and used in this study.

Table 6.1. Structural and thermal properties of the synthesized farnesene-based polymers.

	M_n (kg/mol)[a]	$Đ = M_w/M_n$	T_g (°C)[b]	$T_{d,10\%}$ (°C)[c]
PF	62	6.9	-71.8	331
HPF	61	7.1	-58.5	356
PFGMA (10 mol% GMA)	63	4.2	-69.8	317
PFMAA (10 mol% MAA)	58	4.1	-69.3	341

[a] Measured with GPC relative to PMMA standards
[b] Measured from the second heating cycle of DSC exotherm
[c] Onset temperature at 10% mass loss measured with TGA

6.5.2 Rheological Characterization of Homopolymers

The complex viscosity measurements of the homopolymers taken at 175 °C within the linear viscoelastic region were evaluated to predict the rheological properties during melt-blending (Figure 6.2). At higher frequencies ($\omega > 25$ rad/s), the four farnesene-containing polymers have similar complex viscosities that range from 11 to 29 Pa·s, which is roughly two orders of magnitude lower than that of PLA. To minimize particle size of the dispersed phase during polymer blending and achieve optimal blending, the viscosity ratio between the dispersed phase and the host polymer matrix should ideally be near unity.[50] While the viscosity ratio ultimately plays a significant role in obtaining minimal particle size, a significant mismatch in viscosity ratios can be offset through reactive blending between the two immiscible phases to achieve sub-micron particle dispersions.[51, 52] It has been shown that at higher concentrations of the dispersed phase (i.e., >15%), the suppression of droplet coalescence is the dominant contribution of reactive compatibilizers which help to stabilize the interface.[51] Moreover, using the Flory-Huggins interaction parameter ($\chi = 0.43$ at 190 °C) for poly(isoprene)/PLA blends[53] as a reference, we anticipate the formation of large dispersed phase droplets in our system arising from a high degree of immiscibility between PLA and PF. Therefore, to achieve adequate dispersed phase droplet sizes to obtain favorable mechanical properties, reactive interfacial compatibilization will need to occur during blending.

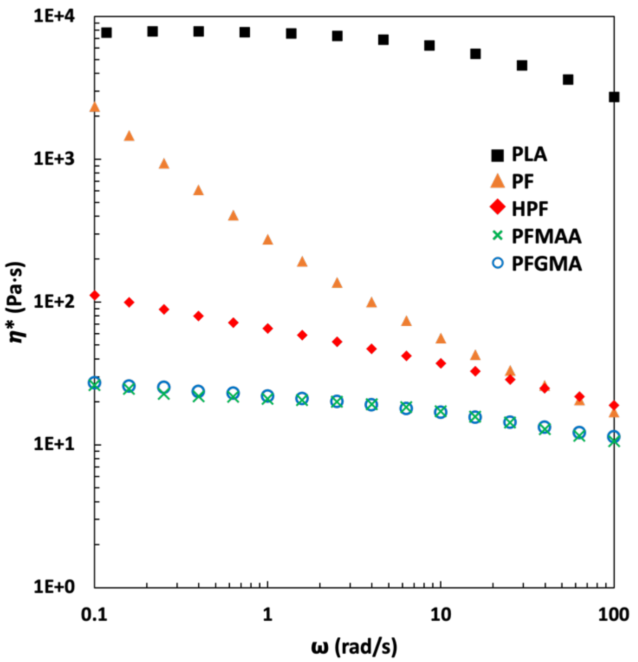

Figure 6.2. Complex viscosity measurements of homopolymers versus frequency measured at 175 °C.

6.5.3 Mechanical Properties of Blends

The elongation at break and notched impact strength of the blends is shown in Figure 6.3 and summarized in Table 6.2. The binary blends exhibited only slight improvements in impact strength (roughly 3-fold) and elongation at break (between 2- and 4-fold) relative to neat PLA at 20 weight % loadings of the farnesene polymers. Compared to neat PLA, a noticeable decrease in the yield stress and elastic modulus was observed in all binary blends, which can be explained by the addition of the soft, rubbery farnesene elastomers. It should also be noted that during testing, the binary blends exhibited distinct yielding before fracture and indicated the enhanced ductility of these blends in relation to neat PLA which underwent brittle fracture. Representative tensile curves are shown in Figure 6.4 which demonstrate the brittle to ductile transitions observed with the PFGMA, PFMAA binary blends. The negligible improvements in mechanical properties are likely due to the immiscibility between the two phases causing large particle sizes of the dispersed phase inside of the PLA matrix.[54] Large rubber particles have previously been shown to lower the strain at which cavitation can occur, leading to the formation of large holes which promote fracture at low strain rates.[55]

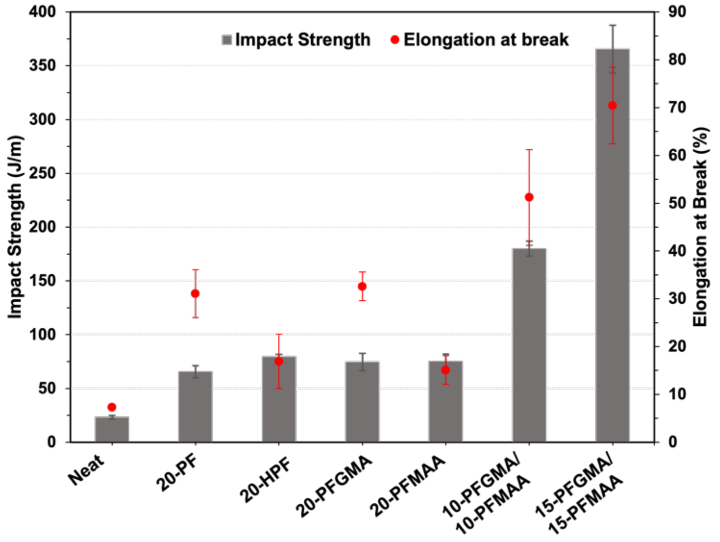

Figure 6.3. Mechanical properties of neat PLA, binary, and ternary blends showing the elongation at break (red dots and dashed line) and notched impact strength (grey bars) (n = 5, error bars represent standard deviation, means are shown).

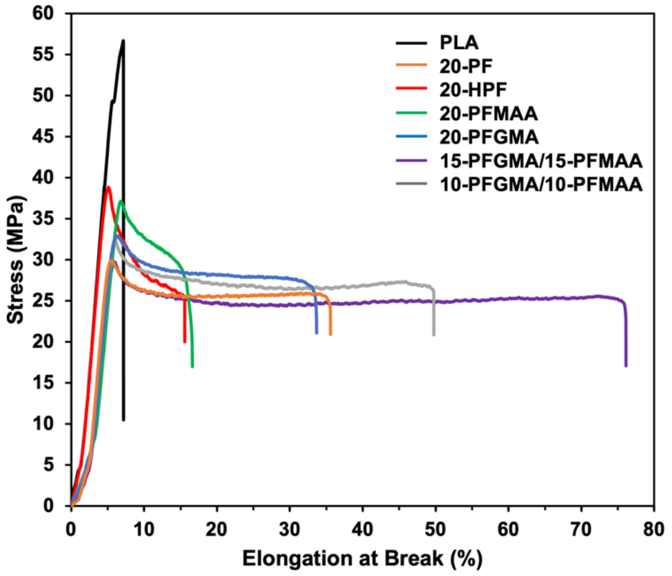

Figure 6.4. Representative strain in elongation at break versus stress curves for the binary and ternary blends.

Evidently, no interfacial compatibilization reactions between the epoxy functionalized PFGMA and the acid/hydroxyl groups on PLA took place under these conditions as all binary blends exhibited similar mechanical properties. Although previous reports have demonstrated the effectiveness of GMA-functionalized polymers as single component impact modifiers of PLA,[17, 49, 56] this proved to not be the case in our system as the incorporation of GMA into the farnesene backbone resulted in only a limited improvement in impact strength relative to neat PLA.

Conversely, the ternary blends consisting of PLA, PFGMA, and PFMAA displayed tremendous improvements in both impact strength and elongation at break. The PLA/(10-PFGMA/10-PFMAA) ternary blend achieved an elongation at break of 51%, and a notched impact strength of 180 J/m, more than 8-fold greater than PLA. Moreover, when the loading was further increased to 30 weight % (15-PFGMA/15-PFMAA in the blend), an impact strength of 366 J/m and elongation at break of 70% was achieved, corresponding to a ~10- and 16-fold increase in elongation at break and impact strength, respectively, over PLA. The improved toughness of the ternary blends was attributed to the occurrence of acid-epoxy/hydroxyl-epoxy cross-linking reactions which took place *in situ* during blending. The cross-linking reactions also led to an improvement in ductility, as both ternary blends demonstrated brittle to ductile transitions accompanied by necking during tensile testing (Figure 6.4). However, improvement in tensile toughness of rubber toughened blends is often accompanied by a significant decrease in yield strength and elastic modulus relative to the neat polymer.[37] A similar relationship was observed with our ternary blends as the modulus dropped from ~2200 MPa to ~1500 MPa and the yield stress decreased from ~57 MPa to ~30 MPa with the toughened 15-PFGMA/15PFMA blend. This was also observed in the previous work by Zhou *et al.* using myrcene grafted PLA blends which demonstrated an elongation at break of 97%, an extremely low elastic modulus of ~70 MPa, and a yield strength of only ~9 MPa.[36]

Table 6.2. Mechanical properties of binary and ternary blends.[a]

Blend	Yield Stress (MPa)	Elongation at Break (%)	Elastic Modulus (MPa)	Notched Impact Strength (J/m)
PLA	57 ± 0.8	7 ± 0.4	2210 ± 48	22 ± 1
20-PF	30 ± 0.6	31 ± 5	1880 ± 26	66 ± 6
20-HPF	39 ± 3	16 ± 6	1930 ± 53	80 ± 2
20-PFGMA	34 ± 2	32 ± 3	1870 ± 46	75 ± 8
20-PFMAA	38 ± 2	15 ± 3	1880 ± 17	75 ± 7
10-PFGMA/10-PFMAA	31. ± 0.9	51 ± 10	1710 ± 24	180 ± 8
15-PFGMA/15-PFMAA	29 ± 3	70 ± 8	1530 ± 27	366 ± 22

[a] Average values reported with standard deviations, n = 5

6.5.4 Thermal Properties

Previous reports have demonstrated a correlation between the degree of crystallization present in the PLA matrix and the impact strength of the resulting blend.[17, 47] A higher degree of crystallization (>40%), obtained through annealing, was shown to improve impact strength in a system comprised of PLA/poly(ethylene-*co*-glycidyl methacrylate);[17] whereas variations between low levels of crystallinity in other PLA blends (0-6%) was shown to have negligible effects on impact strength.[48, 49, 57, 58] Therefore, to evaluate the role of crystallization on impact strength in our system, the melting (T_m) and cold crystallization (T_{cc}) temperatures of samples taken from the fractured impact bars were evaluated. Figure 6.5 shows the DSC exotherms from the first heating cycle of the binary and ternary blends and the values are summarized in Table 6.3. The exotherms obtained for neat PLA and the prepared blends all exhibit similar thermal transitions, with clear glass transition, crystallization, and melting peaks observed for all species. The difference in melting, cold crystallization, and glass transition temperatures of the blends was not significantly different than those obtained for neat PLA. Moreover, the toughened 15-PFGMA/15-PFMAA ternary blend had nearly the same crystallinity as neat PLA at 5.9% and did not differ considerably from the other blends. Altogether, these results suggest that crystallinity did not contribute to the enhanced impact strength observed in the ternary blends.

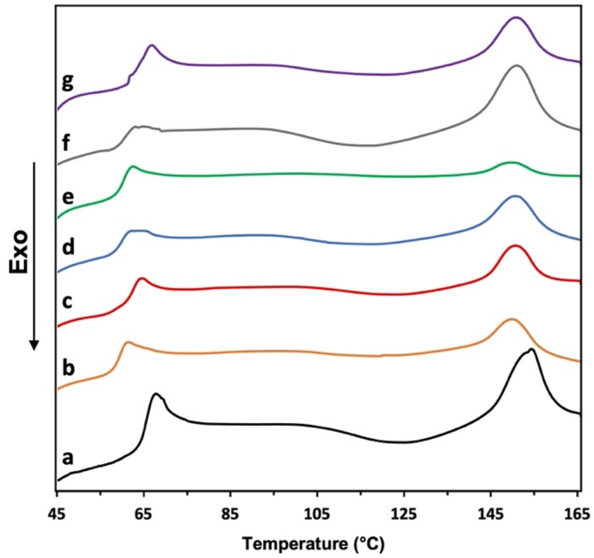

Figure 6.5. DSC exotherms of binary and ternary blends obtained from the first heating cycle: (a) neat PLA; (b) 20-PF; (c) 20-HPF; (d) 20-PFGMA; (e) 20-PFMAA; (f) 10-PFGMA/10-PFMAA; and (g) 15-PFGMA/15-PFMAA. Samples were taken from the fractured impact bars.

The T_gs of the binary and ternary blends are shown in Table 6.3 (see Appendix D, Figure D5 for curves). Each blend exhibits two T_gs which correspond to the T_gs of the individual components in the blends, with the values shifting slightly closer to one another owing to the interactions between the farnesene phase and the PLA phase. The two ternary blends exhibited the highest upward shift of the first T_g, and downward shift of the second T_g, which indicates their partial miscibility with PLA. The thermal stability of the blends was also evaluated with TGA, with all blends exhibiting equal or higher $T_{d,10\%}$ values than PLA (see Appendix D, Figure D4 for curves).

Table 6.3. Thermal properties of binary and ternary blends.

Blend	T_m (°C)[a]	T_{cc} (°C)[a]	X_c (%)	$T_{g1}^{(DSC)}$ (°C)[b]	$T_{g2}^{(DSC)}$ (°C)[b]	$T_g^{(DMTA)}$ (°C)[c]	$T_{d,10\%}$ (°C)[d]
PLA	153.9	125.2	5.9	-	59.6	67.0	328
20-PF	149.8	119.4	4.8	-69.4	57.9	65.4	326
20-HPF	150.5	124.3	1.4	-58.1	58.4	66.1	339
20-PFGMA	150.2	119.4	3.3	-68.0	58.4	64.0	336
20-PFMA	149.9	127.0	3.3	-68.6	57.3	65.8	327
10-PFGMA/10-PFMAA	150.4	115.1	7.9	-67.1	57.8	65.9	339
15-PFGMA/15-PFMAA	150.3	119.7	5.9	-66.5	58.3	65.4	342

[a] Measured from the first heating cycle of DSC exotherm
[b] Measured from the second heating cycle of DSC exotherm
[c] Measured from peak of tan*δ* curve with DMTA
[d] Onset temperature at 10% mass loss measured with TGA

6.5.5 Blend Miscibility

The miscibility between components in polymer blends has significant influence on both the phase behaviour and resultant mechanical properties of the processed materials. Therefore, dynamic mechanical thermal analysis (DTMA) was used to evaluate the miscibility between the components in the prepared blends. In Figures 6.6a and b, the storage modulus (*G'*) and tanδ curves of neat PLA along with the binary and ternary blends are shown. At room temperature, the *G'* of the blends decreases relative to PLA owing to the presence of the soft, rubbery farnesene-based components. Glass transitions were observed between 55-65 °C for the binary and ternary blends, followed by a sharp decrease in *G'* before reaching the rubbery plateau region. In all cases, cold crystallization peaks were clearly observed, with all blends exhibiting a shift to a higher T_{cc} (between 112-120 °C) relative to neat PLA (T_{cc} ~100 °C).

As shown in Figure 6.6b, the tanδ peak for neat PLA was observed at 67 °C which corresponded to its T_g. For the binary and ternary blends a slight decrease in temperature was observed for their tanδ peaks relative to PLA, with the largest shift obtained for the 20-PFGMA binary blend (64 °C). These shifts to slightly lower temperatures were in agreement with our DSC results and are due to the presence of the rubbery farnesene components in the blends which exhibit T_g values ranging from -71.8 to -58.5 °C. The more noticeable shift of the tanδ peak for the 20-PFMGA blend indicated a higher degree of miscibility between the two phases in the blend owing to the presence of the GMA functional groups which are known to enhance compatibility in PLA rubber toughened blends.[59]

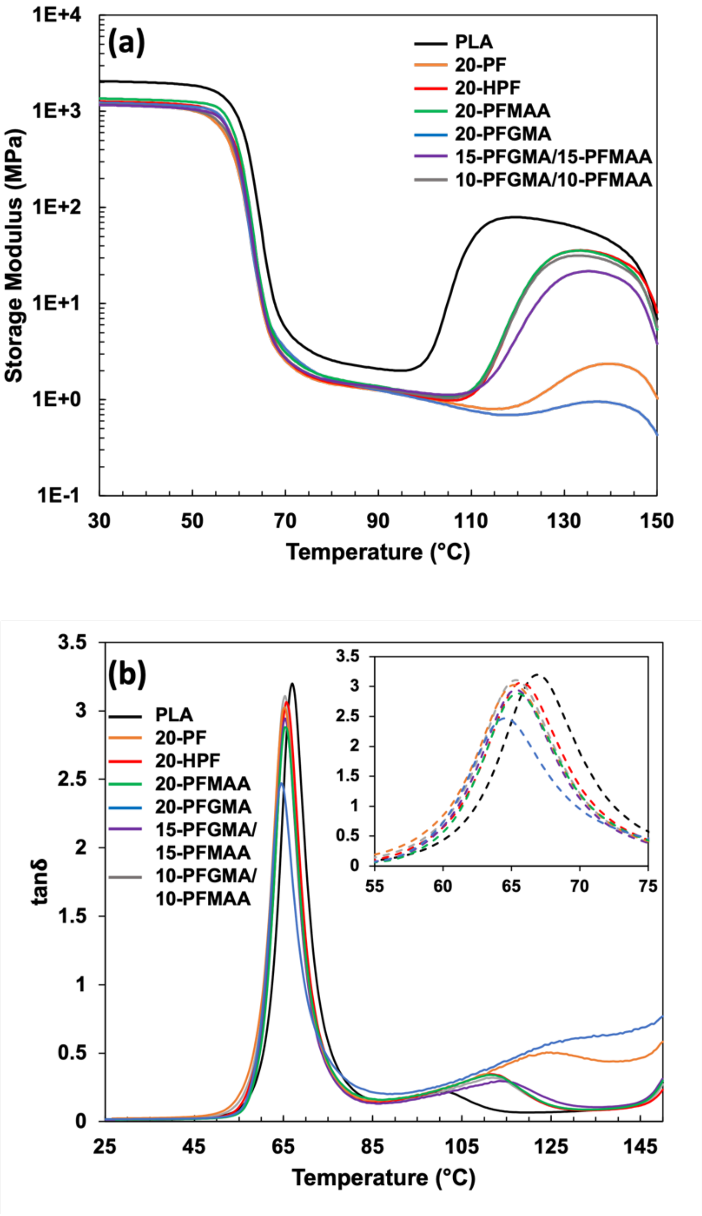

Figure 6.6. DMTA traces of neat PLA, binary, and ternary blends: (a) Storage modulus (G’) vs temperature; (b) tanδ vs temperature.

6.5.6 Blend Morphology

In Figure 6.7, the cryo-fractured and cryo-microtomed surfaces of the binary and ternary blends is shown, while the weighted-average particle diameters (d_w) are summarized in Table 6.4. In the case of the four binary blends, large dispersed phase droplets are clearly visible, with d_w values ranging from 2.9 to 4.3 µm, and polydispersities between 1.8 and 2.5. In immiscible binary systems, this morphology of discrete dispersion of the minor phase with a higher polydispersity is commonly observed,[60] and helps to explain the poor mechanical properties obtained with these blends as the large droplets facilitated fracture during testing.

Conversely, the surface morphologies of the two ternary blends revealed much finer droplet sizes, with more sub-micron particles being observed. In the 10-PFGMA/10-PFMAA blend, the d_w decreased to 1.3 µm, while the d_w of the 15/15 blend further decreased to 1.1 µm. As a result of the interfacial compatibilization reaction, the formed graft copolymers stabilized the interface between PLA and the farnesene phases. This prevented dispersed phase coalescence into larger droplets while retaining relatively monodisperse particle sizes.[51]

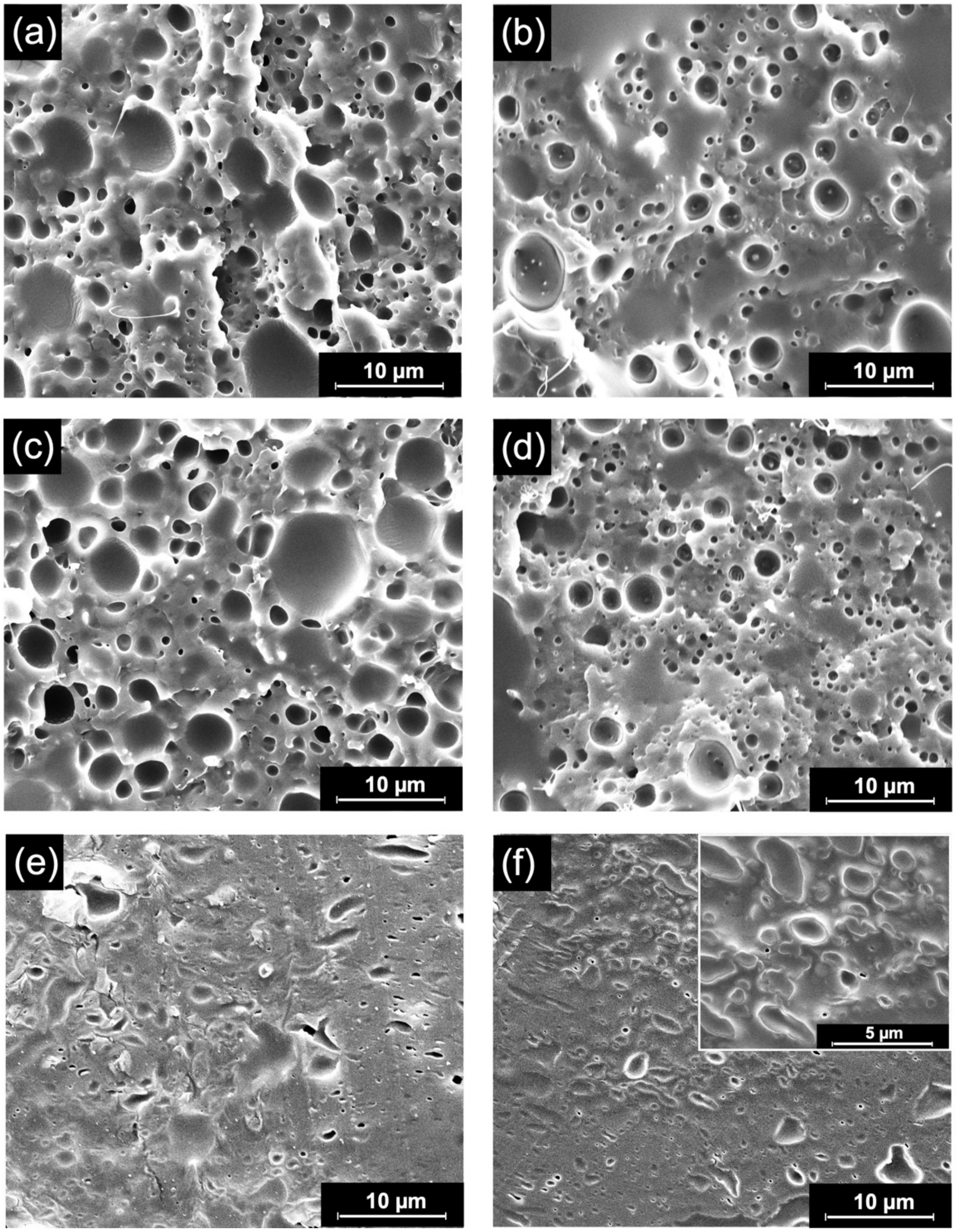

Figure 6.7. Cryo-fractured (a-d) and cryo-microtomed (e,f) SEM images of binary and ternary blends: (a) 20-PF; (b) 20-HPF; (c) 20-PFGMA; (d) 20-PFMAA; (e) 10-PFGMA/10-PFMAA; and (f) 15-PFGMA/15-PFMAA (inset shows higher magnification).

To evaluate the stability of the blends, selected samples were thermally annealed at 100 °C for 8 hours under vacuum. After annealing, the 20-PFGMA and 20-PFMAA binary blends resulted in relatively coarse morphologies, with larger droplets being observed ~ 3-4 μm. In both cases, the d_w and the polydispersity increased after annealing, which suggested that these blends were unstable (Table 6.4 and Appendix D, Figure D6). However, the morphology of the ternary blends did not significantly differ after thermal annealing, as the d_w and the polydispersity remained relatively unchanged. These results suggest that the acid-epoxy/hydroxyl-epoxy compatibilization reaction occurring in the ternary blends was more effective at producing stable morphologies with finer particle size than the non-reactive binary systems.

Table 6.4. Particle diameter measurements of binary and ternary blends.

Blend	**d_w (µm)**	**Polydispersity (d_w/d_n)**
20-PF	3.1	2.3
20-HPF	2.9	2.5
20-PFGMA	4.3 (8.1)[a]	1.9 (2.8)[a]
20-PFMAA	3.2 (5.8)[a]	1.8 (2.5)[a]
10-PFGMA/10-PFMAA	1.3 (1.4)[a]	1.1 (1.2)[a]
15-PFGMA/15-PFMAA	1.1 (1.1)[a]	1.1 (1.1)[a]

[a] After thermal annealing at 100 °C for 8 hours.

6.5.7 Surface Morphology of Fractured Impact Bars

The surface morphology of fractured impact bars was evaluated with SEM to gain insights into the mechanism behind the enhanced impact toughness observed for the ternary blends (Figure 6.8). Neat PLA underwent typical brittle fracture to reveal a smooth and featureless fracture surface,[61] while the 20-PFMAA and 20-PFGMA binary blends began to exhibit fracture lines and ridges in close proximity to the dispersed rubber phase droplets (Figure 6.8a and b). In both cases, phase separation is clear, indicating poor interfacial adhesion between PLA and the farnesene phases which was reflected in the marginal improvements in impact strength obtained with these two binary blends.

In contrast to the binary blends, the interface between the farnesene phases and PLA is harder to discern in the ternary blends, demonstrating the enhanced compatibility arising from the occurrence of cross-linking interfacial reactions (Figures 6.8c and d). Moreover, the fracture surfaces contain several long fibril strands which indicate plastic deformation and ductile fracture during impact, with more fibrils present in the 15/15 blend. In both cases, significant plastic deformation adjacent to the dispersed phase was evident which implies that shear yielding of the PLA matrix has taken place and helps to explain the significant improvement in impact strength observed with these blends.[62] This type of mechanism in which strong interfacial adhesion leading to plastic deformation and shear yielding is one which has been commonly observed in other multiphase blends.[49, 63]

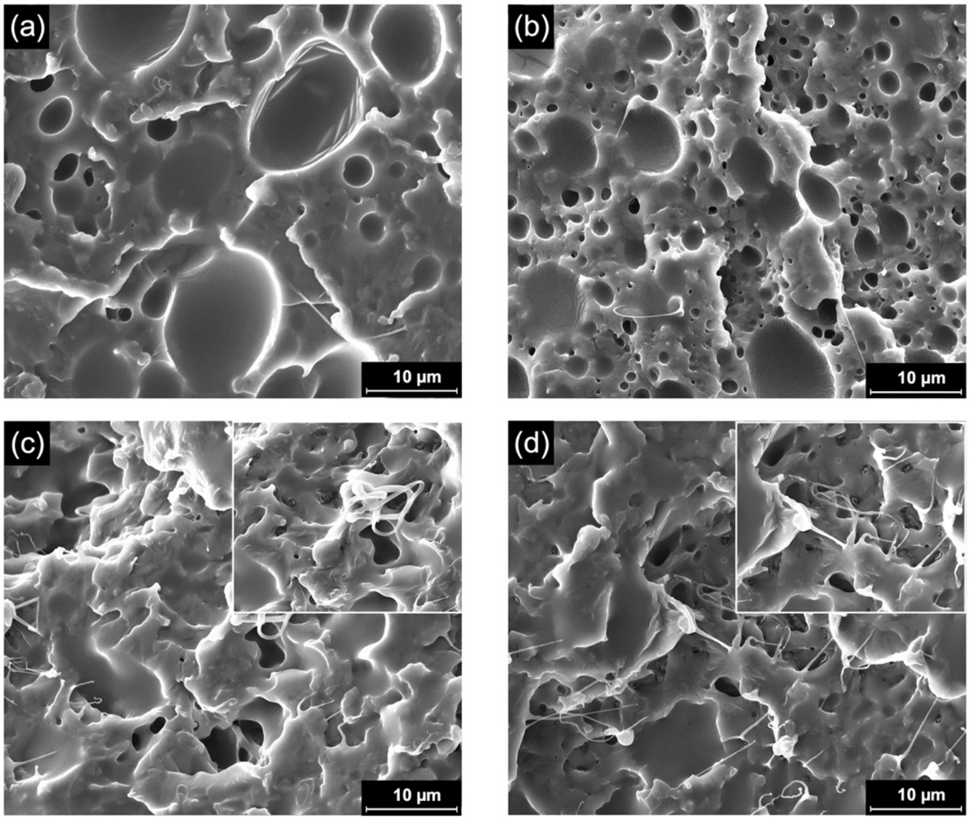

Figure 6.8. SEM images of impact fracture surface adjacent to the notch of selected blends: (a) 20-PFMA; (b) 20-PFGMA; (c) 10-PFGMA/10-PFMAA; and (d) 15-PFGMA/15-PFMAA (2500x magnification, insets show 5000 × magnification of fibrils).

6.5.8 Reactive Compatibilization Mechanism

During mixing, the change in torque was measured over time using the Haake internal batch mixer to monitor the evolution of potential interfacial compatibilization reactions occurring. In general, a higher torque output is correlated with an increase in blend viscosity which can signify copolymer formation.[37] Figure 6.9a shows the torque outputs of the four binary blends which follow similar profiles throughout mixing. Initially, there is a sharp increase in torque as the blends melt inside the chamber and then reach a steady state region after ~ 100 seconds as the torque profiles become flat over time. While the steady state torque profiles illustrate that the blends are stable rheologically under these mixing parameters, they suggest that little to no chemical reaction occurs between the epoxy groups on PFGMA and the acid/hydroxyl groups on PLA as no change in torque was observed.

Previous work has shown that the epoxy-acid/epoxy-hydroxyl interfacial reaction can be promoted through the addition of a catalyst during blending, or through increasing the mixing temperature above 210 °C.[12, 37, 38, 48, 57, 58] Alternatively, the use of multicomponent polymer blends have been successfully employed to promote interfacial compatibilization through dynamic vulcanization in which elastomers are selectively vulcanized during mixing with PLA to generate a cross-linked network.[57, 64] This strategy, when used in conjunction with elevated mixing temperatures, has proven useful in the past to promote epoxy-acid interfacial compatibilization reactions using zinc catalysis to generate toughened PLA blends.[58] Therefore, we postulated whether a ternary system comprised of PLA, PFGMA, and PFMAA could undergo a similar transformation catalyzed through intermolecular hydrogen bonding to promote interfacial reactivity.

In the case of our ternary systems, a large increase in torque was observed after 150 (15-PFGMA/15-PFMAA) and 200 (10-PFGMA/10-PFMAA) seconds of mixing time, as shown in Figure 6.9b. This large and rapid increase in torque was attributed to cross-linking reactions occurring between the epoxy groups on PFGMA, the acid groups on PFMAA, and the acid/hydroxyl groups on PLA. Akin to the work by Liu *et al.,*[57] the generation of a cross-linked elastomeric network in our system led to an increase in blend viscosity and torque output over the course of the reaction. The manifestation of the interfacial compatibilization reactions were substantiated by the reduction in particle size of the dispersed phase coupled with significant improvements in impact strength.

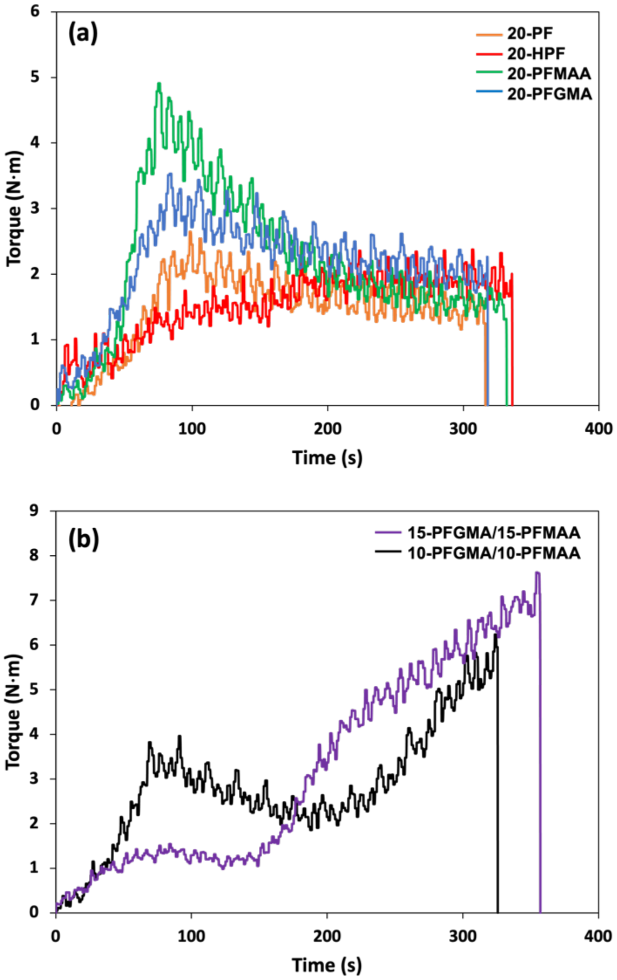

Figure 6.9. Torque vs time plots obtained from the internal batch mixer for (a) binary blends and (b) ternary blends.

To further investigate the cross-linking reaction and identify the chemical structure of the newly formed species, FTIR was employed. Figure 6.10 shows the FTIR absorbance spectra of the three neat homopolymers (PLA, PFGMA, PFMAA) and the cross-linked fractions from the two ternary blends. The ternary blends were etched with chloroform to dissolve PLA, PFGMA, and PFMAA, while the insoluble portion was collected and dried under vacuum prior to analysis (see Appendix D, Figure D7 for the visual appearance). PLA exhibits strong stretching vibration peaks at 1747

cm^{-1} and 1080 cm^{-1} which correspond to the C=O and C-O groups in the backbone, respectively.[65] PFGMA shows strong $-CH_3$ stretching vibration at 2917 cm^{-1}, C=O stretching at 1733 cm^{-1}, and $-CH_3$ bending at 1447 cm^{-1} and 1376 cm^{-1}. In the case of PFMAA, the majority of the free carboxylic acid groups existed as intermolecular dimers which exhibit a stretching vibration at 1698 cm^{-1}.[66]

For the two ternary blends, the insoluble cross-linked portions showed a strong, broadened peak at 1753 cm^{-1} which was attributed to the carbonyl group from the PLA backbone, a broad shoulder peak at 1698 cm^{-1} attributed to the carboxylic acid dimer from PFMAA, as well as a weak alkene stretching peak present at 1667 cm^{-1} which can be associated with the presence of both PFMAA and PFGMA. Furthermore, prominent $-CH_3$ stretching vibrations are evident in both ternary blend samples and are characteristic of the farnesene polymers. Finally, the broad peak ranging from 3200-3600 cm^{-1} indicates the presence of both free and intermolecularly bonded hydroxyl groups[67] resulting from the ring-opening of the epoxy groups of PFGMA through nucleophilic attack of acid/hydroxyl groups. While present in both ternary blends, the signal intensity appears stronger in the 15-PFGMA/15-PFMAA blend, indicating a higher degree of epoxy-acid/epoxy-hydroxyl reactions occurring and helps to explain the enhanced impact strength observed with this blend.

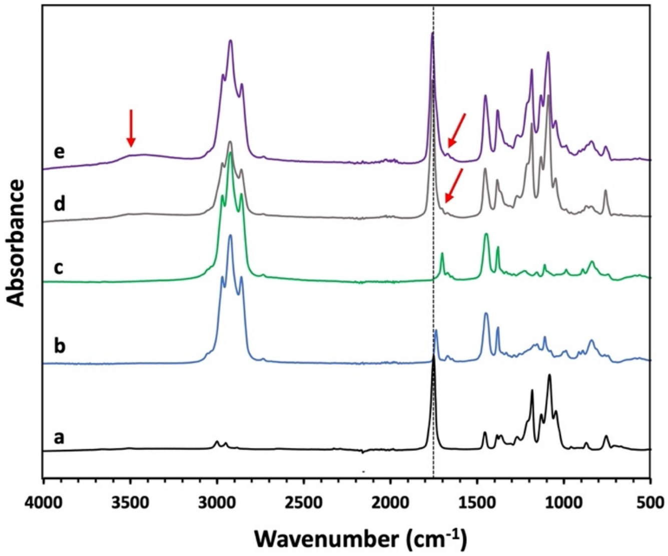

Figure 6.10. FTIR absorption spectra of homopolymers and cross-linked portions from ternary blends: (a) neat PLA; (b) neat PFGMA; (c) neat PFMAA; (d) $CHCl_3$-extracted portion of 10-PFGMA/10-PFMAA; and (e) $CHCl_3$-extracted portion of 15-PFGMA/15-PFMAA.

A proposed reaction mechanism is presented in Scheme 6.1 to account for the enhanced material properties obtained with the ternary blends as well as the formation of the cross-linked species. During the initial stages of mixing, PFGMA and PFMAA will preferentially coalesce with one another inside of the PLA matrix owing to their hydrophobic farnesene chains, with the polar GMA and MA functional groups being positioned on the surface of the droplets. At this interface, the oxygen atom in the epoxide acts as a hydrogen bond acceptor from the neighbouring carboxylic acid donor present in PFMAA; effectively polarizing the carbon-oxygen bond to increase the electrophilicity of the adjacent methylene. This is followed by nucleophilic attack by either the hydroxyl and/or acid group of PLA, or by the acid functionalized PFMAA to generate the corresponding cross-linked polymer network. Previous mechanistic studies with small molecules have shown the effectiveness of hydrogen bonding catalysis on epoxide ring opening,[68-70] although this usually is facilitated by the addition of a phenol-based catalyst. Here, we show that this transformation can also proceed using carboxylic acid as the hydrogen bonding donor to catalyze the interfacial compatibilization reaction between two immiscible phases in the melt.

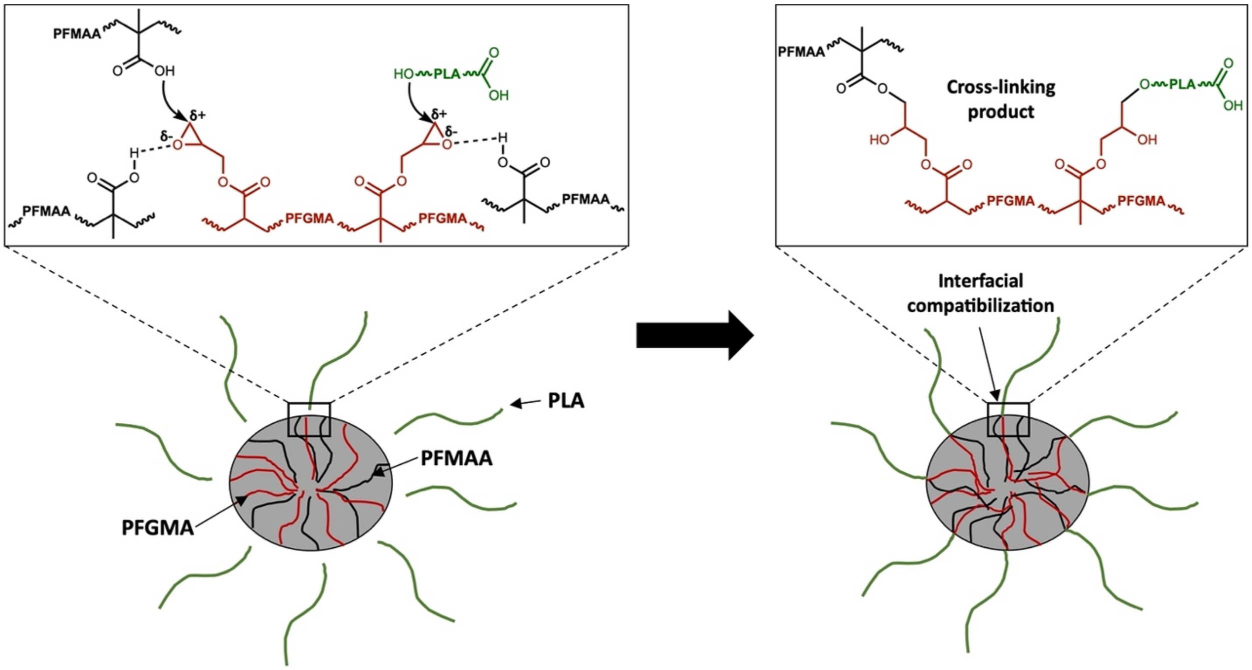

Scheme 6.1. Proposed interfacial compatibilization reaction mechanism during blending leading to formation of cross-linked product with the ternary blends.

6.6 Conclusions

The bio-based monomer farnesene*,* was used as a building block for the design of functionalized elastomeric additives which were then evaluated as rubber toughening agents for PLA. Toughened ternary blends consisting of PLA/PFGMA/PFMAA exhibited an impact strength of 366 J/m (16-fold greater than PLA) which were achieved through interfacial compatibilization reactions to generate a cross-linked polymer network inside of the PLA matrix. The chemical structure of the cross-linked network was elucidated with FTIR and established the occurrence of epoxy-acid/epoxy-hydroxyl reactions between all three components in the blend which occurred via intermolecular hydrogen-bonding catalysis. The morphological analysis of the blends showed a significant reduction in the particle size of the dispersed phase from 4.3 μm in the binary blend, to 1.1 μm in the ternary blend. Finally, improved interfacial adhesion in conjunction with substantial shear yielding of the matrix were determined as the underlying mechanism responsible for enhanced impact strength in the ternary systems. This work demonstrates the applicability of bio-based farnesene polymers as rubber toughening agents to produce sustainably sourced toughened PLA blends.

6.7 Funding

This research was generously supported by the Natural Sciences and Engineering Research Council of Canada (Collaborative Research and Development Grants, CRDPJ 543853-2019 and Discovery Grants Program, RGPIN 05948-2019, RGPIN 06161-2018, 2016-03792) and the James McGill Chair program of McGill University. Student funding was provided by the Fonds de Recherche du Québec - Nature et Technologie (FRQNT), which granted Matthew W. Halloran a Doctoral Scholarship administered under the B2X program.

6.8 Acknowledgements

The authors thank the McGill Chemistry Characterization facility for use of their facility, whose operations are supported by the Quebec Center for Advanced Materials (QCAM). They also acknowledge and thank the Department of Chemical Engineering at Polytechnique Montréal for the use of their facility to perform Izod impact testing. They would also like to thank Dr. Georges Younes for sharing his rheology expertise, and Dr. Sharmaine Luk for her helpful discussions relating to the synthesis. The authors also thank Derek McPhee from Amyris for facilitating the acquisition of the farnesene used in this study. Finally, they would like to acknowledge and thank the McGill Facility for Electron Microscopy Research (FEMR) for use of their equipment and sample preparation.

6.9 References

1. Sangeetha, V. H.; Deka, H.; Varghese, T. O.; Nayak, S. K. State of the Art and Future Prospectives of Poly(Lactic Acid) Based Blends and Composites. *Polym. Compos.* **2018**, *39* (1), 81-101.

2. Reichert, C. L.; Bugnicourt, E.; Coltelli, M. B.; Cinelli, P.; Lazzeri, A.; Canesi, I.; Braca, F.; Martinez, B. M.; Alonso, R.; Agostinis, L.; Verstichel, S.; Six, L.; De Mets, S.; Gomez, E. C.; Issbrucker, C.; Geerinck, R.; Nettleton, D. F.; Campos, I.; Sauter, E.; Pieczyk, P.; Schmid, M. Bio-Based Packaging: Materials, Modifications, Industrial Applications and Sustainability. *Polymers* **2020**, *12* (7), 1558.

3. da Silva, D.; Kaduri, M.; Poley, M.; Adir, O.; Krinsky, N.; Shainsky-Roitman, J.; Schroeder, A. Biocompatibility, Biodegradation and Excretion of Polylactic Acid (Pla) in Medical Implants and Theranostic Systems. *Chem Eng J* **2018**, *340*, 9-14.

4. Singhvi, M. S.; Zinjarde, S. S.; Gokhale, D. V. Polylactic Acid: Synthesis and Biomedical Applications. *J Appl Microbiol* **2019**, *127* (6), 1612-1626.

5. Farah, S.; Anderson, D. G.; Langer, R. Physical and Mechanical Properties of Pla, and Their Functions in Widespread Applications — a Comprehensive Review. *Adv. Drug Deliv. Rev.* **2016**, *107*, 367-392.

6. Halloran, M. W.; Danielczak, L.; Nicell, J. A.; Leask, R. L.; Marić, M. Highly Flexible Polylactide Food Packaging Plasticized with Nontoxic, Biosourced Glycerol Plasticizers. *ACS Appl. Polym. Mater.* **2022**, *4* (5), 3608-3617.

7. Hamad, K.; Kaseem, M.; Ayyoob, M.; Joo, J.; Deri, F. Polylactic Acid Blends: The Future of Green, Light and Tough. *Prog. Polym. Sci.* **2018**, *85*, 83-127.

8. Liu, H.; Zhang, J. Research Progress in Toughening Modification of Poly(Lactic Acid). *J. Polym. Sci. B Polym. Phys.* **2011**, *49* (15), 1051-1083.

9. Zhao, X.; Hu, H.; Wang, X.; Yu, X.; Zhou, W.; Peng, S. Super Tough Poly(Lactic Acid) Blends: A Comprehensive Review. *RSC Advances* **2020**, *10* (22), 13316-13368.

10. Krishnan, S.; Pandey, P.; Mohanty, S.; Nayak, S. K. Toughening of Polylactic Acid: An Overview of Research Progress. *Polym. Plast. Technol. Eng.* **2016**, *55* (15), 1623-1652.

11. Alias, N. F.; Ismail, H. An Overview of Toughening Polylactic Acid by an Elastomer. *Polym. Plast. Technol. Mat.* **2019**, *58* (13), 1399-1422.

12. Thurber, C. M.; Xu, Y.; Myers, J. C.; Lodge, T. P.; Macosko, C. W. Accelerating Reactive Compatibilization of Pe/Pla Blends by an Interfacially Localized Catalyst. *ACS Macro Lett.* **2015**, *4* (1), 30-33.

13. Rigoussen, A.; Verge, P.; Raquez, J.-M.; Habibi, Y.; Dubois, P. In-Depth Investigation on the Effect and Role of Cardanol in the Compatibilization of Pla/Abs Immiscible Blends by Reactive Extrusion. *Eur. Polym. J.* **2017**, *93*, 272-283.

14. Akos, N. I.; Wahit, M. U.; Mohamed, R.; Yussuf, A. A. Comparative Studies of Mechanical Properties of Poly(Ɛ-Caprolactone) and Poly(Lactic Acid) Blends Reinforced with Natural Fibers. *Compos. Interfaces* **2013**, *20* (7), 459-467.

15. Wu, F.; Misra, M.; Mohanty, A. K. Tailoring the Toughness of Sustainable Polymer Blends from Biodegradable Plastics Via Morphology Transition Observed by Atomic Force Microscopy. *Polym. Degrad. Stab.* **2020**, *173*, 109066.

16. Yuryev, Y.; Mohanty, A. K.; Misra, M. Novel Super-Toughened Bio-Based Blend from Polycarbonate and Poly(Lactic Acid) for Durable Applications. *RSC Advances* **2016**, *6* (107), 105094-105104.

17. Oyama, H. T. Super-Tough Poly(Lactic Acid) Materials: Reactive Blending with Ethylene Copolymer. *Polymer* **2009**, *50* (3), 747-751.

18. Wang, M.; Wu, Y.; Li, Y.-D.; Zeng, J.-B. Progress in Toughening Poly(Lactic Acid) with Renewable Polymers. *Polym. Rev.* **2017**, *57* (4), 557-593.

19. Dong, W.; Cao, X.; Li, Y. High-Performance Biosourced Poly(Lactic Acid)/Polyamide 11 Blends with Controlled Salami Structure. *Polym. Int.* **2014**, *63* (6), 1094-1100.

20. Rasselet, D.; Caro-Bretelle, A.-S.; Taguet, A.; Lopez-Cuesta, J.-M. Reactive Compatibilization of Pla/Pa11 Blends and Their Application in Additive Manufacturing. *Materials (Basel)* **2019**, *12* (3), 485.

21. Yeo, J. C. C.; Muiruri, J. K.; Tan, B. H.; Thitsartarn, W.; Kong, J.; Zhang, X.; Li, Z.; He, C. Biodegradable Phb-Rubber Copolymer Toughened Pla Green Composites with Ultrahigh Extensibility. *ACS Sustain. Chem. Eng.* **2018**, *6* (11), 15517-15527.

22. Thakur, S.; Cisneros-Lopez, E. O.; Pin, J.-M.; Misra, M.; Mohanty, A. K. Green Toughness Modifier from Downstream Corn Oil in Improving Poly(Lactic Acid) Performance. *ACS Appl. Polym. Mater.* **2019**, *1* (12), 3396-3406.

23. Mauck, S. C.; Wang, S.; Ding, W.; Rohde, B. J.; Fortune, C. K.; Yang, G.; Ahn, S.-K.; Robertson, M. L. Biorenewable Tough Blends of Polylactide and Acrylated Epoxidized Soybean Oil Compatibilized by a Polylactide Star Polymer. *Macromolecules* **2016**, *49* (5), 1605-1615.

24. Muiruri, J. K.; Liu, S.; Teo, W. S.; Kong, J.; He, C. Highly Biodegradable and Tough Polylactic Acid–Cellulose Nanocrystal Composite. *ACS Sustain. Chem. Eng.* **2017**, *5* (5), 3929-3937.

25. Yang, W.; Weng, Y.; Puglia, D.; Qi, G.; Dong, W.; Kenny, J. M.; Ma, P. Poly(Lactic Acid)/Lignin Films with Enhanced Toughness and Anti-Oxidation Performance for Active Food Packaging. *Int. J. Biol. Macromol.* **2020**, *144*, 102-110.

26. Abdelwahab, M. A.; Jacob, S.; Misra, M.; Mohanty, A. K. Super-Tough Sustainable Biobased Composites from Polylactide Bioplastic and Lignin for Bio-Elastomer Application. *Polymer* **2021**, *212*, 123153.

27. Luk, S. B.; Azevedo, L. A.; Maric, M. Reversible Deactivation Radical Polymerization of Bio-Based Dienes. *React. Funct. Polym.* **2021**, *162*, 104871.

28. Hulnik, M. I.; Vasilenko, I. V.; Radchenko, A. V.; Peruch, F.; Ganachaud, F.; Kostjuk, S. V. Aqueous Cationic Homo- and Co-Polymerizations of Β-Myrcene and Styrene: A Green Route toward Terpene-Based Rubbery Polymers. *Polym. Chem-Uk* **2018**, *9* (48), 5690-5700.

29. Yoo, T.; Henning, S. K. Synthesis and Characterization of Farnesene-Based Polymers. *Rubber Chem. Technol.* **2017**, *90* (2), 308-324.

30. Bolton, J. M.; Hillmyer, M. A.; Hoye, T. R. Sustainable Thermoplastic Elastomers from Terpene-Derived Monomers. *ACS Macro Lett.* **2014**, *3* (8), 717-720.

31. Dalsin, S. J.; Hillmyer, M. A.; Bates, F. S. Linear Rheology of Polyolefin-Based Bottlebrush Polymers. *Macromolecules* **2015**, *48* (13), 4680-4691.

32. Wahlen, C.; Blankenburg, J.; von Tiedemann, P.; Ewald, J.; Sajkiewicz, P.; Müller, A. H. E.; Floudas, G.; Frey, H. Tapered Multiblock Copolymers Based on Farnesene and Styrene: Impact

of Biobased Polydiene Architectures on Material Properties. *Macromolecules* **2020**, *53* (23), 10397-10408.

33. Sarkar, P.; Bhowmick, A. K. Synthesis, Characterization and Properties of a Bio-Based Elastomer: Polymyrcene. *RSC Advances* **2014**, *4* (106), 61343-61354.

34. Rude, M. A.; Schirmer, A. New Microbial Fuels: A Biotech Perspective. *Curr. Opin. Microbiol.* **2009**, *12* (3), 274-281.

35. Cawse, J. L.; Stanford, J. L.; Still, R. H. Polymers from Renewable Sources: 5. Myrcene-Based Polyols as Rubber-Toughening Agents in Glassy Polyurethanes. *Polymer* **1987**, *28* (3), 368-374.

36. Zhou, C.; Wei, Z.; Jin, C.; Wang, Y.; Yu, Y.; Leng, X.; Li, Y. Fully Biobased Thermoplastic Elastomers: Synthesis of Highly Branched Linear Comb Poly(B-Myrcene)-Graft-Poly(L-Lactide) Copolymers with Tunable Mechanical Properties. *Polymer* **2018**, *138*, 57-64.

37. Thurber, C.; Gu, L.; Myers, J. C.; Lodge, T. P.; Macosko, C. W. Toughening Polylactide with a Catalyzed Epoxy-Acid Interfacial Reaction. *Polym. Eng. Sci.* **2018**, *58* (1), 28-36.

38. Yuryev, Y.; Mohanty, A. K.; Misra, M. A New Approach to Supertough Poly(Lactic Acid): A High Temperature Reactive Blending. *Macromol. Mater. Eng.* **2016**, *301* (12), 1443-1453.

39. Luk, S. B.; Métafiot, A.; Morize, J.; Edeh, E.; Marić, M. Hydrogenation of Poly(Myrcene) and Poly(Farnesene) Using Diimide Reduction at Ambient Pressure. *J. Polym. Sci.* **2021**, *59* (19), 2140-2153.

40. Marić, M.; Ashurov, N.; Macosko, C. W. Reactive Blending of Poly (Dimethylsiloxane) with Nylon 6 and Poly (Styrene):Effect of Reactivity on Morphology. *Polym. Eng. Sci.* **2001**, *41* (4), 631-642.

41. Nerkar, M.; Ramsay, J. A.; Ramsay, B. A.; Kontopoulou, M. Dramatic Improvements in Strain Hardening and Crystallization Kinetics of Pla by Simple Reactive Modification in the Melt State. *Macromol. Mater. Eng.* **2014**, *299* (12), 1419-1424.

42. Fetters, L. J.; Lohse, D. J.; Richter, D.; Witten, T. A.; Zirkel, A. Connection between Polymer Molecular Weight, Density, Chain Dimensions, and Melt Viscoelastic Properties. *Macromolecules* **1994**, *27* (17), 4639-4647.

43. Iacob, C.; Yoo, T.; Runt, J. Molecular Dynamics of Polyfarnesene. *Macromolecules* **2018**, *51* (13), 4917-4922.

44. Sahu, P.; Bhowmick, A. K. Redox Emulsion Polymerization of Terpenes: Mapping the Effect of the System, Structure, and Reactivity. *Ind. Eng. Chem. Res.* **2019**, *58* (46), 20946-20960.

45. Luk, S. B.; Maríc, M. Polymerization of Biobased Farnesene in Miniemulsions by Nitroxide-Mediated Polymerization. *ACS Omega* **2021**, *6* (7), 4939-4949.

46. Luk, S. B.; Marić, M. Nitroxide-Mediated Polymerization of Bio-Based Farnesene with a Functionalized Methacrylate. *Macromol. React. Eng.* **2019**, *13* (3), 1800080.

47. Bai, H.; Bai, D.; Xiu, H.; Liu, H.; Zhang, Q.; Wang, K.; Deng, H.; Chen, F.; Fu, Q.; Chiu, F.-C. Towards High-Performance Poly(L-Lactide)/Elastomer Blends with Tunable Interfacial Adhesion and Matrix Crystallization Via Constructing Stereocomplex Crystallites at the Interface. *RSC Advances* **2014**, *4* (90), 49374-49385.

48. Feng, Y.; Zhao, G.; Yin, J.; Jiang, W. Reactive Compatibilization of High-Impact Poly(Lactic Acid)/Ethylene Copolymer Blends Catalyzed by N,N-Dimethylstearylamine. *Polym. Int.* **2014**, *63* (7), 1263-1269.

49. Zhang, K.; Nagarajan, V.; Misra, M.; Mohanty, A. K. Supertoughened Renewable Pla Reactive Multiphase Blends System: Phase Morphology and Performance. *ACS Appl. Mater. Inter.* **2014**, *6* (15), 12436-12448.

50. Favis, B. D.; Chalifoux, J. P. The Effect of Viscosity Ratio on the Morphology of Polypropylene/Polycarbonate Blends During Processing. *Polym. Eng. Sci.* **1987**, *27* (21), 1591-1600.

51. Sundararaj, U.; Macosko, C. W. Drop Breakup and Coalescence in Polymer Blends: The Effects of Concentration and Compatibilization. *Macromolecules* **1995**, *28* (8), 2647-2657.

52. Oxby, K. J.; Marić, M. Compatibilization of Poly(Styrene-Acrylonitrile) (San)/Poly(Ethylene) Blends Via Amine Functionalization of San Chain Ends. *Macromol. React. Eng.* **2014**, *8* (2), 160-169.

53. Chang, K.; Robertson, M. L.; Hillmyer, M. A. Phase Inversion in Polylactide/Soybean Oil Blends Compatibilized by Poly(Isoprene-B-Lactide) Block Copolymers. *ACS Appl. Mater. Inter.* **2009**, *1* (10), 2390-2399.

54. Han, L.; Han, C.; Dong, L. Morphology and Properties of the Biosourced Poly(Lactic Acid)/Poly(Ethylene Oxide-B-Amide-12) Blends. *Polym. Compos.* **2013**, *34* (1), 122-130.

55. Kowalczyk, M.; Piorkowska, E. Mechanisms of Plastic Deformation in Biodegradable Polylactide/Poly(1,4-Cis-Isoprene) Blends. *J. Appl. Polym. Sci.* **2012**, *124* (6), 4579-4589.

56. Bhardwaj, R.; Mohanty, A. K. Modification of Brittle Polylactide by Novel Hyperbranched Polymer-Based Nanostructures. *Biomacromolecules* **2007**, *8* (8), 2476-2484.

57. Liu, H.; Chen, F.; Liu, B.; Estep, G.; Zhang, J. Super Toughened Poly(Lactic Acid) Ternary Blends by Simultaneous Dynamic Vulcanization and Interfacial Compatibilization. *Macromolecules* **2010**, *43* (14), 6058-6066.

58. Liu, H.; Guo, L.; Guo, X.; Zhang, J. Effects of Reactive Blending Temperature on Impact Toughness of Poly(Lactic Acid) Ternary Blends. *Polymer* **2012**, *53* (2), 272-276.

59. Nagarajan, V.; Mohanty, A. K.; Misra, M. Perspective on Polylactic Acid (Pla) Based Sustainable Materials for Durable Applications: Focus on Toughness and Heat Resistance. *ACS Sustain. Chem. Eng.* **2016**, *4* (6), 2899-2916.

60. Ougizawa, T.; Inoue, T. Morphology of Polymer Blends. In *Polymer Blends Handbook*, Utracki, L. A., Wilkie, C. A. Eds.; Springer Netherlands, 2014; pp 875-918.

61. Zhang, K.; Mohanty, A. K.; Misra, M. Fully Biodegradable and Biorenewable Ternary Blends from Polylactide, Poly(3-Hydroxybutyrate-Co-Hydroxyvalerate) and Poly(Butylene Succinate) with Balanced Properties. *ACS Appl. Mater. Inter.* **2012**, *4* (6), 3091-3101.

62. Li, Y.; Shimizu, H. Toughening of Polylactide by Melt Blending with a Biodegradable Poly(Ether)Urethane Elastomer. *Macromol. Biosci.* **2007**, *7* (7), 921-928.

63. Wu, N.; Zhang, H. Mechanical Properties and Phase Morphology of Super-Tough Pla/Pbat/Ema-Gma Multicomponent Blends. *Mater. Lett.* **2017**, *192*, 17-20.

64. Liu, H.; Song, W.; Chen, F.; Guo, L.; Zhang, J. Interaction of Microstructure and Interfacial Adhesion on Impact Performance of Polylactide (Pla) Ternary Blends. *Macromolecules* **2011**, *44* (6), 1513-1522.

65. Chieng, B. W.; Ibrahim, N. A.; Yunus, W. M. Z. W.; Hussein, M. Z. Poly(Lactic Acid)/Poly(Ethylene Glycol) Polymer Nanocomposites: Effects of Graphene Nanoplatelets. *Polymers* **2014**, *6* (1), 93-104.

66. Coleman, M. M.; Lee, J. Y.; Painter, P. C. Acid Salts and the Structure of Ionomers. *Macromolecules* **1990**, *23* (8), 2339-2345.

67. Moskala, E. J.; Howe, S. E.; Painter, P. C.; Coleman, M. M. On the Role of Intermolecular Hydrogen Bonding in Miscible Polymer Blends. *Macromolecules* **1984**, *17* (9), 1671-1678.

68. Büttner, H.; Longwitz, L.; Steinbauer, J.; Wulf, C.; Werner, T. Recent Developments in the Synthesis of Cyclic Carbonates from Epoxides and Co2. *Top. Curr. Chem.* **2017**, *375* (3), 50.

69. Pinto da Silva, L. Mechanistic Study of the Role of Hydrogen Bond Donors in the Two-Component Organocatalysis of the Ring-Opening Reaction of Epoxides. *Mol. Catal.* **2019**, *474*, 110425.

70. Wurst, J. M.; Liu, G.; Tan, D. S. Hydrogen-Bonding Catalysis and Inhibition by Simple Solvents in the Stereoselective Kinetic Epoxide-Opening Spirocyclization of Glycal Epoxides to Form Spiroketals. *J. Am. Chem. Soc.* **2011**, *133* (20), 7916-7925.

7 Discussion and Future Work

In this section, a brief discussion about the results presented in Chapters 3 through 6 will be provided, followed by a summary of the main conclusions from this body of work. Finally, several recommendations for future work are provided.

7.1 Discussion

This thesis aimed to demonstrate the feasibility of improving the mechanical and thermal properties of PVC and PLA blends via renewably sourced additives that can serve as viable replacements for their petroleum-derived counterparts. While this area of research is one which has received considerable attention in recent years, many examples of developments in this field are incomplete as investigations have been limited to only one or two key material properties (i.e., elongation at break, reduction of T_g, impact strength). In contrast, in the present thesis, a broader approach is presented for the development of polymer additives with marketable potential. Therefore, this thesis aimed to illustrate that this strategy is both feasible, and necessary to avoid substitution of problematic chemicals with compounds that have their own regrettable characteristics.

In the first manuscript presented in Chapter 3, a series of heptyl-succinate plasticizers for PVC were synthesized with a varying number of branches to study the relationship between branching and permanence in small molecule plasticizers. Analogous to polymeric plasticizers, it was shown that increased branching of the small molecule plasticizers led to a decrease in migration into non-polar media. However, a significant decrease in plasticizer efficiency was observed with compounds functionalized with four or more heptyl-succinate arms. This was believed to be due to their incompatibility with the PVC matrix which arose from an imbalance between polar and non-polar functional groups on the plasticizers; rendering them too polar and unable to effectively solvate the PVC matrix to function as a plasticizer. Additionally, the application of quantitative ^{1}H NMR for accurately monitoring plasticizer leaching was demonstrated and was shown to be a more reliable method than traditional gravimetric analysis.

In the second manuscript presented in Chapter 4, the focus was shifted away from the use of PVC, and towards the renewably sourced, compostable polymer PLA. Herein, glycerol was used as a building block for the design of bio-plasticizers functionalized with succinate groups and alkyl chains of differing lengths. In contrast to what is seen in the PVC plasticizer literature, there are significantly fewer examples of effective plasticizers being developed for flexible PLA applications. Additionally, many of the studies have relied solely on the use of solvent-casting to produce thin film specimens to evaluate the plasticization efficiency. Although this method has generally become an accepted strategy to evaluate new plasticizers on a lab scale, it has very little industrial relevance as PLA processing is performed industrially using film blowing, calendering or extrusion, which are operated at high temperatures in the melt. Therefore, to bridge the gap between lab and industry, the evaluation of plasticizers in the present work was conducted using solvent-casting as well as melt-mixing. Overall, it was found that the glycerol-succinate plasticizers functionalized with alkyl chains of six or less carbons produced highly flexible film and bulk specimen samples, were more miscible with the PLA matrix, had lower levels of migration, and were also shown to be non-toxic. In particular, the glycerol-succinate compound substituted with a hexyl chain (GS-C6) produced blends with higher elongation at break and greater thermal stability than the commercial plasticizer ATBC.

The third manuscript presented in Chapter 5 served as an extension of the work described in Chapter 4. Herein, the previously developed glycerol compounds were evaluated as potential plasticizers for PVC. At plasticizer loadings of 40 phr, tensile, thermal, morphological, and migration properties of the blends were examined and benchmarked against the commercial *ortho*-phthalate alternative plasticizer DOTP (Eastman 168). Like our group's previous work looking at linear succinate ester plasticizers, it was found that the glycerol-succinate compounds that were functionalized with alkyl chain lengths between four and seven carbons demonstrated the highest plasticization efficiency. The blends produced with these derivatives showed comparable reduction of T_g, and greater improvements in elongation at break relative to DOTP. A clear relationship between alkyl chain length and migration behaviour was also established as the longer chain (and therefore more non-polar) derivatives exhibited higher degrees of migration into non-polar media, and lower degrees of migration into polar media than the shorter chain counterparts. Finally, the blend morphologies revealed phase separation and droplet formation with the shorter chain, more polar plasticizers - agreeing with our calculated HSP values. Overall, this work demonstrated that the glycerol plasticizers were able to effectively serve as dual-purpose plasticizers for both PLA and PVC.

As discussed in Chapter 2, there are two commonly used approaches to improve the mechanical properties of PLA: plasticization to reduce T_g and enhance ductility, and rubber toughening to improve impact strength. As with the earlier plasticizer work, the focus was shifted to target the development of renewably sourced polymeric rubber toughening agents for PLA. As such, the fourth manuscript presented in Chapter 6 describes efforts towards attaining this goal. Here, the terpene monomer, farnesene was used as a building block for the synthesis of GMA and MAA functionalized copolymers and blended with PLA at different loadings with the intent of promoting an interfacial compatibilization reaction to overcome the immiscibility between the phases. It was found that the ternary blends consisting of PFGMA, PFMAA, and PLA displayed remarkable improvements in elongation at break and impact strength (~10-fold and ~16-fold, respectively) relative to neat PLA. Using a combination of SEM, torque mixer measurements, and FTIR, it was deduced that the enhanced toughness arose from the occurrence of cross-linking reactions *in situ* during blending which were catalyzed by intermolecular hydrogen bonding. Additionally, the phase morphologies of the ternary blends showed an approximate 4-fold reduction in particle diameter relative to the binary systems (i.e., from 4.3 to 1.1 μm) with the compatibilized blend morphology deemed stable upon annealing. For many rubber-toughened systems substantial impact strength improvement is observed when the dispersed phase size area ~ 1 μm.

7.2 Conclusions

Altogether, the work described in this thesis represents a significant contribution to the field of renewable polymer additives as it was demonstrated that renewably sourced chemical feedstocks could be used to design plasticizers and impact modifiers without sacrificing performance or functionality of the final product. Moreover, it was established that a broad approach of additive design that considers a wide spectrum of testing while benchmarking performance against commercially relevant products is one which is both attainable and fundamental in the development of viable alternatives to petroleum-based products.

In relation to the proposed objectives in Chapter 1, the following conclusions can be made:

- ^{1}H NMR serves as a more reliable analytical tool to quantify plasticizer leaching than the gravimetric method

- A higher degree of branching in small molecule plasticizers leads to higher permanence; however, the higher branched compounds function poorly as plasticizers
- Glycerol-succinate plasticizers functionalized with linear alkyl chains between four and six carbons in length perform well as plasticizers for both PLA and PVC, are non-toxic, and display similar leaching behaviour to commercial plasticizers.
- When copolymerized with glycidyl methacrylate and methacrylic acid, farnesene can serve as a renewable rubber toughening agent for PLA, while reactive compatibilization can be achieved without the use of external catalysis or elevated blending temperatures.

7.3 Recommendations for Future Work

Based on the work presented in this thesis in conjunction with the results that were obtained, the following recommendations are made for future areas of study:

1. Biodegradation experiments of the glycerol-succinate plasticizers should be performed alongside ATBC and DOTP to identify their respective rates of degradation as well as their metabolites. After being identified, cytotoxicity tests should be conducted on the metabolites. This would be useful to further support claims about the developing non-toxic plasticizers and would allow for future branched plasticizers to be optimized for faster biodegradation.

2. The effect of the glycerol plasticizers on the rate of composting and biodegradation of PLA should be investigated. This would aid in the future design of PLA plasticizers as well as would permit a direct comparison between current commercial plasticizers and our newly developed derivatives.

3. Aging tests should be performed on the plasticized PLA films to evaluate their physical and mechanical properties after a period of one to two months. Plasticized PLA is known to slowly crystallize over time, making the films extremely brittle and leading to mechanical failure. If the films are to be used as food packaging materials, they will need to retain their ductility long enough to serve their purpose.

4. Several avenues for the continuation of the poly(farnesene) rubber toughening agents project should be explored: (a) Farnesene should be co-polymerized with cyclic ketene acetal functional groups to enhance its biodegradability by introducing hydrolysable ester linkages throughout the polymer backbone (Figure 7.1a); (b) bio-derived itaconic acid should be used in place of methacrylic acid to eliminate reliance on petroleum sourced chemicals (Figure 7.2b); (c) Farnesene should be co-polymerized with a monomer containing a UV-sensitive functional group (diazirine, benzophenone, azide) and blended with PLA; i.e., upon irradiation of UV light (or even heat during blending), the photo-sensitive group will form a highly reactive radical species which can generate a cross-linked polymer network with potential as a super toughened PLA blend (Figure 7.2c); and (d) catalysts should be screened to improve the rate of the acid/hydroxyl-epoxy reaction.

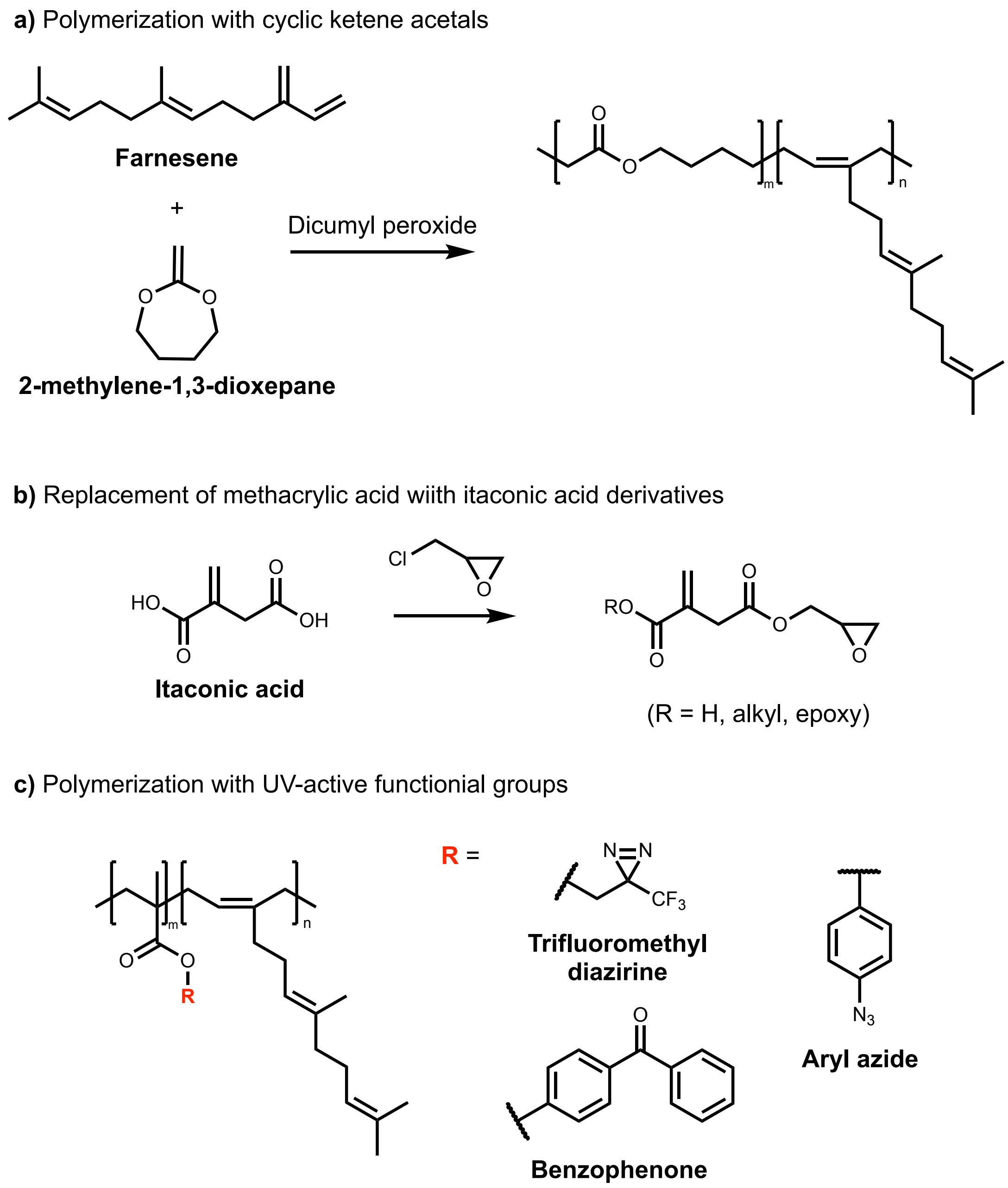
a) Polymerization with cyclic ketene acetals

b) Replacement of methacrylic acid wiith itaconic acid derivatives

c) Polymerization with UV-active functionial groups

Figure 7.1. Proposed future avenues of work for the continuation of the poly(farnesene) rubber toughening project.

5. Life cycle assessments should be performed on the glycerol plasticizers as well as the poly(farnesene) rubber toughening agents. This would help to substantiate our claims of developing renewable polymeric additives as well as provide us with a realistic evaluation of the marketability of these compounds.

8 Original Contributions

The work reported in this thesis consists of several significant contributions to the area of renewable polymer additives. Briefly, the original contributions reported in this work include the following:

1. A significant relationship between branching/molecular weight of small molecule plasticizers and their permanence in PVC blends was established. Plasticizers with higher degrees of branching were proven to be more resistant to leaching than linear compounds; however, the highly branched compounds performed poorly as plasticizers. This was attributed to an imbalance between polar and non-polar moieties on the plasticizer.

2. ^{1}H NMR was shown to be a more effective analytical tool to quantify plasticizer leaching than the gravimetric method. This served as the first report of ^{1}H NMR being used for this application.

3. Glycerol-succinate esters were shown to be excellent candidates as alternative bio-based plasticizers for PLA. The hexyl substituted derivative (GS-C6) was shown to have higher thermal stability, higher elongation at break, and comparable migration behaviour to the commercial plasticizer ATBC.

4. The dual functionality of the glycerol compounds to plasticize two distinct polymer matrices was demonstrated. This contribution sets the stage for further work in the area of developing multi-purpose commodity chemicals as well as identifies several commonalities between what defines an effective PLA/PVC plasticizer.

5. High molecular weight farnesene copolymers consisting of farnesene-methacrylic acid and farnesene-glycidyl methacrylate were shown to be effective rubber toughening agents to significantly improve the impact strength of PLA. A reactive compatibilization mechanism involving intermolecular hydrogen bonding was established in the melt. Overall, this contribution served as the first reported application of poly(farnesene) derivatives as

renewably sourced polymeric additives and provides an excellent starting point for continued work.

9 References

1. Skoczinski, P.; Krause, L.; Raschka, A.; Dammer, L.; Carus, M., Chapter One - Current status and future development of plastics: Solutions for a circular economy and limitations of environmental degradation. In *Methods in Enzymology*, Weber, G.; Bornscheuer, U. T.; Wei, R., Eds. Academic Press: 2021; Vol. 648, pp 1-26.

2. Groh, K. J.; Backhaus, T.; Carney-Almroth, B.; Geueke, B.; Inostroza, P. A.; Lennquist, A.; Leslie, H. A.; Maffini, M.; Slunge, D.; Trasande, L.; Warhurst, A. M.; Muncke, J., Overview of known plastic packaging-associated chemicals and their hazards. *Sci. Total Environ.* **2019,** *651*, 3253-3268.

3. Spevacek, J., A change is gonna come. *Nat. Rev. Chem.* **2017,** *1* (1), 0008.

4. Zhang, Z. M.; Jiang, P. P.; Liu, D. K.; Feng, S.; Zhang, P. B.; Wang, Y. T.; Fu, J. H.; Agus, H., Research progress of novel bio-based plasticizers and their applications in poly(vinyl chloride). *J. Mater. Sci.* **2021,** *56* (17), 10155-10182.

5. Bocque, M.; Voirin, C.; Lapinte, V.; Caillol, S.; Robin, J. J., Petro-Based and Bio-Based Plasticizers: Chemical Structures to Plasticizing Properties. *J. Polym. Sci. A* **2016,** *54* (1), 11-33.

6. Fischer, I.; Schmitt, W. F.; Porth, H. C.; Allsopp, M. W.; Vianello, G., Poly(vinyl chloride). In *Ullmann's Encyclopedia of Industrial Chemistry*, Wiley-VCH: Weinheim, Germany, 2014

7. Godwin, A. D., 28 - Plasticizers. In *Applied Plastics Engineering Handbook*, Kutz, M., Ed. William Andrew Publishing: Oxford, 2011; pp 487-501.

8. Wei, X.-F.; Linde, E.; Hedenqvist, M. S., Plasticiser loss from plastic or rubber products through diffusion and evaporation. *NPJ Mater. Degrad.* **2019,** *3* (1), 18.

9. Czogała, J.; Pankalla, E.; Turczyn, R., Recent Attempts in the Design of Efficient PVC Plasticizers with Reduced Migration. *Materials* **2021,** *14* (4), 844.

10. da Silva, D.; Kaduri, M.; Poley, M.; Adir, O.; Krinsky, N.; Shainsky-Roitman, J.; Schroeder, A., Biocompatibility, biodegradation and excretion of polylactic acid (PLA) in medical implants and theranostic systems. *Chem Eng J* **2018,** *340*, 9-14.

11. Reichert, C. L.; Bugnicourt, E.; Coltelli, M. B.; Cinelli, P.; Lazzeri, A.; Canesi, I.; Braca, F.; Martinez, B. M.; Alonso, R.; Agostinis, L.; Verstichel, S.; Six, L.; De Mets, S.; Gomez, E. C.; Issbrucker, C.; Geerinck, R.; Nettleton, D. F.; Campos, I.; Sauter, E.; Pieczyk, P.; Schmid, M., Bio-Based Packaging: Materials, Modifications, Industrial Applications and Sustainability. *Polymers* **2020,** *12* (7).

12. Sangeetha, V. H.; Deka, H.; Varghese, T. O.; Nayak, S. K., State of the art and future prospectives of poly(lactic acid) based blends and composites. *Polym. Compos.* **2018,** *39* (1), 81-101.

13. Zhao, X.; Hu, H.; Wang, X.; Yu, X.; Zhou, W.; Peng, S., Super tough poly(lactic acid) blends: a comprehensive review. *RSC Advances* **2020,** *10* (22), 13316-13368.

14. Patrick, S., *Practical guide to polyvinyl chloride*. iSmithers Rapra Publishing: 2005.

15. Yu, J.; Sun, L.; Ma, C.; Qiao, Y.; Yao, H., Thermal degradation of PVC: A review. *Waste Manage.* **2016,** *48*, 300-314.

16. Marcilla, A.; Beltran, M., 5 - Mechanisms of plasticizers action. In *Handbook of Plasticizers (Third Edition)*, Wypych, G., Ed. ChemTec Publishing: 2017; pp 119-134.

17. Wypych, G., *Handbook of plasticizers*. ChemTec Publishing: 2004.

18. Sears, J. K.; Darby, J. R., *The Technology of Plasticizers*. John Wiley New York, NY, USA, 1982.

19. Erythropel, H. C.; Maric, M.; Nicell, J. A.; Leask, R. L.; Yargeau, V., Leaching of the plasticizer di(2-ethylhexyl)phthalate (DEHP) from plastic containers and the question of human exposure. *Appl. Microbiol. Biotechnol.* **2014,** *98* (24), 9967-9981.

20. Kastner, J.; Cooper, D. G.; Maric, M.; Dodd, P.; Yargeau, V., Aqueous leaching of di-2-ethylhexyl phthalate and "green" plasticizers from poly(vinyl chloride). *Sci. Total Environ.* **2012,** *432*, 357-364.

21. Jamarani, R.; Erythropel, H. C.; Nicell, J. A.; Leask, R. L.; Maric, M., How Green is Your Plasticizer? *Polymers* **2018,** *10* (8).

22. Koch, H. M.; Preuss, R.; Angerer, J., Di(2-ethylhexyl)phthalate (DEHP): human metabolism and internal exposure - an update and latest results. *Int. J. Androl.* **2006,** *29* (1), 155-165.

23. Richburg, J. H.; Boekelheide, K., Mono-(2-ethylhexyl) phthalate rapidly alters both Sertoli cell vimentin filaments and germ cell apoptosis in young rat testes. *Toxicol. Appl. Pharm.* **1996,** *137* (1), 42-50.

24. Daniels, P. H., A Brief Overview of Theories of PVC Plasticization and Methods Used to Evaluate PVC-Plasticizer Interaction. *J. Vinyl Addit. Technol.* **2009,** *15* (4), 219-223.

25. Kirkpatrick, A., Some relations between molecular structure and plasticizing effect. *J. Appl. Phys* **1940,** *11* (4), 255-261.

26. Aiken, W.; Alfrey, T.; Janssen, A.; Mark, H., Creep Behavior of Plasticized Vinylite VYNW. *J. Polym. Sci.* **1947,** *2* (2), 178-198.

27. Fox, T. G.; Flory, P. J., 2nd-Order Transition Temperatures and Related Properties of Polystyrene 1. Influence of Molecular Weight *J. Appl. Phys* **1950,** *21* (6), 581-591.

28. Zeikus, J. G.; Jain, M. K.; Elankovan, P., Biotechnology of succinic acid production and markets for derived industrial products. *Appl. Microbiol. Biotechnol.* **1999,** *51* (5), 545-552.

29. Dai, Z.; Guo, F.; Zhang, S.; Zhang, W.; Yang, Q.; Dong, W.; Jiang, M.; Ma, J.; Xin, F., Bio-based succinic acid: an overview of strain development, substrate utilization, and downstream purification. *Biofuel. Bioprod. Biorefin.* **2020,** *14* (5), 965-985.

30. Elsiwi, B. M.; Garcia-Valdez, O.; Erythropel, H. C.; Leask, R. L.; Nicell, J. A.; Maric, M., Fully Renewable, Effective, and Highly Biodegradable Plasticizer: Di-n-heptyl Succinate. *ACS Sustain. Chem. Eng.* **2020,** *8* (33), 12409-12418.

31. Erythropel, H. C.; Shipley, S.; Bormann, A.; Nicell, J. A.; Maric, M.; Leask, R. L., Designing green plasticizers: Influence of molecule geometry and alkyl chain length on the plasticizing effectiveness of diester plasticizers in PVC blends. *Polymer* **2016,** *89*, 18-27.

32. Erythropel, H. C.; Dodd, P.; Leask, R. L.; Maric, M.; Cooper, D. G., Designing green plasticizers: Influence of alkyl chain length on biodegradation and plasticization properties of succinate based plasticizers. *Chemosphere* **2013,** *91* (3), 358-365.

33. Jamarani, R.; Halloran, M. W.; Panchal, K.; Nicell, J. A.; Leask, R. L.; Marić, M., Poly(ε-caprolactone)-based additives: Plasticization efficacy and migration resistance. *J. Vinyl Addit. Technol.* **2021,** *27* (4), 821-832.

34. Choi, J.; Kwak, S.-Y., Hyperbranched Poly(ε-caprolactone) as a Nonmigrating Alternative Plasticizer for Phthalates in Flexible PVC. *Environ. Sci. Technol.* **2007,** *41* (10), 3763-3768.

35. Shi, G. X.; Cooper, D. G.; Maric, M., Poly(epsilon-caprolactone)-based 'green' plasticizers for poly(vinyl choride). *Polym. Degrad. Stab.* **2011,** *96* (9), 1639-1647.

36. Karamanlioglu, M.; Preziosi, R.; Robson, G. D., Abiotic and biotic environmental degradation of the bioplastic polymer poly(lactic acid): A review. *Polym. Degrad. Stab.* **2017,** *137*, 122-130.

37. Zaaba, N. F.; Jaafar, M., A review on degradation mechanisms of polylactic acid: Hydrolytic, photodegradative, microbial, and enzymatic degradation. *Polym. Eng. Sci.* **2020,** *60* (9), 2061-2075.

38. Castro-Aguirre, E.; Iñiguez-Franco, F.; Samsudin, H.; Fang, X.; Auras, R., Poly(lactic acid)—Mass production, processing, industrial applications, and end of life. *Adv. Drug Deliv. Rev.* **2016,** *107*, 333-366.

39. Farah, S.; Anderson, D. G.; Langer, R., Physical and mechanical properties of PLA, and their functions in widespread applications — A comprehensive review. *Adv. Drug Deliv. Rev.* **2016,** *107*, 367-392.

40. Jem, K. J.; Tan, B., The development and challenges of poly (lactic acid) and poly (glycolic acid). *Adv. Ind. Eng. Polym. Res.* **2020,** *3* (2), 60-70.

41. Huang, S.; Xue, Y.; Yu, B.; Wang, L.; Zhou, C.; Ma, Y., A Review of the Recent Developments in the Bioproduction of Polylactic Acid and Its Precursors Optically Pure Lactic Acids. *Molecules* **2021,** *26* (21), 6446.

42. Bioplastics market data. https://www.european-bioplastics.org/market/ (accessed July 15th, 2022).

43. Wan, T.; Lin, Y.; Tu, Y., Plasticizing effect of glyceryl tribenzoate, dipropylene glycol dibenzoate, and glyceryl triacetate on poly(lactic acid). *Polym. Eng. Sci.* **2016,** *56* (12), 1399-1406.

44. Shirai, M. A.; Muller, C. M. O.; Grossmann, M. V. E.; Yamashita, F., Adipate and Citrate Esters as Plasticizers for Poly(Lactic Acid)/Thermoplastic Starch Sheets. *J. Polym. Environ.* **2015,** *23* (1), 54-61.

45. Xuan, W. X.; Hakkarainen, M.; Odelius, K., Levulinic Acid as a Versatile Building Block for Plasticizer Design. *ACS Sustain. Chem. Eng.* **2019,** *7* (14), 12552-12562.

46. Zawada, K.; Plichta, A.; Jańczewski, D.; Hajmowicz, H.; Florjańczyk, Z.; Stępień, M.; Sobiecka, A.; Synoradzki, L., Esters of Tartaric Acid, A New Class of Potential “Double Green” Plasticizers. *ACS Sustain. Chem. Eng.* **2017,** *5* (7), 5999-6007.

47. Park, M.; Choi, I.; Lee, S.; Hong, S. J.; Kim, A.; Shin, J.; Kang, H. C.; Kim, Y. W., Renewable malic acid-based plasticizers for both PVC and PLA polymers. *J. Ind. Eng. Chem.* **2020,** *88*, 148-158.

48. Chaochanchaikul, K.; Pongmuksuwan, P., Influence of Ozonized Soybean Oil as a Biobased Plasticizer on the Toughness of Polylactic Acid. *J. Polym. Environ.* **2021**, 1-11.

49. Bagnato, G.; Iulianelli, A.; Sanna, A.; Basile, A., Glycerol Production and Transformation: A Critical Review with Particular Emphasis on Glycerol Reforming Reaction for Producing Hydrogen in Conventional and Membrane Reactors. *Membranes (Basel)* **2017,** *7* (2), 17.

50. Tarique, J.; Sapuan, S. M.; Khalina, A., Effect of glycerol plasticizer loading on the physical, mechanical, thermal, and barrier properties of arrowroot (Maranta arundinacea) starch biopolymers. *Sci. Rep.* **2021,** *11* (1), 13900.

51. Petchwattana, N.; Sanetuntikul, J.; Narupai, B., Plasticization of Biodegradable Poly(Lactic Acid) by Different Triglyceride Molecular Sizes: A Comparative Study with Glycerol. *J. Polym. Environ.* **2018,** *26* (3), 1160-1168.

52. Kulinski, Z.; Piorkowska, E., Crystallization, structure and properties of plasticized poly(l-lactide). *Polymer* **2005,** *46* (23), 10290-10300.

53. Anderson, K. S.; Schreck, K. M.; Hillmyer, M. A., Toughening Polylactide. *Polym. Rev.* **2008,** *48* (1), 85-108.

54. Shrivastava, A., 3 - Plastic Properties and Testing. In *Introduction to Plastics Engineering*, Shrivastava, A., Ed. William Andrew Publishing: 2018; pp 49-110.

55. Alias, N. F.; Ismail, H., An overview of toughening polylactic acid by an elastomer. *Polym. Plast. Technol. Mat.* **2019,** *58* (13), 1399-1422.

56. Mauck, S. C.; Wang, S.; Ding, W.; Rohde, B. J.; Fortune, C. K.; Yang, G.; Ahn, S.-K.; Robertson, M. L., Biorenewable Tough Blends of Polylactide and Acrylated Epoxidized Soybean Oil Compatibilized by a Polylactide Star Polymer. *Macromolecules* **2016,** *49* (5), 1605-1615.

57. Orr, C. A.; Cernohous, J. J.; Guegan, P.; Hirao, A.; Jeon, H. K.; Macosko, C. W., Homogeneous reactive coupling of terminally functional polymers. *Polymer* **2001,** *42* (19), 8171-8178.

58. Liu, H.; Zhang, J., Research progress in toughening modification of poly(lactic acid). *J. Polym. Sci. B Polym. Phys.* **2011,** *49* (15), 1051-1083.

59. Thurber, C.; Gu, L.; Myers, J. C.; Lodge, T. P.; Macosko, C. W., Toughening polylactide with a catalyzed epoxy-acid interfacial reaction. *Polym. Eng. Sci.* **2018,** *58* (1), 28-36.

60. Cobalt bis(2-ethylhexanoate). https://echa.europa.eu/substance-information/-/substanceinfo/100.004.773 (accessed July 19th, 2022).

61. Wang, M.; Wu, Y.; Li, Y.-D.; Zeng, J.-B., Progress in Toughening Poly(Lactic Acid) with Renewable Polymers. *Polym. Rev.* **2017,** *57* (4), 557-593.

62. Bokobza, L., Natural Rubber Nanocomposites: A Review. *Nanomaterials (Basel)* **2018,** *9* (1).

63. Chen, Y.; Yuan, D.; Xu, C., Dynamically Vulcanized Biobased Polylactide/Natural Rubber Blend Material with Continuous Cross-Linked Rubber Phase. *ACS Appl. Mater. Inter.* **2014,** *6* (6), 3811-3816.

64. Wang, Y.; Chen, K.; Xu, C.; Chen, Y., Supertoughened Biobased Poly(lactic acid)–Epoxidized Natural Rubber Thermoplastic Vulcanizates: Fabrication, Co-continuous Phase Structure, Interfacial in Situ Compatibilization, and Toughening Mechanism. *The Journal of Physical Chemistry B* **2015,** *119* (36), 12138-12146.

Appendices

The following appendices contain the supporting information for the published journal articles presented in Chapters 3 through 6.

Appendix A

Supporting information for "*Small molecule plasticizers for improved migration resistance: Investigation of branching and leaching behaviour in PVC blends*."

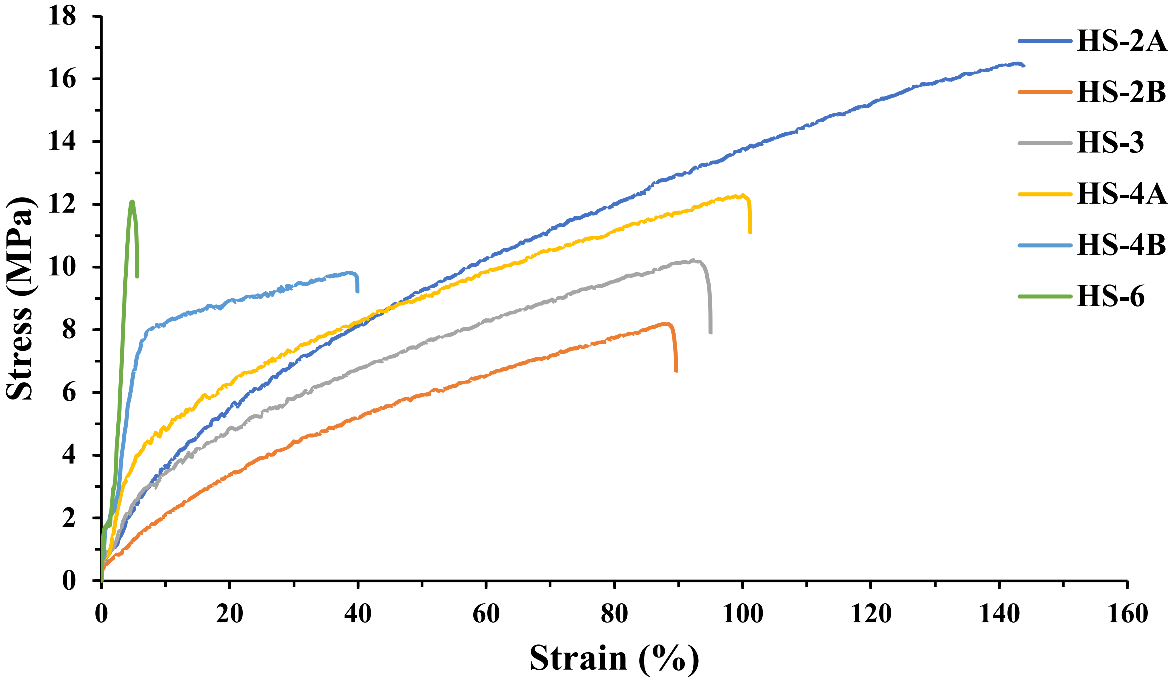

Figure A1. Representative stress/strain curves for branched PVC/plasticizer blends at 40 phr. **HS-2A**, **HS-2B**, **HS-3**, and **HS-4B** display a typical stress-strain relationship of a plasticized PVC sample at 40 phr.

Table A1. Onset temperatures of 5% weight loss of the 40 phr PVC/plasticizer blends

Plasticizer	T_5 (°C)
DEHP	220.7
DHPS	181.9
HS-2A	213.5
HS-2B	224.9
HS-3	219.3
HS-4A	225.9
HS-4B	216.0
HS-6	218.1

The onset of degradation temperature (selected as 5% weight loss) indicates all of the blends produced using the novel branched species display comparable thermal stability to the industrial DEHP.

Table A2. Masses of 40 phr PVC/plasticizer blend disks (2) before and immediately after leaching experiment into hexanes showing the effect of swelling of all blends except for DHPS. (a, b, c denote each of the triplicate experiments)

Plasticizer	Initial Mass (g)	Final Mass (g)	Weight Change (g)
DEHP	**a.** 1.4052 **b.** 1.4413 **c.** 1.4370	**a.** 1.5380 **b.** 1.5752 **c.** 1.5754	**a.** + 0.1328 **b.** + 0.1339 **c.** + 0.1384
DHPS	**a.** 1.3841 **b.** 1.3823 **c.** 1.3867	**a.** 1.3367 **b.** 1.3672 **c.** 1.3708	**a.** – 0.0174 **b.** – 0.0151 **c.** – 0.0159
HS-2A	**a.** 1.4549 **b.** 1.4516 **c.** 1.4662	**a.** 1.4775 **b.** 1.4776 **c.** 1.4917	**a.** + 0.0226 **b.** + 0.0260 **c.** + 0.0255
HS-2B	**a.** 1.4140 **b.** 1.4477 **c.** 1.4467	**a.** 1.4698 **b.** 1.4980 **c.** 1.4979	**a.** + 0.0558 **b.** + 0.0503 **c.** + 0.0512
HS-3	**a.** 1.4554 **b.** 1.4597 **c.** 1.4841	**a.** 1.5068 **b.** 1.5120 **c.** 1.5340	**a.** + 0.0514 **b.** + 0.0523 **c.** + 0.0499
HS-4A	**a.** 1.4505 **b.** 1.4603 **c.** 1.4465	**a.** 1.5345 **b.** 1.5544 **c.** 1.5459	**a.** + 0.0840 **b.** + 0.0941 **c.** + 0.0994
HS-4B	**a.** 1.4465 **b.** 1.4389 **c.** 1.4419	**a.** 1.4894 **b.** 1.4695 **c.** 1.4799	**a.** + 0.0429 **b.** + 0.0306 **c.** + 0.0380
HS-6	**a.** 1.4696 **b.** 1.4739 **c.** 1.4633	**a.** 1.5516 **b.** 1.5562 **c.** 1.5436	**a.** + 0.0821 **b.** + 0.0823 **c.** + 0.0803

Synthesis, Characterization, and Spectral Data for Synthesized Compounds

HS-2A

Reaction yield: 94%
^{1}H NMR (500 MHz, Chloroform-*d*) δ 4.08 (q, *J* = 6.7 Hz, 8H), 2.62 (s, 8H), 1.71 – 1.54 (m, 9H), 1.42 (d, *J* = 10.0 Hz, 2H), 1.37 – 1.22 (m, 17H), 0.93 – 0.82 (m, 6H).

HS-2B

Reaction yield: 92%
^{1}H NMR (500 MHz, Chloroform-*d*) δ 4.13 – 4.01 (m, 4H), 3.93 (d, *J* = 1.8 Hz, 4H), 2.61 (s, 8H), 1.66 – 1.55 (m, 4H), 1.38 – 1.22 (m, 20H), 0.93 – 0.84 (m, 6H), 0.81 (t, *J* = 7.5 Hz, 6H).

HS-3

Reaction yield: 88%
^{1}H NMR (500 MHz, Chloroform-*d*) δ 4.13 – 3.97 (m, 12H), 2.62 (s, 12H), 1.62 (p, *J* = 6.8 Hz, 7H), 1.55 – 1.40 (m, 2H), 1.38 – 1.21 (m, 27H), 0.92 – 0.85 (m, 13H).

HS-4A

Reaction yield: 91%
^{1}H NMR (500 MHz, Chloroform-*d*) δ 4.16 – 3.92 (m, 16H), 3.25 (s, 4H), 2.61 (s, 17H), 1.70 – 1.51 (m, 9H), 1.50 – 1.17 (m, 39H), 0.86 (q, *J* = 6.5 Hz, 18H).

HS-4B

Reaction yield: 80%
^{1}H NMR (500 MHz, Chloroform-*d*) δ 4.14 (s, 4H), 4.07 (t, *J* = 6.7 Hz, 8H), 2.62 (s, 13H), 1.67 – 1.56 (m, 8H), 1.39 – 1.19 (m, 31H), 0.95 – 0.80 (m, 11H).

HS-6

Reaction yield: 75%
^{1}H NMR (500 MHz, Chloroform-*d*) δ 4.19 – 3.99 (m, 22H), 3.40 (s, 3H), 2.62 (d, *J* = 5.7 Hz, 27H), 1.69 – 1.52 (m, 14H), 1.43 – 1.17 (m, 53H), 0.96 – 0.80 (m, 18H).

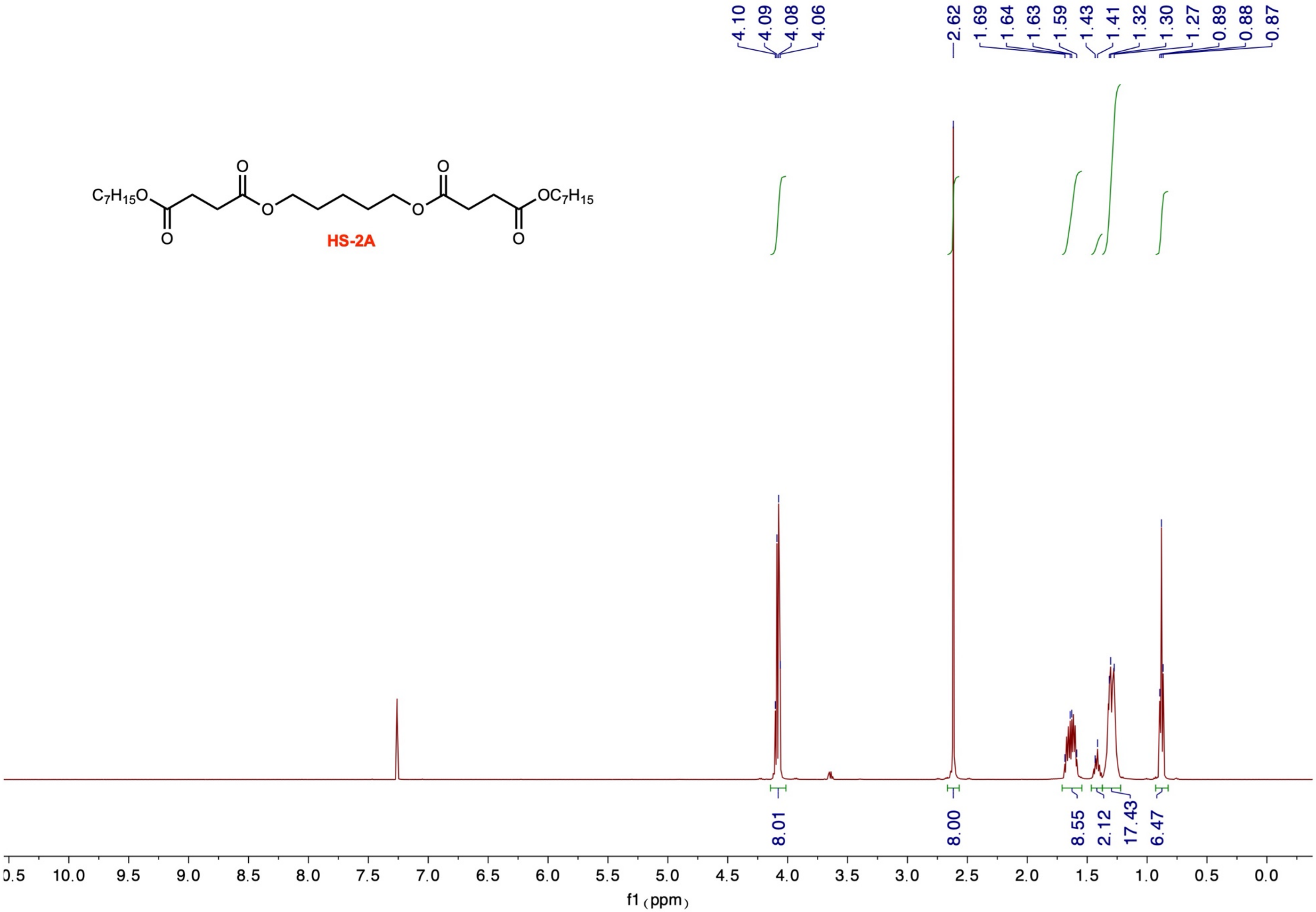
HS-2A
C7H15O
OC7H15
O
4.10
4.09
4.08
4.06
2.62
1.69
1.64
1.63
1.59
1.43
1.41
1.32
1.30
1.27
0.89
0.88
0.87
8.01
8.00
8.55
2.12
17.43
6.47
0.5
10.0
9.5
9.0
8.5
8.0
7.5
7.0
6.5
6.0
5.5
5.0
4.5
4.0
3.5
3.0
2.5
2.0
1.5
1.0
0.5
0.0
f1 (ppm)

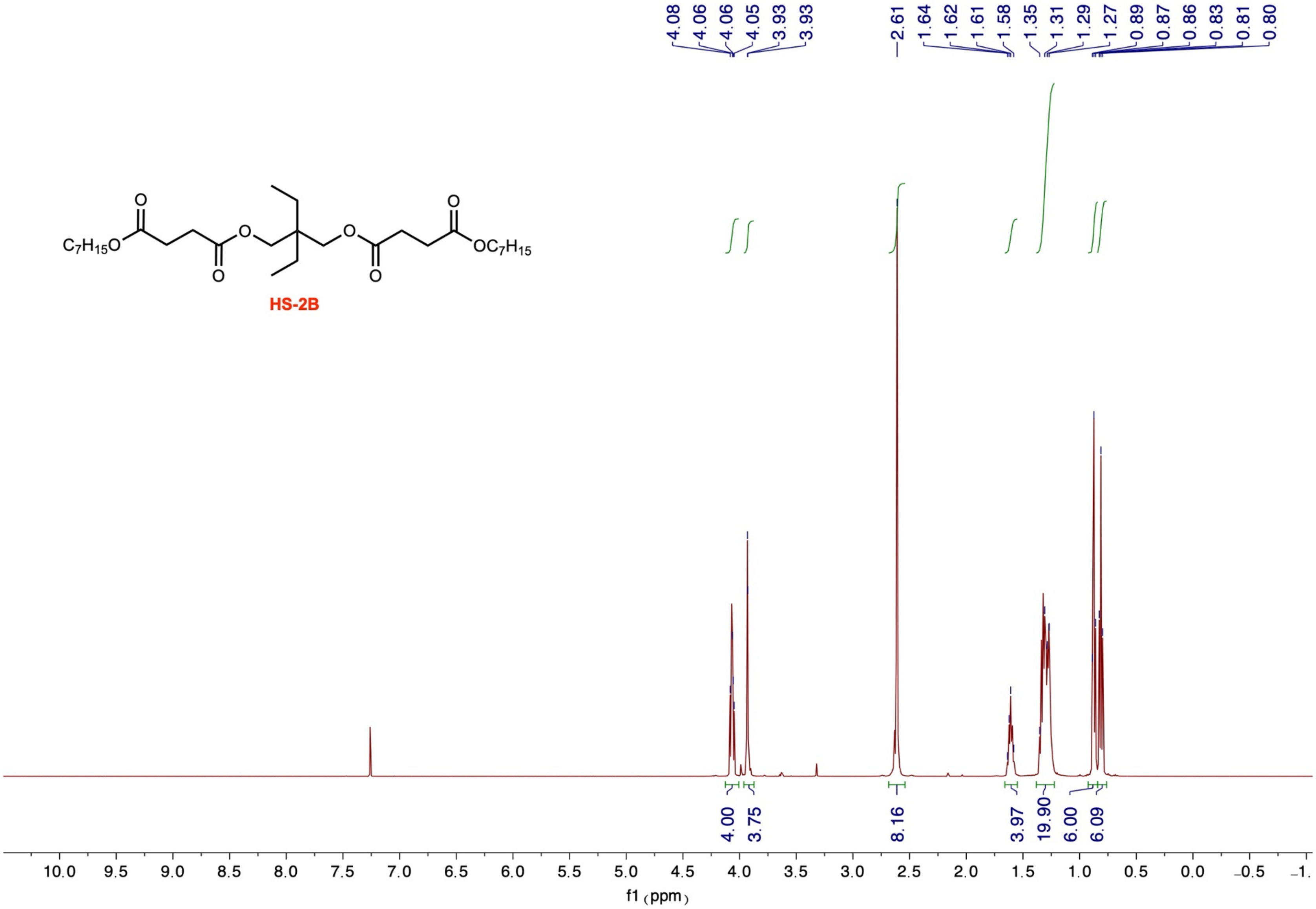
4.08
4.06
4.06
4.05
3.93
3.93
2.61
1.64
1.62
1.61
1.58
1.35
1.31
1.29
1.27
0.89
0.87
0.86
0.83
0.81
0.80
4.00
3.75
8.16
3.97
19.90
6.00
6.09
10.0
9.5
9.0
8.5
8.0
7.5
7.0
6.5
6.0
5.5
5.0
4.5
4.0
3.5
3.0
2.5
2.0
1.5
1.0
0.5
0.0
–0.5
–1.
f1 (ppm)
$C_7H_{15}O$
OC_7H_{15}
O

HS-2B

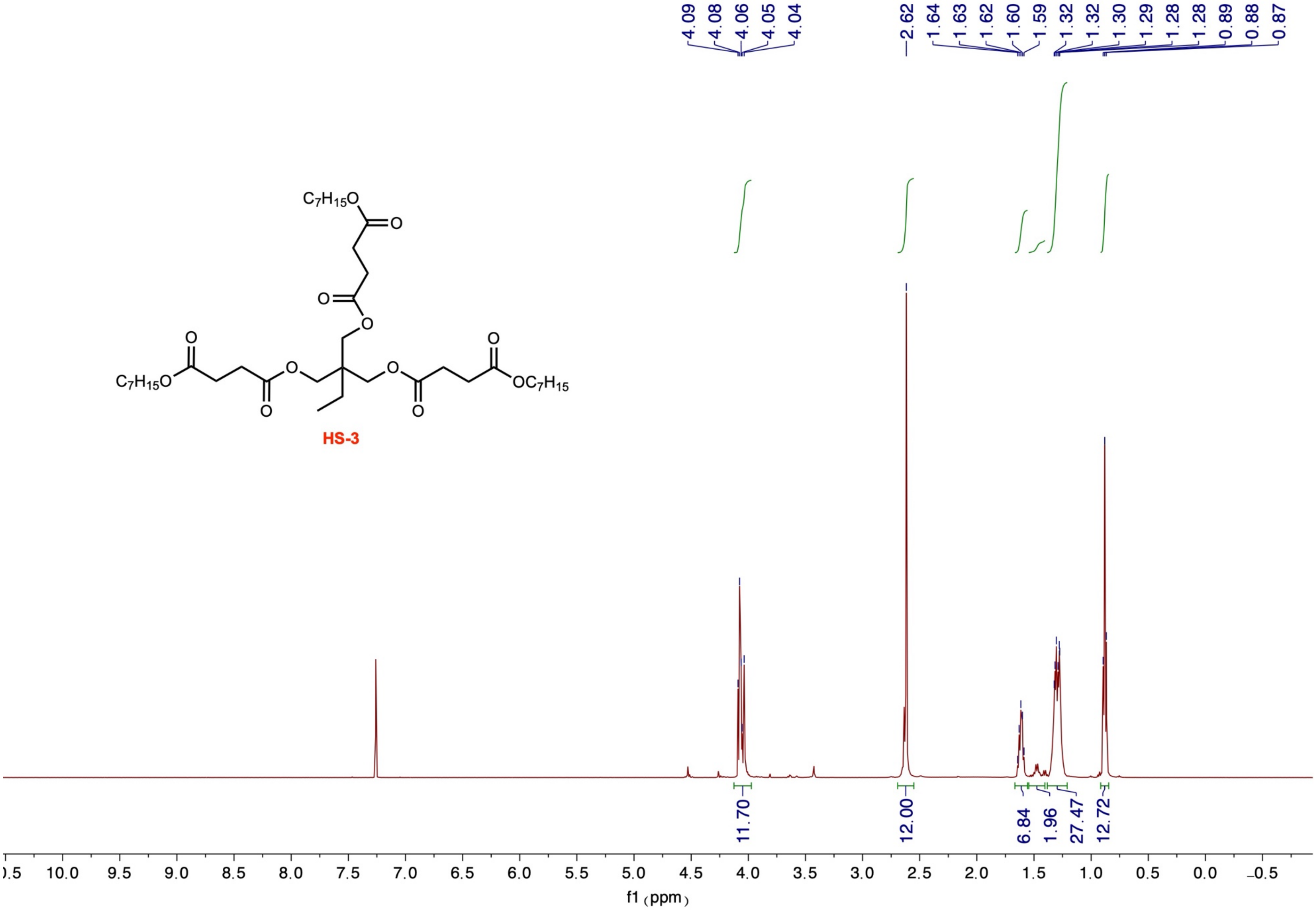
HS-3

4.09
4.08
4.06
4.05
4.04
2.62
1.64
1.63
1.62
1.60
1.59
1.32
1.32
1.30
1.29
1.28
1.28
0.89
0.88
0.87
11.70
12.00
6.84
1.96
27.47
12.72
C7H15O
O
OC7H15
10.0
9.5
9.0
8.5
8.0
7.5
7.0
6.5
6.0
5.5
5.0
4.5
4.0
3.5
3.0
2.5
2.0
1.5
1.0
0.5
0.0
-0.5
f1 (ppm)

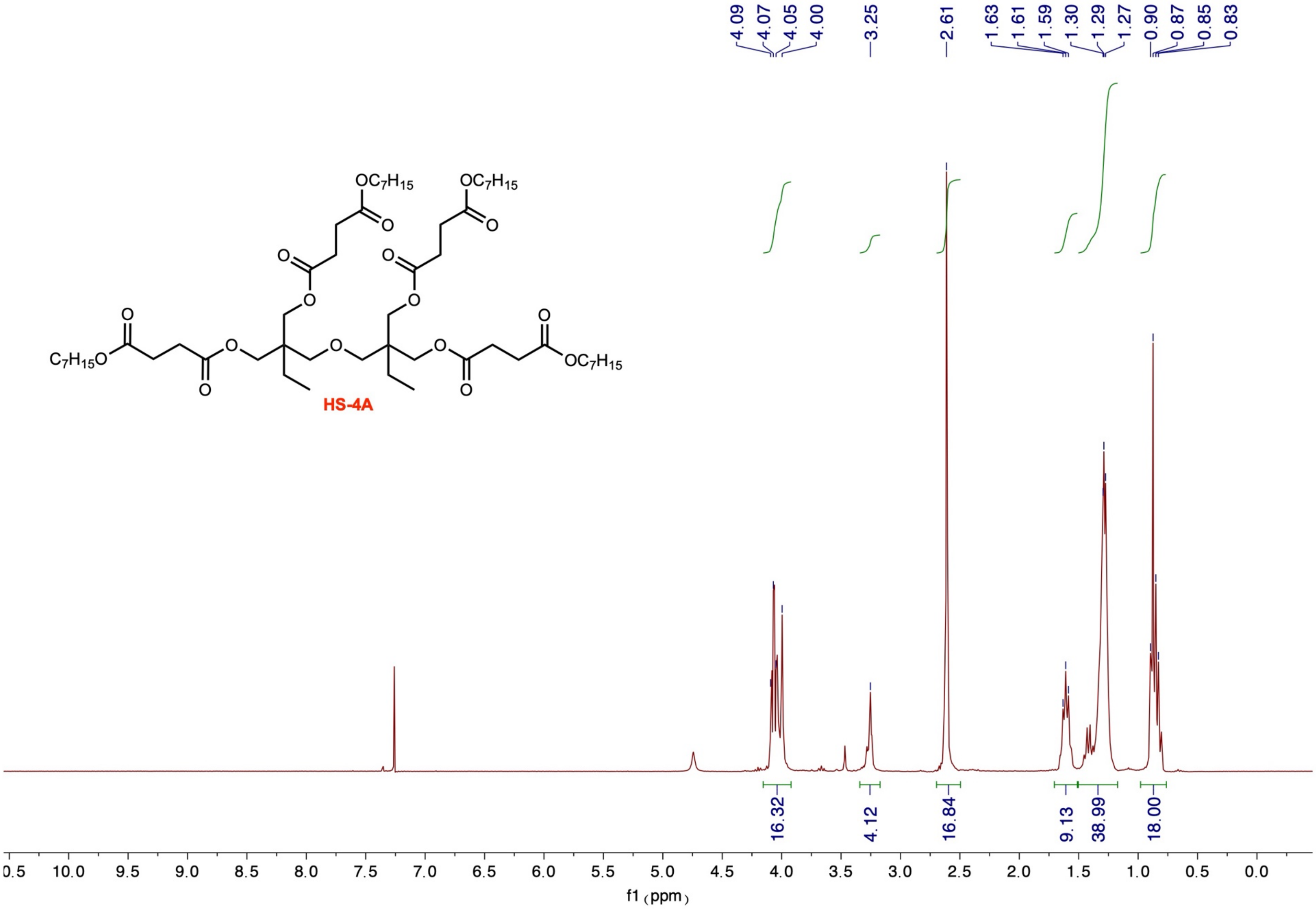
HS-4A
4.09
4.07
4.05
4.00
3.25
2.61
1.63
1.61
1.59
1.30
1.29
1.27
0.90
0.87
0.85
0.83
16.32
4.12
16.84
9.13
38.99
18.00
0.5
10.0
9.5
9.0
8.5
8.0
7.5
7.0
6.5
6.0
5.5
5.0
4.5
4.0
3.5
3.0
2.5
2.0
1.5
1.0
0.5
0.0
f1 (ppm)

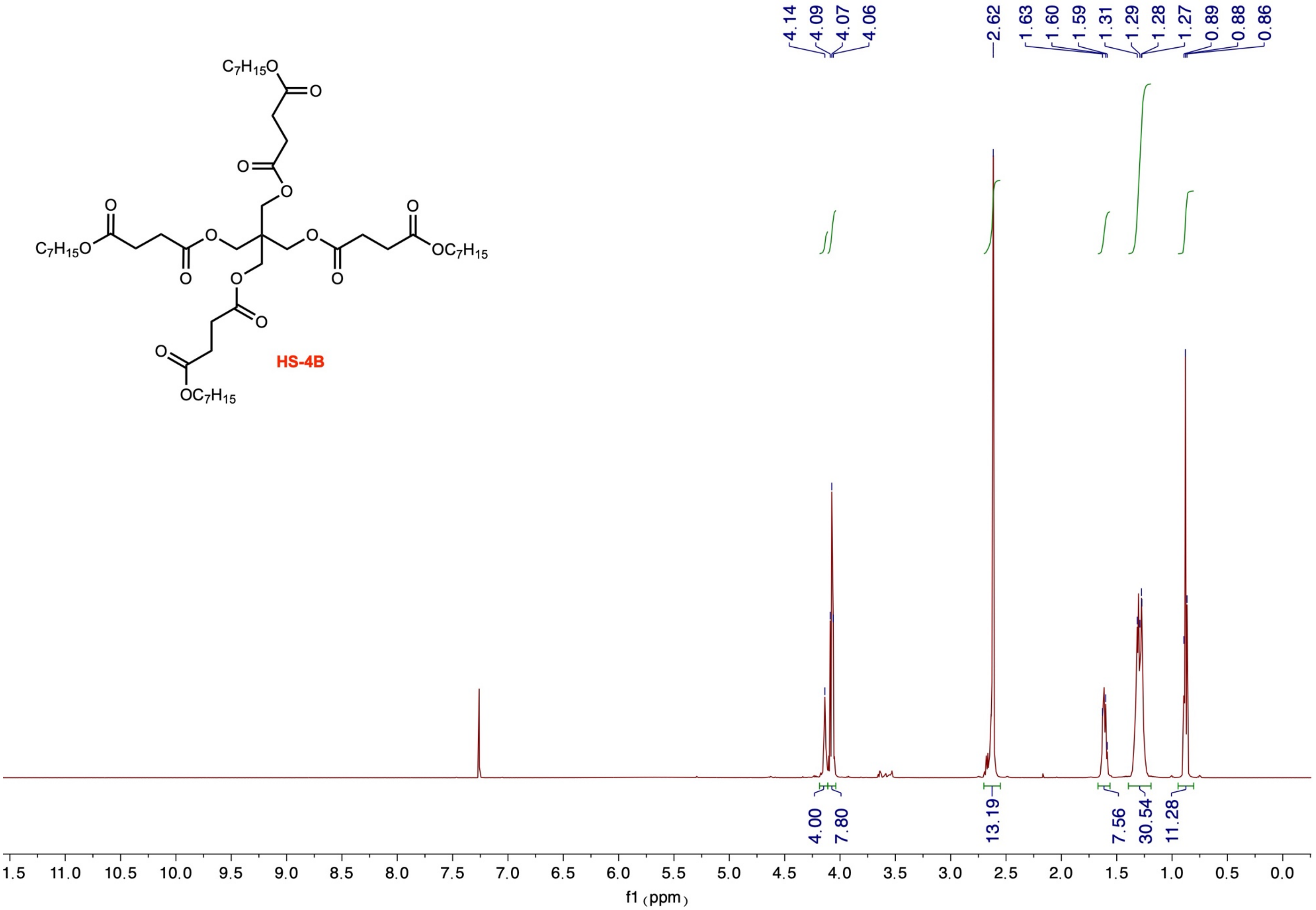
C7H15O
OC7H15
HS-4B
4.14
4.09
4.07
4.06
2.62
1.63
1.60
1.59
1.31
1.29
1.28
1.27
0.89
0.88
0.86
4.00
7.80
13.19
7.56
30.54
11.28
1.5
11.0
10.5
10.0
9.5
9.0
8.5
8.0
7.5
7.0
6.5
6.0
5.5
5.0
4.5
4.0
3.5
3.0
2.5
2.0
1.5
1.0
0.5
0.0
f1 (ppm)

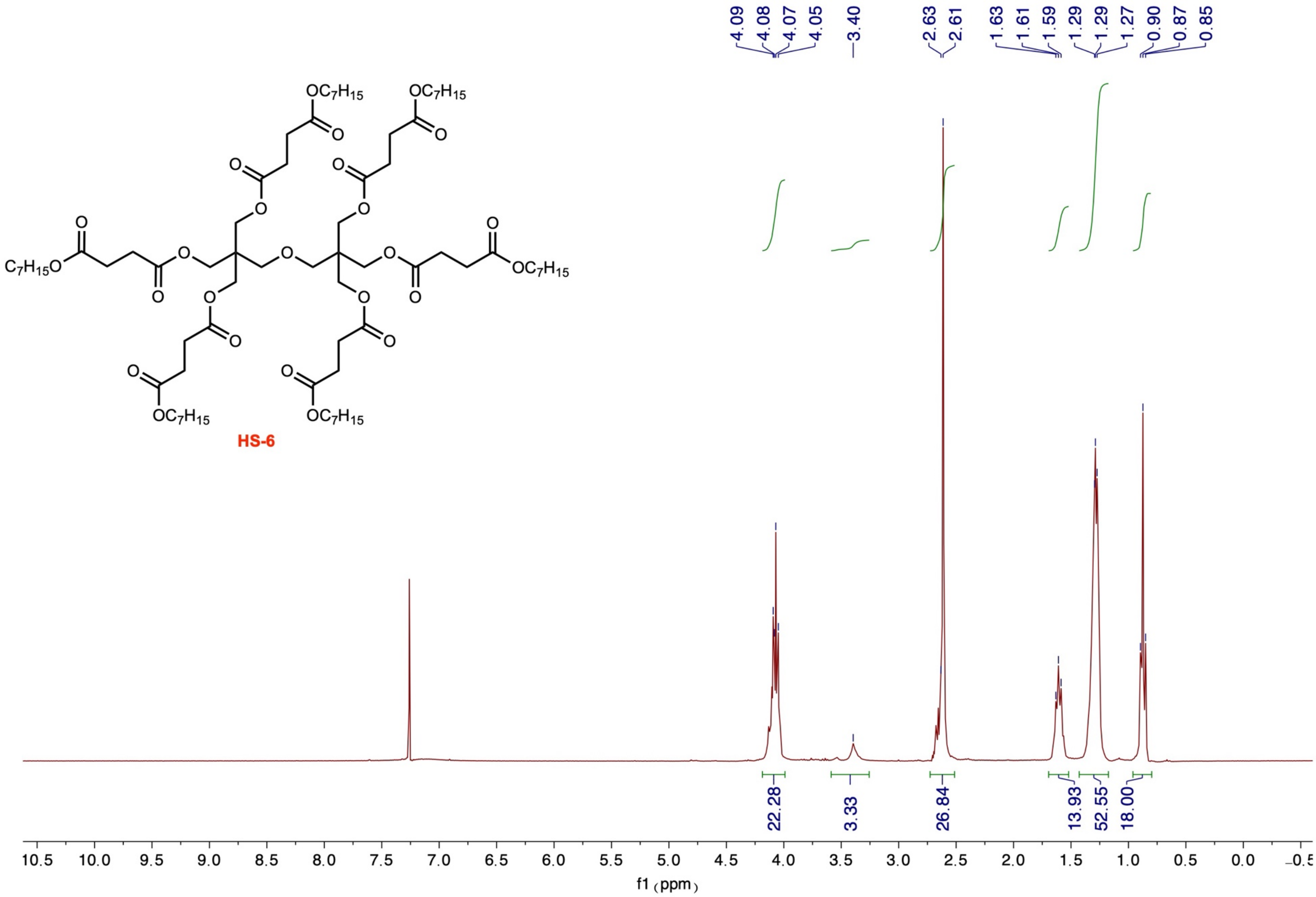
4.09
4.08
4.07
4.05
3.40
2.63
2.61
1.63
1.61
1.59
1.29
1.29
1.27
0.90
0.87
0.85
22.28
3.33
26.84
13.93
52.55
18.00
10.5
10.0
9.5
9.0
8.5
8.0
7.5
7.0
6.5
6.0
5.5
5.0
4.5
4.0
3.5
3.0
2.5
2.0
1.5
1.0
0.5
0.0
-0.5
f1 (ppm)
OC7H15
O
HS-6

Appendix B

Supporting information for "*Highly flexible polylactide food packaging plasticized with non-toxic, bio-sourced glycerol plasticizers.*"

Synthesis and characterization of plasticizers:

a) *Synthesis of mono succinates:*

Mono*iso*propyl succinate

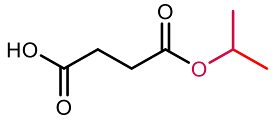

Chemical Formula: $C_7H_{12}O_4$
Molecular Weight: 160.17

Succinic anhydride (50.00 g, 0.50 mol, 1 eq.) was added to a 500 mL round bottomed flask containing a Teflon-coated stir bar, 4-(dimethylamino) pyridine (DMAP) (0.61 g, 5 mmol, 0.01 eq.) and 250 mL *i*-propanol (5 mL/g of succinic anhydride). The mixture was then heated at 70 °C for 18 hours, cooled to room temperature, and the residual solvent was removed *in vacuo*. The crude residue was then dissolved in 100 mL of ethyl acetate (EtOAc), washed with 25 mL of 2M HCl, dried over $MgSO_4$, filtered, and concentrated to afford mono*iso*propyl succinate (75.93 g, 0.474 mol) in a 95% yield as a white solid which was used without further purification.

^{1}H NMR (500 MHz, Chloroform-*d*) δ 5.03 (hept, J = 6.3 Hz, 1H), 2.68 (ddd, J = 7.2, 6.1, 0.9 Hz, 2H), 2.60 (ddd, J = 7.2, 6.0, 1.0 Hz, 2H), 1.24 (d, J = 6.3 Hz, 6H) ppm.

Monopropyl succinate

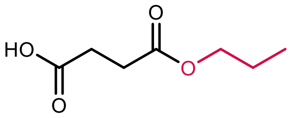

Chemical Formula: $C_7H_{12}O_4$
Molecular Weight: 160.17

Succinic anhydride (50.00 g, 0.50 mol, 1 eq.) was added to a 500 mL round bottomed flask containing a Teflon-coated stir bar, *n*-propanol (39.4 mL, 0.52 mol, 1.05 eq.), and 250 mL of toluene. The mixture was then heated at 95 °C for 18 hours, cooled to room temperature, and the solvent was removed *in vacuo* to afford monopropyl succinate (78.68 g, 0.49 mol) in a 98% yield as a yellow oil which was used without further purification.

^{1}H NMR (500 MHz, Chloroform-*d*) δ 4.08 (q, *J* = 6.7 Hz, 2H), 2.71 (ddd, *J* = 7.2, 5.8, 1.5 Hz, 2H), 2.65 (ddd, *J* = 7.2, 5.7, 1.5 Hz, 2H), 1.67 (dtd, *J* = 14.1, 7.4, 6.6 Hz, 2H), 0.96 (t, *J* = 7.4 Hz, 3H) ppm.

Monobutyl succinate

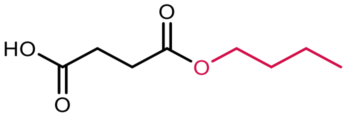

Chemical Formula: $C_8H_{14}O_4$
Molecular Weight: 174.20

Succinic anhydride (50.00 g, 0.50 mol, 1 eq.) was added to a 500 mL round bottomed flask containing a Teflon-coated stir bar, *n*-butanol (45.73 mL, 0.50 mol, 1 eq.), and 250 mL of toluene. The mixture was then heated at 105 °C for 18 hours, cooled to room temperature, and the solvent was removed *in vacuo*. The crude residue was then dissolved in 100 mL of ethyl acetate (EtOAc), washed with 25 mL of DI water, 25 mL of brine, dried over $MgSO_4$, filtered, and concentrated to afford monobutyl succinate (83.0 g, 0.48 mol) in a 95% yield as a yellow oil which was used without further purification.

^{1}H NMR (500 MHz, Chloroform-*d*) δ 4.11 (t, *J* = 6.6 Hz, 2H), 2.69 (ddd, *J* = 7.2, 6.0, 1.4 Hz, 2H), 2.62 (ddd, *J* = 7.6, 6.0, 1.4 Hz, 2H), 1.66 – 1.57 (m, 2H), 1.42 – 1.33 (m, 2H), 0.93 (t, *J* = 7.4 Hz, 3H) ppm.

Mono(2-ethylhexyl) succinate

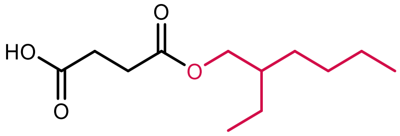
Chemical Formula: $C_{12}H_{22}O_4$
Molecular Weight: 230.30

Succinic anhydride (50.00 g, 0.50 mol, 1 eq.) was added to a 500 mL round bottomed flask containing a Teflon-coated stir bar, 2-ethylhexanol (78.11 mL, 0.50 mol, 1 eq.), and 250 mL of toluene. The mixture was then refluxed for 18 hours and cooled to room temperature. The reaction mixture was then washed with 25 mL of DI water, 25 mL of brine, dried over $MgSO_4$, filtered, and concentrated *in vacuo* to afford mono(2-ethylhexyl) succinate (112.84 g, 0.49 mol) in a 98% yield as a yellow oil which was used without further purification.

^{1}H NMR (500 MHz, Chloroform-*d*) δ 4.08 – 3.98 (m, 2H), 2.70 (ddd, *J* = 7.0, 5.8, 1.5 Hz, 2H), 2.65 (ddd, *J* = 7.8, 5.9, 1.5 Hz, 2H), 1.59 (p, *J* = 6.0 Hz, 1H), 1.42 – 1.24 (m, 8H), 0.91 (td, *J* = 7.5, 7.1, 4.1 Hz, 6H) ppm.

Monohexyl succinate

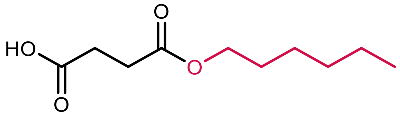
Chemical Formula: $C_{10}H_{18}O_4$
Molecular Weight: 202.25

Succinic anhydride (50.00 g, 0.50 mol, 1 eq.) was added to a 500 mL round bottomed flask containing a Teflon-coated stir bar, *n*-hexanol (62.71 mL, 0.50 mol, 1 eq.), and 250 mL of toluene. The mixture was then refluxed for 18 hours and cooled to room temperature. The reaction mixture was then washed with 25 mL of DI water, 25 mL of brine, dried over $MgSO_4$, filtered, and concentrated *in vacuo* to afford mono(2-ethylhexyl) succinate (97.90 g, 0.48 mol) in a 97% yield as a pale-yellow oil which was used without further purification.

^{1}H NMR (500 MHz, Chloroform-*d*) δ 4.11 (t, *J* = 6.7 Hz, 2H), 2.70 (ddd, *J* = 7.1, 5.9, 1.4 Hz, 2H), 2.64 (ddd, *J* = 7.7, 5.9, 1.4 Hz, 2H), 1.64 (dq, *J* = 8.3, 6.7 Hz, 2H), 1.42 – 1.25 (m, 6H), 0.98 – 0.83 (m, 3H) ppm.

Monoheptyl succinate

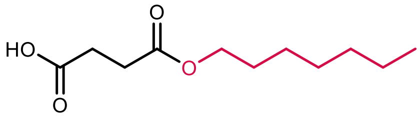

Chemical Formula: $C_{11}H_{20}O_4$
Molecular Weight: 216.28

Succinic anhydride (50.00 g, 0.50 mol, 1 eq.) was added to a 500 mL round bottomed flask containing a Teflon-coated stir bar, *n*-hexanol (70.54 mL, 0.50 mol, 1 eq.), and 250 mL of toluene. The mixture was then refluxed for 18 hours and cooled to room temperature. The reaction mixture was then washed with 25 mL of DI water, 25 mL of brine, dried over $MgSO_4$, filtered, and concentrated *in vacuo* to afford monoheptyl succinate (103.6 g, 0.48 mol) in a 96% yield as a milky yellow oil which was used without further purification.

^{1}H NMR (500 MHz, Chloroform-*d*) δ 4.11 (t, *J* = 6.7 Hz, 2H), 2.70 (ddd, *J* = 7.2, 5.9, 1.4 Hz, 2H), 2.64 (ddd, *J* = 7.6, 5.8, 1.4 Hz, 2H), 1.69 – 1.59 (m, 2H), 1.41 – 1.22 (m, 8H), 0.99 – 0.83 (m, 3H) ppm.

b) Synthesis of plasticizers

Each analog was synthesized according to the same procedure. Glycerol (5.00 g, 54.29 mol, 1 eq.) was mased directly into a 250 mL three-necked round bottomed flask, followed by the addition of the appropriate mono-succinate (3.8 eq.) and *p*-toluene sulfonic acid monohydrate (310 mg, 1.63 mmol, 0.03 eq.). The flask was fitted with a Dean-Stark apparatus and condenser and heated at 110 **°C** for 18 hours under a steady stream of bubbling N_2 which served to remove the water by-product during the reaction. After 18 hours, the mixture was cooled to room temperature, dissolved in 50 mL of ethyl acetate, washed with 25 mL of a saturated sodium bicarbonate solution, dried over magnesium sulfate, filtered, and concentrated under reduced pressure to afford the GS analogs as clear to yellow oils.

GS-*i*P

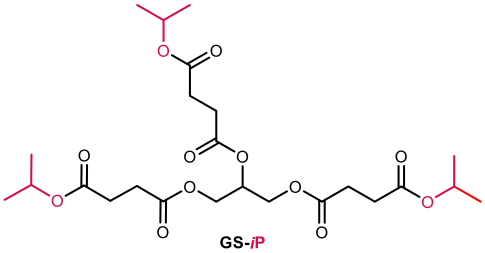

GS-*i*P

Chemical Formula: $C_{24}H_{38}O_{12}$
Molecular Weight: 518.56

Reaction yield: 88%

^{1}H NMR (500 MHz, Chloroform-*d*) δ 5.34 – 5.22 (m, 1H), 5.07 – 4.92 (m, 3H), 4.30 (dd, *J* = 11.9, 4.3 Hz, 2H), 4.18 (dd, *J* = 11.9, 5.9 Hz, 2H), 2.76 – 2.49 (m, 12H), 1.22 (d, *J* = 6.3 Hz, 18H) ppm.

GS-C3

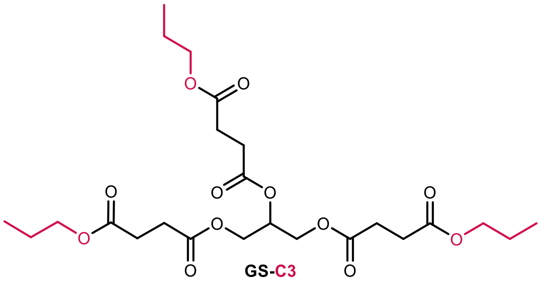

GS-C3

Chemical Formula: $C_{24}H_{38}O_{12}$
Molecular Weight: 518.56

Reaction yield: 92%

^{1}H NMR (500 MHz, Chloroform-*d*) δ 5.33 – 5.18 (m, 1H), 4.30 (dd, *J* = 11.4, 3.7 Hz, 2H), 4.18 (dd, *J* = 11.9, 5.9 Hz, 2H), 4.04 (d, *J* = 6.7 Hz, 6H), 2.62 (s, 12H), 1.69 – 1.59 (m, 6H), 0.92 (t, *J* = 7.4 Hz, 9H) ppm.

GS-C4

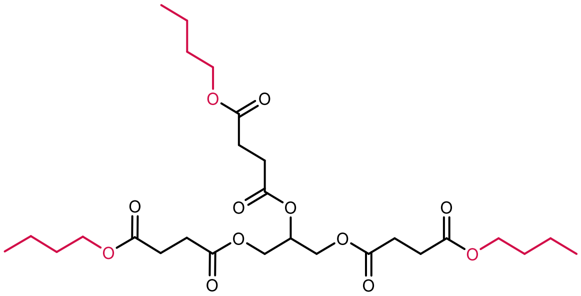

GS-C4
Chemical Formula: $C_{27}H_{44}O_{12}$
Molecular Weight: 560.64

Reaction yield: 95%

^{1}**H NMR** (500 MHz, Chloroform-*d*) δ 5.27 (t, *J* = 5.1 Hz, 1H), 4.30 (d, *J* = 11.9 Hz, 2H), 4.22 – 4.15 (m, 2H), 4.08 (t, *J* = 7.5 Hz, 6H), 2.63 (d, *J* = 11.4 Hz, 12H), 1.65 – 1.54 (m, 6H), 1.37 (q, *J* = 7.5 Hz, 6H), 0.92 (t, *J* = 7.4 Hz, 9H) ppm.

GS-C6

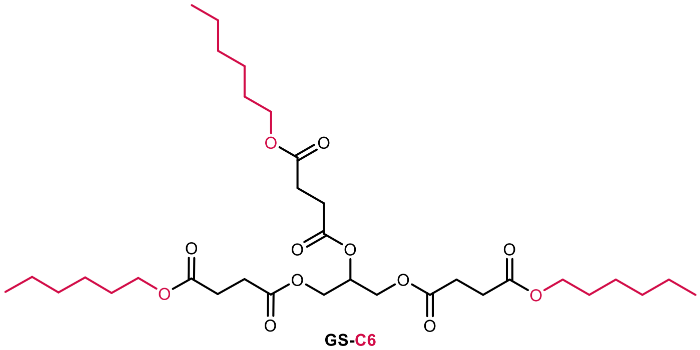

GS-C6
Chemical Formula: $C_{33}H_{56}O_{12}$
Molecular Weight: 644.80

Reaction yield: 86%

^{1}**H NMR** (500 MHz, Chloroform-*d*) δ 5.35 – 5.18 (m, 1H), 4.30 (d, *J* = 11.9 Hz, 2H), 4.19 (d, *J* = 6.0 Hz, 2H), 4.07 (t, *J* = 6.8 Hz, 6H), 2.62 (d, *J* = 11.2 Hz, 12H), 1.66 – 1.56 (m, 7H), 1.32 (d, *J* = 12.8 Hz, 22H), 0.88 (t, *J* = 6.9 Hz, 12H) ppm.

GS-C7

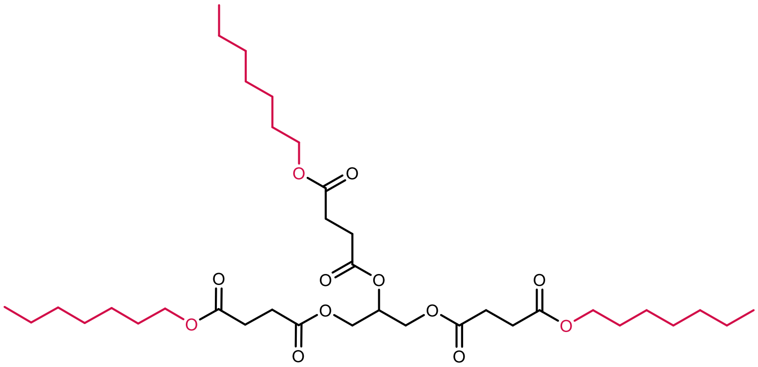

GS-C7

Chemical Formula: $C_{36}H_{62}O_{12}$

Molecular Weight: 686.88

Reaction yield: 91%

^{1}H NMR (500 MHz, Chloroform-*d*) δ 5.26 (d, *J* = 4.4 Hz, 1H), 4.31 (dd, *J* = 11.9, 4.2 Hz, 2H), 4.19 (dd, *J* = 11.9, 5.9 Hz, 2H), 4.07 (t, *J* = 6.8 Hz, 6H), 2.70 – 2.53 (m, 12H), 1.69 – 1.53 (m, 8H), 1.29 (dd, *J* = 15.0, 9.0 Hz, 30H), 0.96 – 0.80 (m, 12H) ppm.

GS-EH

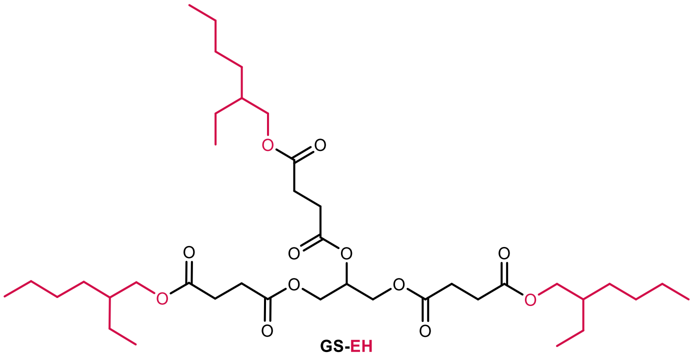

GS-EH

Chemical Formula: $C_{39}H_{68}O_{12}$

Molecular Weight: 728.96

Reaction yield: 82%

^{1}H NMR (500 MHz, Chloroform-*d*) δ 5.36 – 5.16 (m, 1H), 4.30 (d, *J* = 11.9 Hz, 2H), 4.18 (d, *J* = 12.0 Hz, 2H), 4.05 – 3.95 (m, 6H), 2.63 (d, *J* = 7.2 Hz, 12H), 1.61 – 1.50 (m, 3H), 1.42 – 1.21 (m, 25H), 0.88 (t, *J* = 7.5 Hz, 18H) ppm.

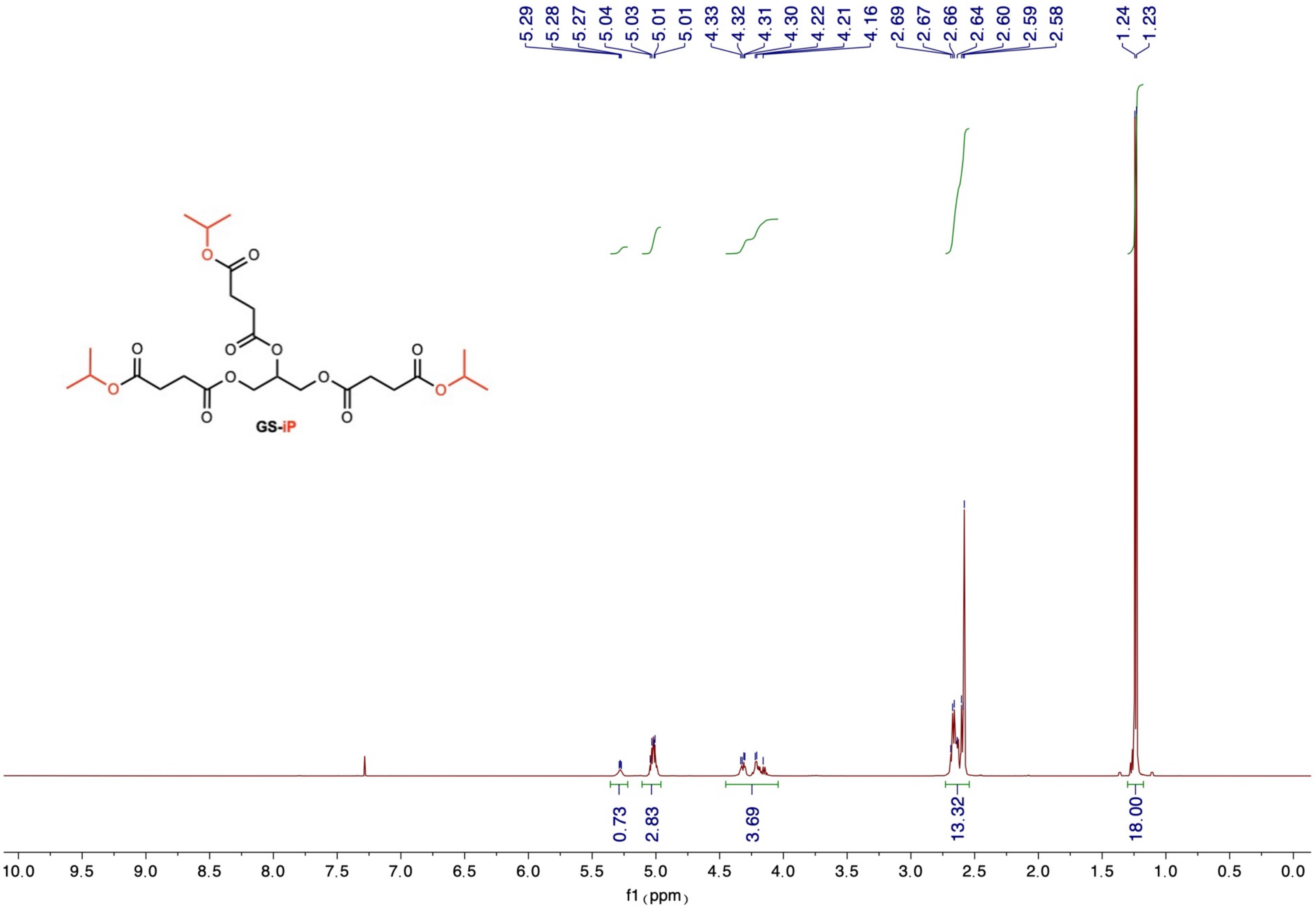
5.29
5.28
5.27
5.04
5.03
5.01
5.01
4.33
4.32
4.31
4.30
4.22
4.21
4.16
2.69
2.67
2.66
2.64
2.60
2.59
2.58
1.24
1.23
0.73
2.83
3.69
13.32
18.00
10.0
9.5
9.0
8.5
8.0
7.5
7.0
6.5
6.0
5.5
5.0
4.5
4.0
3.5
3.0
2.5
2.0
1.5
1.0
0.5
0.0
f1 (ppm)
O
GS-iP

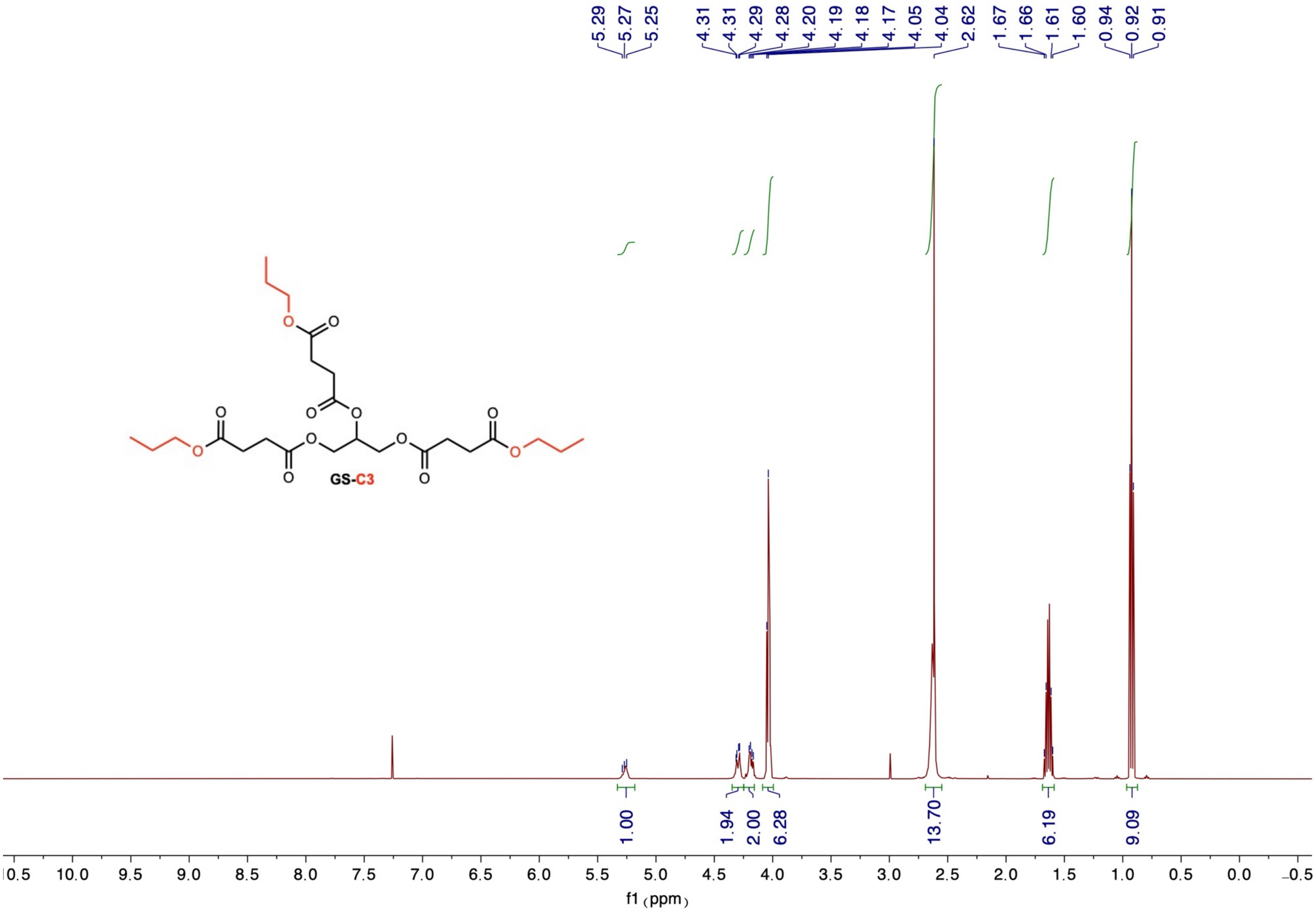
GS-C3
5.29
5.27
5.25
4.31
4.31
4.29
4.28
4.20
4.19
4.18
4.17
4.05
4.04
2.62
1.67
1.66
1.61
1.60
0.94
0.92
0.91
1.00
1.94
2.00
6.28
13.70
6.19
9.09
10.5
10.0
9.5
9.0
8.5
8.0
7.5
7.0
6.5
6.0
5.5
5.0
4.5
4.0
3.5
3.0
2.5
2.0
1.5
1.0
0.5
0.0
-0.5
f1 (ppm)
O

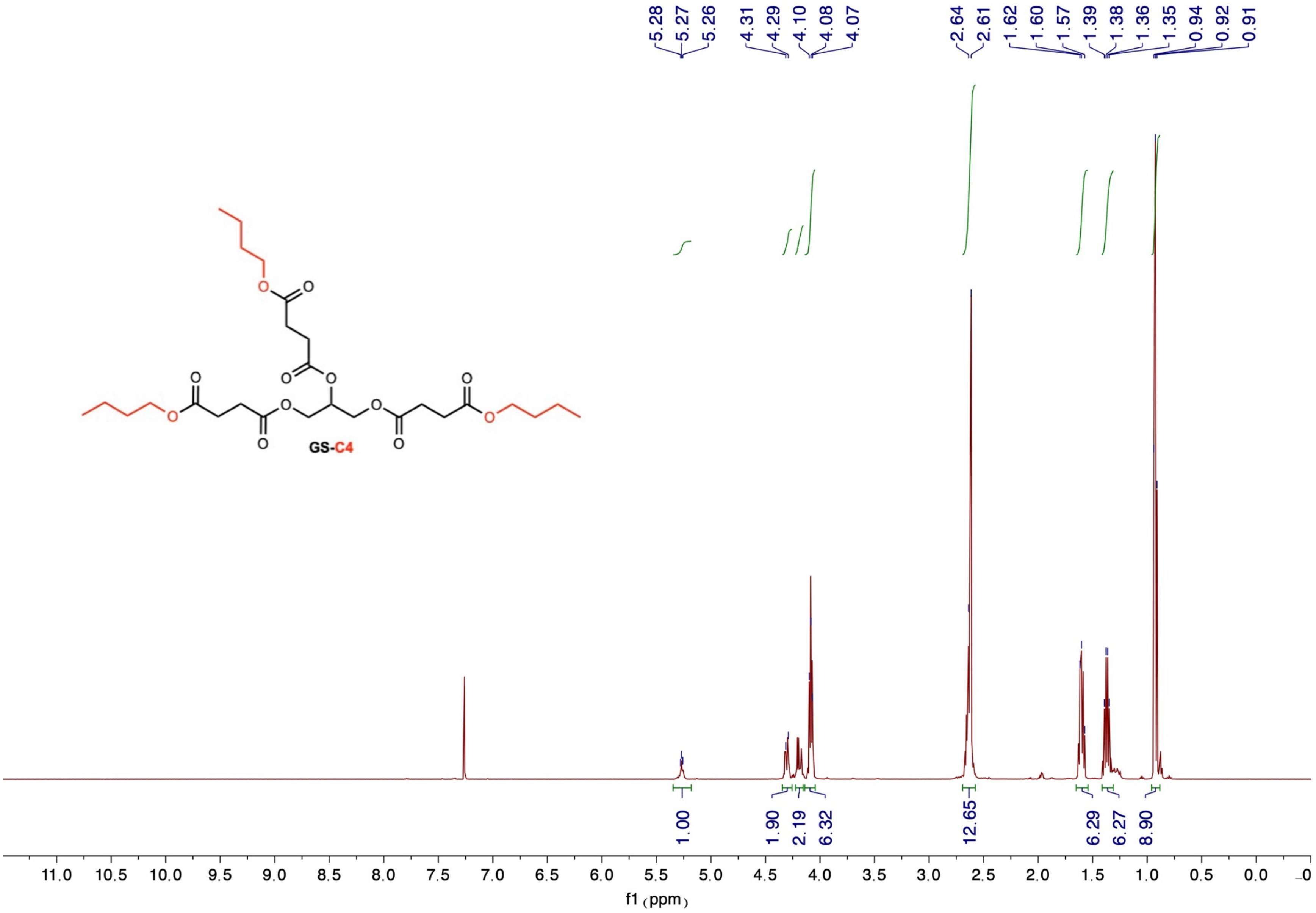
GS-C4
5.28
5.27
5.26
4.31
4.29
4.10
4.08
4.07
2.64
2.61
1.62
1.60
1.57
1.39
1.38
1.36
1.35
0.94
0.92
0.91
1.00
1.90
2.19
6.32
12.65
6.29
6.27
8.90
11.0
10.5
10.0
9.5
9.0
8.5
8.0
7.5
7.0
6.5
6.0
5.5
5.0
4.5
4.0
3.5
3.0
2.5
2.0
1.5
1.0
0.5
0.0
f1 (ppm)

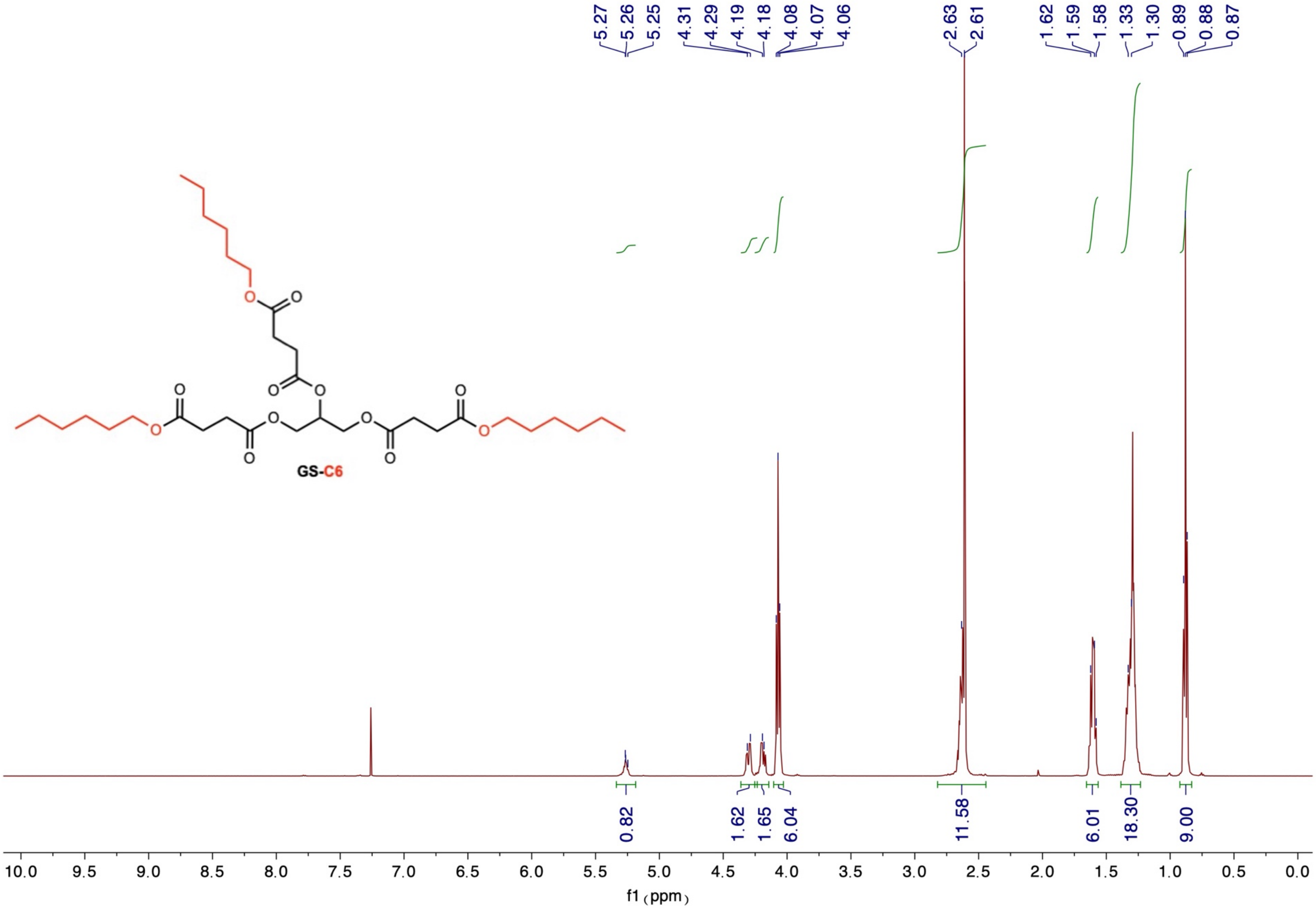
GS-C6
5.27
5.26
5.25
4.31
4.29
4.19
4.18
4.08
4.07
4.06
2.63
2.61
1.62
1.59
1.58
1.33
1.30
0.89
0.88
0.87
0.82
1.62
1.65
6.04
11.58
6.01
18.30
9.00
10.0
9.5
9.0
8.5
8.0
7.5
7.0
6.5
6.0
5.5
5.0
4.5
4.0
3.5
3.0
2.5
2.0
1.5
1.0
0.5
0.0
f1 (ppm)

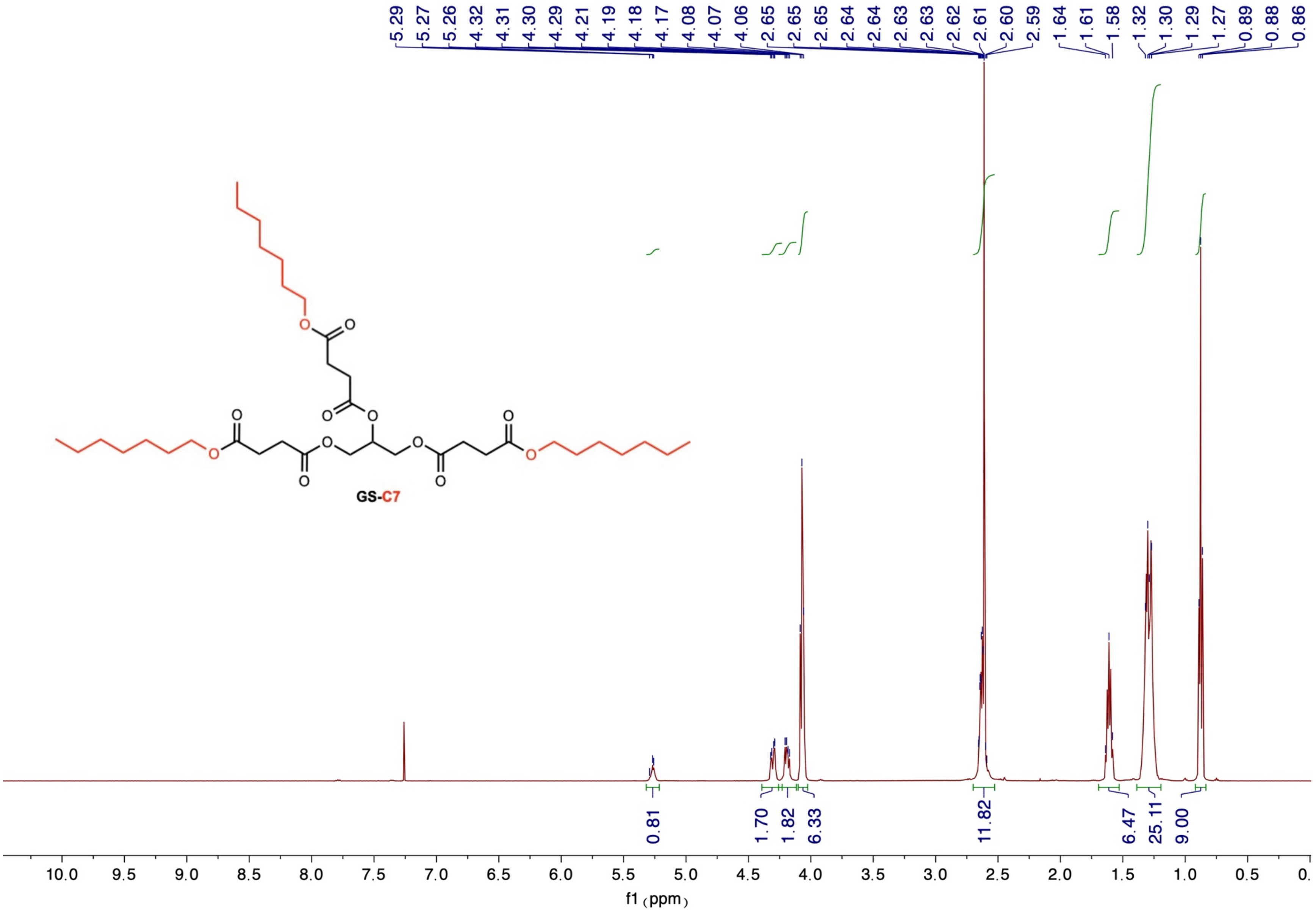
GS-C7

5.29
5.27
5.26
4.32
4.31
4.30
4.29
4.21
4.19
4.18
4.17
4.08
4.07
4.06
2.65
2.65
2.65
2.64
2.64
2.63
2.63
2.62
2.61
2.60
2.59
1.64
1.61
1.58
1.32
1.30
1.29
1.27
0.89
0.88
0.86
0.81
1.70
1.82
6.33
11.82
6.47
25.11
9.00
10.0
9.5
9.0
8.5
8.0
7.5
7.0
6.5
6.0
5.5
5.0
4.5
4.0
3.5
3.0
2.5
2.0
1.5
1.0
0.5
0.
f1 (ppm)
O

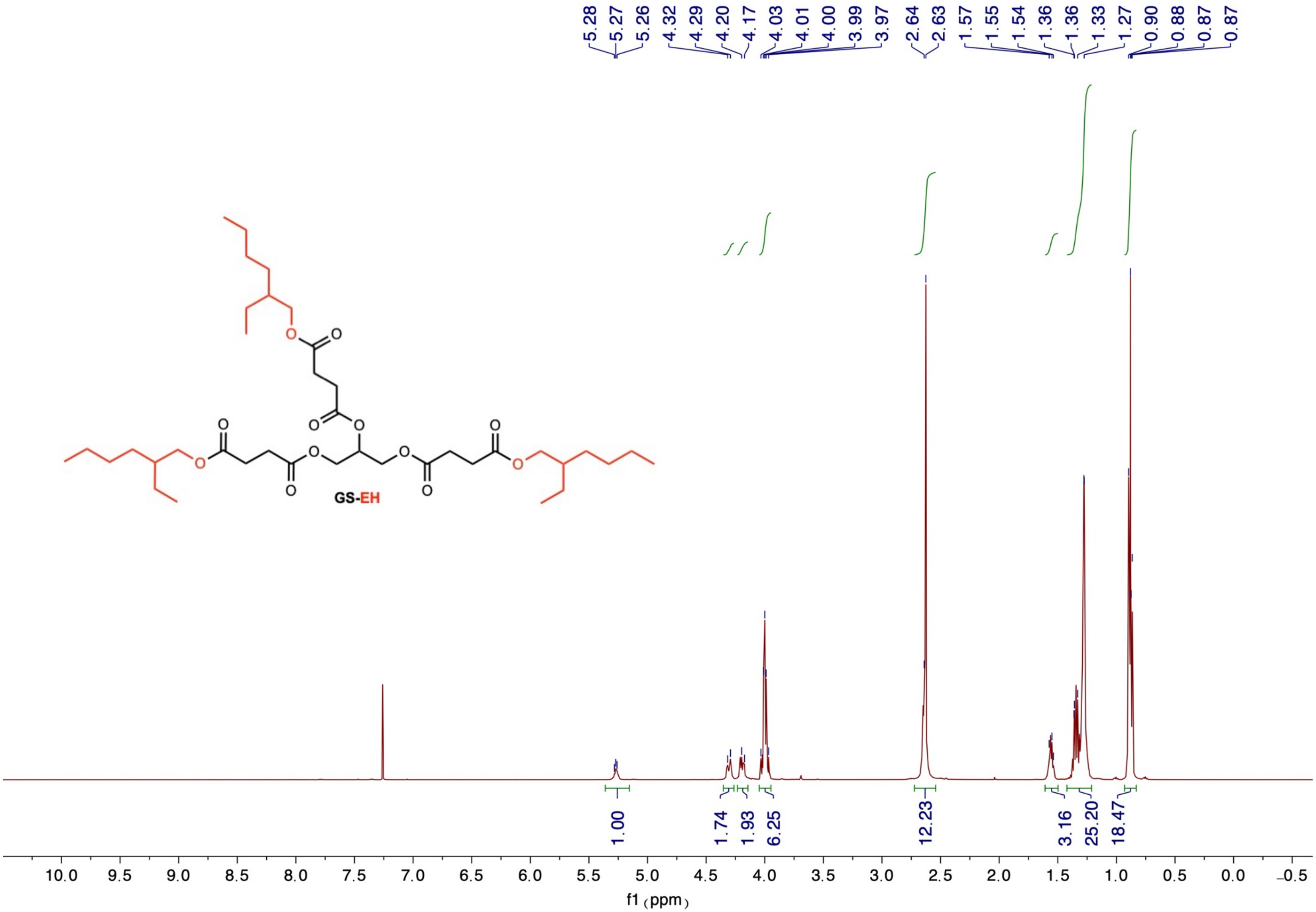
5.28
5.27
5.26
4.32
4.29
4.20
4.17
4.03
4.01
4.00
3.99
3.97
2.64
2.63
1.57
1.55
1.54
1.36
1.36
1.33
1.27
0.90
0.88
0.87
0.87
1.00
1.74
1.93
6.25
12.23
3.16
25.20
18.47
10.0
9.5
9.0
8.5
8.0
7.5
7.0
6.5
6.0
5.5
5.0
4.5
4.0
3.5
3.0
2.5
2.0
1.5
1.0
0.5
0.0
–0.5
f1 (ppm)
O
GS-EH

Table B1. Onset temperatures of 5% weight loss of the film blends

Blend	**10 wt% Blend**	**20 wt% Blend**
ATBC	222 °C	207 °C
GS-iP	279 °C	261 °C
GS-C3	279 °C	271 °C
GS-C4	244 °C	195 °C
GS-C6	258 °C	213 °C
GS-C7	293 °C	235 °C
GS-EH	256 °C	225 °C

T_5 of nPLA film: 278 °C

Table B2. Onset temperatures of 5% weight loss of the melt-mixed blends

Blend	**10 wt% Blend**	**20 wt% Blend**
ATBC	272 °C	221 °C
GS-iP	280 °C	227 °C
GS-C3	306 °C	242 °C
GS-C4	279 °C	258 °C
GS-C6	292 °C	260 °C
GS-C7	295 °C	265 °C
GS-EH	280 °C	281 °C

T_5 of nPLA blend: 321 °C

Table B3. Melting temperatures (T_m) of PLA film blends obtained from the second heating cycle in DSC.

Wt%	**ATBC**	**GS-*i*P**	**GS-C3**	**GS-C4**	**GS-C6**	**GS-C7**	**GS-EH**
10	143 °C	142 °C	146 °C	143 °C	143 °C	142 °C	144 °C
20	142 °C	145 °C	146 °C	142 °C	145 °C	145 °C	141 °C

T_m of nPLA film: 151 °C

Table B4. Cold crystallization temperatures (T_{cc}) of PLA film blends obtained from the second heating cycle in DSC.

Wt%	ATBC	GS-*i*P	GS-C3	GS-C4	GS-C6	GS-C7	GS-EH
10	N/A	122 °C	108 °C	116 °C	111 °C	106 °C	N/A
20	93 °C	110 °C	101 °C	94 °C	90 °C	80 °C	N/A

T_{cc} of nPLA film: N/A

Table B5. Crystallinity (X_c) of PLA film blends obtained from the second heating cycle in DSC.

Wt%	ATBC	GS-*i*P	GS-C3	GS-C4	GS-C6	GS-C7	GS-EH
10	5.5%	6.3%	6.9%	4.6%	9.4%	5.5%	4.5%
20	8.3%	6.1%	6.2%	5.2%	9.8%	9.8%	1.5%

X_c of nPLA film: 3.4%

Table B6. Melting temperatures (T_m) of PLA melt-mixed blends obtained from the second heating cycle in DSC.

Wt%	ATBC	GS-*i*P	GS-C3	GS-C4	GS-C6	GS-C7	GS-EH
10	144 °C	142 °C	148 °C	143 °C	149 °C	145 °C	148 °C
20	144 °C	145 °C	142 °C	145 °C	147 °C	148 °C	141 °C

T_m of nPLA melt-mixed sample: 152 °C

Table B7. Cold crystallization temperatures (T_{cc}) of PLA melt-mixed blends obtained from the second heating cycle in DSC.

Wt%	**ATBC**	**GS-*i*P**	**GS-C3**	**GS-C4**	**GS-C6**	**GS-C7**	**GS-EH**
10	109 °C	110 °C	120 °C	108 °C	103 °C	111 °C	106 °C
20	94 °C	102 °C	108 °C	84 °C	86 °C	107 °C	107 °C

T_{cc} of nPLA melt-mixed sample: 131°C

Table B8. Crystallinity (X_c) of PLA melt-mixed blends obtained from the second heating cycle in DSC.

Wt%	**ATBC**	**GS-*i*P**	**GS-C3**	**GS-C4**	**GS-C6**	**GS-C7**	**GS-EH**
10	4.2%	N/A	6.3%	2.9%	3.1%	1.3%	1.1%
20	3.6%	1.3%	6.1%	4.9%	6.3%	5.1%	6.4%

X_c of nPLA melt-mixed sample: 3.2%

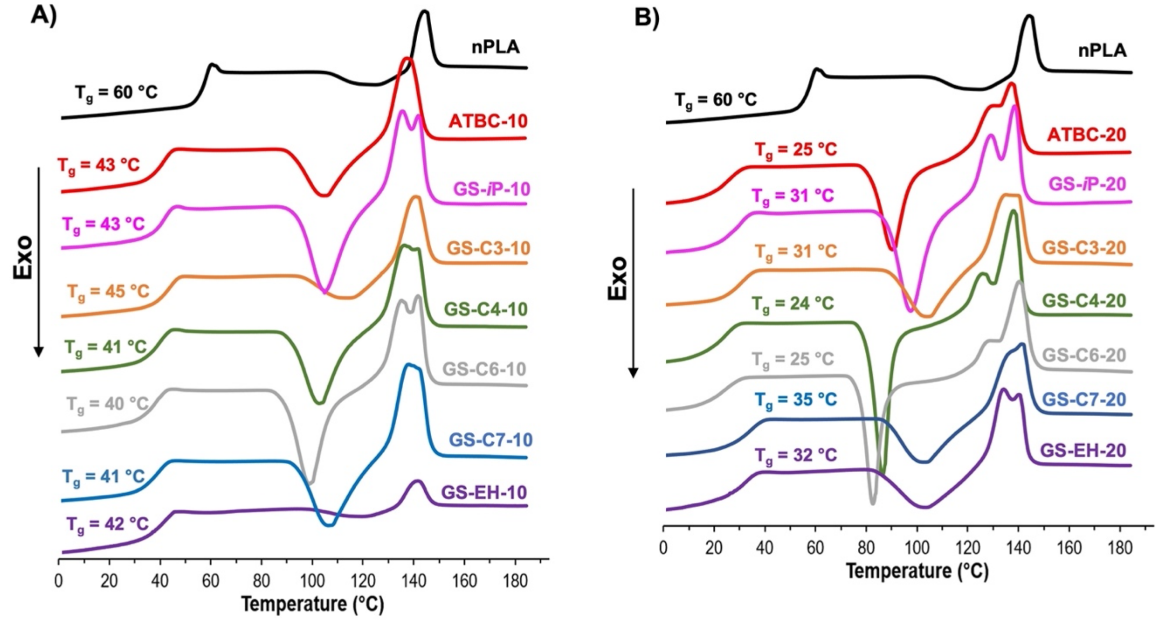

Figure B1. DSC thermograms of PLA melt-mixed blends obtained from the second heating cycle with (A) 10wt% and (B) 20wt% glycerol plasticizers.

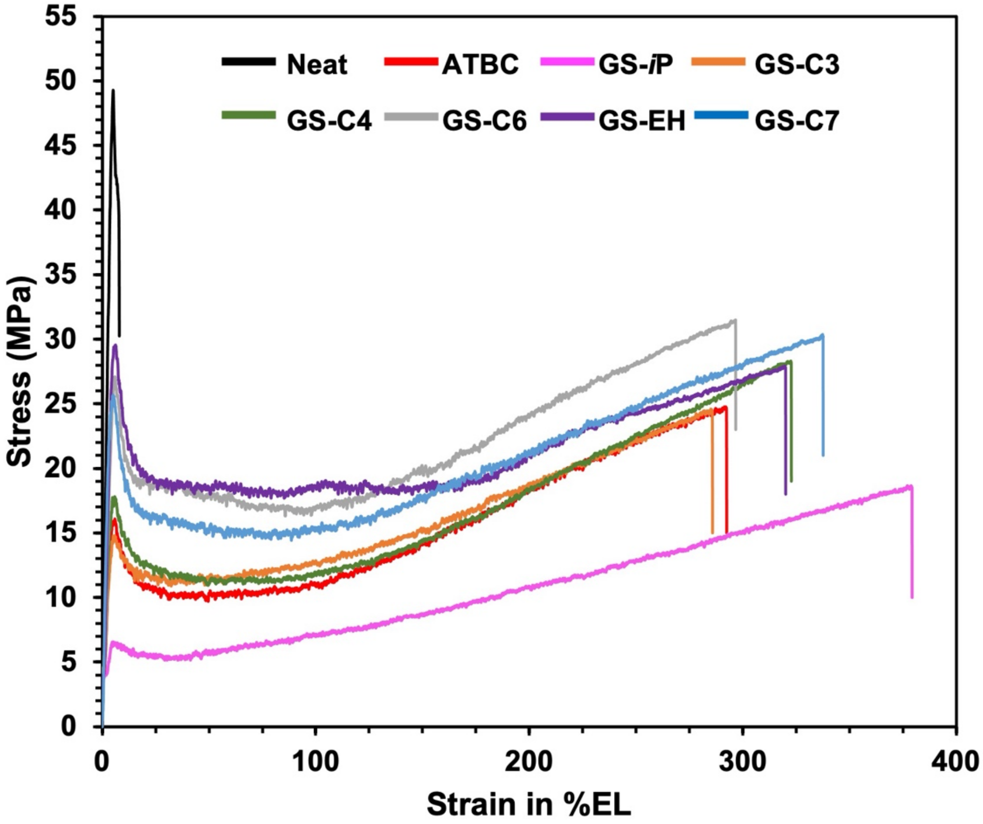

Figure B2. Stress versus strain in % elongation of PLA film blends with 10wt% glycerol plasticizers.

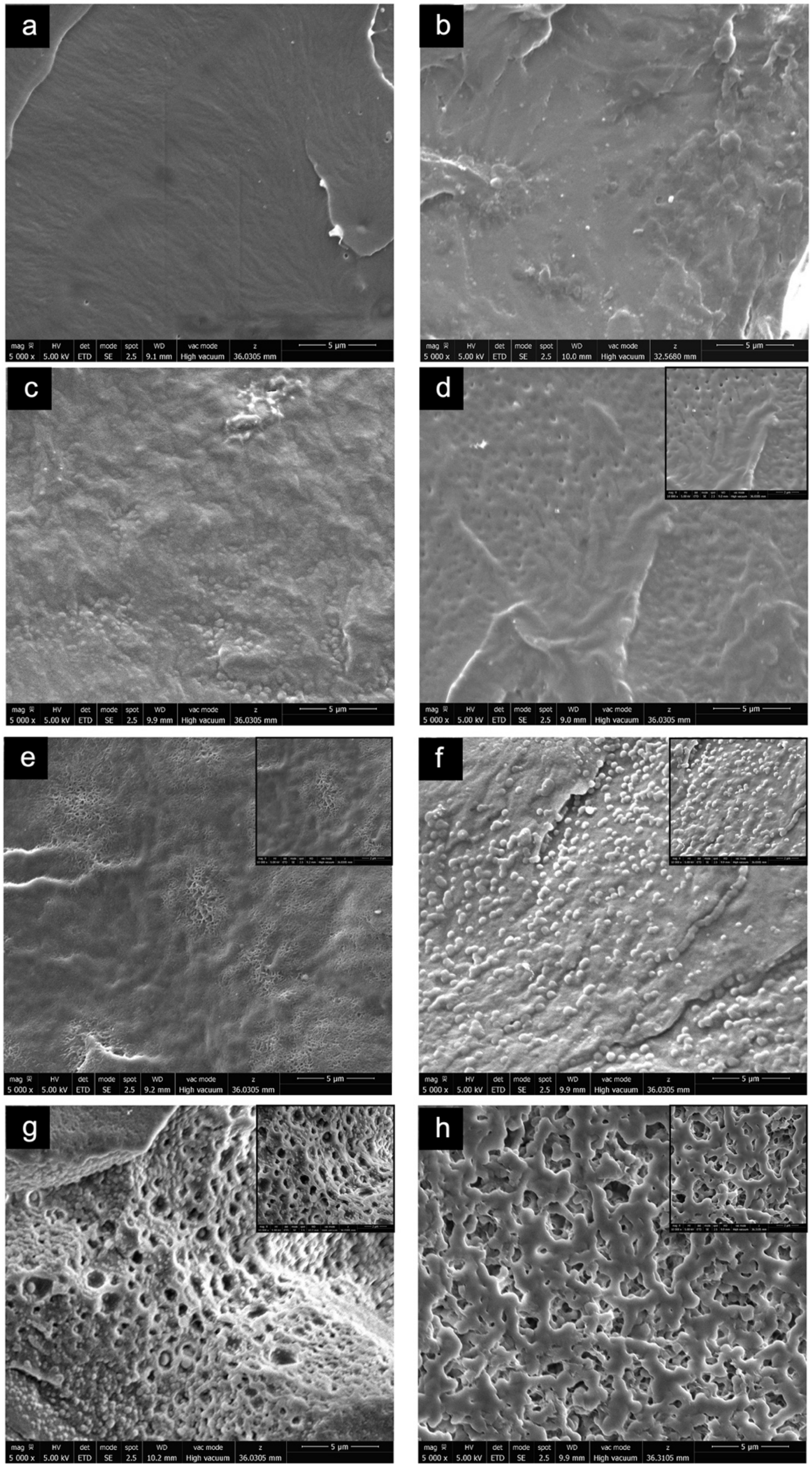

Figure B3. Freeze fractured surface SEM images of nPLA and 20 wt% solvent-cast film blends (5000× mag., 10,000 mag. in insets).

(a) nPLA, (b) ATBC, (c) GS-C3, (d) GS-*i*P, (e) GS-C4, (f) GS-C6, (g)

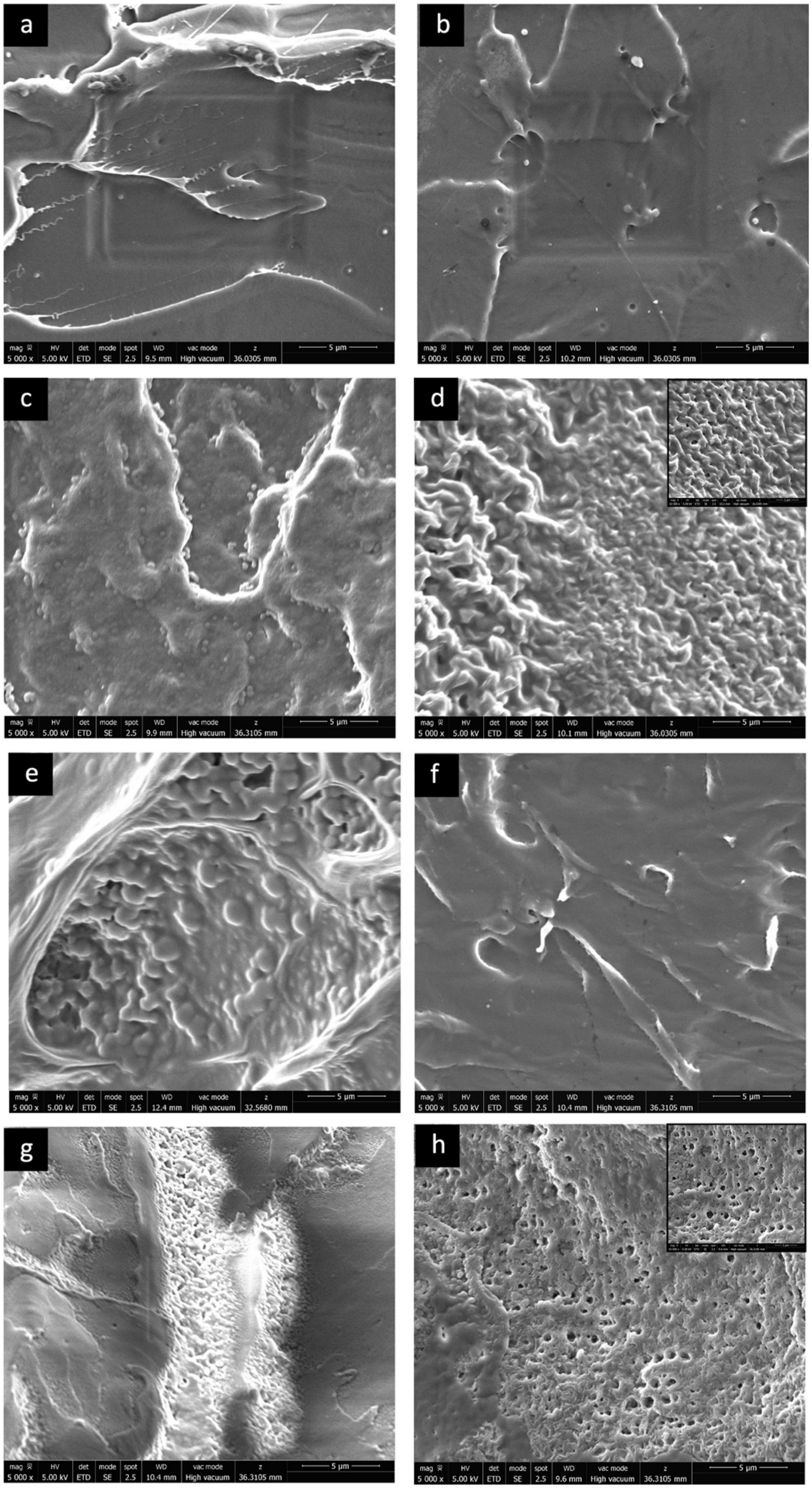

Figure B4. Freeze fractured surface SEM images of nPLA and 20 wt% melt-mixed blends (5000× mag., 10,000 mag. in insets).

(a) nPLA, (b) ATBC, (c) GS-C3, (d) GS-*i*P, (e) GS-C4, (f) GS-C6, (g)

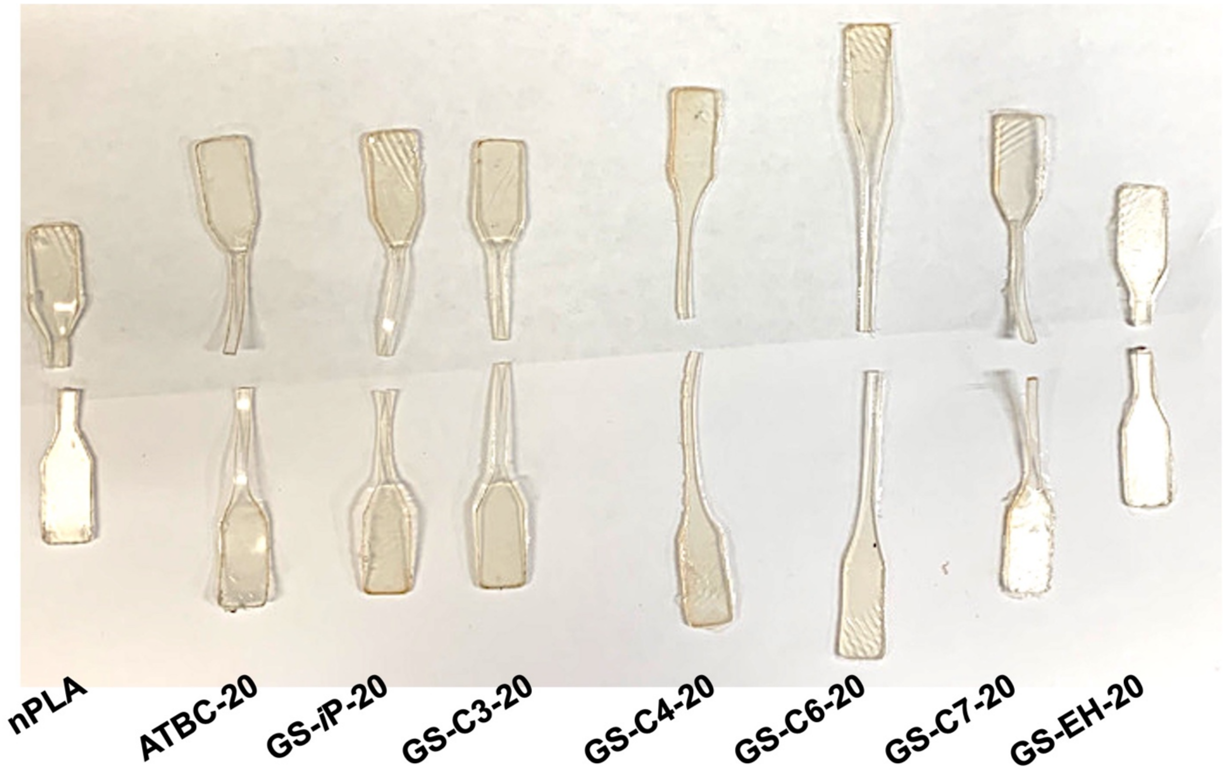

Figure B5. Tensile testing specimens of the 20wt% melt-mixed blends showing typical necking before fracture.

Hansen Solubility Parameters:

The below HSPs were calculated using the group contribution theory with Hoftyzer–Van Krevelen method. Assumptions: density was assumed as 1.0 g/cm^3 for glycerol plasticizers and 1.24 g/cm^3 for PLA. Radius value of PLA was found to be 10.7.[1]

---

[1] Abbott, S., Chemical compatibility of poly (lactic acid): A practical framework using Hansen solubility parameters. *Poly (Lactic Acid) Synthesis, Structures, Properties, Processing, and Applications* **2010**, 83-95.

Table B9. Calculated Hansen-Solubility parameters for each plasticizer and PLA.

Compound	MW (g/mol)	Density (g/cm³)	Molar Volume (cm³/mol)	# of Groups	Contribution of Group	Fdi (MJ/m3)$^{1/2}$•mol^{-1}	Fpi² (MJ/m3)$^{1/2}$•mol^{-1}	Ehi (J/mol)	δd (MJ/m³)1/2	δp (MJ/m³)$^{1/2}$	δh (MJ/m³)$^{1/2}$	δ (MJ/m³)$^{1/2}$	RED
ATBC	402.5	1.05	384.7	4	CH_3-	420	0	0	16	2.5	8.5	18.3	0.6
				11	CH_2	270	0	0					
				4	COO -	390	240100	7000					
				1	>C<	-70	0	0					
GS-C4	560.6	1	560.6	3	CH_3-	420	0	0	14.8	2.1	8.7	17.3	0.6
				17	CH_2	270	0	0					
				6	COO -	390	240100	7000					
				1	>C-	80	0	0					
GS-C3	518.6	1	518.6	3	CH_3-	420	0	0	14.4	2.3	9	17.1	0.6
				14	CH_2	270	0	0					
				6	COO -	390	240100	7000					
				1	>C-	80	0	0					
GS-iP	518.6	1	518.6	6	CH_3-	420	0	0	14.2	2.3	9	17	0.6
				8	CH_2	270	0	0					
				6	COO -	390	240100	7000					
				4	>C-	80	0	0					
GS-EH	728.9	1	728.9	6	CH_3-	420	0	0	15.6	1.6	7.6	17.4	0.7
				23	CH_2	270	0	0					
				6	COO -	390	240100	7000					
				4	>C-	80	0	0					
GS-C6	644.8	1	644.8	3	CH_3-	420	0	0	15.3	1.9	8.1	17.4	0.7
				23	CH_2	270	0	0					
				6	COO -	390	240100	7000					
				1	>C-	80	0	0					
GS-C7	686.9	1	688.9	3	CH_3-	420	0	0	15.5	1.7	7.8	17.4	0.7
				26	CH_2	270	0	0					
				6	COO -	390	240100	7000					
				1	>C-	80	0	0					
PLA	72.1	1.24	58.1	1	>C-	80	0	0	15.3	8.4	11	20.6	
				1	CH_3-	420	0	0					
				1	COO -	390	240100	7000					

Appendix C

Supporting information for "*Bio-based glycerol plasticizers for flexible Poly(vinyl chloride) blends.*"

Calculations & Formulas

The formulas used for the calculation of Hansen Solubility Parameters and Interaction Radii are as follows:[2, 3]

The below parameters were calculated using the group contribution method of Van Krevelen.

$$\delta_d = \frac{\sum F_{di}}{V},\ \delta_p = \frac{\sqrt{\sum F_{pi}^2}}{V},\ \delta_h = \frac{\sqrt{\sum E_{hi}}}{V},\ \delta = \sqrt{\delta_d^2 + \delta_p^2 + \delta_h^2}$$

where*:* F_{di} represents the dispersive functional group value, F_{pi} represents the polar functional group values, E_{hi} represents the cohesive energy of the hydrogen bonding forces, V represents the molar volume, δ_d represents the dispersion forces, δ_p represents the permanent dipoles, δ_h represents the hydrogen bonding, and δ represents the overall Hansen Solubility Parameter.

$$\delta_v = \sqrt{(\delta_d^2 + \delta_p^2)}$$

where*:* δ_v represents the combination of the dispersion and permanent dipole forces.

$$Interaction\ Radius = \sqrt{((\delta_{v,PVC} - \delta_{v,plasticizer})^2 + (\delta_{h,PVC} - \delta_{h,plasticizer})^2)}$$

---

[2] Van Krevelen, D. W.; Te Nijenhuis, K., Chapter 7 - Cohesive Properties and Solubility. In *Properties of Polymers (Fourth Edition)*, Van Krevelen, D. W.; Te Nijenhuis, K., Eds. Elsevier: Amsterdam, 2009; pp 189-227.

[3] Hansen, C. M., *Hansen solubility parameters: a user's handbook.* CRC press: 2007.

DSC Exotherms of Blends

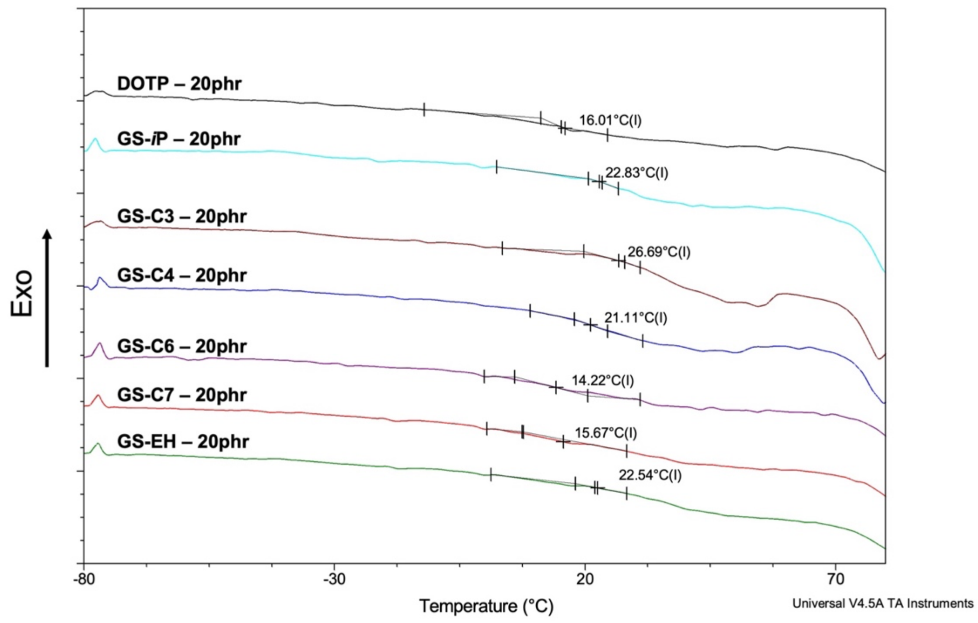

Figure C1. DSC exotherms of 20 phr PVC/plasticizer blends

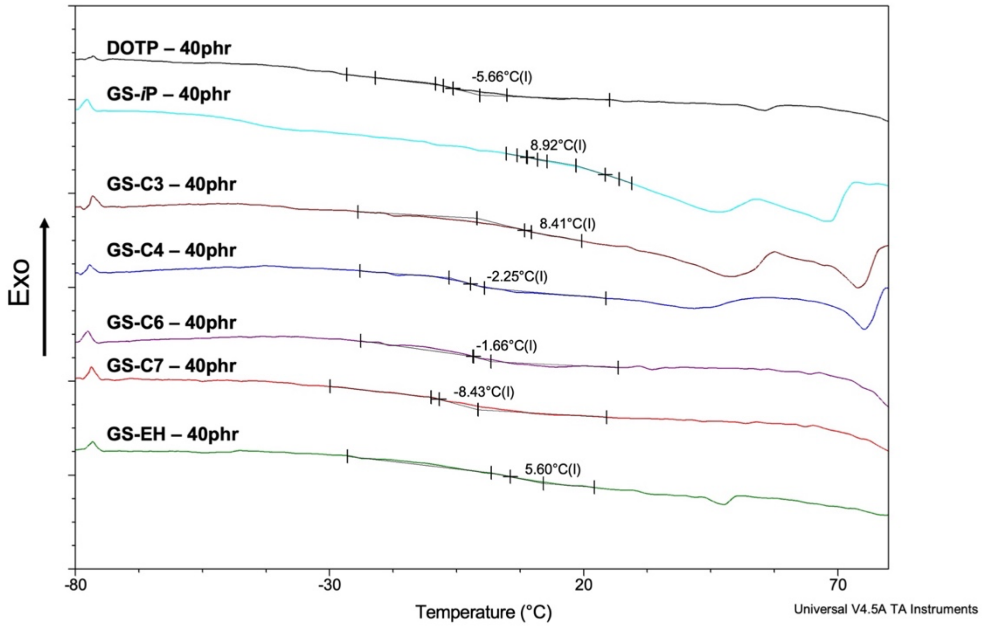

Figure C2. DSC exotherms of 40 phr PVC/plasticizer blends.

Appendix D

Supporting information for "*Toughening poly(lactide) with bio-based poly(farnesene) elastomers.*"

*Glossary of terms: poly(farnesene) (**PF**), poly(farnesene-co-methacrylic acid) (**PFMAA**), poly(farnesene-co-glycidyl methacrylate) (**PFGMA**), hydrogenated poly(farnesene) (**HPF**), poly(lactide) (**PLA**).*

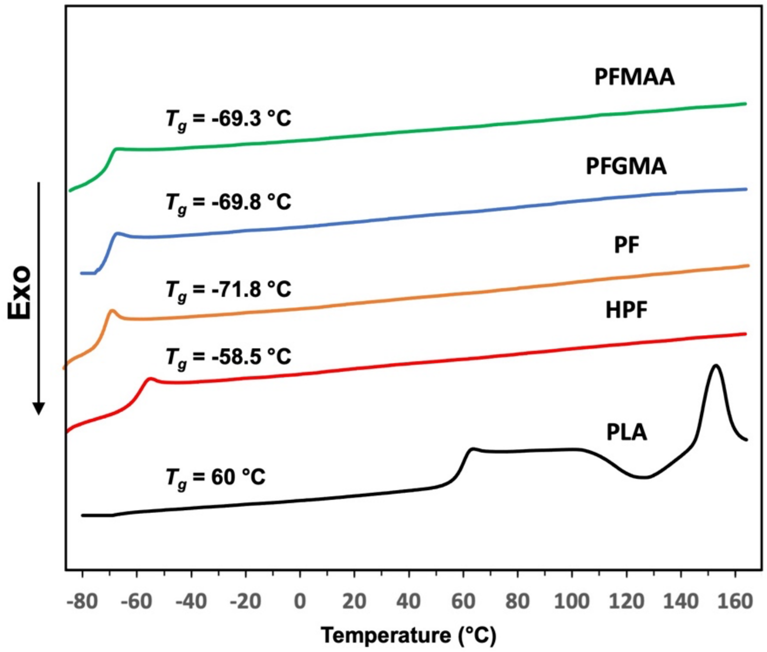

Figure D1. DSC traces of homopolymers obtained from the second heating cycle.

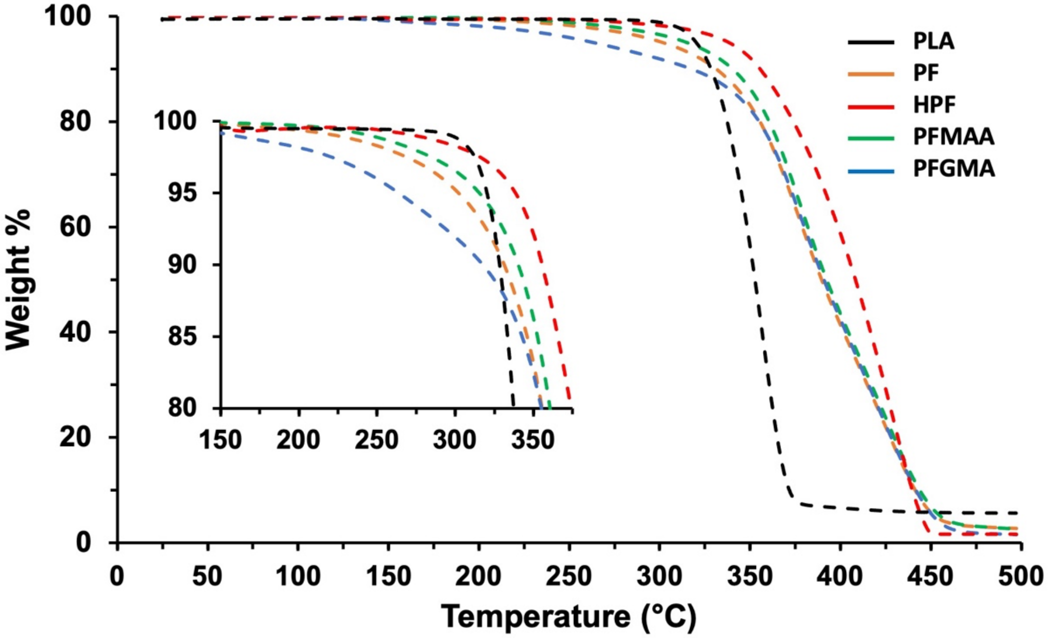

Figure D2. TGA traces of homopolymers.

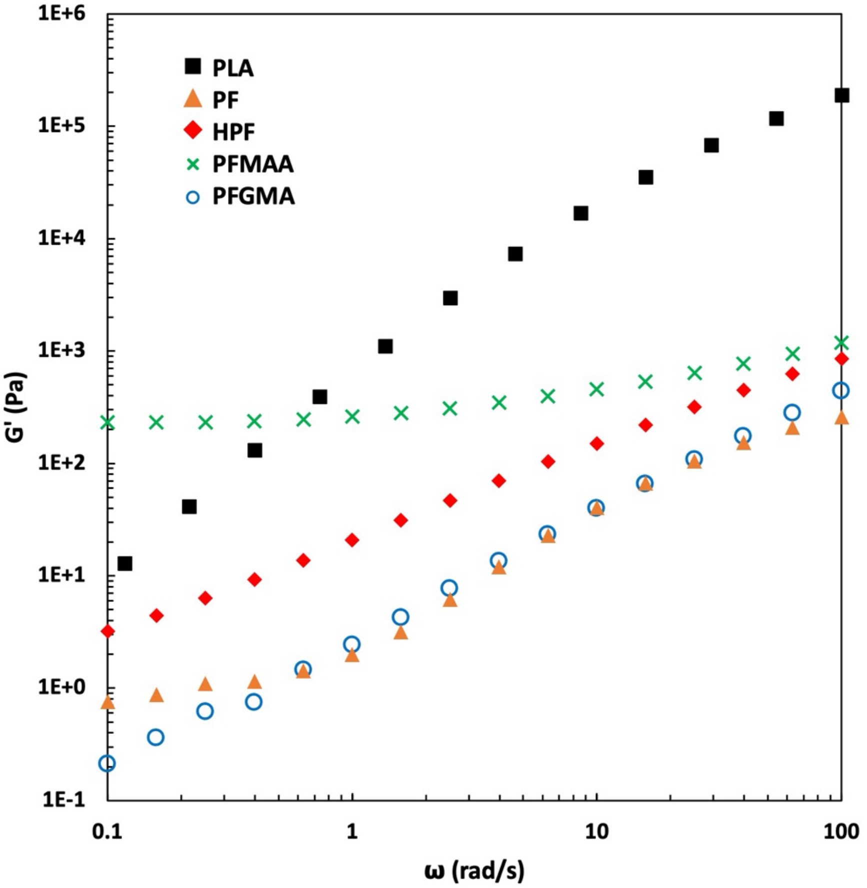

Figure D3. Storage modulus versus frequency of homopolymers taken at 175 °C.

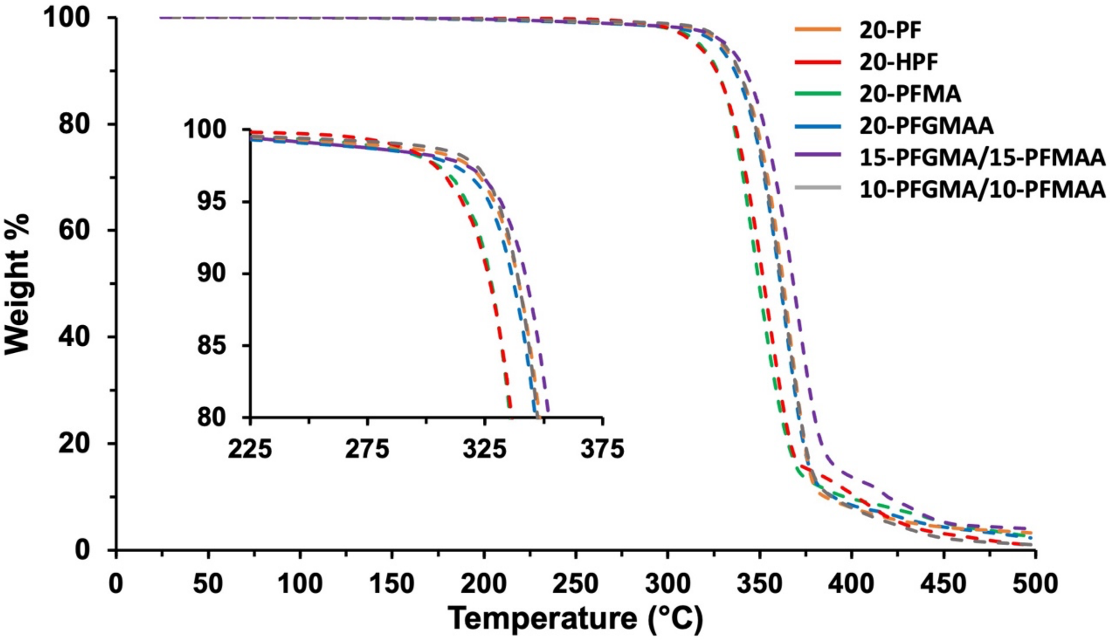

Figure D4. TGA traces of binary and ternary blends.

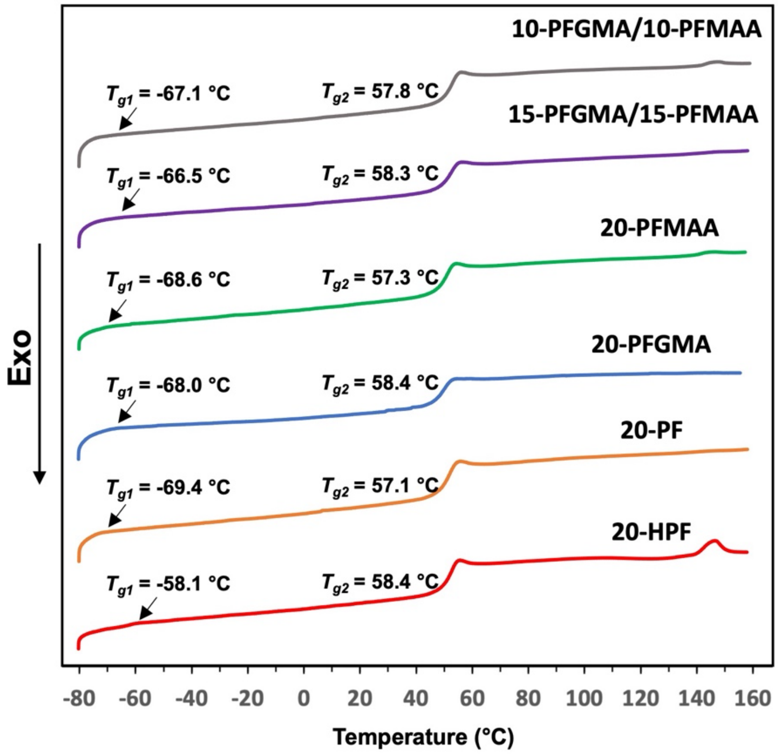

Figure D5. DSC traces of binary and ternary blends obtained from the second heating cycle.

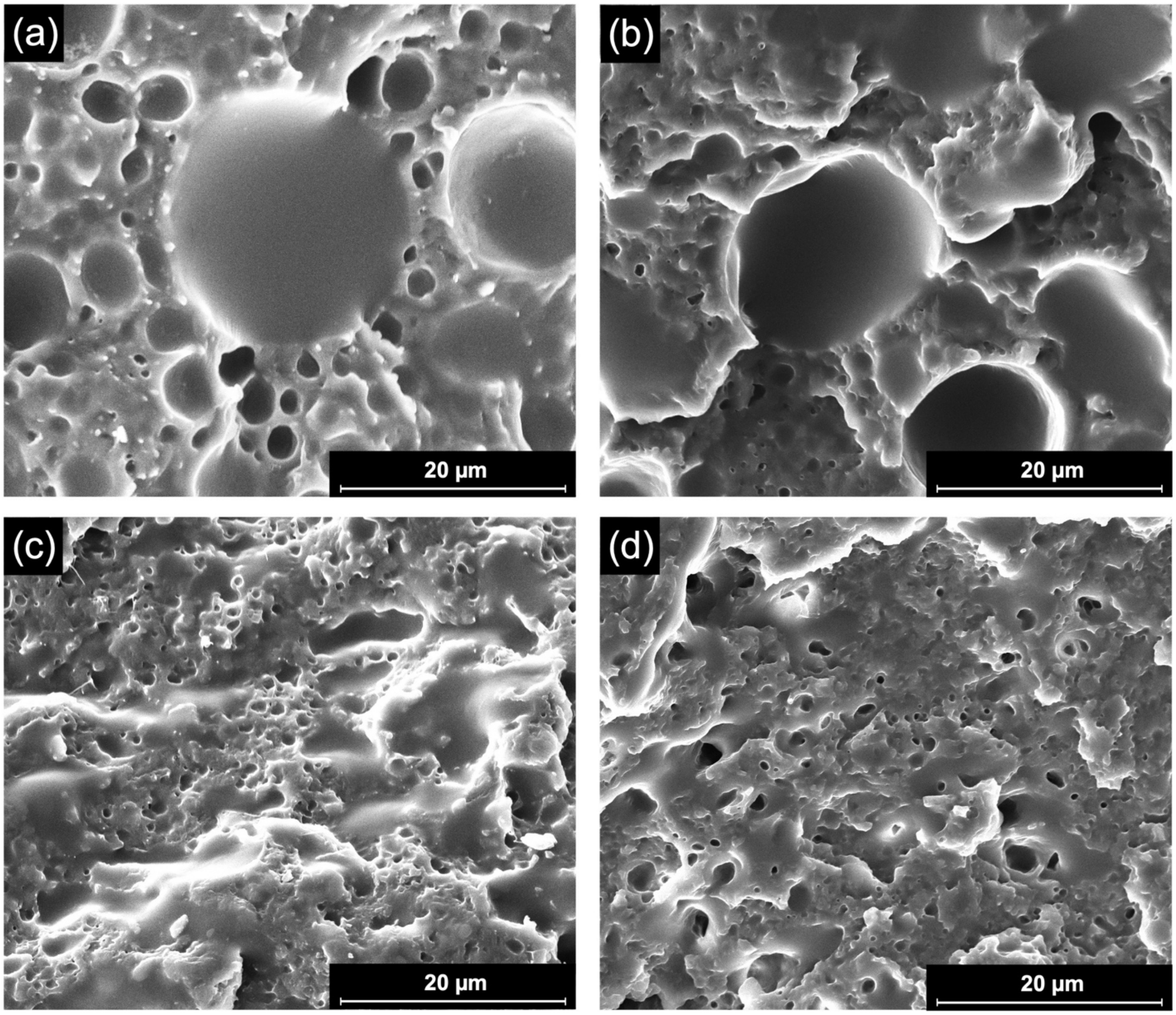

Figure D6. SEM images of cryo-fractured surfaces of binary and ternary blends after thermal annealing for 8 hours under vacuum at 100 °C: (a) 20-PFMAA, (b) 20-PFGMA, (c) 15-PFGMA/15-PFMAA, (d) 10-PFGMA/10-PFMAA.

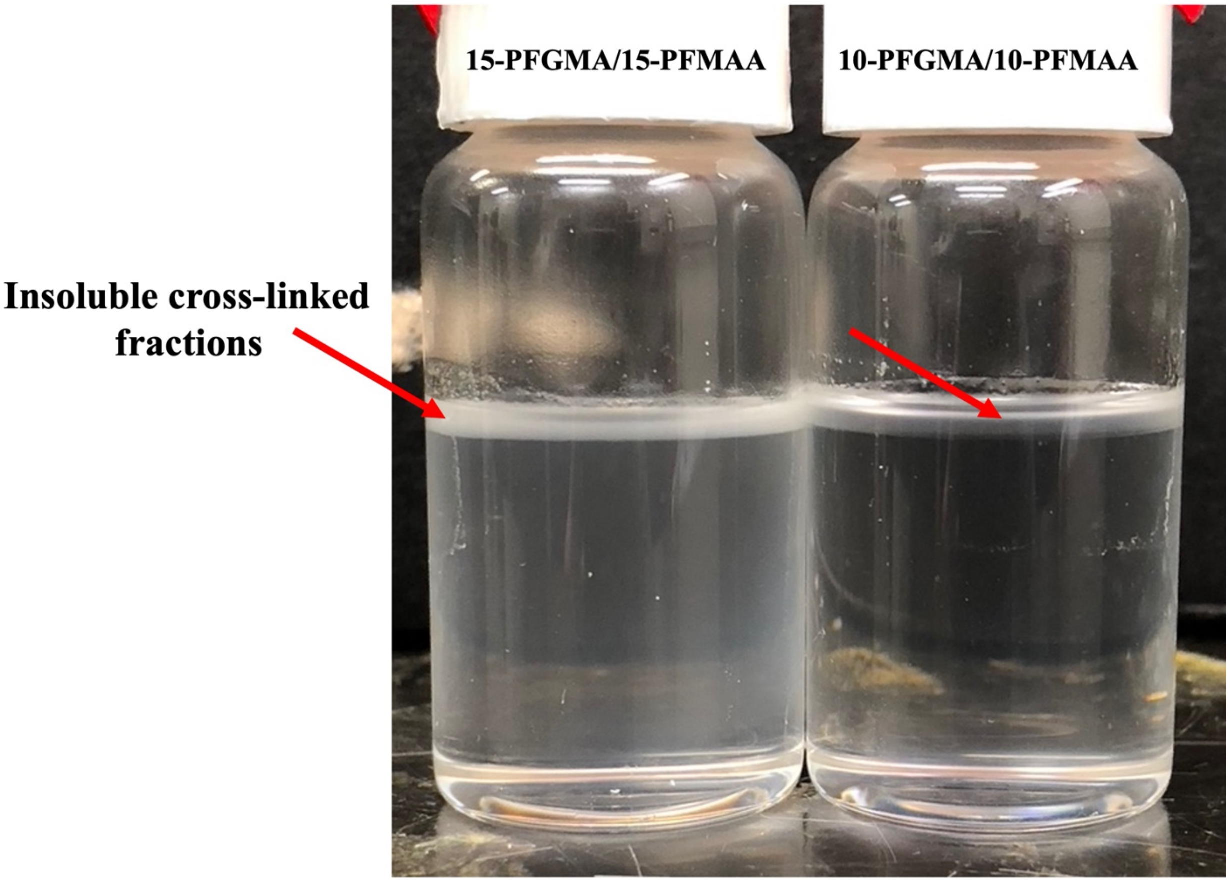

Figure D7. Isolated insoluble fraction obtained for the ternary blends after stirring in $CHCl_3$ for 48 hours (repeated three times). The insoluble fraction was isolated and dried and then analyzed with FTIR.